APPENDIX 1
ENGINEERING ANALYSIS AND DESIGN

Shoalwater Bay Shoreline Erosion, Washington

FLOOD AND COASTAL STORM DAMAGE REDUCTION

Shoalwater Bay Indian Reservation

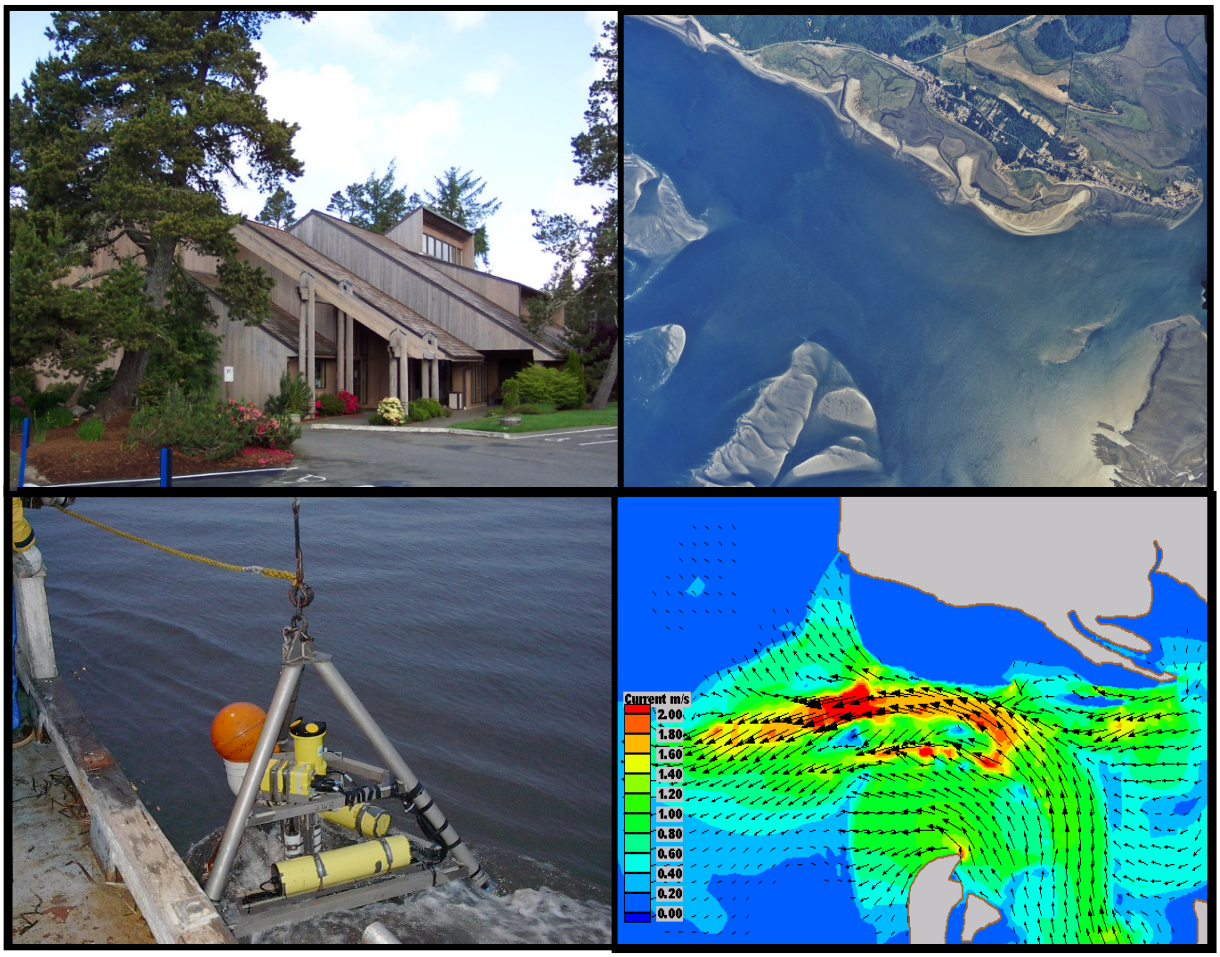

US Army Corps
of Engineers®
Seattle District

U.S. ARMY ENGINEER RESEARCH AND DEVELOPMENT CENTER
CERL CHL GSL EL ITL CRREL TEC

April 2009

REPORT DOCUMENTATION PAGE

Form Approved
OMB No. 0704-0188

PLEASE DO NOT RETURN YOUR FORM TO THE ABOVE ORGANIZATION.

1. REPORT DATE *(DD-MM-YYYY)*	2. REPORT TYPE	3. DATES COVERED *(From - To)*
04-2009	Final	2009

4. TITLE AND SUBTITLE
Appendix 1--Engineering Analysis and Design
Shoalwater Bay Shoreline Erosion, Washington
Flood and Coastal Storm Damage Reduction
Shoalwater Bay Indian Reservation

5a. CONTRACT NUMBER

5b. GRANT NUMBER

5c. PROGRAM ELEMENT NUMBER

6. AUTHOR(S)
U.S. Army Corps of Engineers, Seattle District
U.S. Army Engineer Research and Development Center, Coastal Hydraulics Laboratory
U.S. Geological Survey, Coastal and Marine Geology Program
Washington Department of Ecology, Coastal Monitoring and Analysis Program
Shoalwater Bay Indian Tribe

5d. PROJECT NUMBER

5e. TASK NUMBER

5f. WORK UNIT NUMBER

7. PERFORMING ORGANIZATION NAME(S) AND ADDRESS(ES)
U.S. Army Corps of Engineers, Seattle District
Post Office Box 3755
Seattle, Washington 98124-3755

8. PERFORMING ORGANIZATION REPORT NUMBER

9. SPONSORING/MONITORING AGENCY NAME(S) AND ADDRESS(ES)
U.S. Army Corps of Engineers, Seattle District
Post Office Box 3755
Seattle, Washington 98124-3755

10. SPONSOR/MONITOR'S ACRONYM(S)
USACE

11. SPONSOR/MONITOR'S REPORT NUMBER(S)

12. DISTRIBUTION/AVAILABILITY STATEMENT
Approved for public release; distribution unlimited.

13. SUPPLEMENTARY NOTES
Appendix 1 to Post-Authorization Decision Document and Environmental Assessment, April 2009, U.S. Army Corps of Engineers, Seattle District.

14. ABSTRACT

The study was conducted in accordance with Section 545 of the Water Resources Development Act (WRDA) of 2000, as amended by Section 5153 of WRDA 2007. Section 545(a) of WRDA 2000 directed the Secretary of the Army to conduct a study to determine the feasibility of providing coastal erosion protection for the tribal reservation of the Shoalwater Bay Indian Tribe in the State of Washington. The interagency investigation conclusively demonstrated that (1) erosion of the natural barrier dune on Graveyard Spit has reached a critical stage and (2) modest engineering solutions are technically feasible to significantly reduce coastal erosion and the risk to the Shoalwater Reservation from flooding and coastal storm damage. The report identifies restoration of the eroded 12,500 foot-long barrier dune as the most appropriate long-term solution to coastal erosion, flooding, and storm damage problems affecting the Shoalwater Bay Indian Reservation. This plan is a complete solution to identified problems, is cost effective, is environmentally acceptable, and will improve the economic and social conditions of the Shoalwater Bay Indian Tribe. Sand to restore the barrier dune will be dredged from an aquatic borrow site in Willapa Bay.

15. SUBJECT TERMS
Willapa Bay, Washington; coastal erosion; shoreline erosion; coastal storm damage reduction; flood damage reduction; barrier dunes; storm-generated waves; Shoalwater Bay Indian Tribe.

16. SECURITY CLASSIFICATION OF:			17. LIMITATION OF ABSTRACT	18. NUMBER OF PAGES	19a. NAME OF RESPONSIBLE PERSON
a. REPORT	b. ABSTRACT	c. THIS PAGE			Chief, Civil Programs and Projects Branch
U	U	U	UU	240	19b. TELEPHONE NUMBER *(Include area code)* 206-764-6747

Reset

Standard Form 298 (Rev. 8/98)
Prescribed by ANSI Std. Z39.18
Adobe Professional 7.0

(This page intentionally left blank)

Interagency Project Delivery Team

An interagency team, under direction of the U.S. Army Corps of Engineers, Seattle District and in consultation with the Shoalwater Bay Indian Tribe, conducted comprehensive studies to determine the technical feasibility of, and to formulate alternative plans for, providing coastal erosion protection to the Shoalwater Bay Indian Reservation at Willapa Bay, Washington. The interagency team included the following entities:

Project Management, Preparation of Decision Document and Environmental Assessment:

- U.S. Army Corps of Engineers, Seattle District

Technical Studies, conducted under direction of Seattle District:

- U.S. Army Corps of Engineers, Seattle District
- U.S. Army Engineer Research and Development Center, Vicksburg, Mississippi
  - Coastal and Hydraulics Laboratory
  - Environmental Laboratory
- U. S. Geological Survey interagency team
  - Coastal and Marine Geology Program, Menlo Park, California
  - Delft Hydraulics, Netherlands
  - Rutgers University, Institute of Coastal and Marine Services
- Washington Department of Ecology, Lacey, Washington
  - Coastal Monitoring and Analysis Program
- Shoalwater Bay Indian Tribe: Tribal Council and staff

Agency Technical Reviews:

- U.S. Army Corps of Engineers, Alaska District (Draft and Final Decision Document)
- U.S. Army Corps of Engineers, Walla Walla District (Cost and Schedule)

This document is also available online at:

http://www.nws.usace.army.mil/ers/doc_table.cfm

Table of Contents

FIGURES AND TABLES

Acronyms Used in the Appendix

ADCIRC	Advanced Circulation numerical model
ADCP	Acoustic Doppler current profiler
ADVO	Acoustic Doppler velocitmeter ocean hydra system
BEB	Beach Erosion Board
CDIP	Coastal Data Information Program
CMS-WAVE	Coastal Modeling System – Wave Action Balance Equation Diffraction Model
CHL	Coastal and Hydraulics Laboratory at ERDC
Corps	U.S. Army Corps of Engineers
DRO	USACE Dredging Research Program
EHI	Evans-Hamilton, Inc
ENSO	El Niño Southern Oscillation
EST	Empirical Simulation Technique
ERDC	Engineer Research and Development Center, U.S. Army Corps of Engineers
GIS	Geographic information system
GWCE	Generalized Wave Continuity Equation
HQUSACE	Headquarters, U. S. Army Corp of Engineers
M-CACES	Micro-computer aided cost engineering system
MAT	Maximum astronomical tide
MHHW	Mean higher high water
MLLW	Mean lower low water
MTL	Mean Tide Level
NAD	North American Datum
NDBC	National Data Buoy Center
NEPA	National Environmental Policy Act 1969
NIMA	U.S. National Imaging and Mapping Agency
NMFS	National Marine Fisheries Service
NWS	Seattle District, U.S. Army Corps of Engineers
NOAA	National Oceanic and Atmospheric Administration
NOS	National Ocean Service
OMRR&R	Operation, maintenance, repair, replacement and rehabilitation
PDO	Pacific Decadal Oscillation
SBEACH	Storm induced BEAch Change model
Shoalwater Reservation	Shoalwater Bay Indian Reservation
Shoalwater Tribe	Shoalwater Bay Indian Tribe
SR-105	Washington State Route 105
SPM	Shore Protection Manual
sstoi	Sea surface temperature optimum interpolation indices

STWAVE	Steady-state spectral wave model
USC&GS	U.S. Coast and Geodetic Survey
USGS	U.S. Geological Survey
UTM	Universal Trans Mercator
WA DOE	Washington Department of Ecology
WA DOT	Washington Department of Transportation
WGS	World Geodetic System

Conversion Factors – Non-SI to SI Units of Measurement

The Metric System, a system of units used for physical measurements, is called the International System of Units, and its units are called SI units. Non-SI units of measurement used in this report can be converted to SI units as follows:

Multiply	By	To Obtain
Acres	4,046.873	square meters
cubic yards	0.7645549	cubic meters
Feet	0.3048	meters
Inches	2.54	centimeters
miles (U.S. statute)	1.609347	kilometers
Pounds	4.5359×10^2	grams
Tons	1.016×10^3	kilograms
square miles	2,589,998	square meters

1.0 Problem Definition and Study Approach

1.1 Introduction

The proposed Shoalwater Bay Shoreline Erosion Project is located on the Shoalwater Bay Indian Reservation (Shoalwater Reservation). The Shoalwater Reservation is located on the northern shore of Willapa Bay, a large estuary located on the southwest coast of Washington State (see Figure 1.1). With a spring diurnal range tidal prism of more than 10^{10} cubic feet, Willapa Bay is one of the largest inlets on the coast of the continental United States, (Jarrett 1976). At the mean maximum tidal flow of 2.5 knots, the main (northernmost) Willapa channel transports about 400,000 cubic feet per second, or about twice the average annual discharge rate of the Columbia River at The Dalles, (Richey et al., 1966). The massive tidal flow, combined with energetic waves, has created one of our country's most actively eroding coasts. The northern shoreline of Willapa Bay to the west of the project area has changed drastically since the Shoalwater Reservation was established in 1866, (Terich and Levensellar, 1986). Over the last century, portions of the Cape Shoalwater shoreline have retreated more than three miles (see Figure 1.2). By the 1990's, the Shoalwater Reservation's only remaining protection from storm wave attack was a barrier dune that is located on Graveyard Spit and the islands fronting the Tokeland Peninsula. Tidal currents and storm waves have severely eroded the barrier dune, exposing the Shoalwater Bay Indian Reservation to increasing levels of flooding due to wave overtopping of the shoreline during periods of extreme high tides (see Figures 1.3 and 1.4).

1.2 Shoreline Erosion and Storm Induced Flooding

On March 3, 1999, a combined storm and high tide caused severe flooding of the Shoalwater Reservation shoreline and the surrounding community. The flooding prompted the initiation of a Corps of Engineers emergency flood protection planning process. As a consequence, in March 2001, the Corps of Engineers constructed a riprap flood berm along a small portion (1,700 feet) of the Shoalwater Reservation shoreline. This flood berm provides protection from direct wave attack and further shoreline erosion during combined storm and high tide events only to this portion of the Reservation shoreline, including the Tribal headquarters building. Since the flood berm protects only a portion of the Reservation shoreline, however, it does not address flooding of all tribal uplands caused by overtopping of the adjacent unprotected shoreline areas. In February 2006, another storm at extreme high tide caused significant flooding and damage to areas not protected by shoreline flood berm. Portions of the shoreline that is not protected by the flood berm – and the tribal infrastructure located on these lands – will continue to be overtopped by storm waves at extreme high tide, causing flooding of all the low lying backshore areas of the Shoalwater Reservation with elevations lower than approximately +15 feet mean lower low water (MLLW) (see Figure 1.5). A 300-foot-long extension was constructed in December 2007.

Coastal erosion and storm induced flooding is a serious problem for the entire one-square-mile Shoalwater Reservation. It is the direct result of the erosion and breaching of the barrier dune on Graveyard Spit that fronts the Tokeland Peninsula. The uplands portion of the original Shoalwater Reservation is only 335 acres. The Tribe has acquired an additional 105 acres, increasing their uplands area to approximately 440 acres. Essential public facilities and housing are being constructed on these lands, to support the growing needs of the tribal community. The balance of the Shoalwater Reservation,

totaling some 700 acres, extends into Willapa Bay and includes tidelands (part of North Cove) extending to MLLW. These tidelands, which have been used by the Shoalwater Tribe for subsistence shellfish gathering, have been seriously degraded and chocked with sand as a direct result of extreme high tide storm events that have overtopped the barrier dune on Graveyard Spit. Accordingly, planning objectives for this project include reducing coastal erosion and resulting flooding of the uplands portion of the Shoalwater Reservation, as well as protecting intertidal habitat in North Cove from further infilling and loss due to storm waves that overwash the Graveyard Spit barrier dune.

1.3 Design Goals and Study Approach

The stated goal of this project's enabling legislation [1] is to **"**construct and maintain a project to provide coastal erosion protection for the tribal reservation of the Shoalwater Bay Tribe." The project is to be "cost-effective," "environmentally acceptable and technically feasible;" and "improve the economic and social conditions of the Shoalwater Bay Tribe." Initially, the prognosis for addressing any one, let alone all three, of these requirements appeared to be extremely bleak. The magnitude of the ongoing erosion and the seemingly inexorable northward advance of the Willapa channel led initially to considerable uncertainty that an economically feasible engineering solution could be formulated and substantiated. Before initiating any engineering work on structural alternatives, a major interagency effort was expended to understand the geology, geomorphology, and hydraulics of Willapa Bay and the Willapa Bay entrance. The Seattle District office of the U.S. Army Corps of Engineers entered into formal agreements with an interdisciplinary team of scientists from the following entities to assist in conducting the required comprehensive investigations:

- U.S. Army Engineer Research and Development Center (ERDC), Coastal and Hydraulics Laboratory, Vicksburg, Mississippi.
- U.S. Geological Survey, Coastal and Marine Geology Program, Menlo Park, California.
- Washington Department of Ecology, Coastal Monitoring and Analysis Program, Lacey, Washington.

These studies – the results of which are documented in this report – led to some unexpected findings that paved the way for what appears to be a relatively straightforward, economically viable, and environmentally acceptable engineering solution. The recommended plan also has the very strong support of the Shoalwater Bay Indian Tribe.

1.4 Summary of Findings

Comprehensive geologic studies found that the erosion processes, driven by the channel migration, are undergoing a profound change. The northward migration of the Willapa channel has stopped in the vicinity of the proposed project. Since the mid-1980s, the slope of the north bank of the main channel has been constant and has remained in a fixed position. This strongly indicates that the channel encountered hard strata that are resistant to erosion, sparing the last of the severely damaged dunes fronting the Shoalwater Reservation shoreline. Engineering solutions will not have to attempt to turn aside the advance of the Willapa Channel but will only have to address the barrier dune erosion and resultant flooding caused by locally generated waves or waves that enter from the ocean. Wave studies, including the collection of field data and numerical modeling determined that while these waves were capable of eroding the dunes and causing flooding of Shoalwater Reservation uplands, they are relatively small by coastal engineering standards. Three protective structure alternatives were formulated to address the

[1] Section 545 of the Water Resources Development Act of 2000, Public Law 106-541.

erosion and flooding problems on the Shoalwater Reservation. These alternatives included a sea dike (two variations), dune restoration, and dune restoration combined with shoreline flood berm extension. Each alternative plan would provide a complete solution to the coastal erosion and related storm damage threat to Shoalwater Reservation lands and infrastructure. Barrier dune restoration (see Figure 1.6) has been determined to be the most appropriate long term solution to the coastal erosion and associated storm damage problems affecting the Shoalwater Bay Indian Reservation. Plan formulation and evaluation of alternative plans is documented in the Decision Document report to which this report is appended.

References

Jarrett, J. T. 1976. "Tidal prism-inlet area relationships," GITI Report 3, U.S. Army Engineer Waterways Experiment Station, Vicksburg, MS.

Richey, E. P., Dean, R. G., Ekse, M. I., and Kent, J. C. 1966. "Considerations for the temporary arresting of the erosion at Cape Shoalwater, Washington," State of Washington, Department of Conservation, Olympia, WA.

Terich, T., and Levenseller, T. 1986. The Severe Erosion of Cape Shoalwater, Washington. *Journal of Coastal Research,* Vol. 2, No. 4, pp. 465-477.

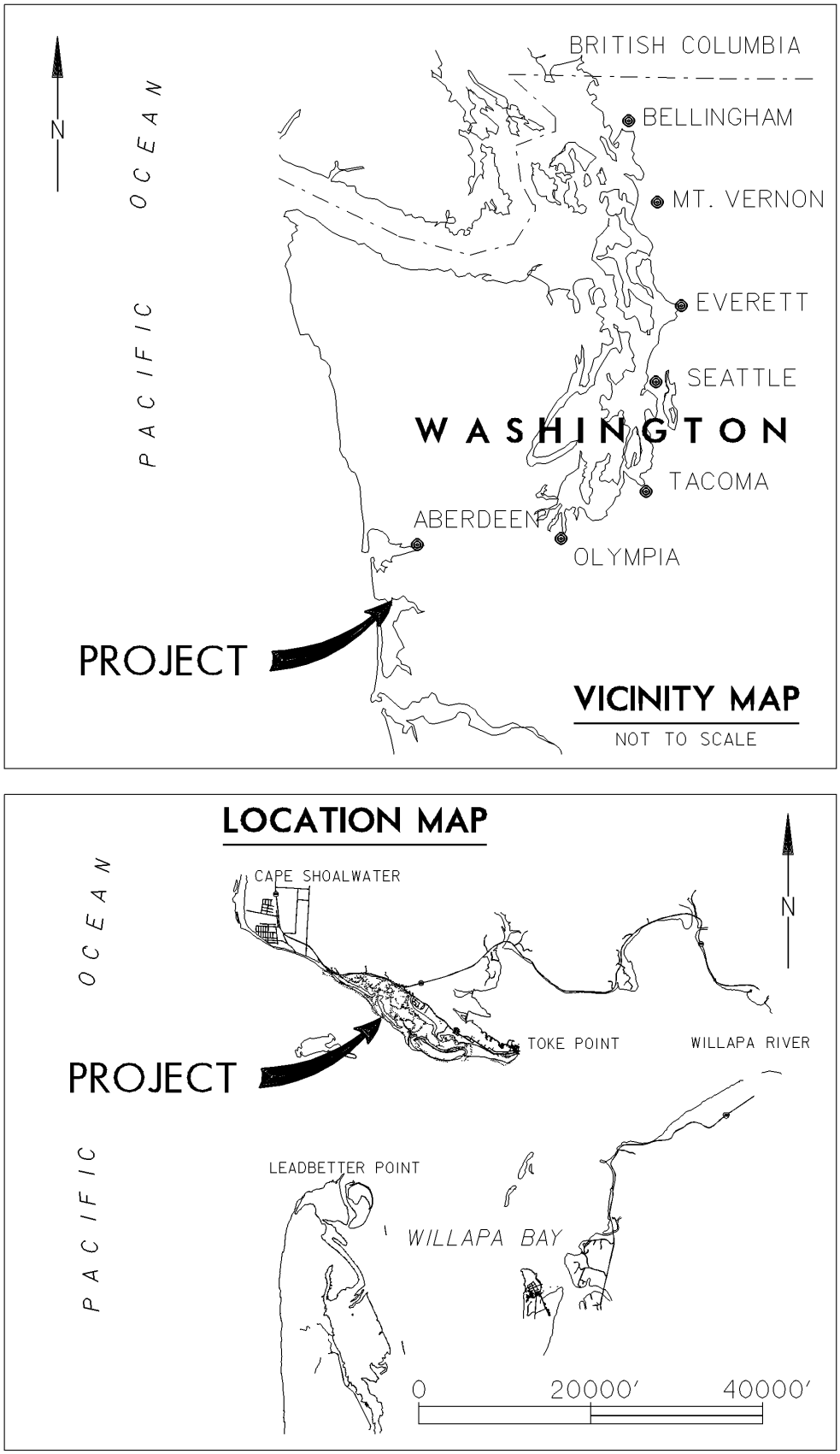

Figure 1.1 - Project vicinity and location maps.

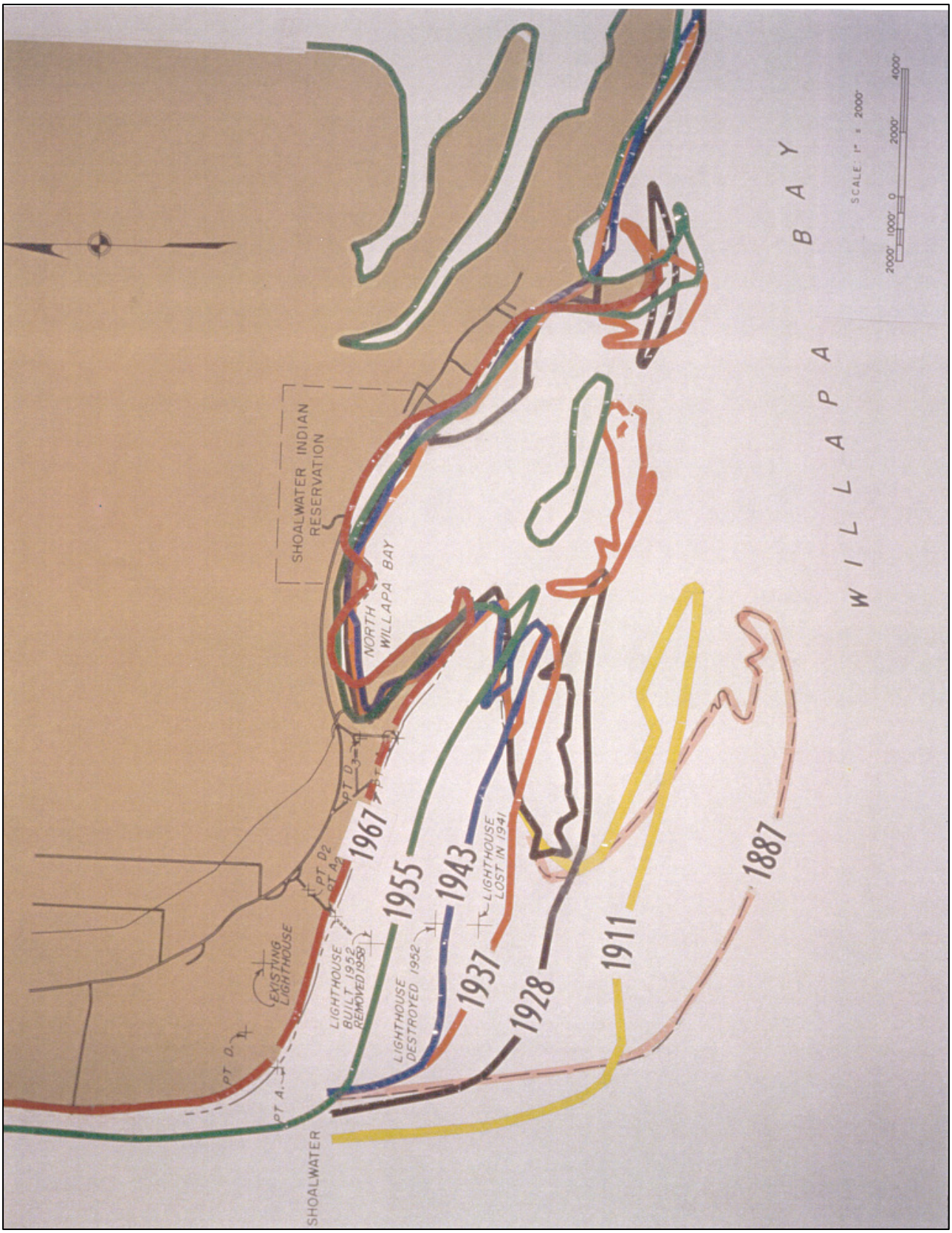

Figure 1.2 Willapa Bay shoreline erosion 1887 to 1967.

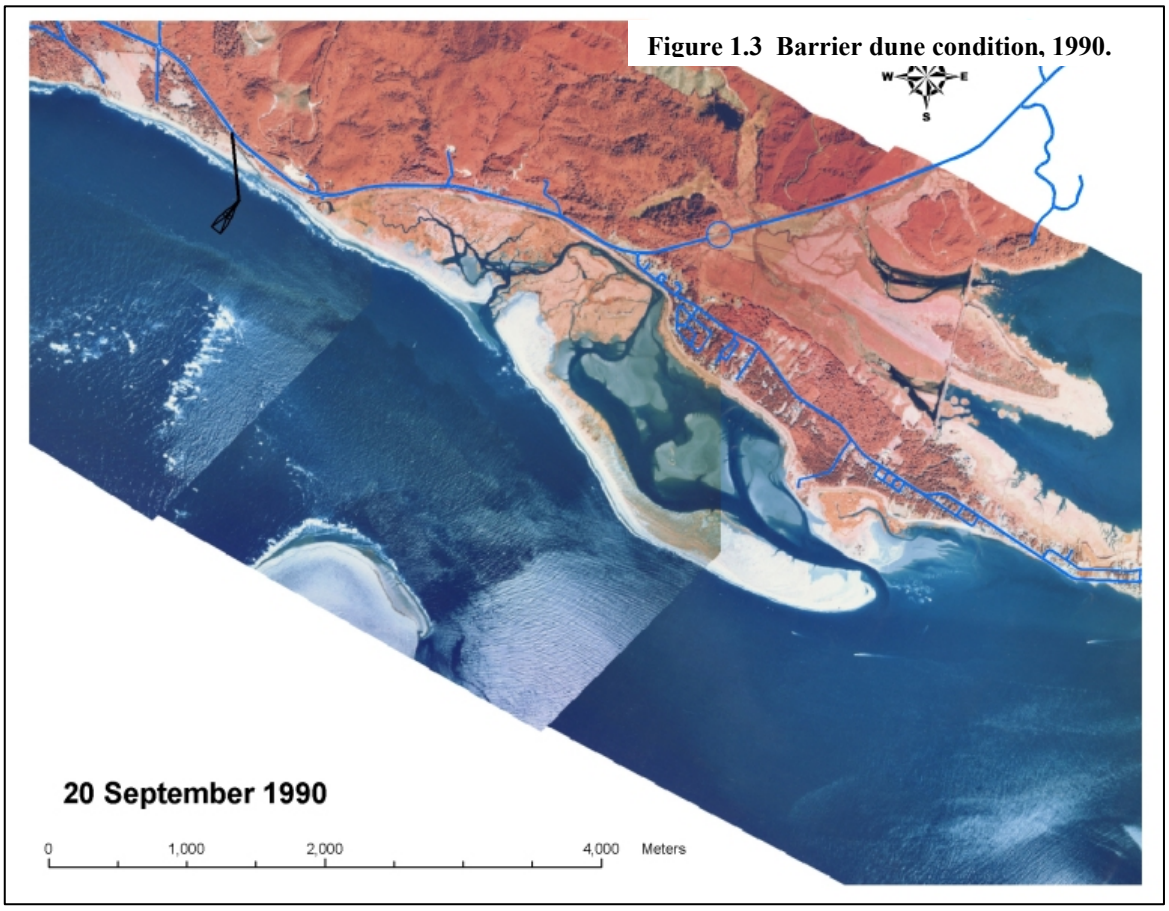

Figure 1.3 Barrier dune condition, 1990.

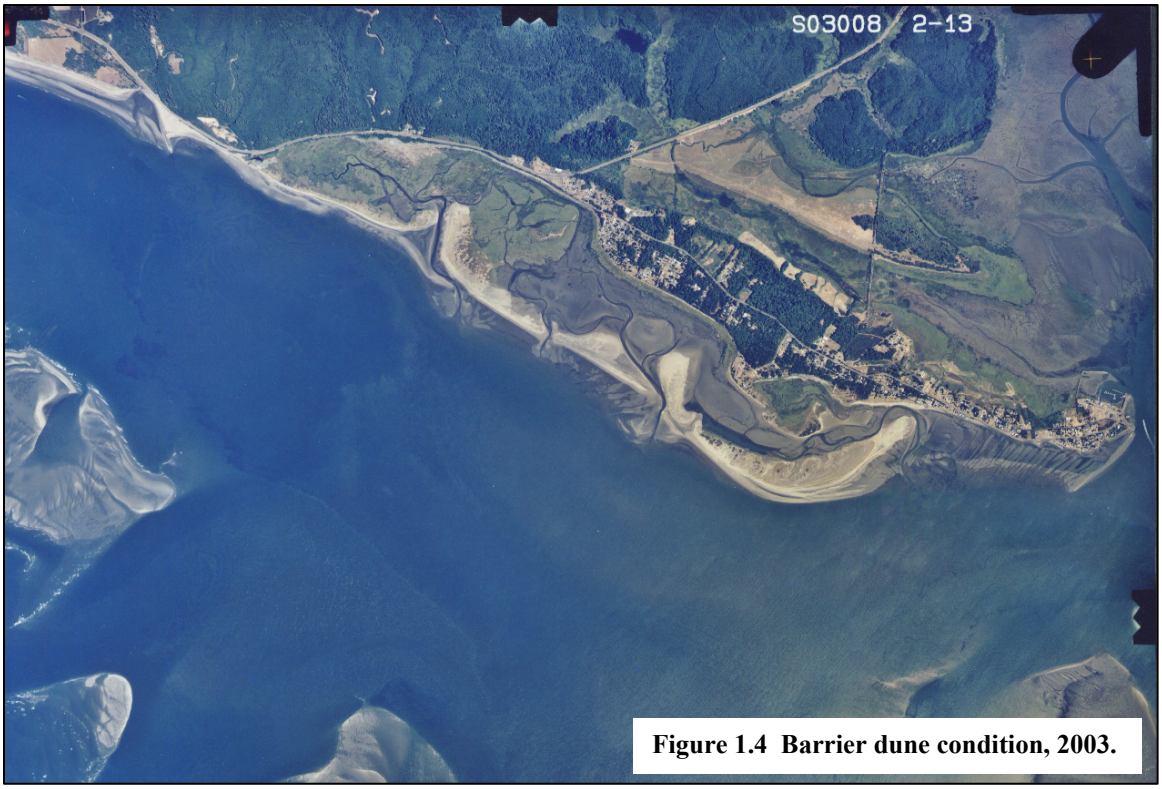

Figure 1.4 Barrier dune condition, 2003.

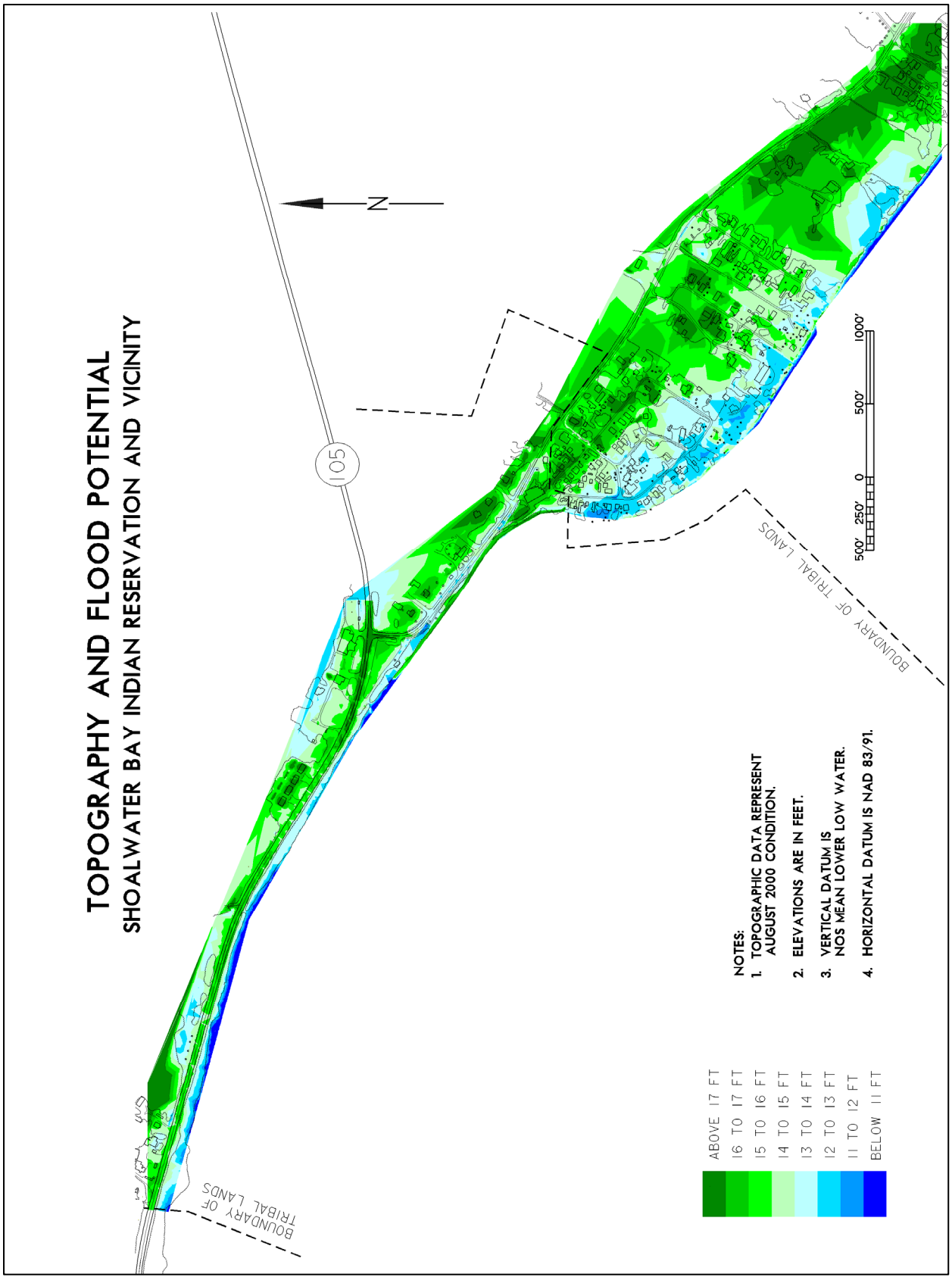

Figure 1.5 Topography and flood potential, Shoalwater Bay Indian Reservation and vicinity.

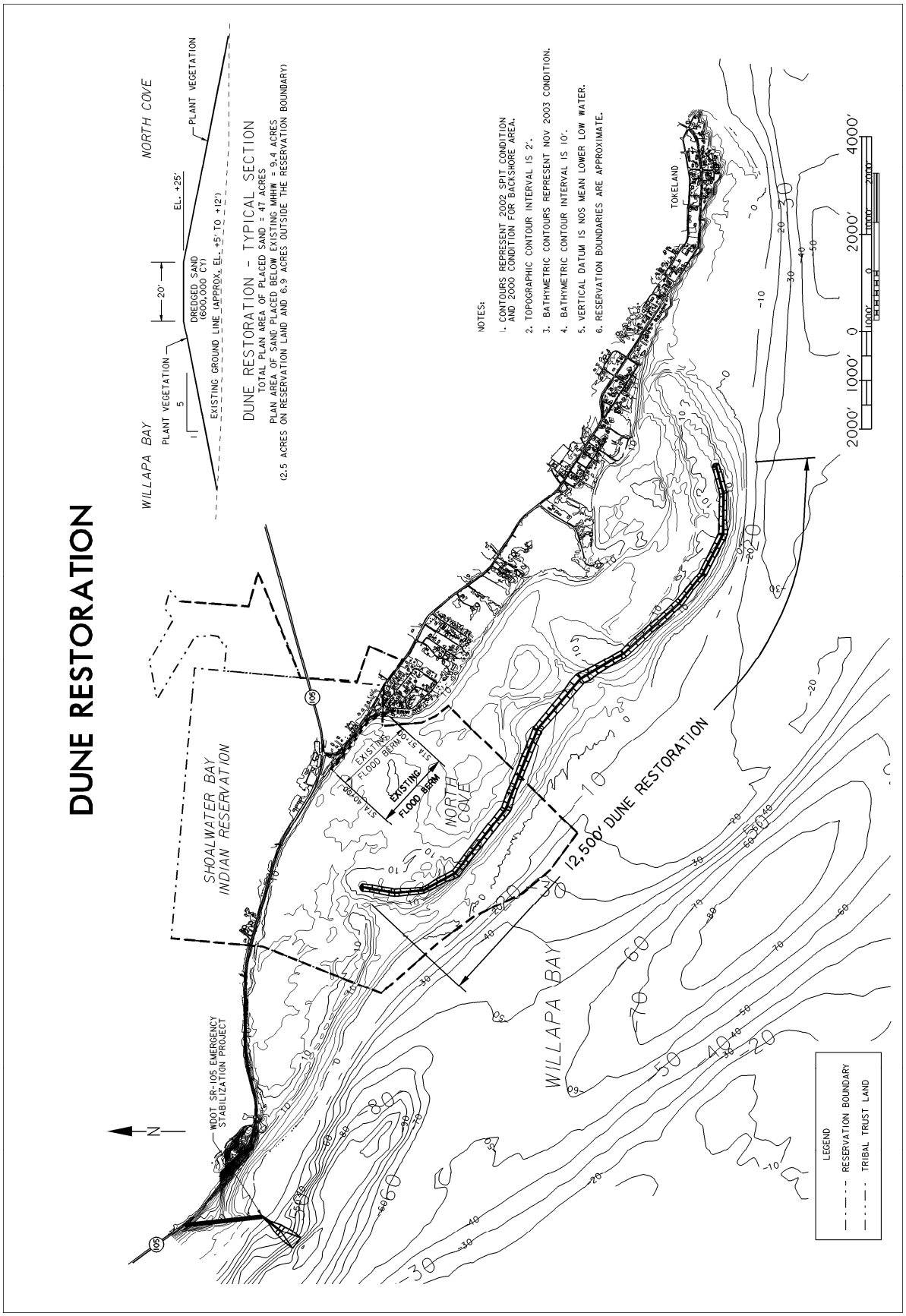

Figure 1.6 Barrier dune restoration, plan and section.

2.0 Underlying Geologic Conditions and Processes

2.1 Geologic Framework[2]

2.1.1 Coastal Features

The northern portion of Willapa Bay near its entrance is characterized by a broad shallow shoal, a deep main channel, and three prominent sand ridges that protrude obliquely into the bay (Figure 2.1.1) (Morton et al., 2002). Marshes and tidal flats form fringing wetlands that occupy the low elevations between the sand ridges. The oldest exposed sand ridge, Kindred Island, is low (< 4 m above MLLW), uninhabited, and serves as an anchor point for dikes that transform the adjacent marshes into grazing pasture. A dense forest originally covered the island that was cleared for the cattle ranching operation. Tokeland Peninsula, the relatively large middle ridge, is also about 4 m above MLLW. It is densely forested, and supports a small community of residences and businesses, as well as a portion of the Shoalwater Bay Indian reservation. Both Tokeland Peninsula and Kindred Island are stable landforms that are experiencing wave-generated erosion of their southeastern margins.

Empire Spit fronts Tokeland Peninsula and helps protect it from direct exposure to waves from the Pacific Ocean. In general, Empire Spit is a low (< 4 m above MLLW), relatively young, segmented and unstable beach-washover deposit that is covered with grasses and low shrubs. Its recent formation is thought to be related to the rapid northward migration of the entrance channel and attendant 3.8 km historical beach retreat at Cape Shoalwater (Terich and Levensellar, 1986; Dingler and Clifton, 1994; Kaminsky et al., 1999). Two relatively shallow tidal inlets divide Empire Spit into three segments (Figure 2.1.1). The northwestern segment, which is attached to the Pleistocene upland, is a transgressive beach that is migrating landward as the beach retreats. Overwash sand is deposited into the adjacent North Cove marsh. At low tide, muddy marsh sediments are exposed along most of the beach of the northwestern spit segment (Figure 2.1.2).

The central segment of Empire Spit is also a transgressive feature that is migrating landward as a result of beach erosion and storm washover. The convex-seaward shape of the central spit segment is a result of rapid retreat along the margins of the two tidal inlets that form the lateral boundaries of the island. The southeastern spit segment is also arc shaped, but it has a different depositional history than the other segments of Empire Spit. The southeastern spit segment is

2 Written by Guy R. Gelfenbaum, Ph.D., Peter Ruggiero, Ph.D., Laura A. Landerman, Ph.D., and Giles Lesser, U.S. Geological Survey, Coastal and Marine Geology Program, Menlo Park, CA; and George Kaminsky and Diana McCandless, Washington Department of Ecology, Coastal Monitoring and Analysis Program, Lacey, WA.

retreating along its western section while simultaneously extending eastward and northward as a result of wave refraction and sand supplied by updrift erosion, (Gelfenbam, et al, in publication).

2.1.2 Historical Trends

The historical trends of primary concern in this project are related to the evolution of the spits and associated islands fronting the Tokeland Peninsula. These spits formed the genesis of North Cove and have historically defined the environmental setting in which the Shoalwater Bay Reservation was established. As Cape Shoalwater rapidly eroded during the early part of the 20th century, the main spit, which became known as Graveyard Spit, retreated landward to the north-northeast (Figure 2.1.3). By 1955, the shoreline retreated to the point where it approximately merged with the most interior spit that defined North Cove (Figure 2.1.4). In fact, this interior spit was the site of the town of North Cove and home of the Shoalwater Bay Lifesaving Station, which was established in 1878 and operated until it was lost to erosion in 1956. By 1974 (Figures 2.1.5 and 2.1.6), the shoreline had nearly just begun to reach the landward side of this old interior spit, and by 1985 (Figure 2.1.7), the shoreline had retreated to the point that Graveyard Spit was located mostly landward of the old spit, occupying what was North Cove tidal marsh.

The reason for this long-term shoreline retreat is clearly related to the northerly migration of the entrance channel. By 1985, the channel encountered the erosion-resistant Pleistocene sediments at the base of the terrace bordering the present day State Route (SR) 105, and its northerly migration at this location essentially halted. In fact, since that time, the channel thalweg has migrated slightly to the south.

Presently, Graveyard Spit (located immediately west of Empire Spit – see Figure 2.1.1) exists as a thin and fragmented landform that is anchored and aligned by consolidated and erosion-resistant Pleistocene substrate in the vicinity of the SR 105 emergency stabilization project groin. Extending to the east of Graveyard Spit is a series of segmented sand islands sometimes referred to as Empire Spit. In contrast to historical conditions, this fragile line of barrier beaches no longer appears to receive sand supply from the eroding beach plain to the northwest. The lack of sand supply indicates that this landform will remain of low relief, compromising its historical function as a flood barrier for the Tokeland Peninsula.

Shoreline retreat along this northwest corner of North Cove has slowed substantially relative to historical rates of change, but the present condition and orientation of the spit suggest that it will continue to pivot towards the north-northeast from its hinge point at the base of the Pleistocene terrace. Thus, the present condition of the spit is locally controlled by the geological framework of the region. However, the alignment, depth and extent of the consolidated-erosion resistant substrate are not completely known. Such material may be a contributing factor to the relative stability of the associated island shoreline to the southeast of cross-section line 7 (see Figure 2.2.1). Alternatively, the confluence of westward and northward ebb flows may maintain a local dynamic morphological equilibrium. Regardless of the mechanism(s) responsible for this relatively stable point, the alignment and recent erosion trends along cross-section lines 5, 6, and 7 suggest that the shoreline may pivot landward about this southeasterly point.

The present situation suggests that although the potential for spit breaching is enhanced by periods of elevated water levels, Graveyard Spit and the sand islands located to the east will likely continue their landward retreat, under normal climatic conditions, particularly as the crest elevation and width of the spit and associated island continues to diminish. The geometry and position of the main channel does not appear to have a significant or direct influence on the present shoreline behavior.

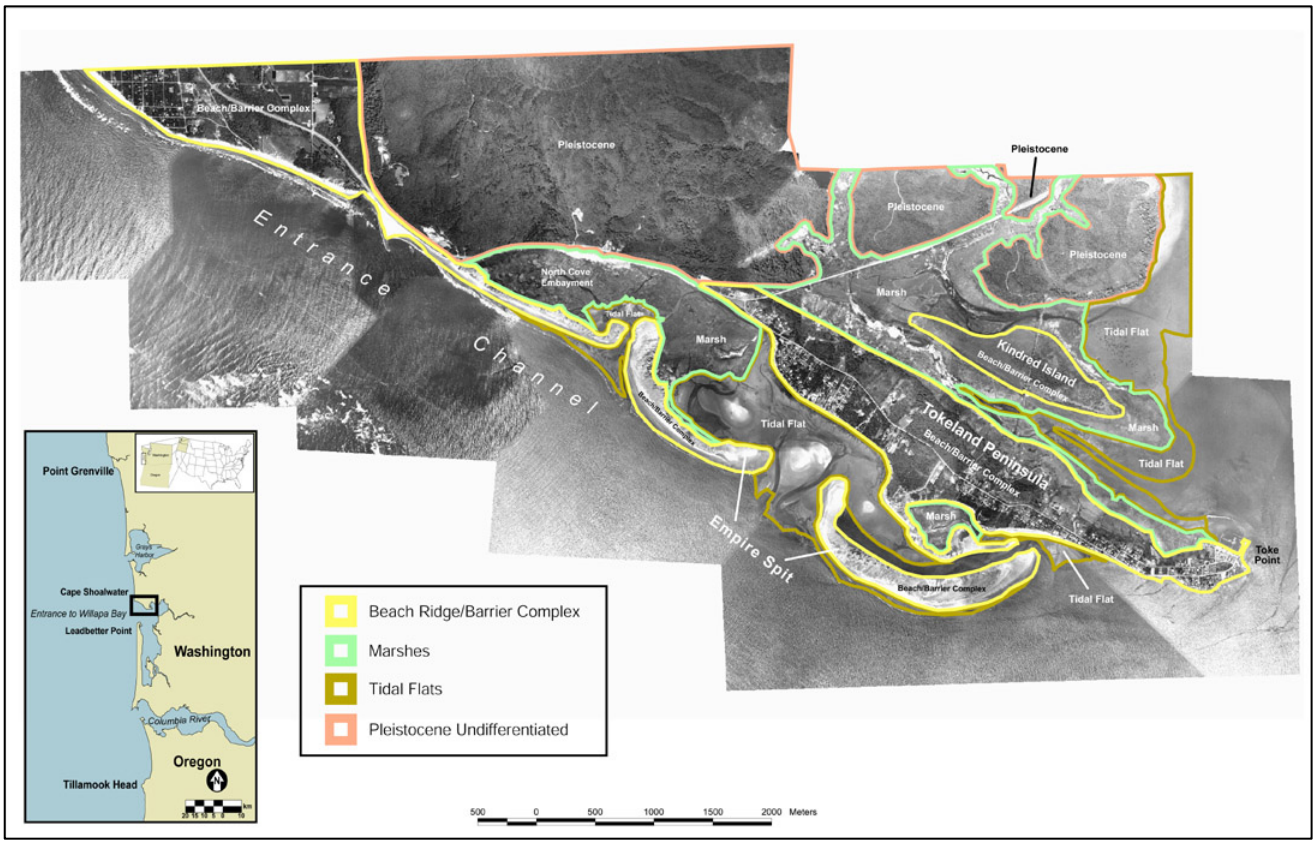

Figure 2.1.1 Distribution of Holocene and modern depositional environments of north Willapa Bay interpreted from field observations, topographic maps, and the 1999 aerial photograph.

Figure 2.1.2 Graveyard spit – exposed marsh sediments.

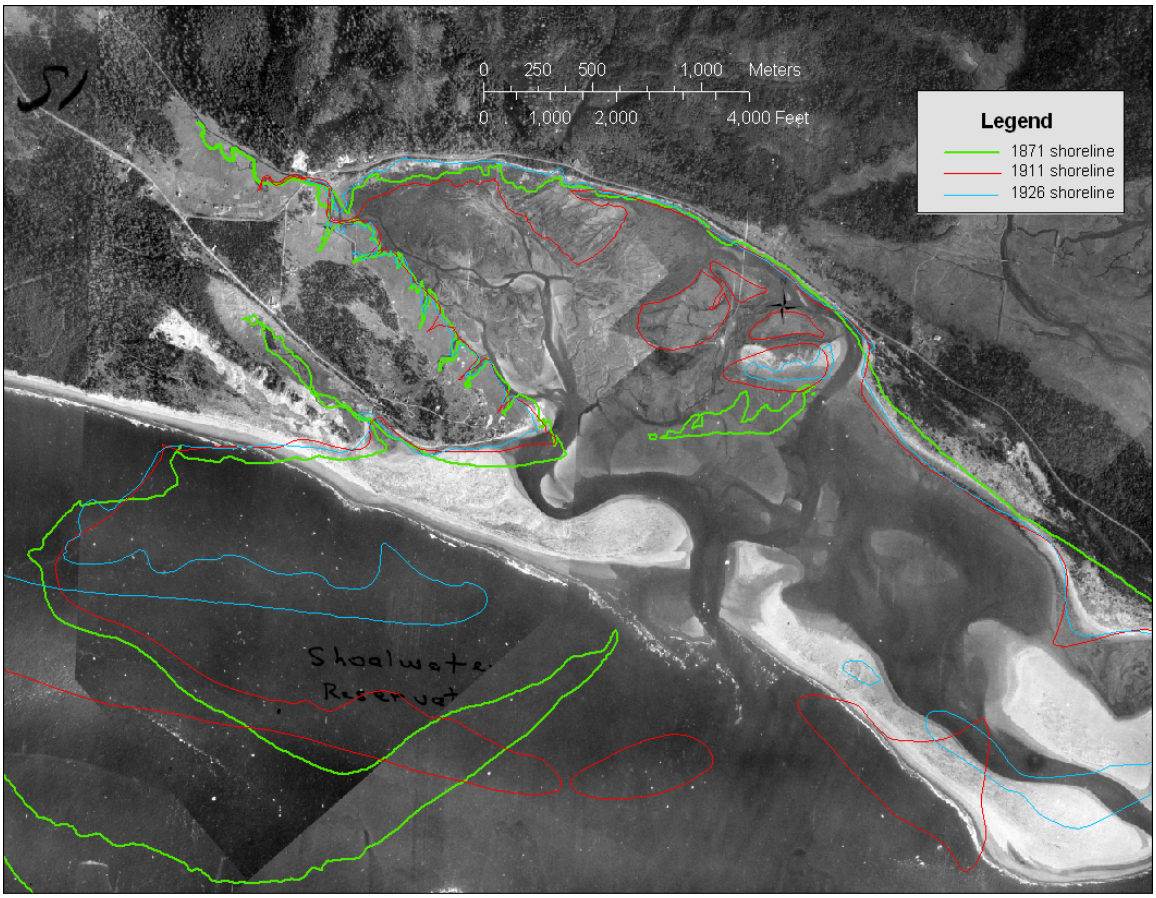

Figure 2.1.3 Map of North Cove showing historical shoreline positions of 1871, 1911 and 1926 on the 1945 aerial photo mosaic.

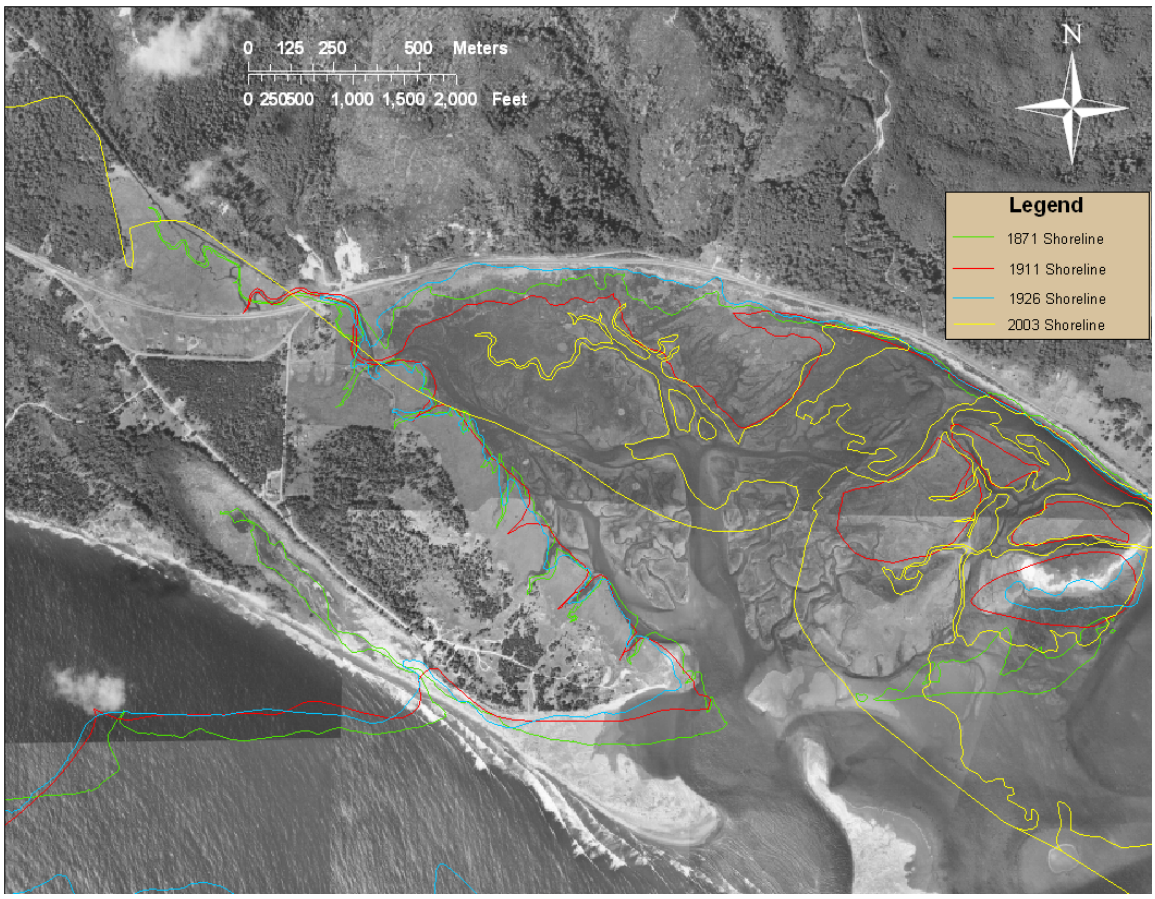

Figure 2.1.4 Map of North Cove showing historical shoreline positions of 1871, 1911, 1926, and 2003 on the 1955 aerial photo mosaic.

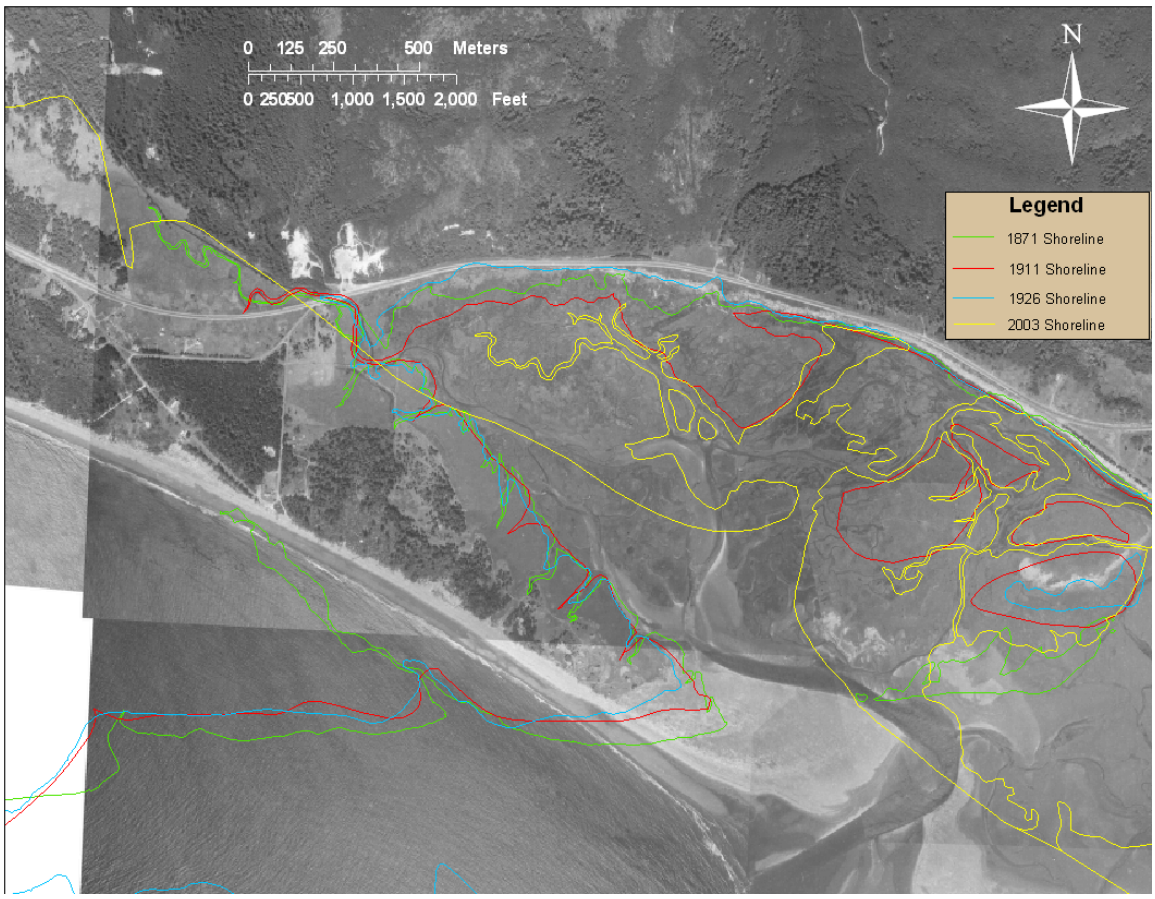

Figure 2.1.5 Map of North Cove showing historical shoreline positions of 1871, 1911, 1926, and 2003 on the 1963 aerial photo mosaic. Note the retreat of the shoreline through the old spit where the Town of North Cove was located.

Figure 2.1.6 Map of North Cove showing historical shoreline positions of 1871, 1911, 1926, and 2003 on the 1974 aerial photo mosaic. Note the retreat of the shoreline, approaching the northeastern side of the old spit that defined North Cove. Also note the elongation of Graveyard Spit as compared to Figure 2.1.5 (1963 photo).

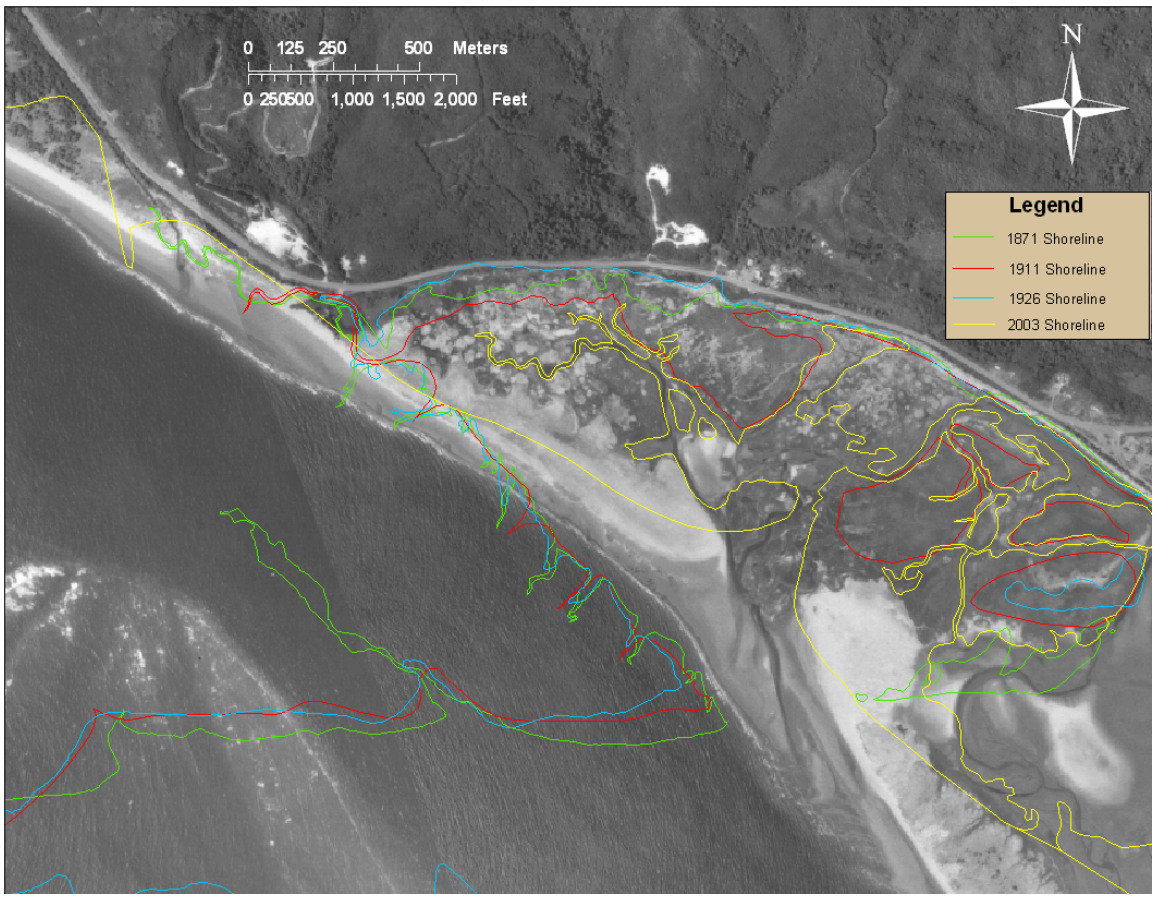

Figure 2.1.7 Map of North Cove showing historical shoreline positions of 1871, 1911, 1926, and 2003 on the 1985 aerial photo mosaic. Note the position of the 1985 shoreline is mostly landward of the old spit, occupying what was North Cove. Also not the breach through Graveyard Spit located landward of the old spit.

References

Dingler, J. R. and Clifton, H.E., 1994. Barrier systems of California, Oregon, and Washington, in Davis, R. A., ed., Geology of Holocene Barrier Islands: Springer-Verlag, Berlin, p. 115-165.

Gelfenbaum, G. R., Kaminsky, G. M., Lauderman, L. A., Lesser, G., McCandless, D. In publication. "Shoalwater Bay Tribe Erosion Study Report", Scientific Investigation Report XX, December 6, 2004 DRAFT, U.S. Geological Survey, Menlo Park, CA, 362 pages. Prepared in cooperation with Washington State Department of Ecology.

Jarrett, J. T. 1976. "Tidal prism-inlet area relationships," GITI Report 3, U.S. Army Engineer Waterways Experiment Station, Vicksburg, MS.

Kaminsky, G. M., Daniels, R. C., Huxford, R., McCandless, D., and Ruggerio, P., 1999, Mapping erosion hazard areas in Pacific County, Washington: Journal of Coastal Research Special Issue28, p. 158-170.

Morton, R.A., Purcell, N. A., and Peterson, R. L. 2002. "Large-scale Cycles of Holocene Deposition and Erosion at the entrance to Willapa Bay, Washington – Implications for Future Land Loss and Coastal Change, Open File Report 2002-46," U.S. geological Survey, St. Petersburg, FL, 124 p.

Richey, E. P., Dean, R. G., Ekse, M. I., and Kent, J. C. 1966. "Considerations for the temporary arresting of the erosion at Cape Shoalwater, Washington," State of Washington, Department of Conservation, Olympia, WA.

Terich, T., and Levenseller, T. 1986. The Severe Erosion of Cape Shoalwater, Washington. *Journal of Coastal Research,* Vol. 2, No. 4, pp. 465-477.

2.2 Geomorphic Cycles

The evolution of the spits and islands at the Shoalwater Bay Indian Reservation (Shoalwater Reservation) during the last 150 years has been intimately related to changes and migration of the main (northernmost) Willapa channel. Sections 2.2.1 and 2.2.2 will examine the bathymetry of the channel and will describe changes of the surficial features based on maps, aerial photographs, and bathymetric surveys. Section 2.2.3 will examine the link between climatology and morphological changes.

2.2.1 Historical Data Sources and Analysis[3]

Cross-section Lines

To compute the movement of the channel and the morphologic features at the study area, we established a base line and cross-section lines spaced at 610 m (2,000 ft) intervals (Figure 2.2.1). The cross-section lines were approximately parallel to and overlapping the Seattle District, U.S. Army Corps of Engineers (NWS) bathymetric survey lines for 2000-2003. Table 2.2.1 lists State Plane coordinates of the endpoints of the cross-section lines.

Table 2.2.1
Baseline and cross-section line coordinates

Line	Endpoint	Easting	Northing
Baseline	1	771,094	519,349
	2	748,458	533,339
D-west	1	743,720	524,511
	2	748,978	533,018
D-east	1	745,422	523,460
	2	750,679	531,966
1	1	747,123	522,408
	2	752,380	530,915
2	1	748,824	521,357
	2	754,081	529,863
3	1	750,525	520,305
	2	755,783	528,812
4	1	752,227	519,254
	2	757,484	527,760
5	1	753,928	518,202
	2	759,185	526,709
6	1	755,629	517,151
	2	760,887	525,657
7	1	757,331	516,099
	2	762,588	524,606
8	1	759,032	515,048

[3] Written by Andrew Morang, Ph.D., U.S. Army Engineer Research and Development Center, Coastal and Hydraulics Laboratory, Vicksburg, MS.

	2	764,289	523,554
9	1	760,733	513,997
	2	765,991	522,503
10	1	762,435	512,945
	2	767,692	521,452
11	1	764,136	511,894
	2	769,393	520,400
12	1	765,837	510,842
	2	771,094	519,349

Notes:
1. State plane coordinates, Washington South Zone, NAD83, feet.
2. Endpoint 2 of each cross-section line is at the junction with the base line.

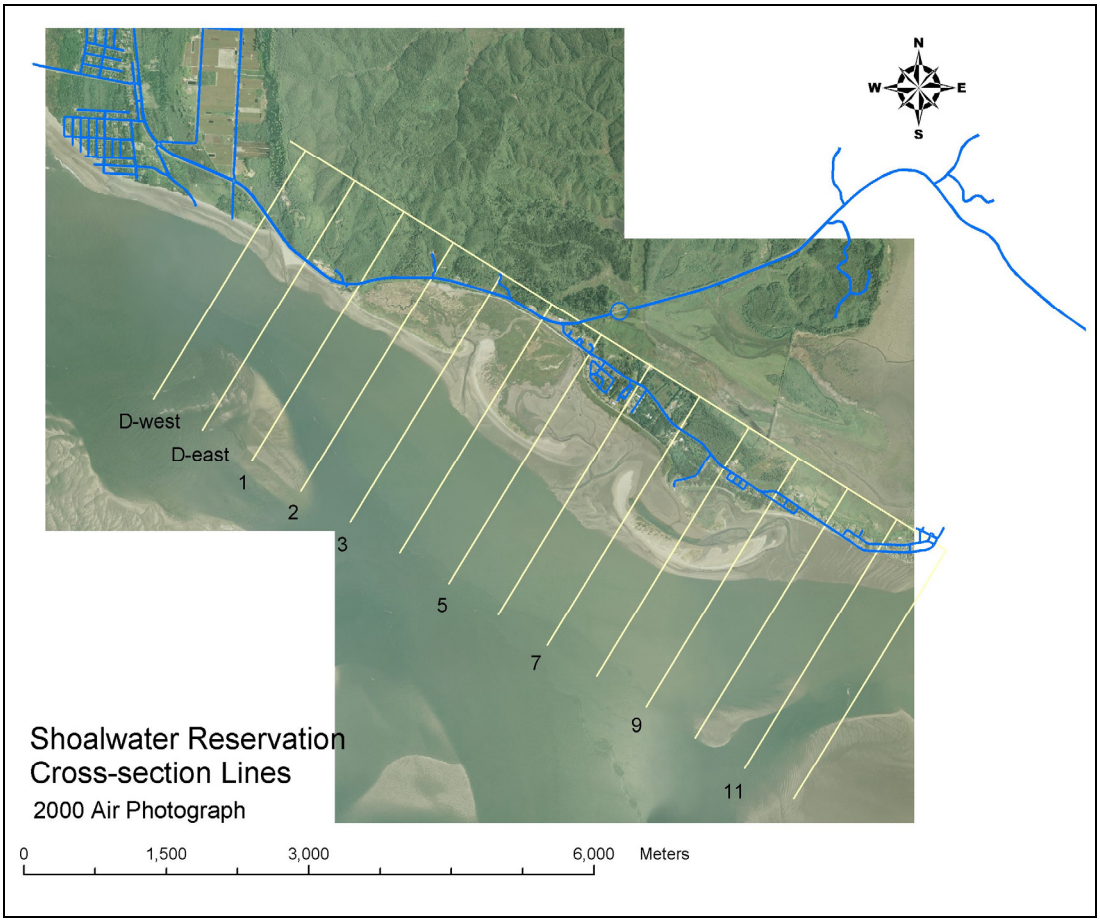

Figure 2.2. 1 . Cross-section lines used for analysis of channel bathymetry and movement of spits and islands. D-east and D-west are on either side of the SR-105 highway groin. Cross-line 1 is at the west end of the marshy bay that is protected by the spit and islands. The cross lines are 610 m (2,000 ft) apart.

Bathymetric Data

The Seattle District (NWS) has conducted hundreds of hydrographic surveys of portions of Willapa Bay in the last 150 years. Between 1852 and 1922, Seattle District surveyors prepared charts of the entrance area on irregular intervals. This was an era of growth of the timber and oyster industries, during which wood products were shipped to ports in the United States and the Orient and oysters were shipped to California. Almost annually between 1927 and 1978, District surveyors prepared charts of the entire entrance based on soundings taken in July or August. Following World War II, ship traffic through the mouth of Willapa Bay declined, and Federal maintenance dredging of the navigation channel across the ebb shoal ceased in 1974. From 1981 to 1983, surveys were only made in the area immediately adjacent to the navigation channel. The next comprehensive survey was 1993, followed by a three-year gap. After 1996, annual surveys have been run in the northern part of the bay.

During 1998-2000, ERDC conducted an analysis of dredging alternatives at the mouth of Willapa Bay. To document cycles of channel migration, Hands (2000) collected and digitized 60 historical charts that he obtained from the archives at Seattle District. These are reproduced in Appendix A of ERDC Technical Report TR-00-6 and will not be included in this Engineering Appendix. Most of these charts provided partial data coverage of the channel adjacent to the Shoalwater Reservation, and are therefore of value in examining the link between climate cycles and historical shoreline changes (Section 2.2.3 below).

To examine recent shoreline changes at the Shoalwater Reservation and to identify effects of the construction of the SR-105 Emergency Stabilization Project rock dike on the Willapa channel and the nearby shore, we have concentrated on the recent bathymetry surveys that were available in digital form (Table 2.2.2). NWS and the U.S. Geological Survey (see Ruggiero and Voigt 2000 for survey methods) supplied these files to ERDC.

Table 2.2.2
Digital bathymetric surveys

Date	Source	Notes
Aug 1993	USACE, Seattle	File wb93an.dat
Feb-Mar 1996	USACE, Seattle	File wb96an.dat
Jan 1997	USACE, Seattle	File wb97an.dat
Jul 1998	USACE, Seattle	More comprehensive than previous years, to support ERDC alternatives study. File wb98an.dat.
Aug 1998	JALBTCX	SHOALS hydrographic LIDAR (not used, coverage only over ebb shoal at mouth of bay)
Oct 1999	USACE, Seattle	Annual, file wb99an.dat
Mar-May 2000	USACE, Seattle	Annual, file wb00an1.dat
Aug 2000	USGS	Overlap with 2000 USACE survey data
Sep-Nov 2000	USACE, Seattle	Annual no. 2, file wb00an2.dat
Mar 2001	USACE, Seattle	Annual, file wb01an.dat
May 2001	USGS	Overlap with 2001 USACE survey data
Jul 2001	USACE, Seattle	Disposal site monitoring, file 01wi035a,b,
Mar, July 2002	USACE, Seattle	Annual, file wb02an.dat
Oct 2003	USACE, Seattle	Annual, file wb03an_new.dat

Notes:
LIDAR = Light Detection and Ranging
JALBTCX = Joint Airborne LIDAR Bathymetry Technical Center of Expertise, Mobile, AL
SHOALS = Scanning Hydrographic Operational Airborne LIDAR Survey

Processing Bathymetry Data

Historical bathymetry data were imported into ESRI® ArcView™ v. 3.2 software. Data were contoured and grids created with the Spatial Analyst software module. Some of the data already existed in project files from the previous Willapa Bay project (Kraus 2000). Once the bathymetry was gridded, the thalwegs were visually traced (Figure 2.2.2).

The plot of all the thalwegs reveals some important details (Figure 2.2.3). In the east, the Willapa River has barely deviated from its channel over a century. South of the reservation bay, the Willapa River and the main bay channels join at a junction near cross-section line 7. The location of this junction has been surprisingly constant over time. Then, further to the west, the thalwegs show a steady progression to the north, a rotation with the pivot point at the junction. Over a period of 75 years, the thalweg has changed from an east-west orientation to a southeast-northwest orientation.

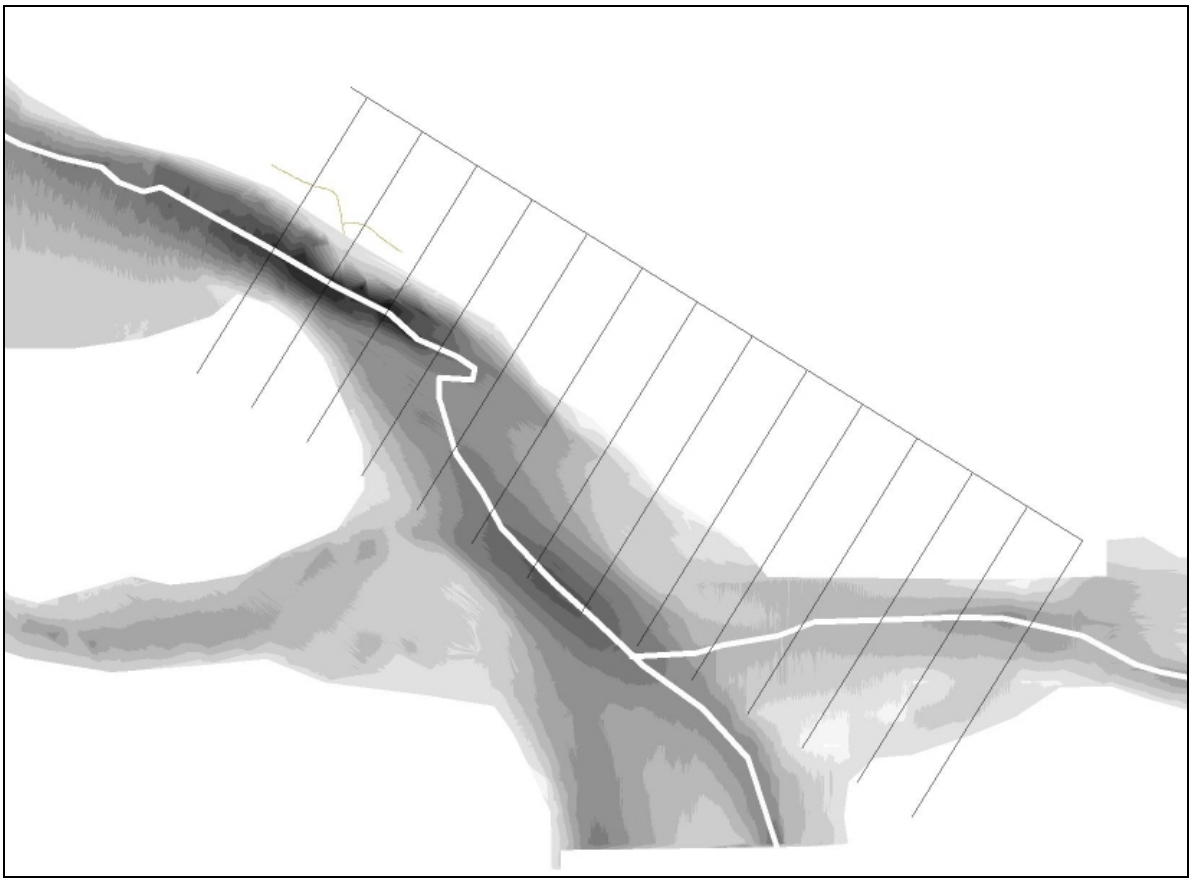

Figure 2.2. 2. November 2000 bathymetry, gridded and shaded with each gray tone representing 5-foot depth intervals. The thalweg was traced visually to follow the deepest portion of the channel.

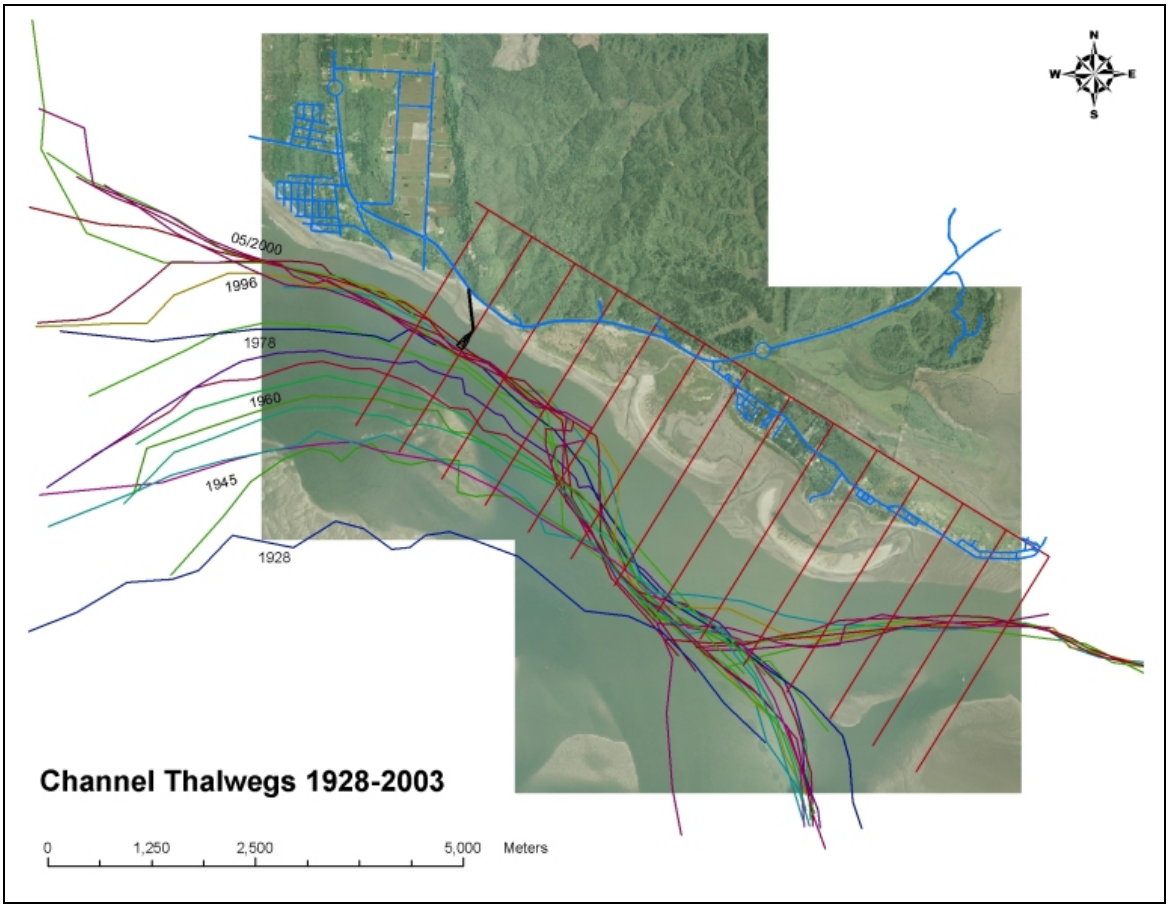

Figure 2.2. 3. Thalwegs from 1928 to 2003, based on bathymetry data provided by NWS. Cross-section lines are 610 m (2,000 ft) apart. Background photo: October 2000.

Analysis Using ArcMap™ Software

All rectified aerial photographs, shorelines, bathymetry, cross-section lines, and other features were organized and displayed in ESRI® ArcMap™ GIS software. This software conveniently displays the features at any selected scale and allows the user to turn on and off various features, make measurements, and prepare graphics. Figures in this chapter were prepared with the ArcMap software.

Aerial Photograph Sources

Aerial photographs have proven to be an invaluable source of information on changes that have occurred to Graveyard Spit, the islands, the bay, and the nearby shorelines over the last 60 years. Table 2.2.3 lists the dates and sources of photographs used in the analysis of the spits and other features. The 1942, 1945, and 1955 photographs came from the archives of the U.S. Army Corps of Engineers' Beach Erosion Board (BEB) (Morang 2003). NWS and the Washington State Department of Ecology (WA DOE) provided more recent dates.

Table 2.2.3
Aerial photographs used for spit and island analysis

Date	Type	Original Print Scale	Source	ERDC version	Scan resolution (if scanned at ERDC)	Ortho-rectification
1-Jul-42	B&W aircraft		BEB archives	Paper 9x9"	1200	WA DOE mosaic
19-Sep-45	B&W aircraft	1:16,000 ?	BEB archives	Paper 9x9", digital	800	WA DOE mosaic
4-Aug-55	B&W aircraft	1" = 800'	WA DOT	Paper 9x9"	600	WA DOE mosaic
1-Jan-63	B&W aircraft	1:12,000	WA DOE	Paper 9x9"		WA DOE mosaic
24-May-70	B&W aircraft	1:12,000	WA DOE			WA DOE mosaic
19-Jul-78	B&W aircraft	1" = 2000'	USACE NWS	Paper 9x9", digital		ERDC
16-Jul-79	B&W aircraft	1" = 2000'	USACE NWS	Digital		ERDC
22-Oct-80	B&W aircraft	1" = 2000'	USACE NWS	Digital		ERDC
15-Jul-81	Color IR aircraft	1" = 2000'	USACE NWS	Digital, paper	600 (118-2 only)	ERDC
12-Jul-82	Color IR aircraft	1" = 2000'	USACE NWS	Paper 9x9", digital TIFF	600 (118-3 only)	ERDC
21-Jun-83	Color IR aircraft	1" = 2000'	USACE NWS	Digital		ERDC
28-May-84	Color IR aircraft	1" = 2000'	USACE NWS	Digital		ERDC
26-Jun-85	B&W aircraft	1" = 3500'	USACE NWS	Paper 9x9"	2400	WA DOE mosaic
30-May-86	Color IR aircraft	1" = 2000'	USACE NWS	Digital		ERDC
3-Jun-87	Color IR aircraft		USACE NWS	Digital		ERDC
20-Jun-88	Color IR aircraft		USACE NWS	Digital		ERDC
24-Jun-89	Color IR aircraft		USACE NWS	Digital		ERDC
20-Sep-90	Color IR aircraft	1" = 2000'	USACE NWS	Paper 9x9", digital TIFF	600	WA DOE mosaic
23-Jul-91	Color IR aircraft		USACE NWS	Digital		ERDC
15-Jul-92	Color IR aircraft	1" = 2000'	USACE NWS	Digital		ERDC
26-Jul-92	Color IR aircraft	1" = 2000'	USACE NWS	Paper 9x9"		ERDC
12-Sep-93	Color IR aircraft	1" = 2000'	USACE NWS	Paper 9x9"		ERDC
17-Dec-93	Color aircraft	1:6,000	USACE NWS	Paper 9x9"		ERDC
19-Feb-94	Color IR aircraft	1" = 2000'	USACE NWS	Digital		ERDC
28-Jun-95	Color IR aircraft	1" = 2000'	USACE NWS	Digital		ERDC
7-Aug-96	Color aircraft	1" = 1000'	USACE NWS	Paper 9x9", digital TIFF	600	WA DOE mosaic
2-Apr-97	Color aircraft	1" = 1000'	USACE NWS	Paper 9x9", digital TIFF	600	WA DOE mosaic
15-Sep-98	Color aircraft	1" = 3333'	USACE NWS	Paper 9x9", digital TIFF	600	ERDC
26-May-99	Color aircraft		WA DOE			WA DOE mosaic

27-Oct-00	Earthdata false-color satellite digital orthophotos	5000 x 5000 pixels (10,000 x 10,000 ft)	ERDC purchase	Digital	Digital	Earthdata, rectified lat-long.
12-Jul-02	Color aircraft	1:3600	USACE NWS	Paper 9x9", digital	300	WA DOE mosaic
14-Aug-03	Color aircraft	1:40,000	USACE NWS	Digital		WA DOE mosaic

Notes:
DOT = Washington State Dep. of Transportation.
DOE = Washington State Dep. of Ecology.
NWS = U.S. Army Engineer District, Seattle.
BEB = USACE Beach Erosion Board

Aerial Photograph Preparation

Aerial photographs, without special processing, are simply photographic images of the ground. Even when taken from an aircraft with a commercial aerial mapping camera, air photographs contain numerous distortions caused by the optics of the camera and the geometry of the aircraft (tilt and pitch). Therefore, although photographs can be invaluable to document qualitative changes over time, they are generally unsuitable for measurements of features or for mapping purposes. One of the most valuable uses of historical vertical air photographs is for shoreline change measurements. But, before measurements can be made, images have to be photogrammetrically rectified to remove distortions and create map projections with real earth coordinates (e.g., latitude-longitude, state plane, etc.). Once the photos have been transformed, they can be superimposed in mapping or geographic information system (GIS) software, and features can be outlined and measured (i.e., distances from feature to feature or surface areas).

To convert the photographs into photomosaics (Table 2.2.3), the paper prints had to be scanned and processed in a multi step procedure. The process evolved into a fruitful cooperative effort between ERDC and the WA DOE:

1. Identify suitable single or sets of photographs that cover the study area (ERDC and WA DOE).
2. Based on the scale of the original print (a function of altitude and lens focal length), scan the print at appropriate resolution to generate digital files with a ground pixel size of approx. ½ m. Scan resolution ranged from 300x300 dots per inch (dpi) to 2400x2400 dpi, with files saved as uncompressed TIFF format (ERDC).
3. Transfer scanned images to WA DOE.
4. Prepare triangulation and orthorectify individual frames, then mosaic individual frames together (DOE). Convert to MrSID compressed format.
5. Transfer mosaic digital files to ERDC.
6. Import mosaics into ArcGIS software, allowing features to be displayed in correct map projection (ERDC).

Some flight dates were only available as digital JPEG image files provided by Seattle District (i.e., ERDC did not have 9 x 9 inch paper prints). These frames were lower resolution, with a ground pixel size greater than five meters. These frames were rectified at ERDC, based on identifying features on the photograph and matching them with known ground locations. The procedure was less rigorous than the one used by WA DOE but was suitable considering the pixel size. By combining the WA DOE aerial mosaics and the photo flights processed at ERDC, aerial coverage spans 1942 to 2003.

Inventory of Aerial Photographs

Figures 2.2.4 through 2.2.25 are a sequence of Willapa Bay aerial photographs listed in Table 2.2.3, covering 1942 to 2003. All have been plotted with north to the top and at the same scale. The modern road network is shown for reference. In addition, the SR-105 rock groin's position is shown on all photographs, although it was constructed in 1998. The channel thalweg has been plotted when the year of the photo flight and the bathymetry survey coincided, or were less than, 12 months apart.

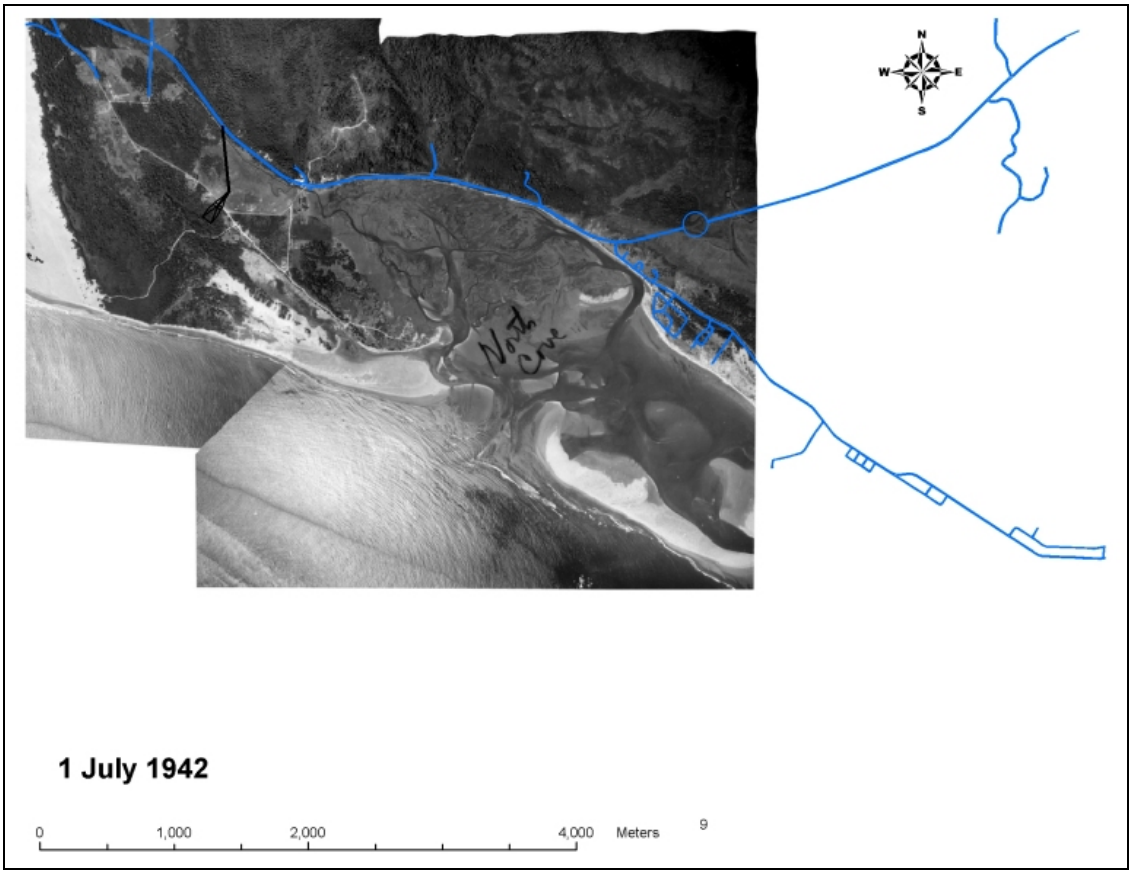

Figure 2.2. 4. 1942 aerial photograph. Original prints from the archives of USACE Beach Erosion Board.

Figure 2.2. 5. 1945 aerial photograph. Original prints from the Beach Erosion Board archives.

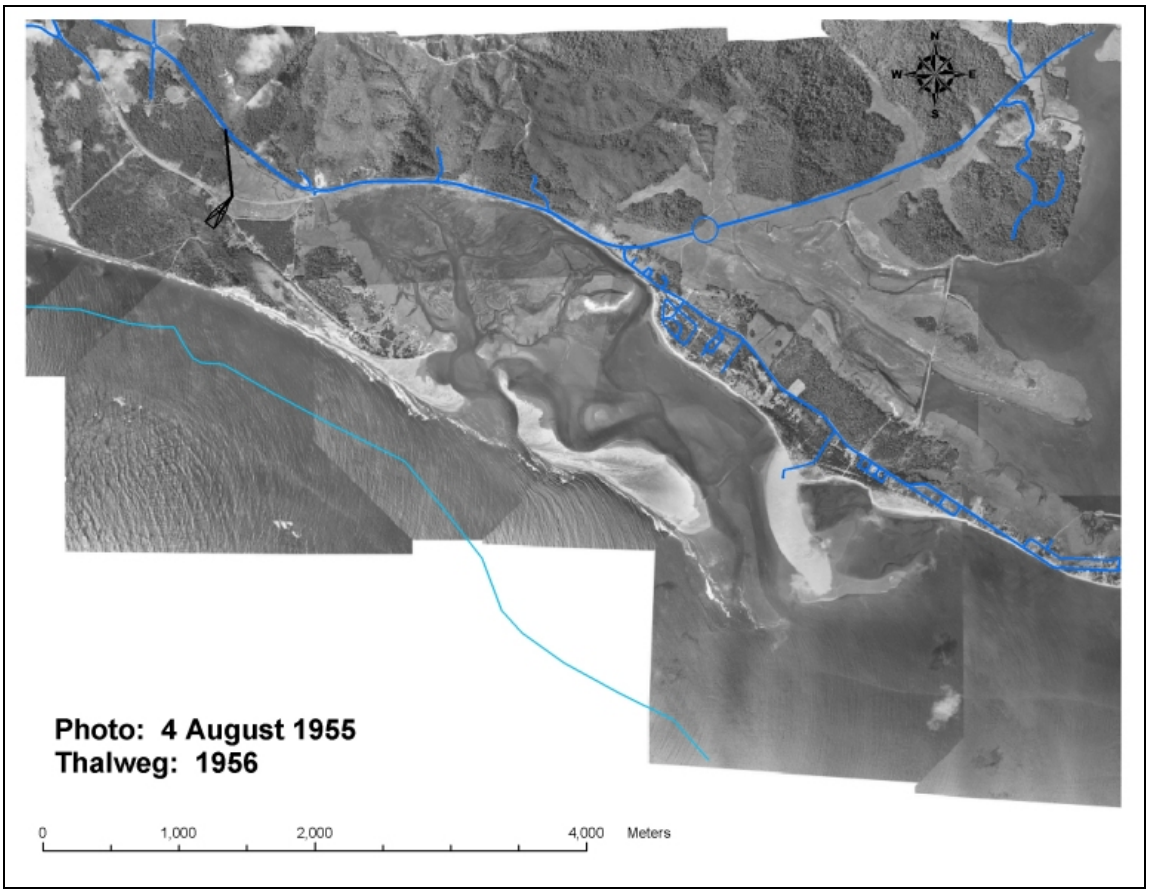

Figure 2.2. 6. 1955 aerial photograph. Original prints from Washington Department of Transportation.

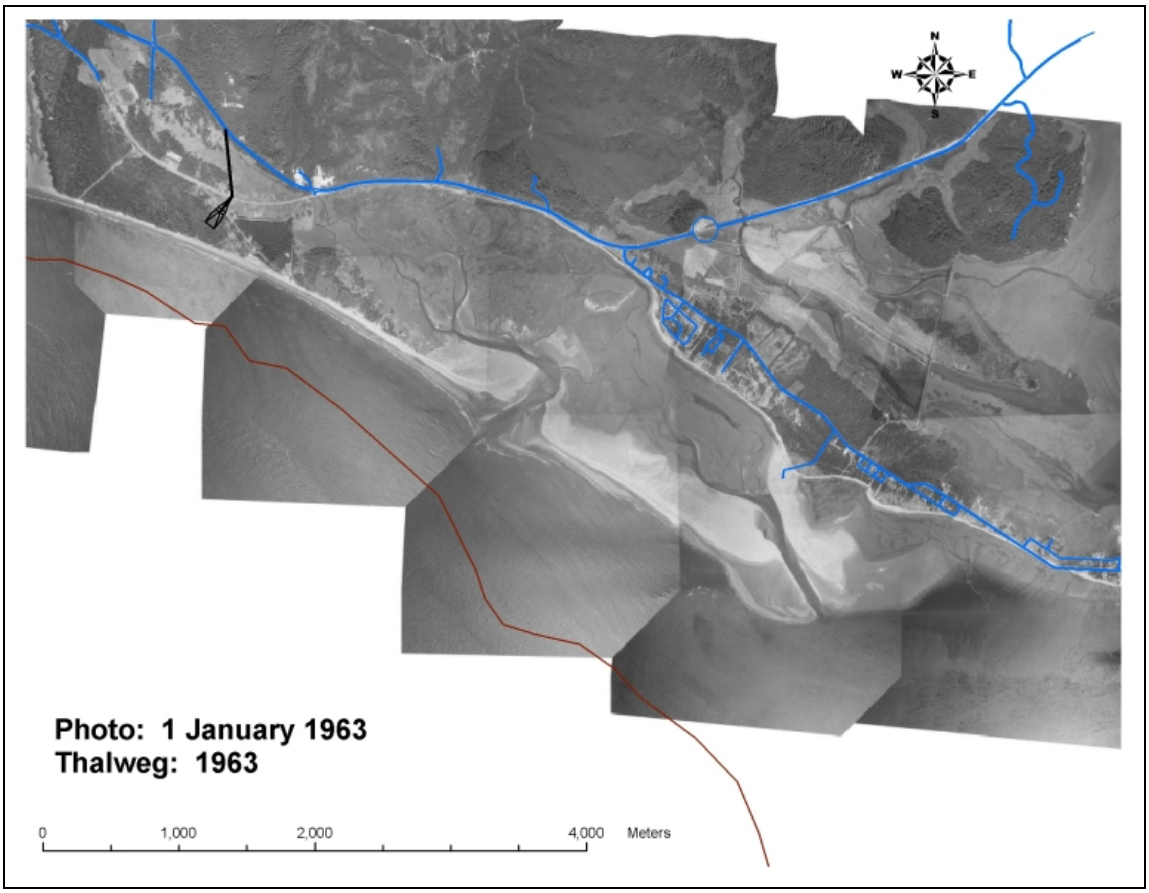

Figure 2.2. 7. 1963 aerial photograph. Original prints from Washington Department of Ecology.

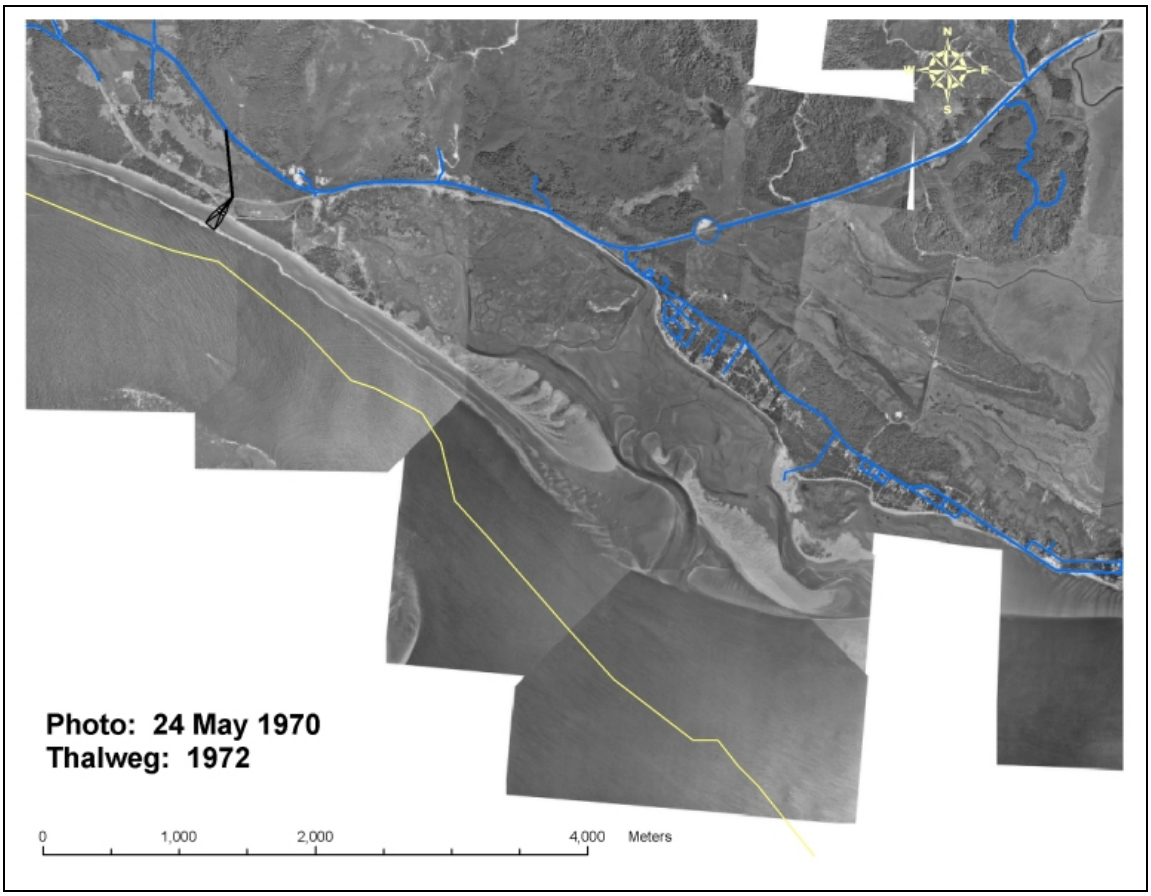

Figure 2.2. 8. 1970 aerial photograph. Original prints from WA DOE. Note that Empire spit is a continuous feature as far as the tidal opening just south of the community.

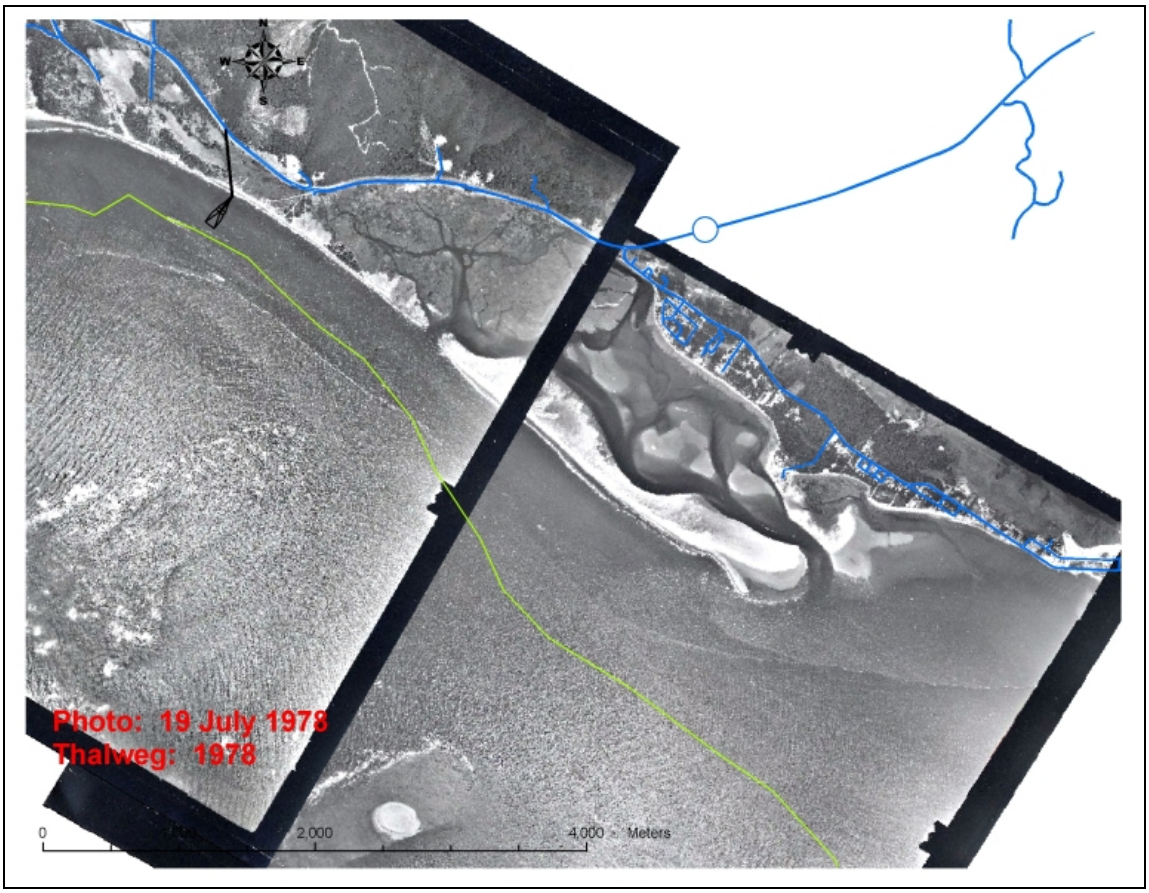

Figure 2.2. 9. 1978 aerial photograph. Original prints NWS. Between this date and the previous photo, a new tidal opening formed in Empire Spit closer to the west end of the bay, approximately in the same location as the 1956 opening.

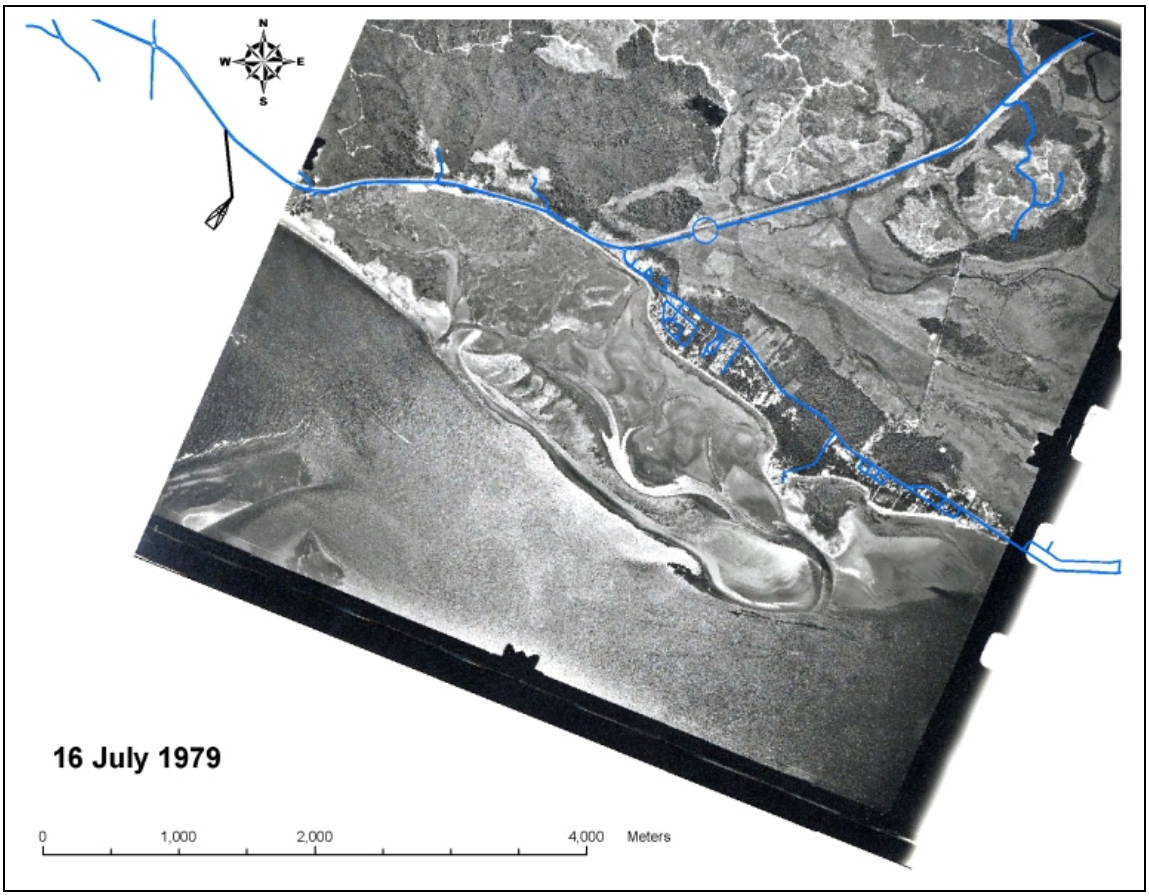

Figure 2.2. 10. 1979 aerial photograph. Original prints NWS.

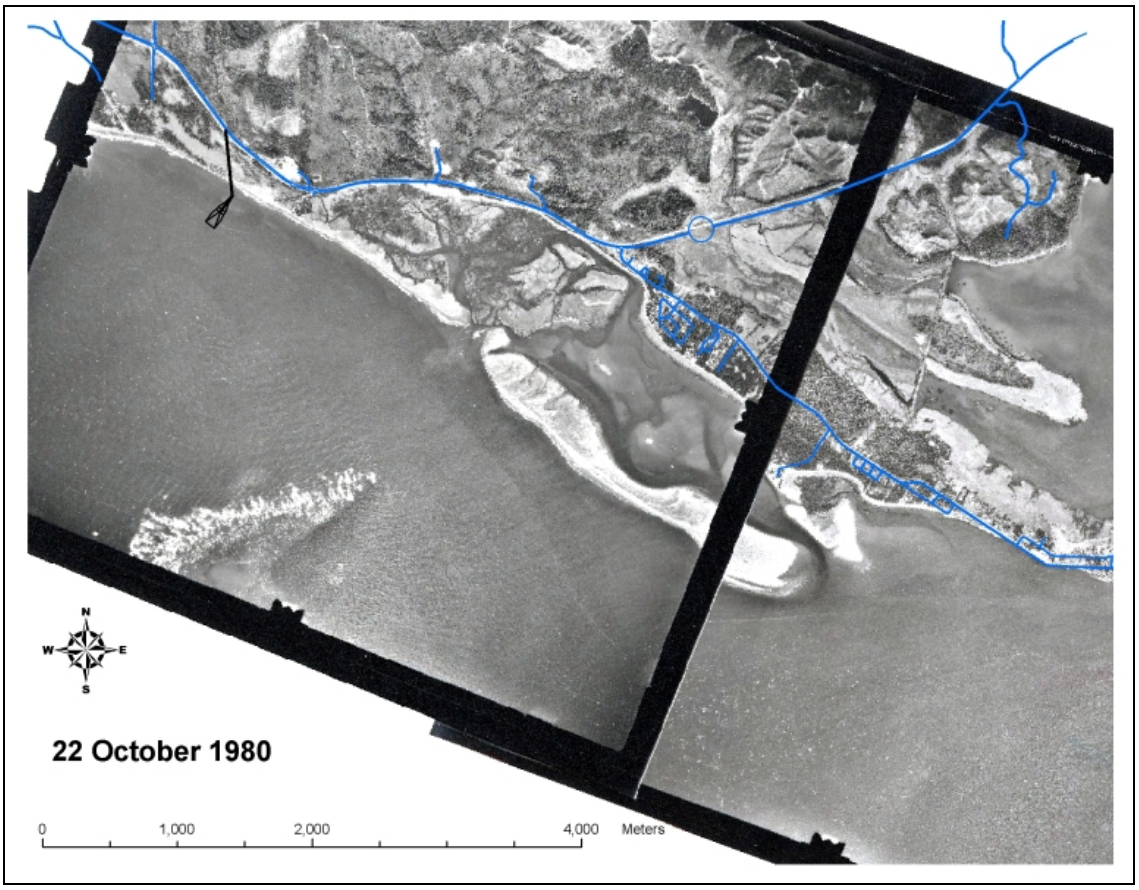

Figure 2.2. 11. 1980 aerial photograph. Original prints NWS.

Figure 2.2. 12. 1981 aerial photograph. Original prints NWS. Note that Graveyard spit is thin and appears to have recently been overwashed.

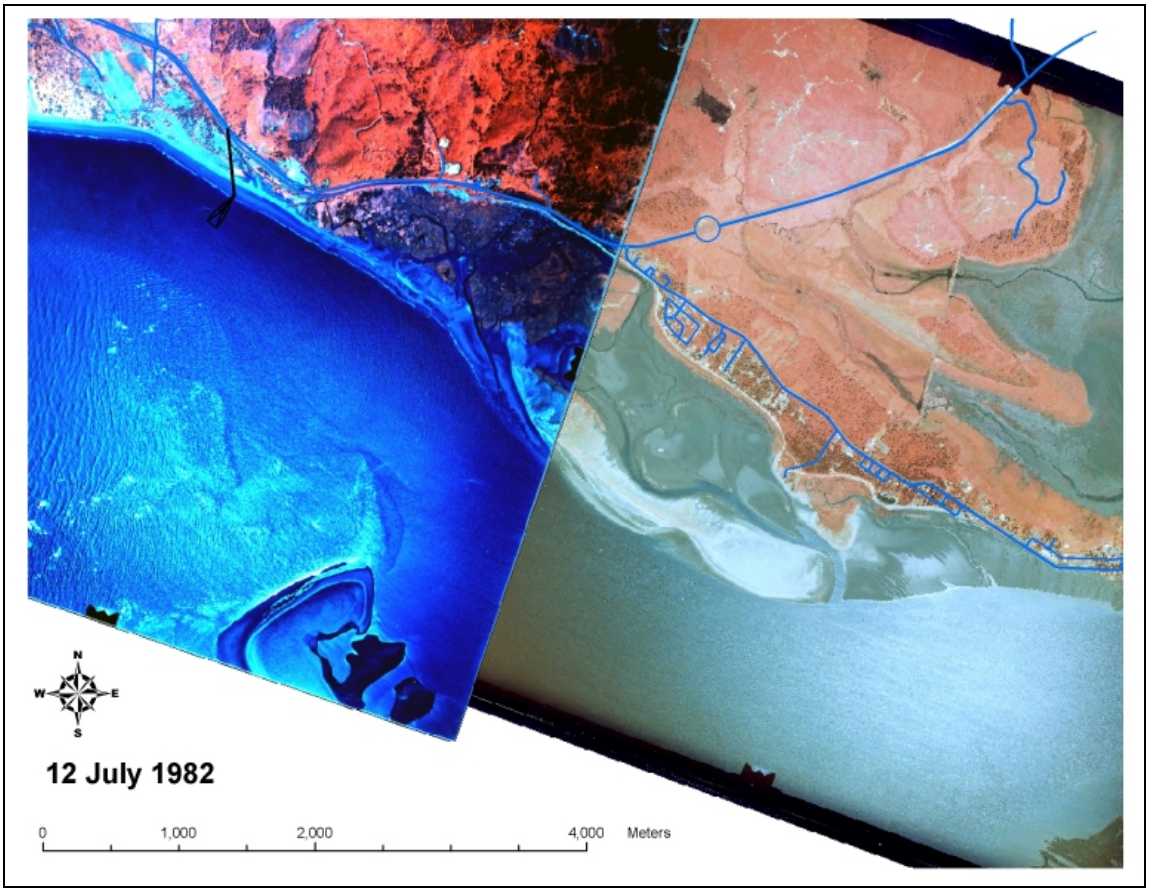

Figure 2.2. 13. 1982 aerial photograph. Original prints NWS. Graveyard spit has almost disappeared except for some narrow sand shoals.

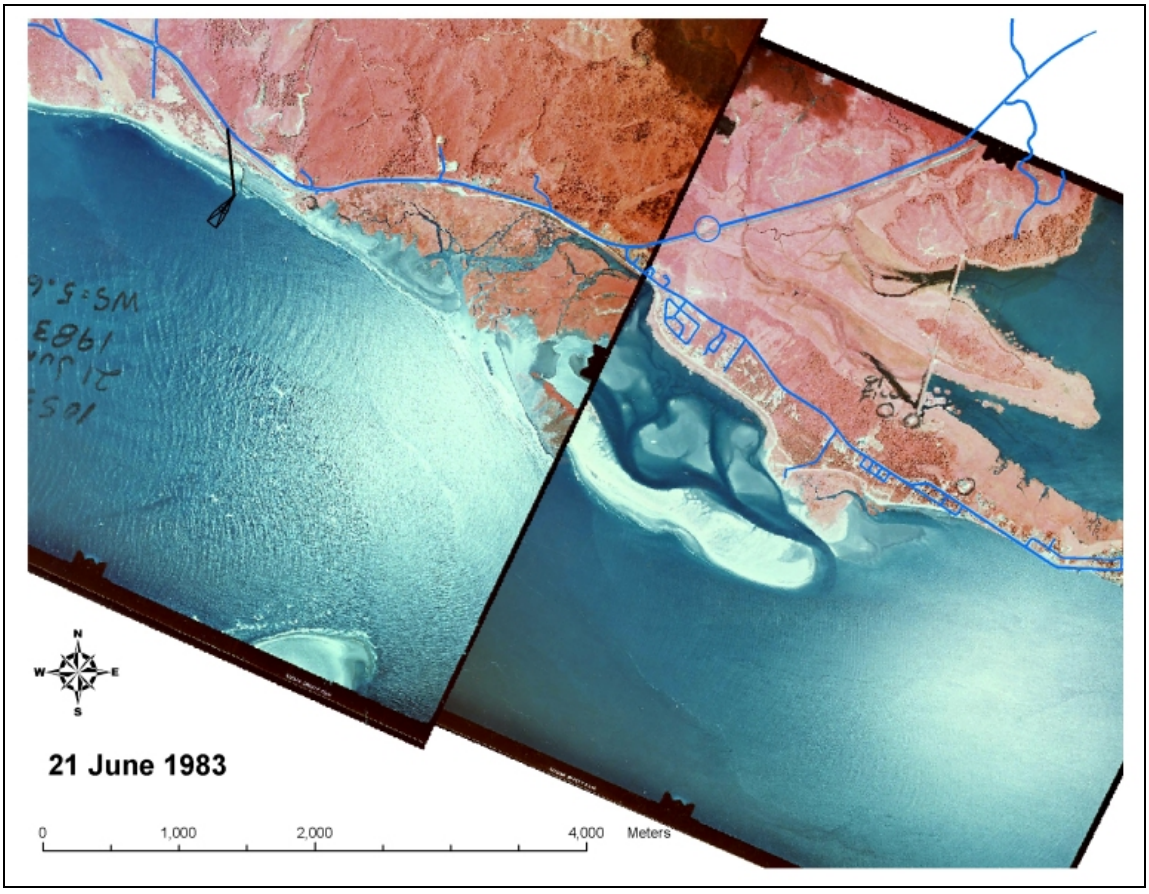

Figure 2.2. 14. 1983 aerial photograph. Original prints NWS. Graveyard Spit is more substantial than in 1982.

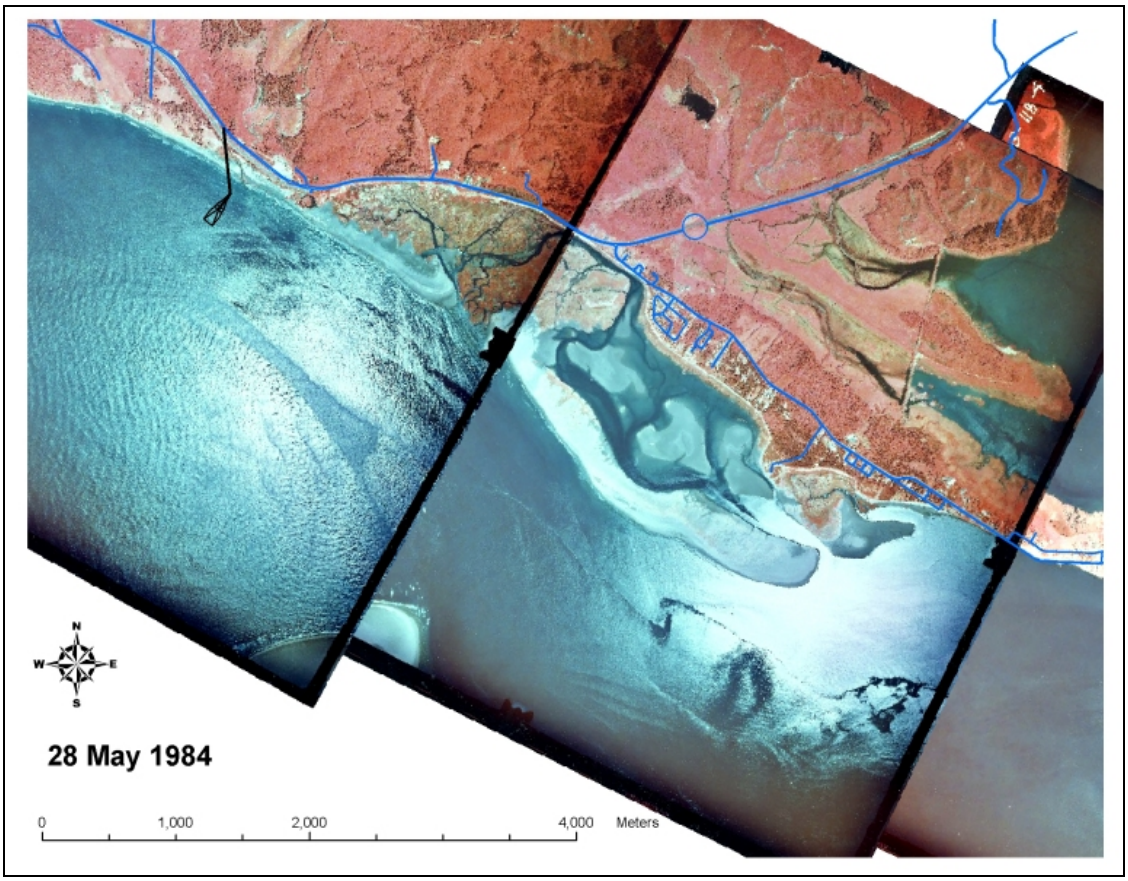

Figure 2.2. 15. 1984 aerial photograph. Original prints NWS.

Figure 2.2. 16. 1985 aerial photograph. Original prints NWS.

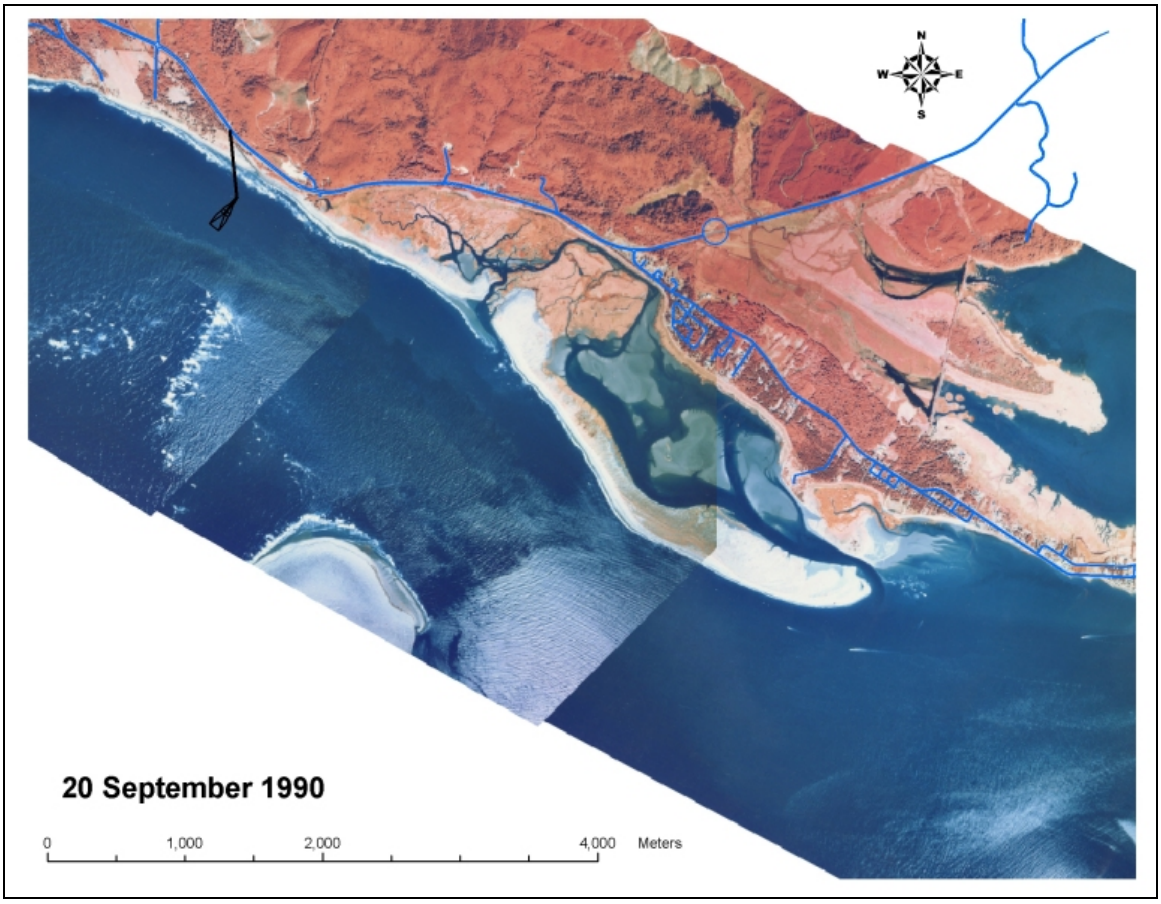

Figure 2.2. 17. 1990 aerial photograph. Original print NWS.

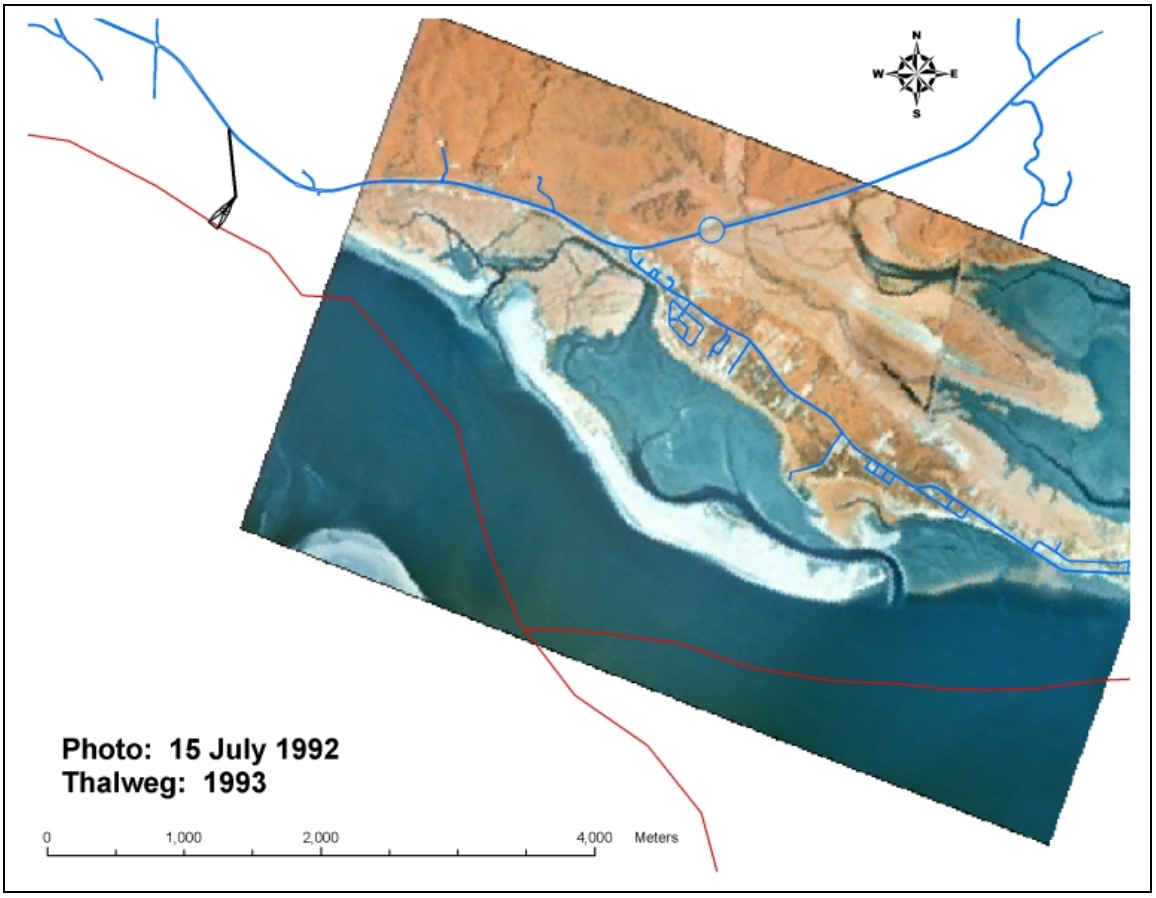

Figure 2.2. 18. 1992 aerial photograph. Original print NWS.

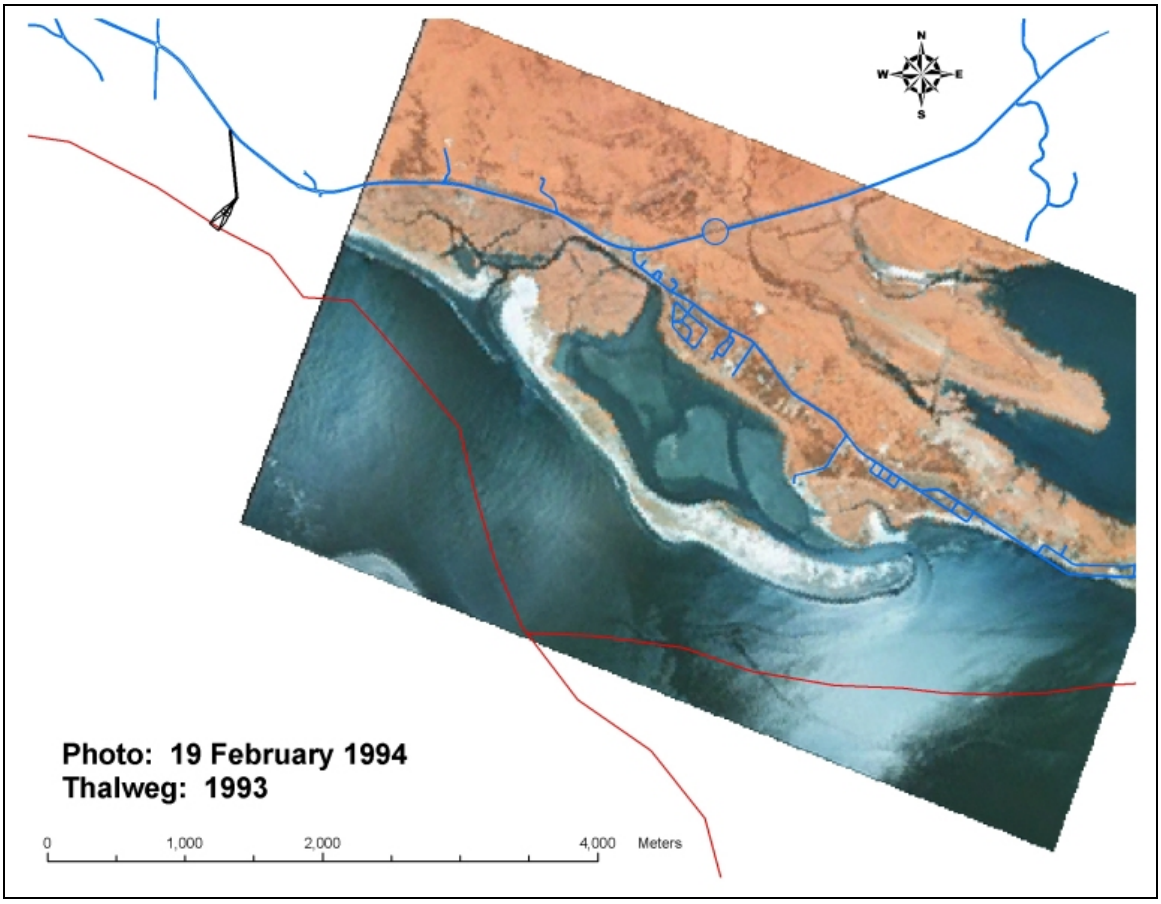

Figure 2.2. 19. 1994 aerial photograph. Original print NWS. Notice the thin section in the island just south of the community.

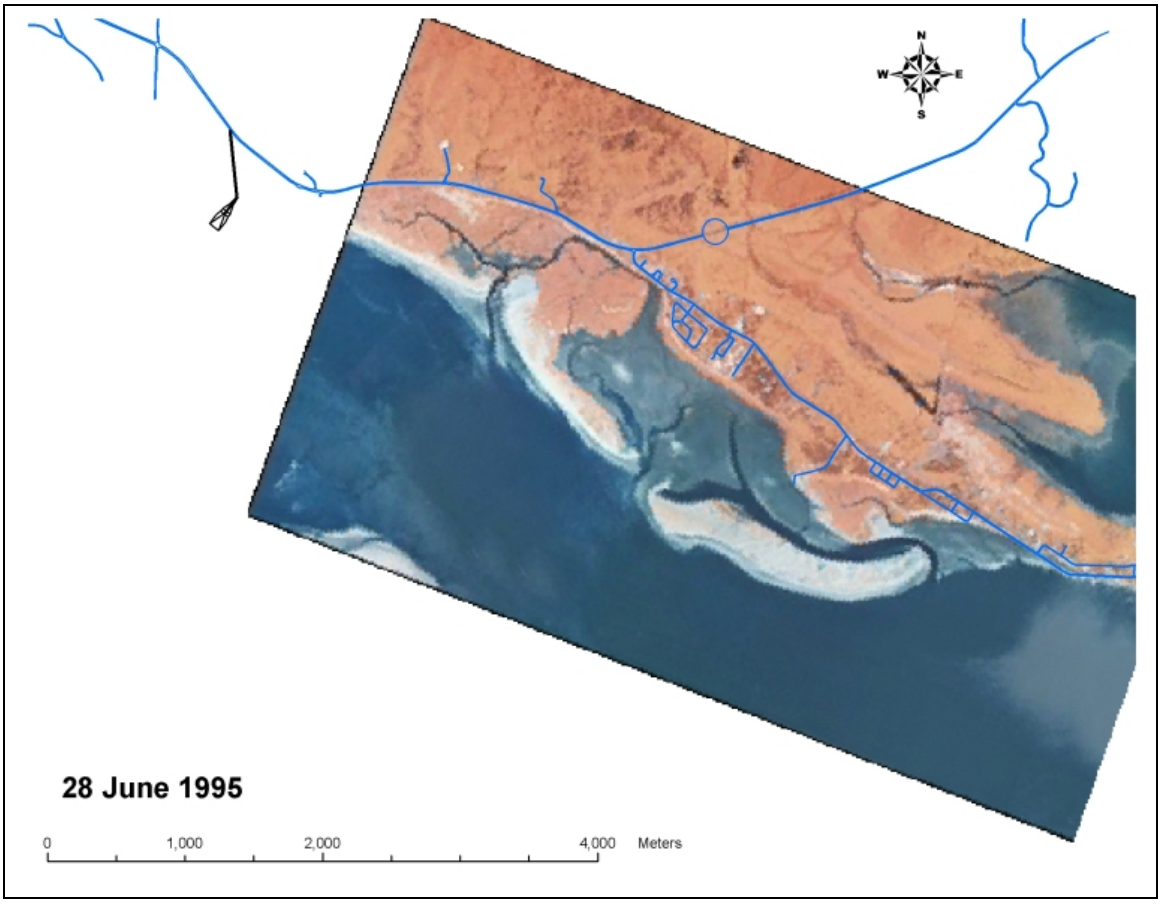

Figure 2.2. 20. 1995 aerial photograph. Original print NWS. The long island seen in the 1994 photograph has been breached and a tidal channel has formed through the opening.

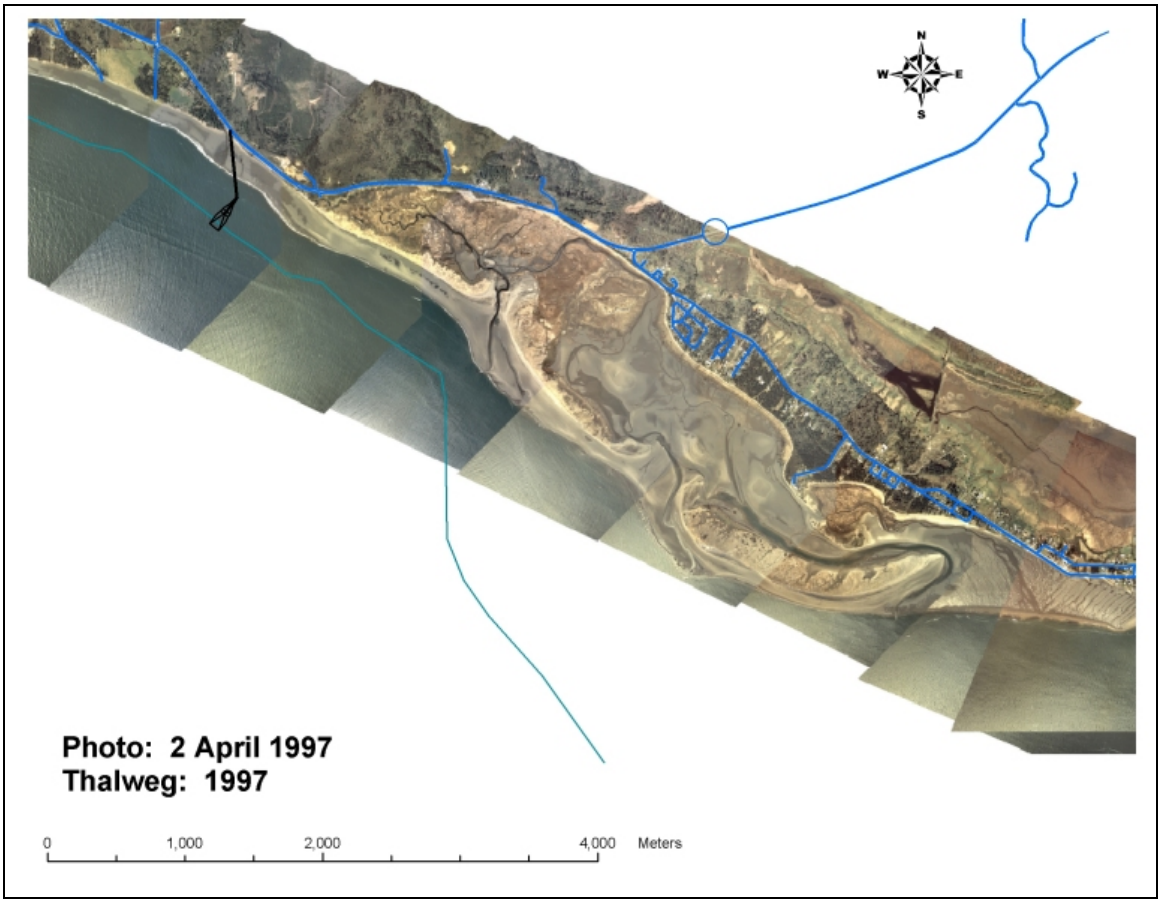

Figure 2.2. 21. 1997 aerial photograph. Original prints NWS.

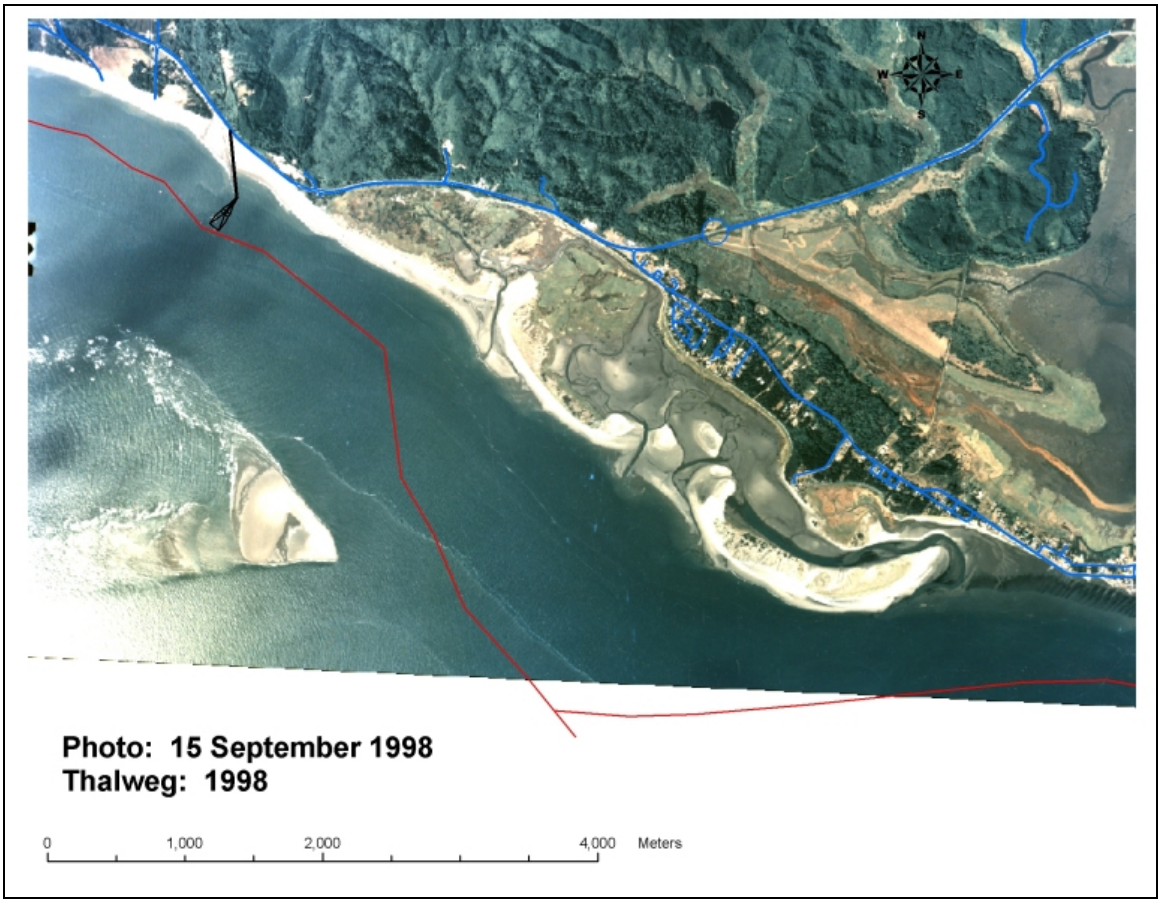

Figure 2.2. 22. 1998 aerial photograph. Original print NWS. This photograph was taken when construction of the SR-105 Emergency Stabilization Project dike and groin was underway.

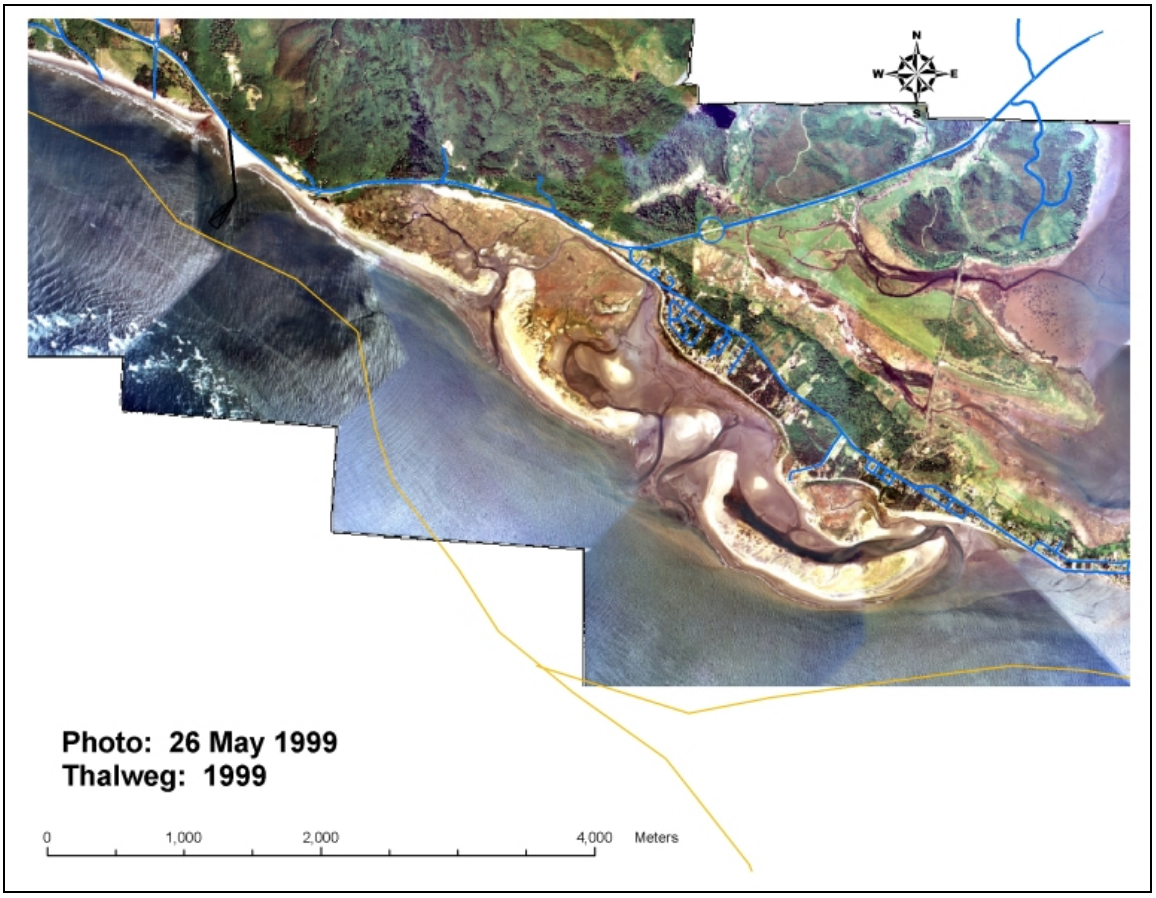

Figure 2.2. 23. 1999 aerial photograph. Original prints NWS.

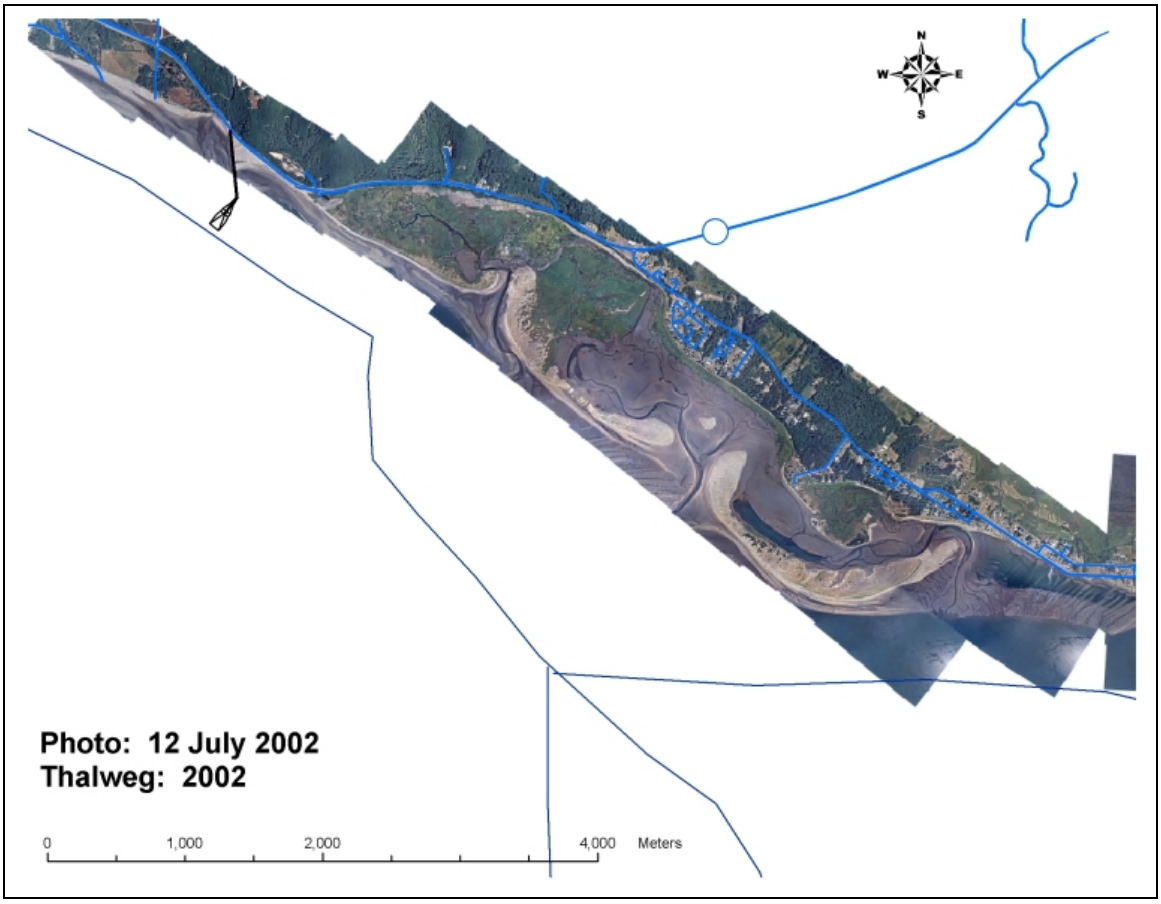

Figure 2.2. 24. 2002 aerial photograph. Original prints NWS.

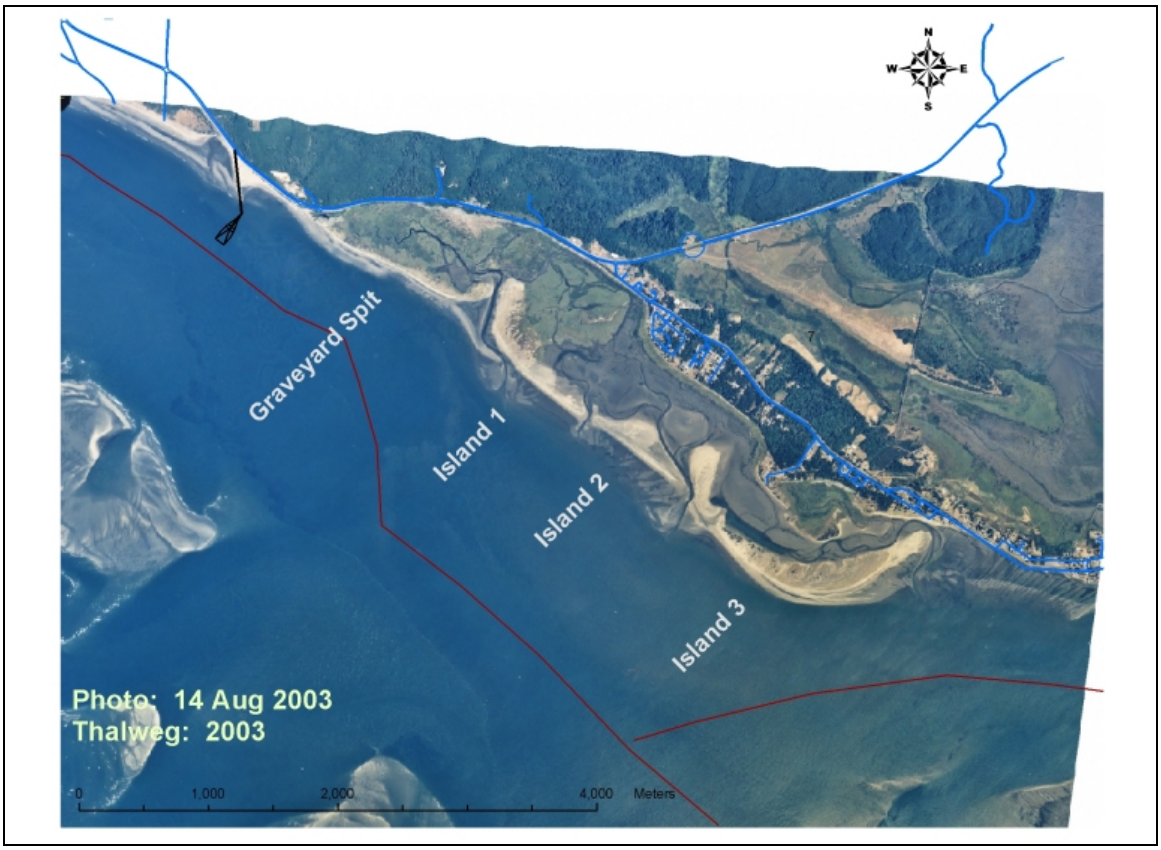

Figure 2.2. 25. 2003 aerial photograph. Original prints NWS. Labels refer to features discussed in the text.

Historical Shorelines: 1871, 1926, and 1950

Washington DOE provided ERDC with three historical shorelines, 1871, 1926, and 1950. DOE digitized these shorelines from U.S. Coast and Geodetic Survey (USC&GS) T-sheets as part of a historical data recovery project for the whole Washington Coast. For the Shoalwater study, the DOE GIS specialist clipped the shorelines to include only the Shoalwater study area and then re-projected them to State Plane, WA south zone, NAD83, with units in feet. This allowed us to import these shoreline files directly into the ArcGIS project, without need to convert coordinate systems.

The shoreline from 1871 is some of the oldest known map data for the Willapa Bay area (Figure 2.2.26). It is especially valuable because it shows the series of spits that once formed Cape Shoalwater. Modern maps still call the northern mouth of Willapa Bay "Cape Shoalwater," even though now it does not have the morphology of a cape.

1911 T-sheet

Washington DOE scanned and projected a 1911 T-sheet into State Plane coordinates. In the ArcGIS project, this historical chart can also be compared with the other data sets and the shoreline position can be interpreted at the cross-section lines (Figure 2.2.27).

The next known shoreline was from a 1926 T-sheet (Figure 2.2.28). This shoreline, along with 1871 and 1911, were valuable additions to the project dataset because they were older than the earliest photo flight (1942). The 1950 shoreline closely matched the 1955 photo mosaic, underscoring that the various parties involved in digitizing, data reduction, and GIS operations had conducted their tasks rigorously (Figure 2.2.29).

Post-1950 Shorelines

ERDC digitized the post-1950 shorelines using the aerial photographs as the source data. On the seaward (south) side of the islands and spits, we interpreted the wet-dry line to be the shoreline. This approximated the most recent high water line before the time that the photograph was taken. On the bay (north) side of the islands, selecting a shoreline required a greater degree of interpretation because it was often difficult to determine what was swamp and wetland vegetation, and what was dune grass (Figure 2.2.30). The features were outlined as polygons and were then converted to ESRI Shape files. These shape files can be projected with one another, showing the progression of changes overtime.

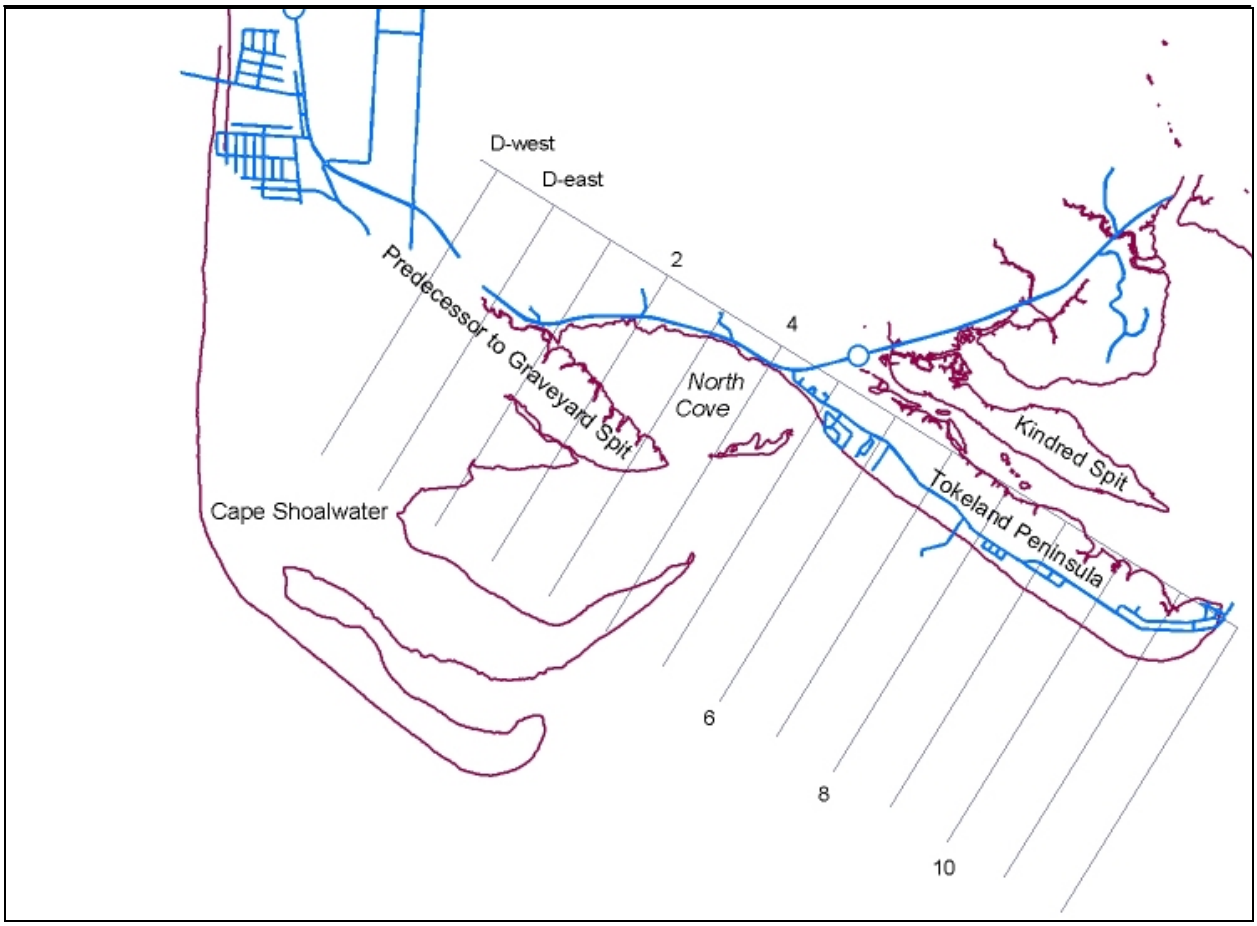

Figure 2.2. 26. 1871 shoreline based on U.S. Coast and Geodetic Survey T-sheet, with superimposed cross-section lines and contemporary roads. Shoreline digitized from T-sheet by WA DOE.

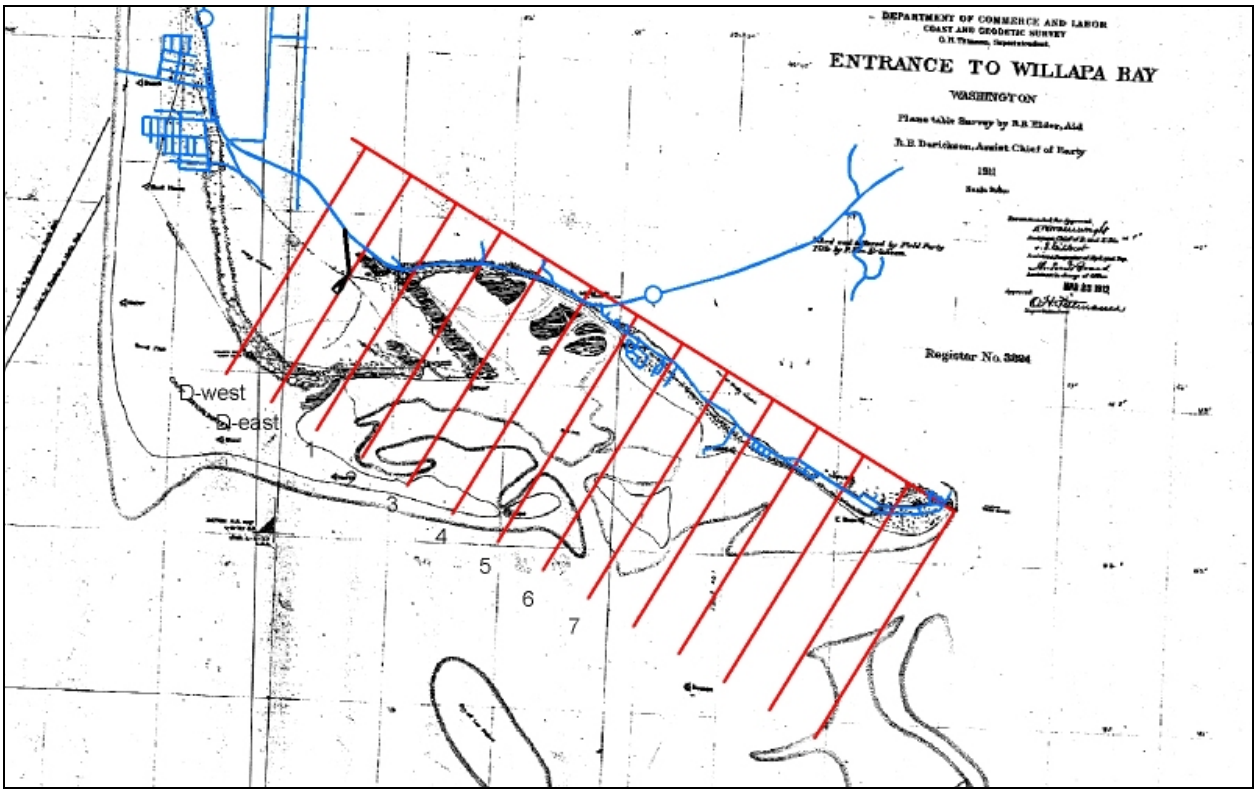

Figure 2.2. 27. 1911 shoreline based on U.S. Coast and Geodetic T-sheet, projected into State Plane, Washington South Zone, NAD83. The cross-section grid and contemporary roads are shown for reference. Digital map provided by WA DOE.

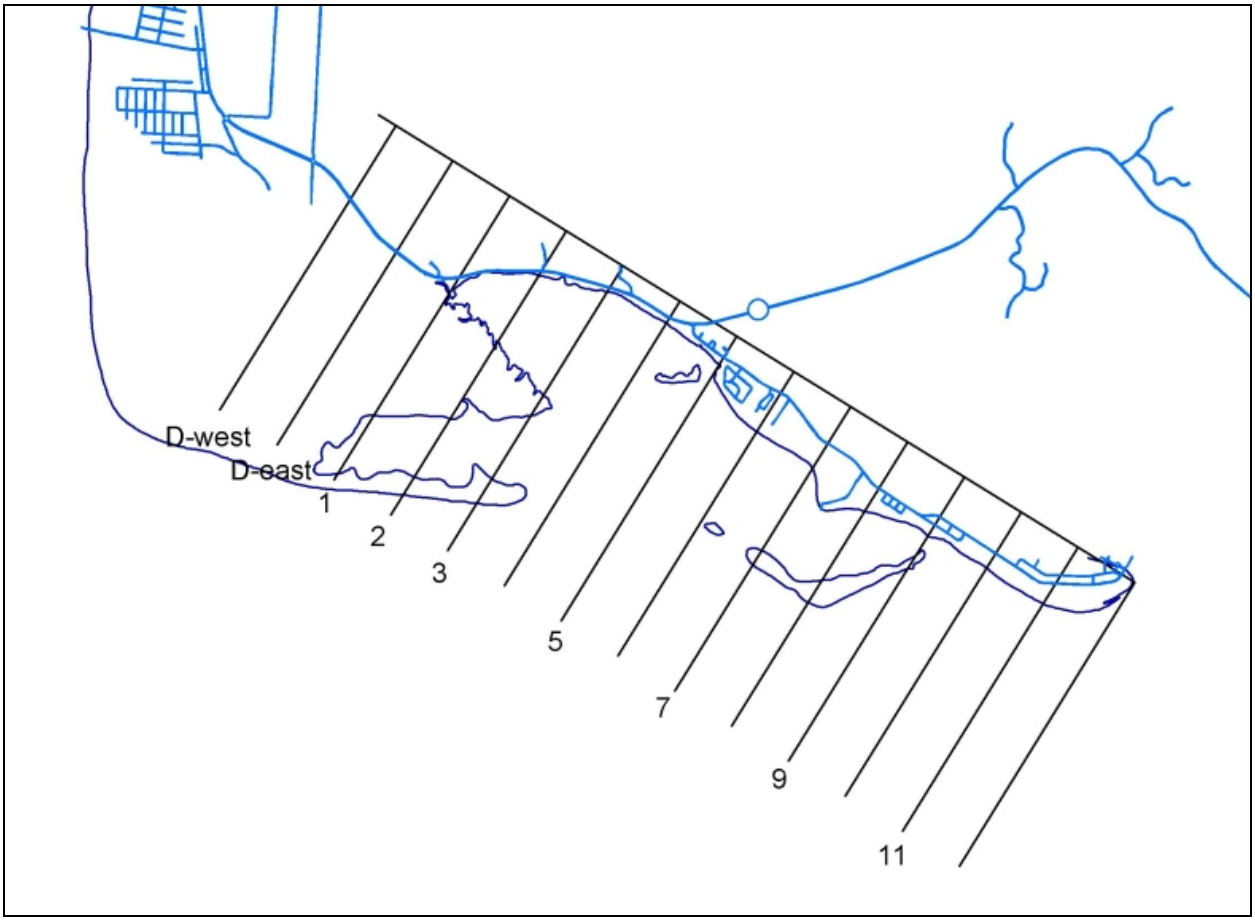

Figure 2.2. 28. 1926 shoreline from USC&GS T-sheet. This predates the earliest known aerial photographs of Willapa Bay. Digitized mapping provided by WA DOE.

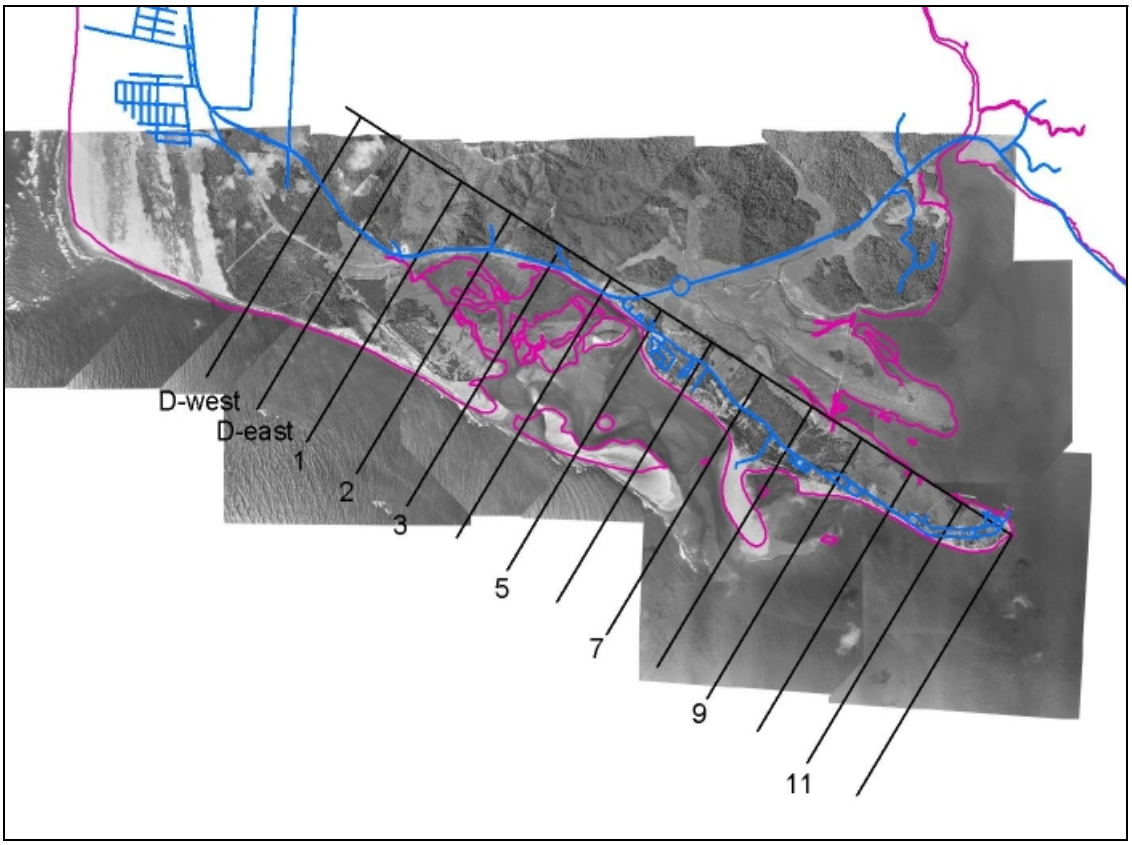

Figure 2.2. 29. 1950 T-sheet shoreline superimposed on 1955 photo mosaic. The close match shows that all data reduction and GIS operations were conducted rigorously.

Figure 2.2. 30. Example of outline of Graveyard spit shoreline on 1966 photo mosaic. This procedure was used to outline the spits and islands on all the aerial photo dates.

2.2.2 Historical Bathymetric and Morphologic Changes[4]

Island and Spit Migration and Channel Location

Cape Shoalwater's dramatic erosion during the 20th century has been well documented in the literature (Lowell, 1997; Morton, Purcell, and Peterson, 2002; Richey, et al., 1966; Terich and Levenseller, 1986). Most of these reports concentrated on the cape at the mouth of Willapa Bay because this was one of the most extreme examples of erosion in the United States. This chapter addresses shore retreat and channel changes inside the mouth of the bay near the Shoalwater Reservation.

Figure 2.2.31 is a plan view of the changes that have occurred to Graveyard spit and the sand islands. The features were outlined in ArcGIS software and superimposed on one frame. The figure shows some interesting patterns:

1. The greatest retreat of Graveyard Spit occurred during the first few decades of the 20th century. By about 1980, the spit had moved to approximately the position it occupies today.
2. For much of the 20th century, the sand islands to the east of Graveyard Spit (sometimes referred to as Empire Spit) were a continuous feature. It breached in 1995, forming two thin islands. When the spit was intact, it bulged out to the south as much as 2000 ft from the location of the present opening. After the 1995 breach, sand moved into the opening, similar to the pattern seen at drumstick barriers on non-structured, open coast tidal inlets. By 2003, three narrow islands existed (labeled in Figure 2.2.25).
3. The channel between Island 3 and Tokeland Peninsula was narrower in 2002 than at any time in the past. It is likely that as the breach between Islands 2 and 3 gets wider, less tidal flow is moving through the Tokeland-Island 3 gap, and the east tip of Island 3 is slowly moving towards Tokeland Peninsula. We cannot predict if the island will eventually weld to the peninsula, closing the opening.

To determine if the retreat rate has changed over the years, the position of the shoreline versus time were plotted. In each subsection below, the first figure is a graph of shoreline and thalweg position over time based on all trustworthy shoreline and bathymetric data. The second figure shows the cross-section of the channel at the same cross line based on the 1993-2003 bathymetry surveys. In the figures below, distances are referenced to the baseline shown in Figures 2.2.1 and 2.2.31 and tabulated in Table 2.2.1. The distance shown is from the baseline to the seaward (south) side of Graveyard Spit or the sandy islands. Land is to the left of the figure, and the viewer is looking towards the southeast.

[4] Written by Andrew Morang, Ph.D., U.S. Army Engineer Research and Development Center, Coastal and Hydraulics Laboratory, Vicksburg, MS.

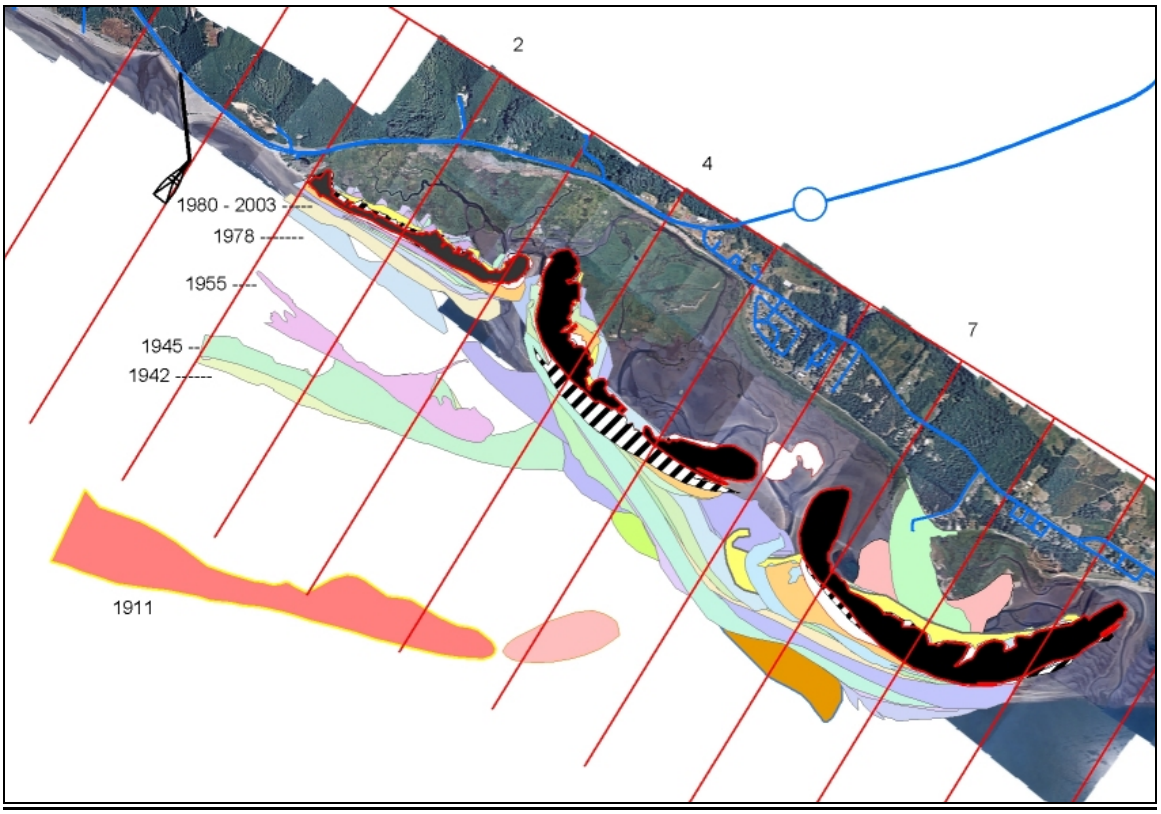

Figure 2.2.31. Plan view of locations of Graveyard Spit and sand islands, 1911 to 2003. The spit moved much more rapidly during the first few decades of the 20th century. By 1980, the spit had stabilized in approximately the same position that it occupies today. Background photograph: July 2002. North is to the top. Cross-section lines are 2,000 feet apart.

Cross-section Line D-west

The shoreline at D-west, about 2000 ft west of the underwater portion the SR-105 dike, retreated over 10,000 feet, or almost two miles, in a century, an average of about 115 feet/year (Figure 2.2.32). The rate of shoreline retreat decreased in the early 1980's, and the curve leveled off by about 1995. The shape of the thalweg curve is similar to the shoreline curve and also shows a reduced retreat rate after the 1980's.

The channel cross-sections (Figure 2.2.33) demonstrate how the channel bottom scoured after construction of the SR-105 dike in 1998. The channel became wider and deepened from about 80 feet to over 100 feet. It is clear that in this area, channel cross-section increased greatly after 1998.

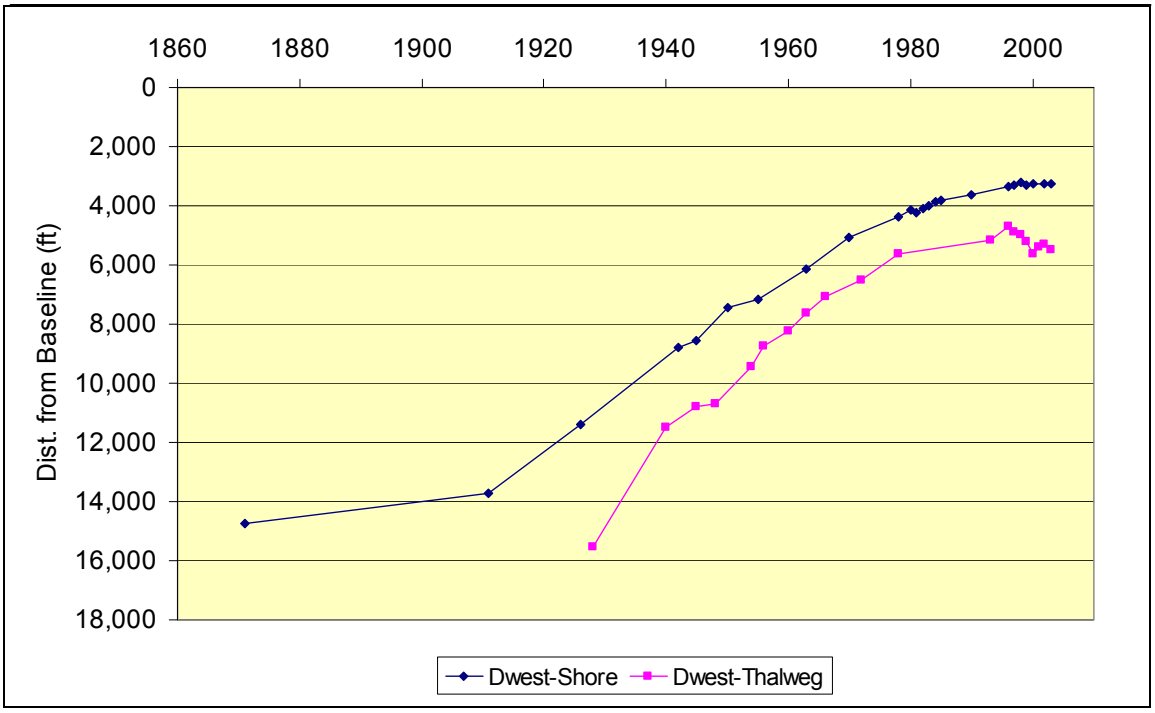

Figure 2.2.32. Cross-section line D-west: shoreline and thalweg position.

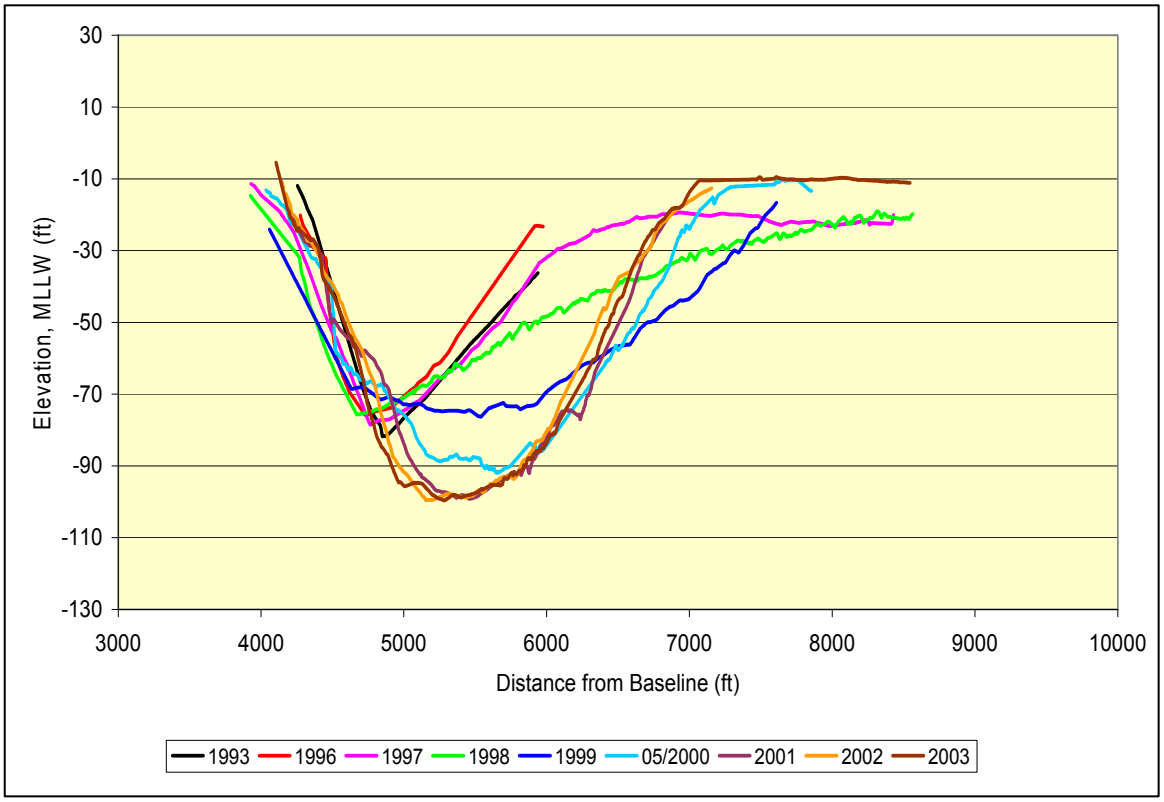

Figure 2.2.33. D-west: channel cross-sections. The channel scoured after construction of the SR-105 dike in 1998, and its depth increased from 80 to about 100 feet. In this plot, land is to the left and the Willapa Bay ebb shoal is to the right.

Cross-section Line 1

At cross-section line 1, the channel thalweg also retreated at about 115 feet/year for the century after 1870, and the shoreline retreated at a similar rate (Figure 2.2.34). The channel and shoreline curves both began to level off in the early 1980's, and the thalweg started moving south, away from shore, in 1998. The cross-sections show that the channel became deeper and wider after 1999, with total depth increase of almost 40 feet (Figure 2.2.35). This is part of the scour zone that first formed at the toe of the SR-105 dike and then spread along the axis of the channel.

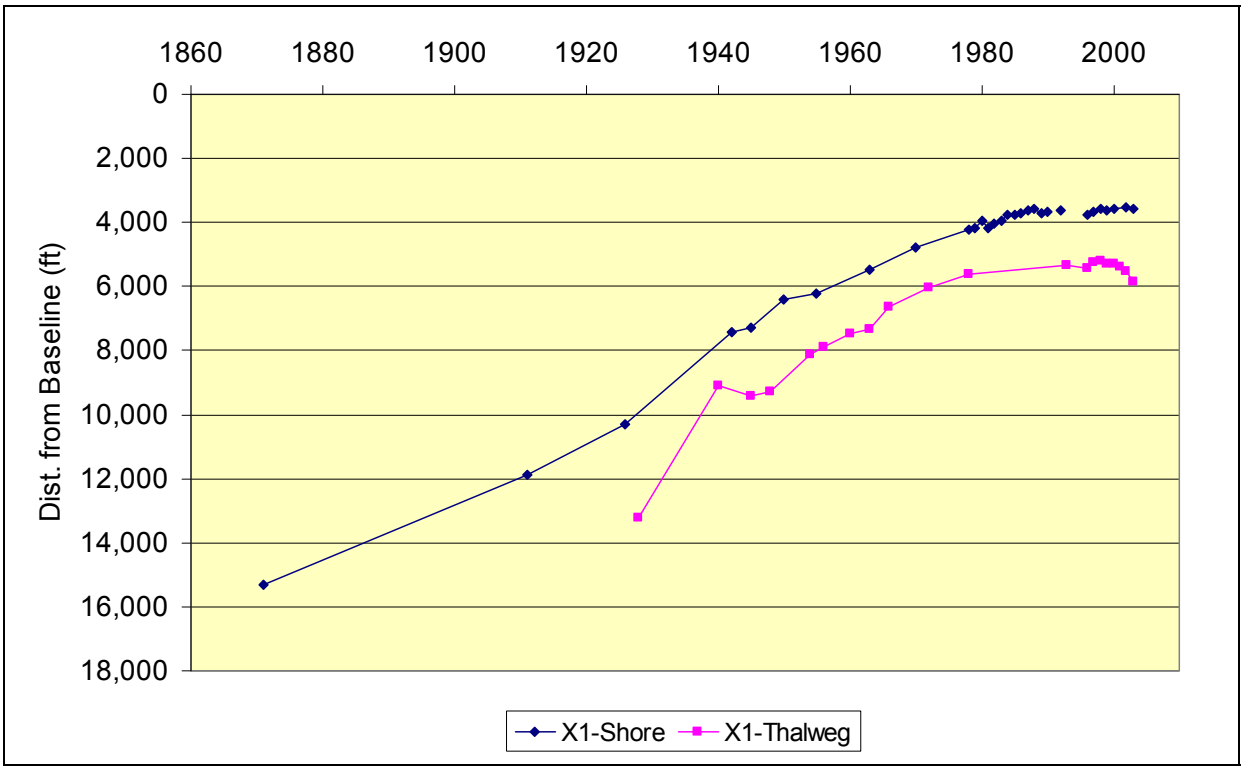

Figure 2.2.34. Cross-section line 1: shoreline and thalweg position. The shoreline position stabilized after 1980, and the thalweg began to move away from shore.

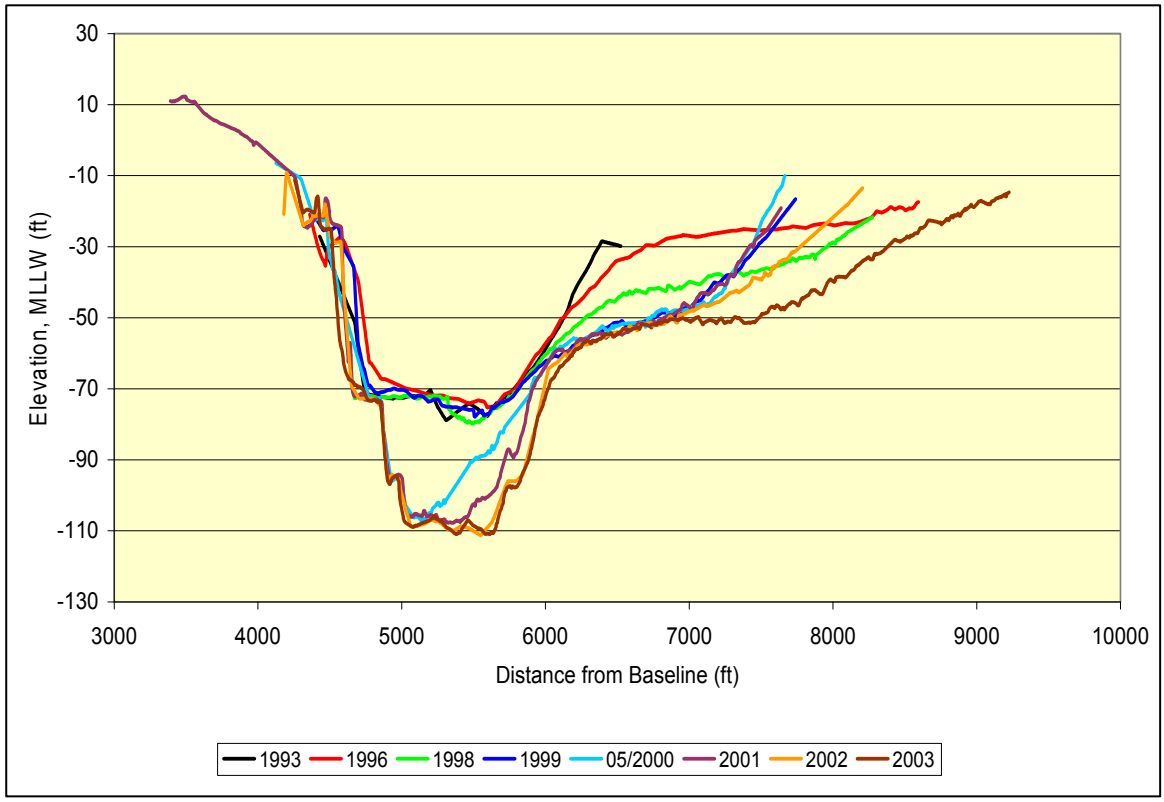

Figure 2.2.35. Line 1: channel cross-sections. Between 1998 and May 2000, the channel here scoured about 40 feet.

Cross-section Line 2

At cross-line 2, the retreat of the shoreline and the thalweg paralleled each other, as at D-west and cross-line 1 (Figure 2.2.36). The cross-section curves show how the south flanks of the channel began to deepen as early as 1996, well before construction of the SR-105 dike began. Although the thalweg remained in approximately the same position, by 2003, the overall channel had a significantly greater cross-section than in 1993 (Figure 2.2.37). Around 8,000 feet from the baseline, the 2003 channel was 40 feet deeper than in 1993.

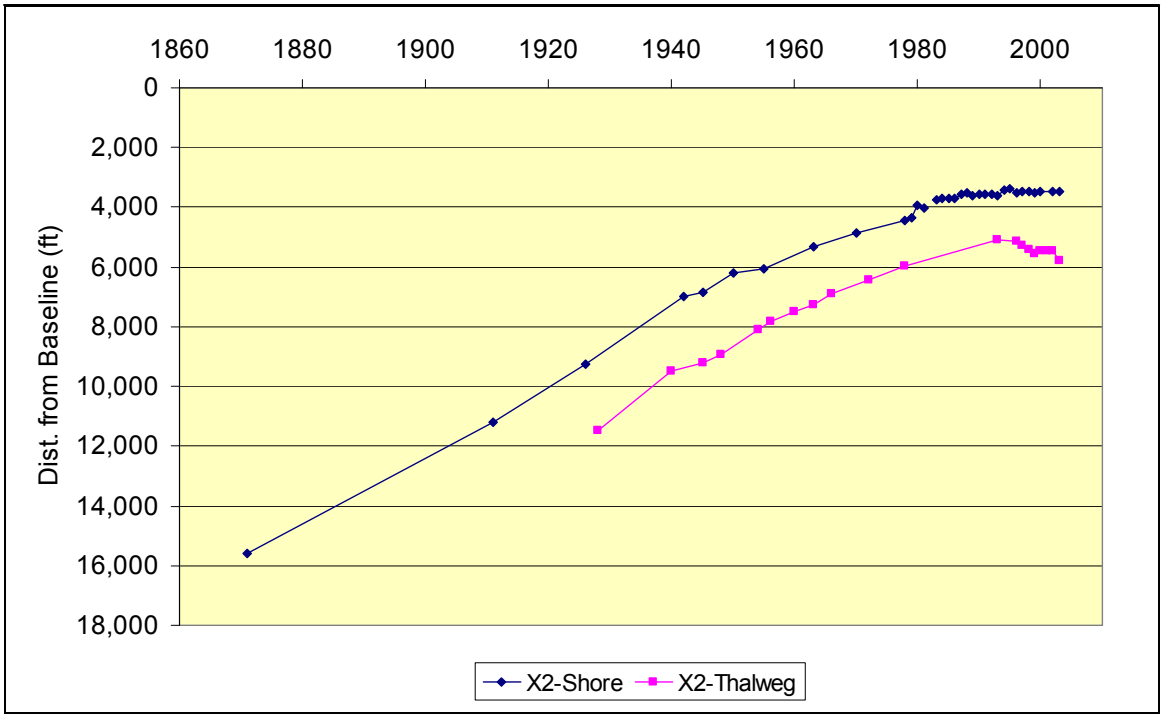

Figure 2.2.36. Cross-section line 2: shoreline and thalweg position. The shoreline position stabilized in the early 1980's, while the thalweg moved away from shore (to the south) after 1996.

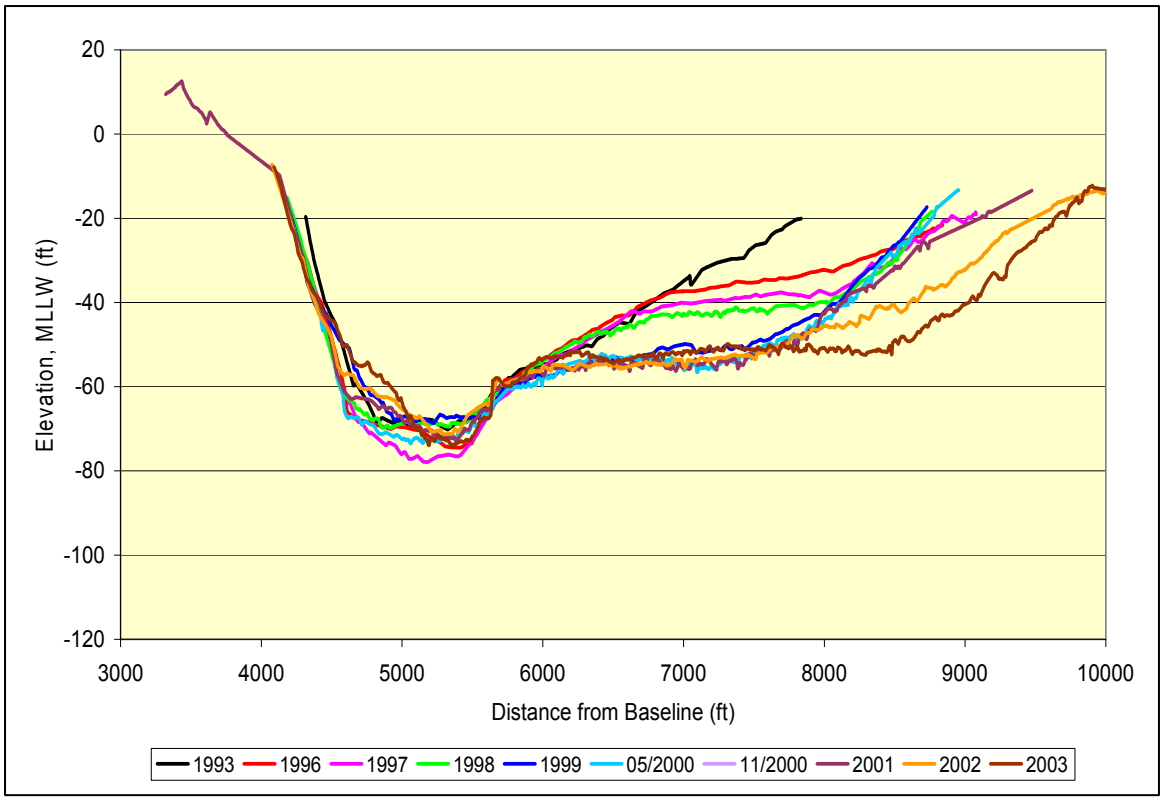

Figure 2.2.37. Line 2: channel cross-sections. After 1993, the south flanks of the channel began to deepen, although the thalweg remained in approximately the same position.

Cross-section Line 4

At cross line 4, the shore retreated until about 1950, when it reached approximately the same position that it has today (Figure 2.2.38). The thalweg also moved shoreward (to the north) until 1996, when it reversed its direction and began to move southward. The cross-section plots show how the channel changed shape after 1996 (Figure 2.2.39). In 1993 and 1996, the channel was about 4,000 feet wide and had an approximately flat bottom. By 1997, the south end of the channel had deepened, while the north side (closest to the beach) had begun to get shallower. By 2003, the south side was 30 feet deeper than in 1993, while the north side was 20 feet shallower. Note that the north bank was fixed for a decade. As at Line 2, the channel edge resisted erosion by tidal currents. When the Washington State Department of Transportation rerouted part of SR-105, they made a number of borings along the proposed highway route. At borings B-1-97, B-2-97, and B-3-97, they encountered a unit they identified as "Very dense, brown Pleistocene Terrace" (Jackson, Allen, and Lowell 1997). We believe this unit extends under the Shoalwater bay and under the present spit and islands. Rotary borings at a number of locations along the islands will be needed to verify this hypothesis.

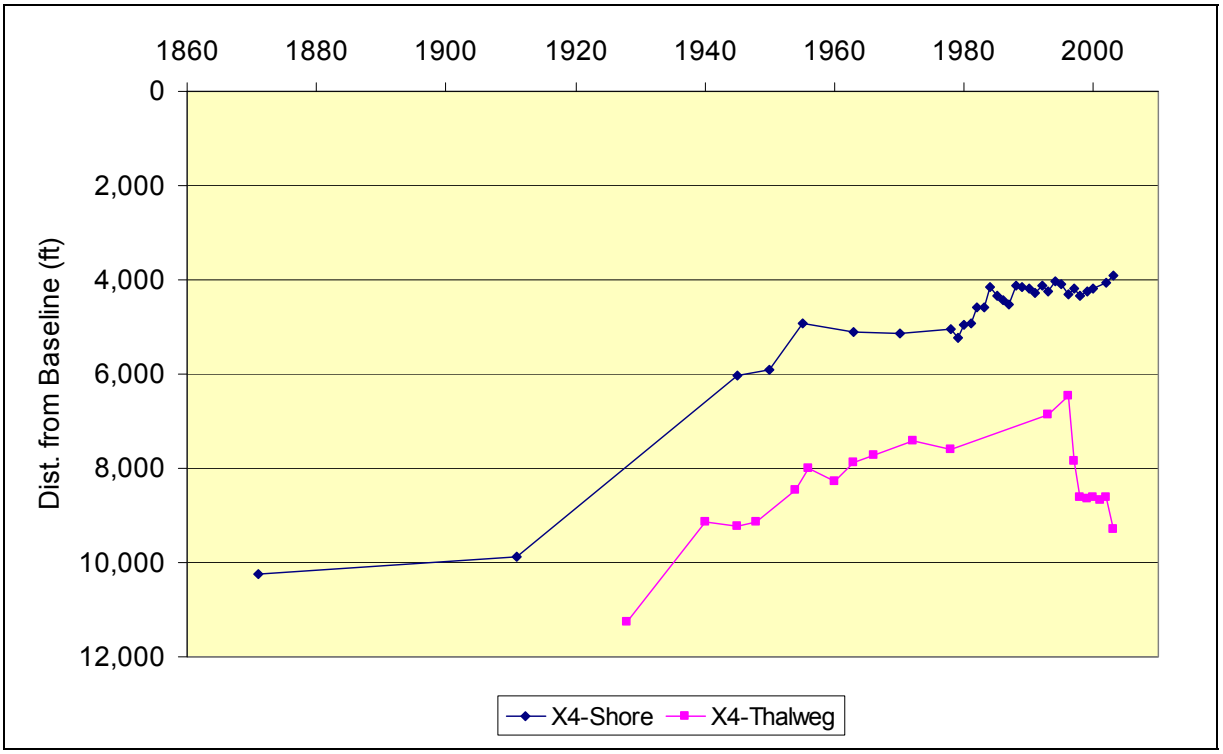

Figure 2.2.38. Cross-section line 4: shoreline and thalweg position. By 1980, the shoreline had stopped retreating. The thalweg moved away from shore after 1996.

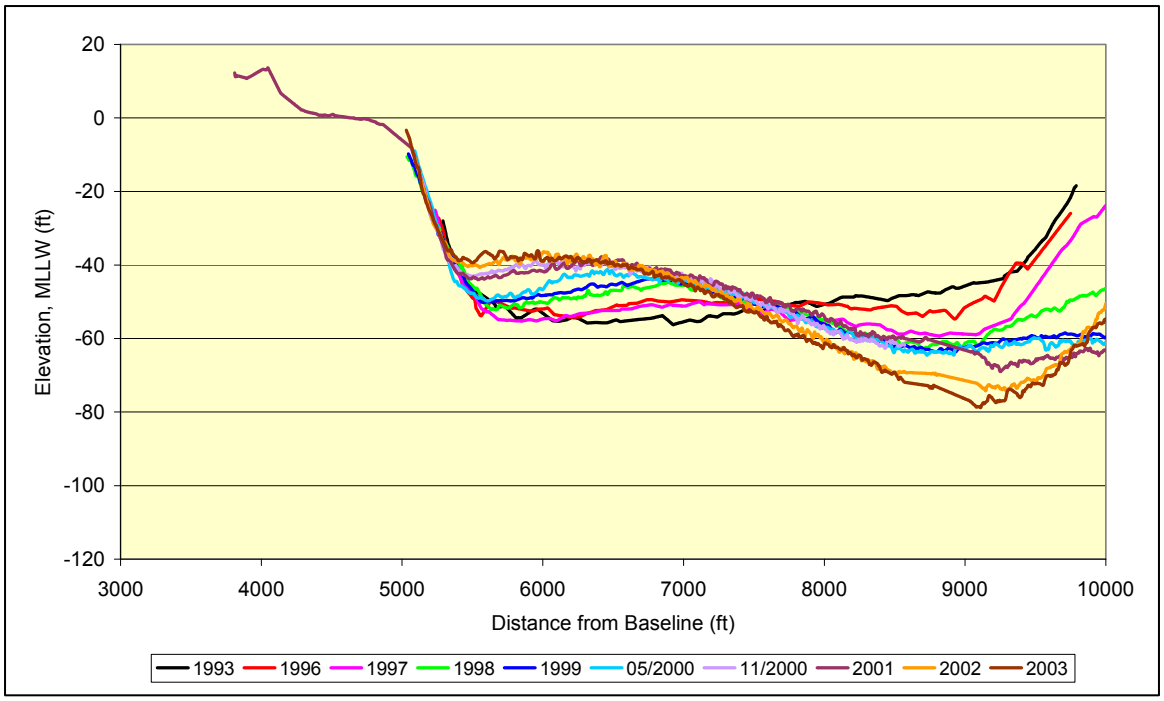

Figure 2.2.39. Line 4: channel cross-sections. Since 1993, the north edge of the channel was fixed. Over time, the thalweg migrated south (to the right) as the area beyond 8,000 feet to the south deepened.

Cross-section Line 7

Cross-section line 7 is near the southeast end of the study zone, extending over Island 3. This is the zone where the main Willapa Bay channel and the Willapa River channels merge. For almost a century, the shoreline (sometimes Island 2, other times Island 3) has remained between 5,000 an 7,000 ft from the baseline (Figure 2.2.40). However, since 1987, the shoreline has moved north about 1,000 feet, which is in contrast to cross-section lines D-west, 1, 2, and 4, where the shore position stabilized during the 1980s. The reason for the recent retreat is likely a loss of sand supply from the west, during which time the island became lower and thinner. Until the 1980s, the thalwegs also moved north, but at a much lower rate than further west (Figure 2.2.41). After 1996, the thalweg moved south about 2,000 feet and then fluctuated as the channel made minor adjustments.

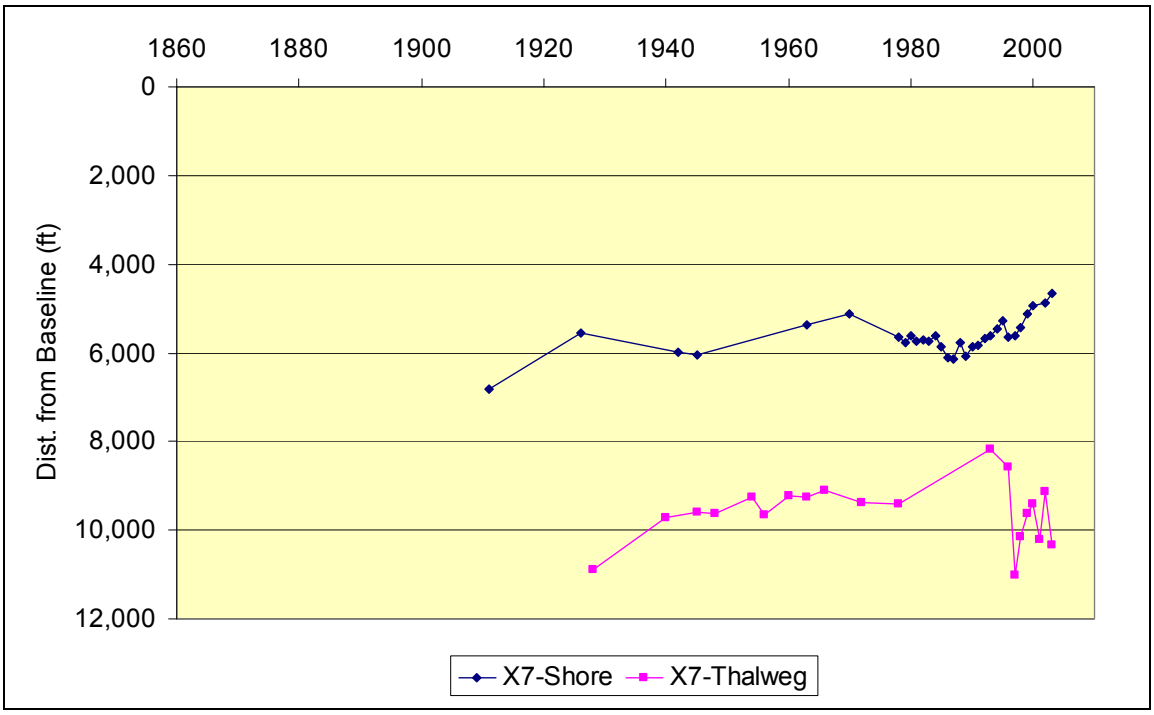

Figure 2.2.40. Cross-section Line 7: shoreline and thalweg position.

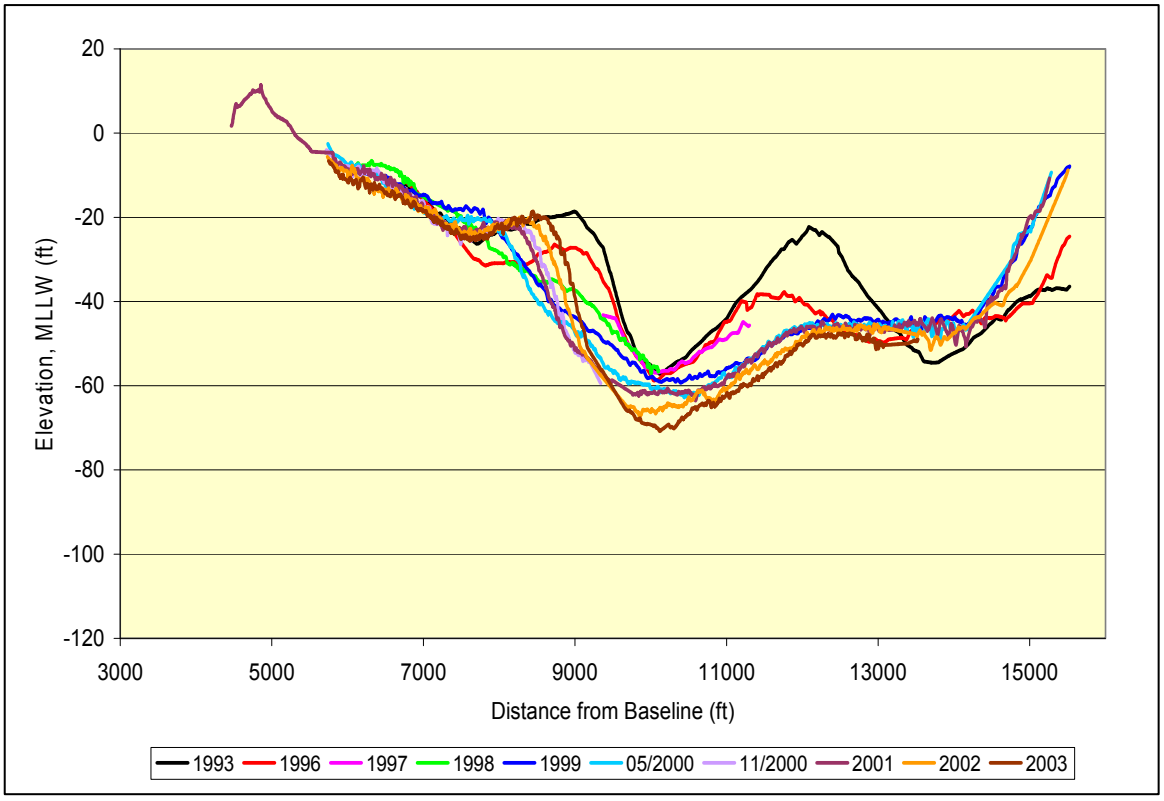

Figure 2.2.41. Line 7: channel cross-sections. The 1993 curve shows two distinct deep sections. But, over time, the channels merged into one deeper trough with a lobe to the south (the right).

Tabulated Data

Table 2.2.4 lists the distances from the baseline to the shoreline, as plotted in the figures above. Table 2.2.5 lists distances from the baseline to the thalweg.

Table 2.2.4
Distance (in ft), baseline to seaward edge of feature

	Cross-section line					
Year	D-west	1	2	4	5	7
1871	14,760	15,330	15,600	10,260		
1911	13,700	11,880	11,210	9,880	8,970	6,810
1926	11,400	10,320	9,270			5,560
1942	8,770	7,430	7,000		5,850	5,980
1945	8,570	7,300	6,850	6,030	4,860	6,034
1950	7,450	6,380	6,190	5,900	5,620	
1955	7,175	6,220	6,058	4,910	5,730	
1963	6,146	5,460	5,320	5,115	5,280	5,360
1970	5,050	4,800	4,860	5,130	5,430	5,120
1978	4,370	4,230	4,436	5,052	5,200	5,638
1979		4,160	4,370	5,230	5,300	5,754
1980	4,150	3,940	3,950	4,950	5,310	5,605
1981	4,230	4,190	4,025	4,936	5,660	5,727
1982	4,110	4,050		4,575	5,280	5,712
1983	4,015	3,950	3,750	4,590	5,220	5,730
1984	3,880	3,770	3,710	4,140	5,120	5,605
1985	3,820	3,760	3,700	4,330	5,230	5,860
1986		3,720	3,680	4,445	5,400	6,120
1987		3,600	3,560	4,530	5,320	6,150
1988		3,570	3,503	4,110	4,890	5,775
1989		3,720	3,625	4,160	4,860	6,073
1990	3,620	3,650	3,566	4,190	4,960	5,846
1991			3,585	4,275		5,845
1992		3,640	3,542	4,130	4,880	5,677
1993			3,600	4,250	4,890	5,600
1994			3,433	4,040	4,700	5,470
1995			3,382	4,100	4,670	5,270
1996	3,360	3,770	3,510	4,300	4,800	5,650
1997	3,300	3,670	3,487	4,170	4,700	5,620
1998	3,230	3,550	3,448	4,340	4,720	5,420
1999	3,280	3,610	3,520	4,240	4,460	5,130
2000	3,260	3,550	3,475	4,190	4,420	4,935
2002	3,260	3,540	3,470	4,070	4,310	4,860
2003	3,265	3,560	3,450	3,920	4,300	4,650

Table 2.2.5 Distance (in ft), baseline to channel thalweg						
	Cross-section line					
Date	D-west	1	2	4	5	7
1928	15,550	13,240	11,470	11,250	11,230	10,900
1940	11,470	9,100	9,500	9,130	9,570	9,720
1945	10,800	9,400	9,200	9,220	9,260	9,590
1948	10,680	9,300	8,920	9,140	9,580	9,620
1954	9,440	8,100	8,100	8,460	9,090	9,250
1956	8,750	7,900	7,840	8,000	8,850	9,650
1960	8,230	7,460	7,510	8,290	8,950	9,230
1963	7,630	7,340	7,270	7,890	9,190	9,260
1966	7,060	6,640	6,910	7,720	8,820	9,100
1972	6,520	6,020	6,410	7,410	8,220	9,390
1978	5,640	5,620	5,960	7,590	8,620	9,400
1993	5,150	5,330	5,100	6,850	8,650	8,180
1996	4,720	5,410	5,130	6,450	9,230	8,590
1997	4,880	5,240	5,280	7,850	9,550	11,000
1998	4,990	5,200	5,430	8,600	9,880	10,160
1999	5,220	5,300	5,550	8,660	9,510	9,620
2000	5,650	5,280	5,480	8,630	9,770	9,420
2001	5,390	5,360	5,440	8,680	9,540	10,220
2002	5,310	5,500	5,470	8,620	9,190	9,130
2003	5,470	5,850	5,800	9,280	9,490	10,340

Channel Bathymetry Changes

As part of the analysis, we examined the progressive changes in bathymetry from one survey date to the next. The most useful comparison for this report is the summary difference plot showing the changes between 1993 and 2003 (Figure 2.2.42). The figure reflects the following geomorphic changes:

1. West of cross-line 2, the bottom became deeper as the thalwegs clustered along one path during the 1980s and 1990s. The channel was unable to continue moving northward, and as a result, the bottom became deeper as the flow was concentrated against the shore.
2. In the area between cross-lines 3 and 4, the process of the channel developing a platform to the south is reflected in the red zone south of the thalwegs.
3. From cross-lines 4 to 7, the flow was concentrated in a narrow zone shown by the thalweg paths, resulting in bottom scour.
4. From cross-lines 2 to 8, there is no evidence that the bottom is deepening near the spits or islands (i.e., the channel is not progressively moving north). This conclusion is verified by examining the cross-section curves (shown earlier).

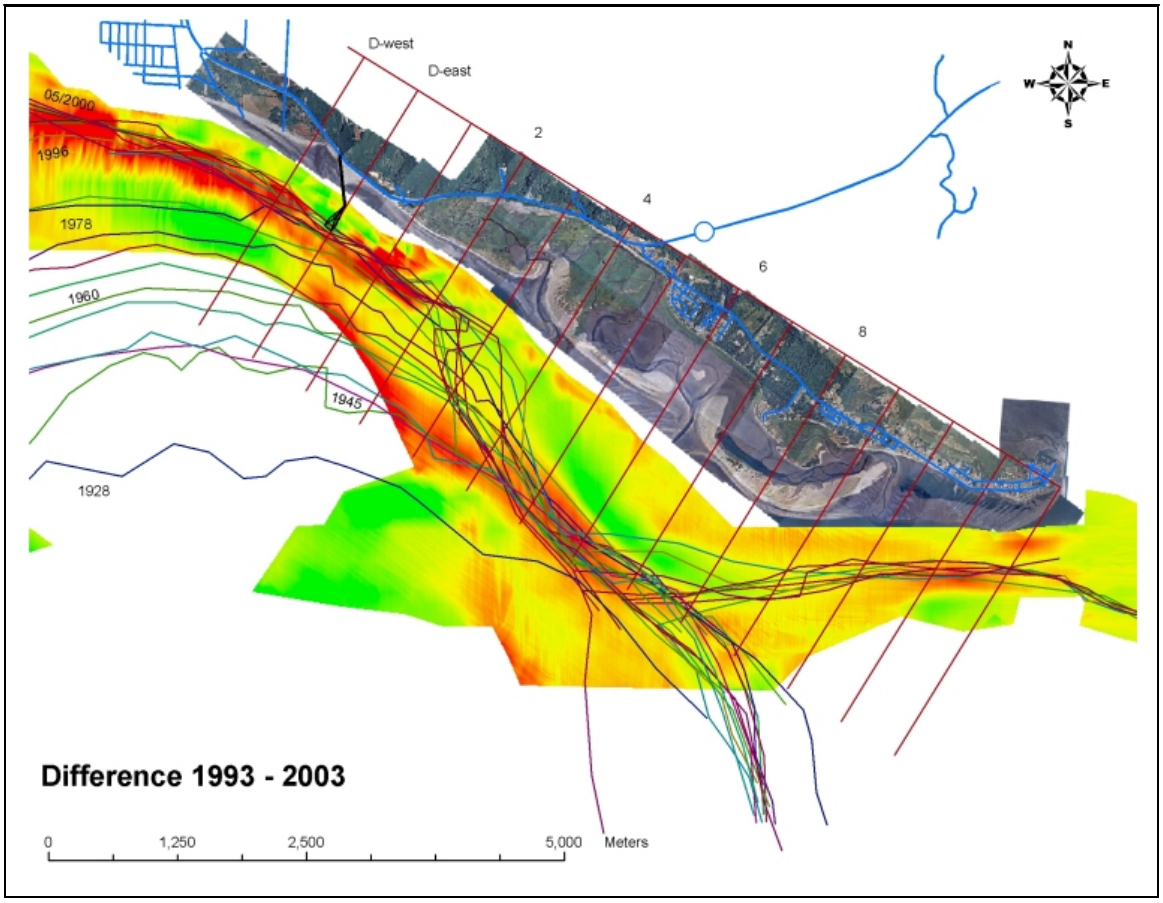

Figure 2.2.42. Difference plot showing bottom elevation changes between 1993 and 2003. Red means the bottom became deeper, while green means the bottom became shallower over the decade. Background photo mosaic: 2002. Thalwegs: 1928 – 2002. Individual thalwegs are shown in Figures 2.2.4 – 2.2.24.

References

Hands, E. B. 2000. "Chapter 3, Geomorphology," In: Kraus, N. C. (editor), Study of Navigation Channel Feasibility, Willapa Bay, Washington. Technical Report ERDC/CHL TR-00-6, Engineer Research and Development Center, Vicksburg, MS.

Jackson, D., Allen, T.M., and Lowell, S. M. 1997. SR-105: Geological Study of the North Channel of Willapa Bay – Vicinity of north Cove, Washington. Geotechnical Report, Willapa Bat Channel Restoration Project, C.S. 2532, OL- 2431, Washington State Department of Transportation, Olympia, WA.

Komar, P.D. 1998. *The Pacific Northwest Coast: Living with the Shores of Oregon and Washington.* Duke University Press, Durham, NC.

Kraus, N.C. (Editor). 2000. Study of Navigation Channel Feasibility, Willapa Bay, Washington. Technical Report ERDC/CHL TR-00-6, Engineer Research and Development Center, Vicksburg, MS.

Morang, A. 2003. Photographic Archives of the Beach Erosion Board. *Shore and Beach*, Vol. 71, No. 4, pp. 17-21.

Morton, R.A., Purcell, N. A., and Peterson, R. L. 2002. Large-scale Cycles of Holocene Deposition and Erosion at the entrance to Willapa Bay, Washington – Implications for Future Land Loss and Coastal Change, Open File Report 2002-46, U.S. geological Survey, St. Petersburg, FL, 124 p.

Pacific International Engineering, 1998. SR-105 Emergency Stabilization Project, Monitoring Program Report #9, October 24, 1998. Monitoring report prepared for Pacific County, Washington State Department of Transportation, Pacific International Engineering, Edmonds, WA.

Ruggiero P., and Voigt, B. 2000. Beach Monitoring in the Columbia River littoral cell, 1997-2000, Publication Number 00-06-26, Coastal Monitoring & Analysis Program, Washington Department of Ecology, 113 pp.

Terich, T., and Levenseller, T. 1986. The Severe Erosion of Cape Shoalwater, Washington. *Journal of Coastal Research,* Vol. 2, No. 4, pp. 465-477.

2.2.3 Linking Reservation Erosion to Climate and Other Factors[5]

Introduction

Section 2.2.3 explores possible links between climatic processes and morphologic changes in the vicinity of the Shoalwater Bay Indian Reservation (Shoalwater Reservation) on the northern shore of Willapa Bay, Washington.

Hypothesis

The hypothesis to be tested is that climate variations (such as changing intensity, frequency, or location of storms, rainfall, sea level elevation, and water temperature) could have combined to modify river discharge, nearshore sediment transport, tidal channel migration, or rates of shore erosion is such a way as to be responsible for a significant portion of the land and cove losses in and near the Shoalwater Reservation. Techniques for exploring possible erosion/climate links were developed that would apply also to event linkages that were non-climatologic and not representable in terms of annual time series, but that could have modified the erosion patterns. Examples of such events are fluctuating numbers of major Willapa Bay entrance channels, existence and size of channels connecting Willapa Bay to North Cove, stages of the Cape Shoalwater Spit Cycle, the construction of SR-105 Dike, and alternating episodes of dredging and non-dredging.

Background

Most U.S. Army Corps of Engineers (USACE) design plans consider climate. Climate can, in general, alter the effectiveness of various engineering alternatives. For this study, climate analysis is of more than customary importance. The Pacific Ocean is known to undergo substantial changes not just seasonally, but on interannual, decadal, and longer time scales (e.g., Wooster 1960, Bjerknes 1972, Wyrki, 1973, Ebbesmeyer and Coomes 1989, Ebbesmeyer, Coomes, and Tangborn 1993). On the decadal scale, physical and biological factors in the North Pacific have been reported to undergo major changes linked to a climate index known as the PDO or Pacific Decadal Oscillation (Trenberth and Hurrell, 1994, Trenberth and Hoar 1996, Hare and Mantua 2000, Chavez et al. 2003). On the interannual scale, rapid progress is being made relating changes in ocean dynamics to phases of the global climate cycle known as the El Niño Southern Oscillation (ENSO). ENSO is primarily a tropical climate cycle, but has a global influence. It is reportedly the strongest signal in the interannual variation of ocean-atmosphere system and demonstrably correlates with landforms changes in the Pacific Northwest as well as weather and biology in the region. Andrews (1965), Richey et al. (1966), Terich and Levenseller (1986), and Shepsis, Hosey, and Phillips (1996) describe cyclic movements of the ocean extension of the main Willapa Channel where it crosses the Willapa ebb delta. A recent study (Kraus 2000) documented ten cycles of massive sediment movement on the Willapa ebb delta and tied them to El Niño. The channel and ebb delta sediment dynamics follow predictable patterns for years then repeat these patterns during subsequent cycles.

All ten ebb delta cycles involved counterclockwise rotation of the Willapa bar channel and sand shoals in the entrance. Each cycle began during the El Niño phase of an ENSO cycle. The recorded cycles of channel rotation and sediment circulation persisted for 5 to 27 years before the next cycle began

[5] Written by Edward B. Hands, Consultant to U.S. Army Engineer Research and Development Center, Coastal and Hydraulics Laboratory, Vicksburg, MS.

with the initiation of a new outlet on the northern portion of the ebb shoal. During the early phase of each cycle, the bar channel is aligned toward the northwest. Survey records clearly show position, depth, alignment, and rate of rotation of the bar channel are synchronized through the cycle. Massive shoals on the ebb delta predictably change size, location, and stability during these cycles (Hands 2000a). A short record of erosion at Cape Shoalwater, just three km west of the Shoalwater Reservation, suggests that shore erosion accelerates toward the end of the cycles and then declines (as do channel migration rates) for several years following El Niños. The influences of ebb channel cycles, ENSO, and other climate variables on the Shoalwater Reservation erosion problems are investigated here in the context of recent findings that climate changes are more understandable and significant that formerly recognized.

Methodology

The science of geomorphology systematically examines, classifies, and interprets landforms. This section discusses the methods for developing a number of long-term geomorphic time series to quantify rates of change related to the evolution of the north shore of Willapa Bay in general and to the historic losses around North Cove in particular. Corresponding climatologic time series are then developed to identify the timing and magnitude of forces that potentially drove or moderated the geomorphic changes. The two types of time series, geomorphic and climatologic, are analyzed in various ways (primarily graphically and statistically) to identify possible direct links.

For this portion of the investigation, the study area centered on the Shoalwater Reservation, but also extended a considerable distance beyond its boundaries in order to assess larger scale processes to which reservation erosion may be simply the local response. Accordingly, the northern boundary of study area extends along the present-day north shore of Willapa Bay from Cape Shoalwater eastward to Toke Point, Washington. The southern boundary coincides with the south side of the 1930 main tidal channel between these same two meridians.

Channels, spits, peninsulas, and islands within these bounds are subject to rapid changes. *Erosion* (for this chapter, loss of emergent and shallow lands) prevails. Erosion follows trends as well as cycles that are well documented by charts and aerial photographs. Climatologic time series are calculated using meteorological measurements and compared to the geomorphic time series. Statistical comparisons were accomplished by transforming high-frequency measurements (e.g., hourly measurements of waves over 15-minutes intervals and sampled at many Hz) into times series of parameters at longer intervals matching intervals at which the geomorphic responses were updated. The basic climatic times series were thus reduced to representative annual series (usually of extremes). For graphical comparison, additional series were calculated to obtain typical monthly values so that brief, but unusual climate extremes would not be diluted, lagged responses not obscured, and processes that led responses could be eliminated as causes.

Geomorphic Losses

Features Quantified in Time Series

To extrapolate past erosion and to predict likely future losses as well as aid in the selection of engineering alternatives at the Shoalwater Reservation, several distinct morphologic features were defined and their rates of change were quantified. The chosen morphologic features are listed in Table 2.2.6. Changes in the first four features will be treated as the *primary responses* for which explanations and mitigation are sought. Which processes were the dominate drivers for the primary responses was sought by looking for correlated fluctuations in the last three features listed in Table 2.2.6, in events mentioned in

the Introduction, and in climate-related process to be discussed in the next section. Engineering alternatives, designed to mitigate losses represented by the first four features, can then be better evaluated. The last three morphologic features are of thus of interest only to the extent they might relate to and possibly explain changes in the four primary features.

Table 2.2.6
Geomorphology

Geomorphologic Feature	Measurements Made to Quantify Feature
1. Shoreline Position	Locations of the shore at equal-spaced cross-section lines along the bay- or South-side of Graveyard Spit and associated island(s). For dates of post-1931 USACE charts, Washington Department of Ecology (WADOE) surveys, and USGS T-Sheets, and rectified aerial photographs of the study area.
2. Plan Area of Graveyard Spit	As digitized east of a common meridian selected near the west side of North Cove. For same dates indicate above.
3. Plan Area of Islands East of Graveyard Spit	Digitized the charted shorelines from historic surveys and approximate water line on USACE and Washington Department of Ecology digital surveys and photographs.
4. Area of North Cove	As defined by charted shorelines on USACE and early historic survey charts, as well as recent surveyed shorelines. All available dates unless there are multiple surveys per year, in which case the most consistent representative time of the year was chosen. Used USACE surveys up to 1978 and rectified photos and WDOE surveys thereafter. Operational definition given in subsequent Table.
5. Channel Cross-Sectional Area of the Willapa Bay Tidal Channel On the South Side of North Cove	At fixed locations (cross-sections) along a dog-legged baseline that roughly parallels the average alignment of North Channel. Areas were measured below the highest common datum included on both North and South sides of the Channel on every survey.
6. Depth Contour Location in Channel	Coordinates of where -18, -24, -30, and -42 ft contours intersect the North and South slopes of the Channel for each cross section.
7. Thalweg Location	Coordinates of deepest interpolated point in channel for each cross section.

Bathymetry Sources

The Seattle District (NWS) has conducted on the order of a thousand hydrographic surveys of various portions of Willapa Bay. Between 1927 and 1978, NWS surveyed the entire entrance to Willapa Bay annually (primarily in July and August) and prepared charts for each year. Between 1852 and 1922, charts were prepared less frequently. After 1967, when Federal maintenance dredging for the Willapa River channel ceased, NWS began surveying only portions of the Bay near the navigation channel.

For a general understanding of study area, sixty NWS bathymetric charts were examined from the years 1852 to 1978, plus digital sounding files from 12 annual surveys covering the years 1981-84, 1993, and 1996-2002. Because collection of consistent, relevant meteorological data started about 1928, and the pre-1920 bathymetric surveys were at intervals of several years, bathymetric features were quantified and reduced to annual time series using a subset of the geomorphic data: 31 annual surveys between 1928 and 2002 and a set of aerial photographs. With the exceptions of 2000-2002, smaller scale versions of all charts consulted in this study can be reviewed in Appendix A of Kraus 2000.

Detailed, quasi-monthly surveys conducted in support of this study were not included in the climate investigations. These recent measurements document details of rapid change within a smaller area over a period of time too short to correlate with climate. Their relevance to the overall study is presented in another chapter.

Photography Analyzed

Approximately 200 oblique and vertical photographs from NWS and ERDC/CHL archives were reviewed in developing hypotheses about erosion patterns. A subset of 28 vertical photographs (covering years 1978 to 2000) was selected for digitization to quantify island and spit changes when surveys were infrequent.

Primary Geomorphic Time Series

Area measurements were chosen to quantify Shoalwater Reservation losses based on the available long-term chart and photographic records in a manner that would allow statistical and graphical exploration of links with climate. Three physiographic units were specified for area determinations: North Cove lagoon, Graveyard Spit, and the islands that form at the eastern end of Graveyard Spit. Graveyard Spit and the islands constitute the southern boundary of North Cove. Table 2.2.7 lists the operational definitions of these areas.

Table 2.2.7
Bay and land area definitions

BAY AREA (also see Figure 2.2.43)
North boundary. For charts: As drawn. For photographs, boundary set at landward (north) edge of the lumber in the western bay. Further east (near the town) boundary set along base of the revetment (where the white zone met the bay.)
West boundary. For charts: As drawn, approx. where bog drainage ditch enters the bay. For photographs: The west edge of the bay was difficult because it was unclear where the wetted bound was, but tried to set between tidal grass and trees.
South boundary. Along high tide line of Graveyard spit, and from there across the narrowest distance between spit and sand bar/island, and across narrowest distance from island to sand spit extending south of monument "Jim." If there is no obvious minimal opening between the easternmost island and the eastern spit, a line is drawn extending south from "Jim" and where this line intersects the shore, a line is drawn to the island across the opening to the west. For photographs: Coincides with the north boundary of the islands and the spit.
East boundary. For charts and photographs: If a spit does not extend south from the mainland near monument "Jim," then a line is drawn due south from "Jim" to the sand bar offshore and this line serves as the east boundary. (This procedure necessary because most of the USACE charts do not extend east far enough to determine the full size of the eastern islands). The line from monument JIM was drawn to the closest part of the adjacent island, with the line typically at an azimuth of 200 - 270 deg.
GRAVEYARD SPIT AREA (also see Figure 2.2.43)
Pre-1955: Original spit. West boundary defined by a line drawn from the westernmost point of the bay across the narrow extent of the spit (approx. SW-NE orientation). Once the spit is wider than approx. 5 mm on paper charts, line is drawn due south from the west point of bay. For photographs: Seaward boundary chosen to be the wet/dry line. The north side of the spit was approximately the line where bright red vegetation met dark red vegetation (for infrared photographs).
ISLANDS 1, 2, and 3 (also see Figure 2.2.43) **(any island directly east of 1 was labeled 2, and any additional island was labeled 3)**
For charts and photographs: Same criteria as Graveyard Spit. The entire area of Island 2 was included even if the east boundary of the island extended further east than the east boundary of the bay.

By digitizing the area of North Cove, Graveyard Spit, and the 1-to-3 islands, five geomorphic time series were determined. Seventy-two quasi-annual area measurements comprise each series (1928 to 2001). At least one island appears on 90 percent of the charts. Two appear on 43 percent, and three appear about one percent of the time. Time series of *annual* area changes were interpolated from each of the initial five time series based on the dates of the area measurements. The second and third islands appear too infrequently to be very useful by themselves for correlations. Therefore the island areas were combined into a single time series *of total island area*. Another time series, *land area* refers to the sum of the total island area plus spit areas (Graveyard and an earlier spit[6] to the south of Graveyard Spit). The land area series is assumed to be a reasonable representation of the volume of emergent sand at the southern boundary to North Cove because there is no data on elevation changes.

Figure 2.2. 43. Nomenclature and definitions of areas for which losses were quantified and for which causes and predictions are sought. A time series of annual changes in area were developed for each of the geomorphic features shown in bold (Spits, Islands, and North Cove).

In addition to the three primary time series characterizing area losses, several other time series where developed to characterize the location, shape, cross-section, and depth of the Willapa North Channel based on interpolating survey data for the 19 ranges shown in Figure 2.2.44. These channel changes were treated as processes (in addition to climate) whose role in the area losses needed examining. Channel time series are, therefore, discussed more in the following *Climate Section* along with other independent processes like dredging cycles, climate phases, and different events whose links with area losses were questioned.

[6] The unnamed spit south of Graveyard Spit can be seen in Figures 2.2.26 - 2.2.28. Its area was included in the s*pit time series* until erosion finally completely eliminated it in 1945.

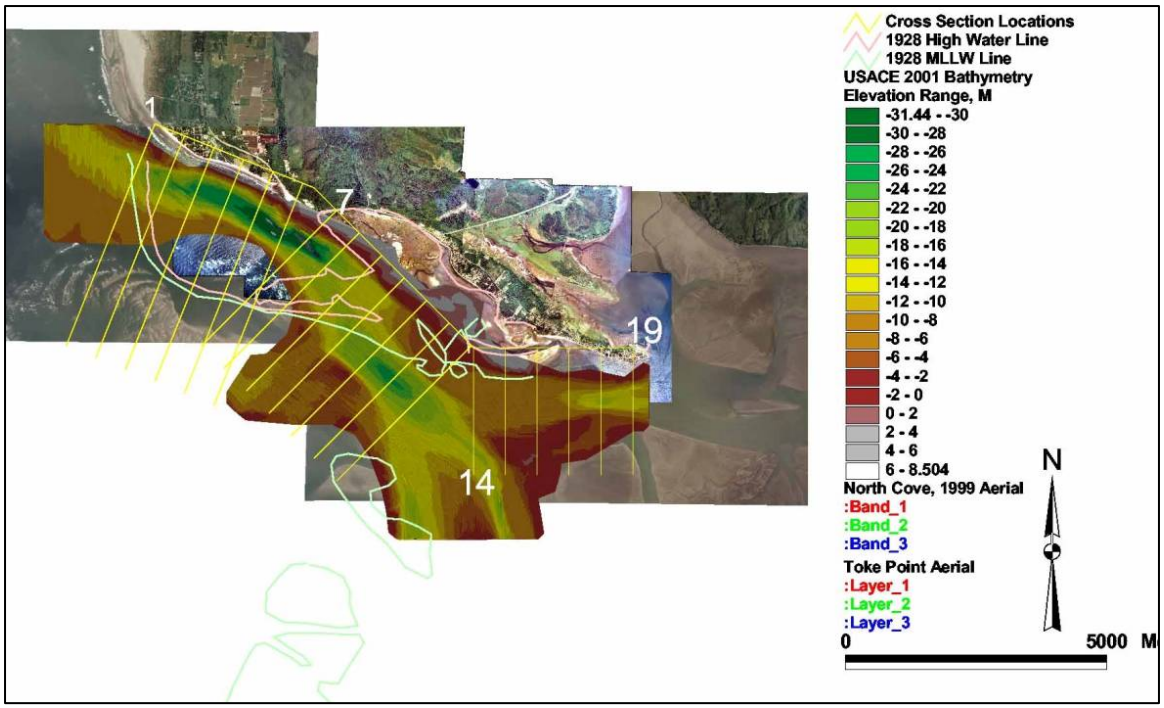

Figure 2.2. 44. Nineteen range lines on which cross-sections were cut to characterize North Channel changes. Ranges 7-13 are approximately perpendicular to the channel opposite North Cove and the Shoalwater Reservation.

Climate and Other Potential Explanatory Processes

Prior Climate Studies

Storm paths across the north Pacific shift southward during El Niños. Seymour (1998); Inman, Jenkins, and Elwany (1996); and Komar (1986, 1997, and 1998) attribute dramatic increases in shore damage along the coasts of California, Oregon, and Washington to significantly higher waves coincident with the 1982 and 1998 El Niños. Changes in storm paths and frequency as well as increased wave heights and altered wave directions during El Niño are other potential factors that could alter erosion patterns at Willapa Bay.

Six Specific climate processes listed in Table 2.2.8 were the basis for calculating a larger number of potential erosion parameters (column 2). Measurements of the parameters were obtained from USACE, National Ocean Service (NOS), and U.S. Geological Survey (USGS) databases. Trends, cycles, and extremes in the parameter time series were compared with perturbations in the geomorphic time series to identify any lagged or simultaneous fluctuations between climate and erosion. Locations where the climate parameters where measured are indicated in Table 2.2.8.

Table 2.2.8
Climatology

PROCESSES	PARAMETERS	UNITS
Storm Potential	Sea Surface Temperature	deg C
Waves	Height, Period, Direction	m, sec, deg
Wave energy factor	Directional energy component	m^2sec
Wind	Wind speed	m/sec
	Wind stress	m^2/sec^2
Water Surface Elevation	Mean from tide gages	m
Run off	Ave summed stream discharges	m^3 /sec
FACTORS	**EVENTS, CYCLES, AND PHASES**	**UNITS**
ENSO	Cyclic	Indexed by year/month
PDO	Phases	Indexed by year
Storminess between surveys	Number of occurrences of exceedance* based on criteria including wave height, water levels, and wind vectors.	nondimensional
Storminess	hours	Duration of exceedance*
SR-105 Dike and Groin	Before and After	nondimensional
Inlet Channel Orientation	Progressive	nondimensional
Stage in Cape Shoalwater Spit	Cyclic	nondimensional
Dredging Episodes	Three periods of dredging separated by four periods of no dredging	Indexed by year
Spit Breaches	Times when erosion cut through Graveyard Spit or one of associated islands to the east.	Indexed by date

*Exceedances can be defined by wind and wave data from:
NDBC Station 46010 off the mouth of the Columbia River.
NDBC Station 46029 farther offshore of Station 46010.
NDBC Station 46041 Offshore of Point Grenville.
NDBC Station 46050 off Oregon.
Pacific Ocean Phase II WIS Station 2046 off the mouth of the Columbia River, OR.
Coast of California Information Data Station 05401 over Grays Canyon, WA.
Coast of California Information Data Station 03601 off Long Beach Peninsula, WA.

Climate Parameters

Conventional Definitions

The term El Niño-Southern Oscillation (ENSO) acknowledges that cycles between El Niño and La Niña phases and movement of atmospheric pressure gradients (both so prominent in the equatorial Pacific) are expressions of a single global phenomenon that couples oceanic and atmospheric cycles.

Quinn et al. (1978) established the years of early El Niños. Quinn's index is widely cited by climatologists and has been used in other coastal investigations (e.g., Seymour 1998). We adopt it here to investigate the timing between El Niños and early changes at North Cove.

The warm phase of equatorial sea surface temperatures is referred to as El Niño. The cool phase is La Niña. Deviations in sea surface temperatures from their base values for the period 1951-1979 are the basis for the modern definition for El Niño and La Niña (Trenberth 1977). These deviations, **sstoi** (for sea surface temperature optimum interpolation indices) were obtained from the NOAA database. The sea surface temperature in a specific part of equatorial Pacific Ocean must deviate in excess of a specified threshold for a certain period of time to initiate or end the different ENSO phases (Figure 2.2.45).

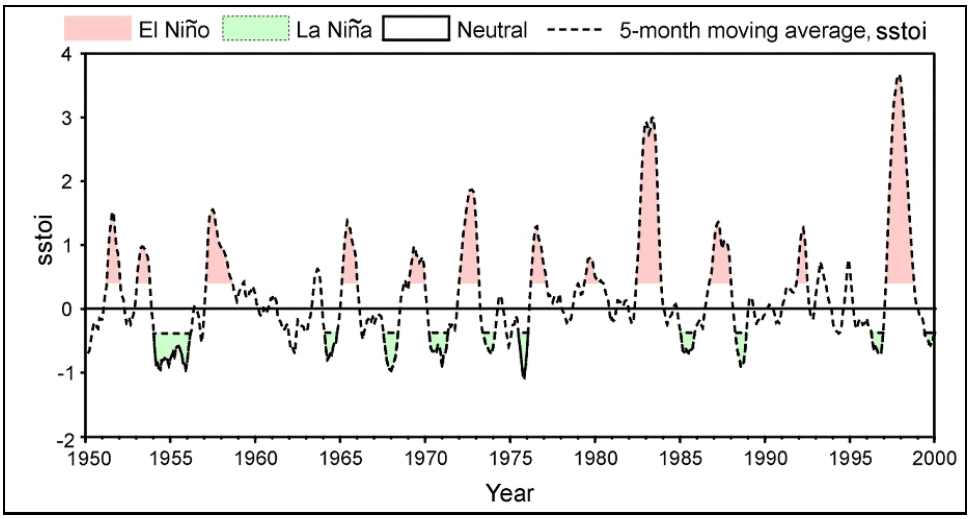

Figure 2.2. 45. Sea surface temperature anomalies (sstoi) are the basis for distinguishing El Niño and La Niña phases in post-1950 ENSO cycles.

Modified Quinn Index

The sstoi data do not exist, however, prior to 1951. For this study, an index to ENSO that spans 1927 to present was needed. Therefore, a modified Quinn-like index for the period 1980 to present was created that optimized the fit during the overlap between Quinn's multifactor index and the universal modern index, sstoi (Figure 2.2.46).

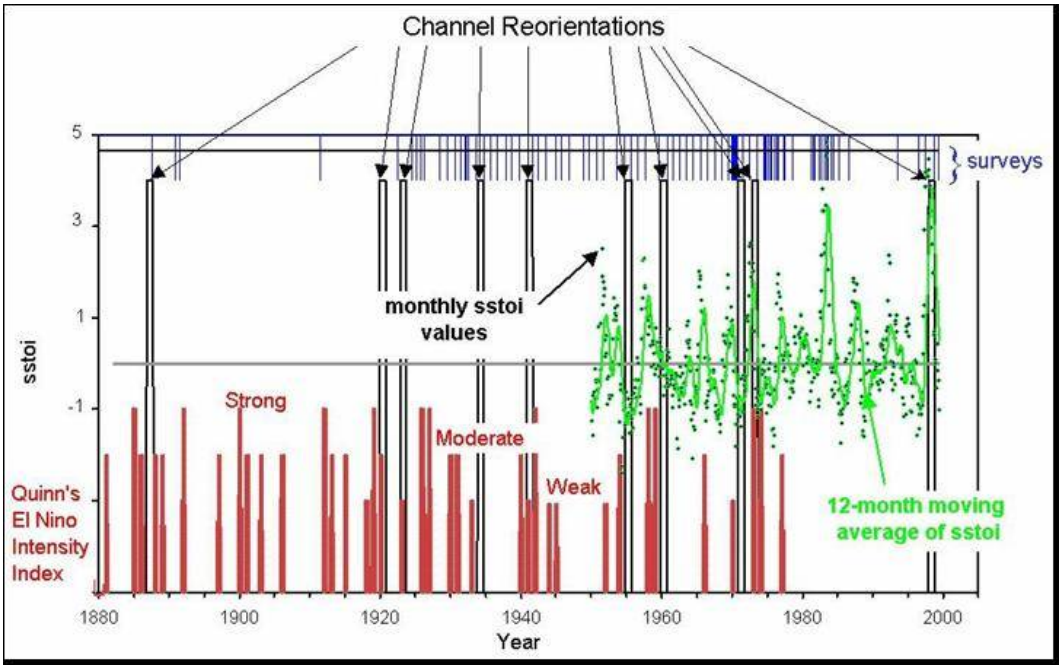

Figure 2.2. 46. Quinn's El Niño index identifies pre-1950 El Niños. A modified El Niño index, used in subsequent figures, is based on the correspondence between Quinn and sstoi indices in the overlap 1950-1977. Cycles of bar channel migration and sediment dynamics on the ebb delta are separated by vertical 6-month wide bars that can be seen to correlate well with El Niños.

Quinn did not attempt to specify the month of initiation or the duration of El Niños. Therefore a second modification was developed here to represent Quinn's index as bars on a monthly time line (Figure 2.2.46). The bars are centered on 31 December because the typical El Niño is most distinct at that time in the tropics and causes warmest waters there at the end of the calendar year. Bar widths were arbitrarily set to span the six months from 1 October to 31 March. After 1980, the width of the vertical bars in figures later in this chapter linking geomorphology and climate reflects the actual onset and duration of El Niños as identified by sstoi. Heights of the bars reflect Quinn's intensity categories. Note that where bar and smooth-curve indices overlap, all of Quinn's bars align with a peak in the sstoi index (Figure 2.2.46).

Hands (2000a) showed that the El Niños years, during which northwest-oriented incipient bar channels formed, were years in which waves tended to be higher from the southwest. But, the local climate factor that correlated best with El Niño was the long-term sea level. New bar channels formed when the winter sea levels were unusually high even for that time of year. The correspondence shown in Figure 2.2.46 suggests that tidal flows out of Willapa Bay are most capable of eroding new and shorter bar channels under conditions when monthly mean sea levels are on the order of 0.7 to 1 ft higher than seasonally normal persistently for several months.

All entrance sediment recirculation cycles began with a new bar channel opening within a year of an El Niño. Hands (2000b 2000c) found evidence of repeated increases in monthly mean sea level on the order of 0.7 to 1 ft for several months during El Niño events that coincided with new channel initiation. However, the three primary geomorphic time series for North Cove failed to show as strong a link to ENSO.

Geomorphic Cycles, Events, and Phases

In addition to the four primary geomorphic features for which protection is sought, a number of other geomorphic features were quantified from a chronological series of charts and aerial photographs. Though not necessarily acting on North Cove problems, these neighboring processes might place North Cove losses in a broader context that would assist prediction of future trends in land and lagoon loss at North Cove and therefore aid in the selection of the best engineering response. These geomorphic processes were subjected to the same algorithms as the climate time series. Both represent possible explanatory processes potentially correlated with one of the four primary response time series (Shore, Spit, Islands, or Cove area losses).

Shore Rotation

The north shore of Willapa Bay has rotated clockwise around a pivot point near the Cove. Throughout most of this century the Bay Shore recessed rapidly at a fairly constant long-term rate near 150feet/year. Only recently does this rate decline. Lowell (1997) reports that the rapidly receding north shore encountered increasingly older, higher, and more consolidated sediments. Similarly resistant sediments may be present in the adjacent, relatively stable area behind the North Cove lagoon and in a second location of channel stability offshore of Empire Spit at eastern side of North Cove (Figure 2.2.43)

Statistics on the long-term trend in channel depth are given in Table 2.2.9 for each range shown in Figure 2.2.44. Because depths were usually well below keel clearance in this reach of the main channel, soundings were often far apart on the earlier surveys. Where the deepest parts of the channel were missed spuriously shallow depths corrupted the triangulated network from which the thalwegs were estimated. Thus noise entered the time series. The bold statistics never the less indicate statistically significant deepening at most ranges. Noteably, all but one of six ranges opposite North Cove fail to show

significant deepening. This section of the North Channel is also different in that it migrated southward significantly during two episodes.

Table 2.2.9
Trends in main Willapa Channel thalweg depth along the north shore

Cross Section Number	Number of Annual Surveys	Fill Trend m/year	Student's t-value	Std Error of Estimate	Correlation Coefficient
1	31	**-0.11**	**-6.71**	**1.93**	**-0.78**
2	32	**-0.1**	**-3.69**	**3.02**	**-0.56**
3	32	**-0.09**	**-2.62**	**4.19**	**-0.43**
4	32	**-0.09**	**-2.24**	**4.85**	**-0.38**
5	32	**-0.14**	**-2.74**	**5.84**	**-0.45**
6	32	**-0.17**	**-3.08**	**6.37**	**-0.49**
7	31	**-0.18**	**-2.95**	**6.72**	**-0.48**
8	31	**-0.08**	**-1.73**	**5.03**	**-0.31**
9	32	0	0.05	4.65	0.01
10	33	-0.03	-0.82	4.01	-0.15
11	33	**-0.09**	**-2.36**	**4.36**	**-0.39**
12	33	-0.07	-1.51	5.47	-0.26
13	33	0.01	0.28	5.98	0.05
14	32	**0.09**	**2.28**	**4.67**	**0.38**
15	32	0.01	0.66	1.44	0.12
16	21	0.01	0.69	1.16	0.16
17	33	**-0.16**	**-4.74**	**4.02**	**-0.65**
18	16	**-0.12**	**-3.23**	**2.07**	**-0.65**

Island Cycle

Major breaches through Graveyard Spit form new islands along the southern boundary of North Cove. The islands migrate eastward to a point south of middle of Tokeland Peninsula. There, their migration switches from eastward to northward. Much of the island sand eventually welds to the Peninsula near the location of Empire Spit in Figure 2.2.43.

The shoreline west of North Cove has persistently eroded northward at rates that increase toward the ocean. In contrast to this northward (clockwise) shoreline recession, the seaward end of the North Channel typically migrates southward across the ebb shoal while an offshore, but shore-tied submerged spit grows southward from Cape Shoalwater. This submerged spit seems to push the bar channel in its counterclockwise rotation. Periodically, southward channel migration is interrupted. At such times, multiple incipient outlets cross the spit. One of these new bar channels grows sufficiently to dissect the spit to the -18 feet MLLW contour, allowing ebb currents to flow directly seaward out of the main North Channel. At this stage, the distal end of the submerged spit becomes isolated from the Cape Shoalwater-attached spit. The resulting separate shoal, typically, begins migrating toward the southeast at a rate relatively rapid compared to previous rate of spit extension. In a few years this distinct sand body merges with other inner entrance shoals offshore of North Cove (Figures 2.2.43 and 2.2.47). Therefore, erosion opposite the reservation could conceivably be directly correlated with the El Niño-synchronized cycles on

the ebb delta. So, the periods of new bar channel initiation and the subsequent dates when the isolated shoal begins to migrate landward are two additional time series analyzed (along with climatologic time series) for correlations to North Cove erosion problems in an attempt to relate changes in annual North Cove erosion to larger sediment-movement and climate-change patterns.

Middle Channel Linked to North Cove

The channel that previously existed in the middle of the 6-mile-wide (20 km) entrance to Willapa Bay shared the Willapa Bay tidal prism with the North Channel. Middle and North Channels interacted in an area south of North Cove, and could have altered sediment movement patterns along the south side of the Cove.

It is convenient to use the term fairway to identify zones in which channels exist from time to time in Willapa Bay. The South Fairway lies off Leadbetter Point, which is the south boundary of the entrance. The North Fairway lies off the north shore. A prominent channel occupied the North Fairway on all of the examined historical charts (1852-1984) and all of the recent surveys. As the north shore receded and rotated, the North Channel rotated northward with it. Where the North Channel was in 1928, the 1993 63rd edition National Oceanic and Atmospheric Administration chart of Willapa Bay shows a Middle Channel almost as prominent. This Middle Channel began as a minor channel directly off Leadbetter Point in 1945. It grew gradually and migrated north and by the 1980s became the largest Middle Channel ever charted in Willapa Bay. As evidenced by USACE surveys in 1998 and 1999, it was considerably diminished in the 1990s by filling from the ocean end – a process still ongoing.

Risks to the northwestern side of North Cove are less significant. The existing barrier dune in this location of Graveyard Spit (a.k.a. Empire Spit) has a large hard Pleistocene rock terrace attached to the mainland and is been observed to be more resistant to erosion (see Engineering Appendix, section 2.1).

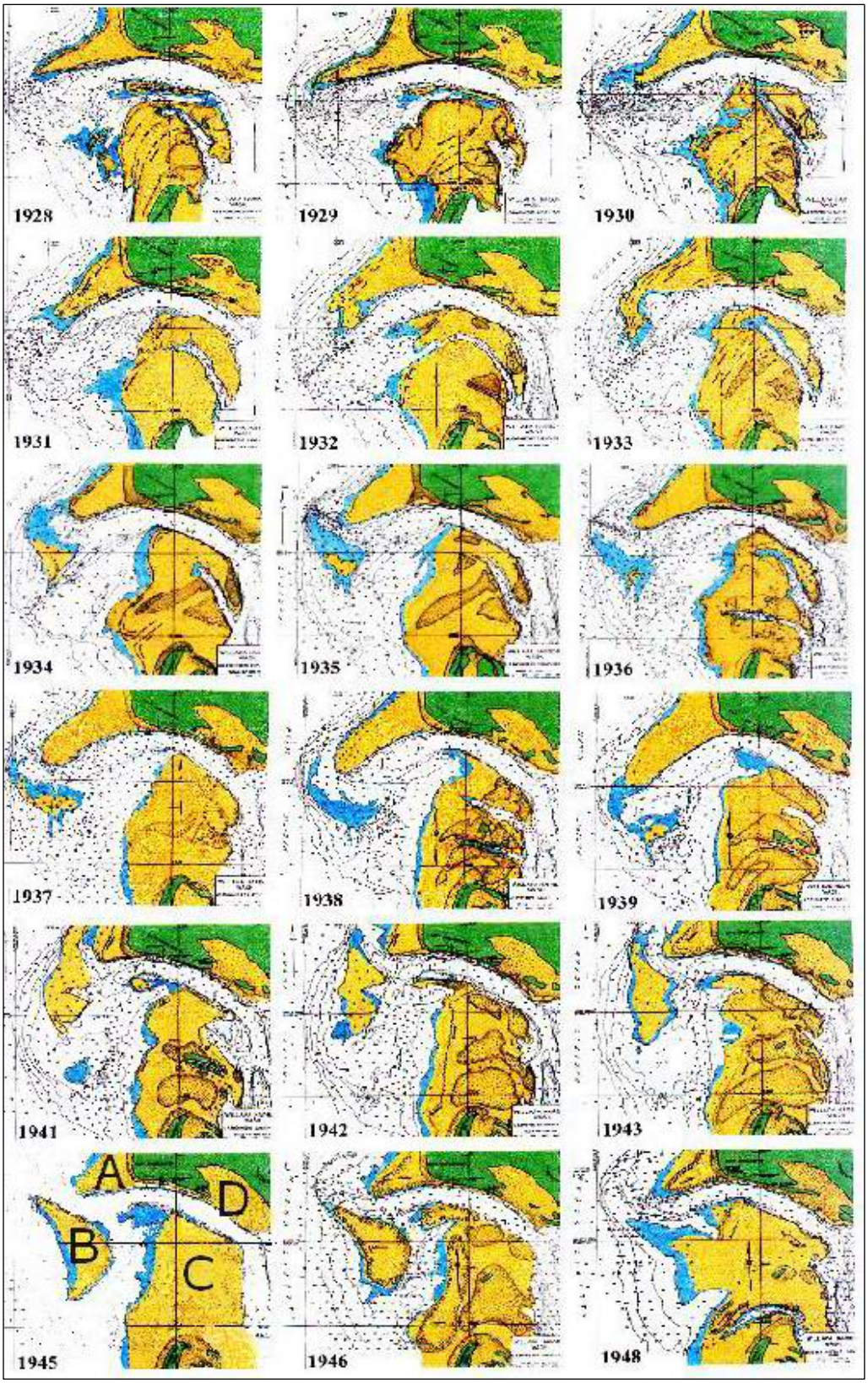

Figure 2.2. 47. Sequence of charts (1928-48) illustrating cycle of channel rotation and shoal migration. New bar channels dissect a submerged spit (A in lowest panel on left) creating a dynamic shoal (B) that migrates rapidly eastward to merge with other entrance shoals (C) near North Cove (D) in the 1945 panel.

Since at least 1928, the ebb currents emptying South Bay flowed north through two major channels that joined almost directly south of Empire Spit. Their combined flow joined with the Willapa River discharge near Empire Spit (Figure 2.2.43). This juncture is off the east edge of the panels shown in Figure 2.2.47. From there the ebb flowed northwest, past Graveyard Spit and to the Pacific Ocean (Figure 2.2.43). In the 1950s, the upper west limb of the channels draining South Bay began veering westward in a shortcut that joined the other South Bay and Willapa River flows approximately opposite Graveyard Spit. When the Middle Channel began to shoal in the 1980s, conservation of flow augmented the portion of the tidal prism that North Channel handled through the connection near the Willapa River and (probably to an even greater extent) through a new juncture south of Graveyard Spit. In response, along the reach near North Cove, the North Channel widened in cross-section primarily by cutting away its south bank. In the reach farther west, the channel enlarged by eroding deeper. Rerouting of flow when the Middle Channel shoaled thus seems to have been an important part of the southward shift of the main channel away from North Cove. The Middle Channel participated in diverting flow away from North Cove at the culmination of its growth-migration cycle that begun in 1945. The charts from 1928 to 1950 suggest part of a similar cycle. The latest diversion of South Bay flow appears, however, to have changed the bathymetry more profoundly. It thus seems unlikely that South Bay will ever channel so much of its tidal prism into the North Channel through the old confluence east of North Cove.

Non-climate Factors Linked to Geomorphic Loss

Bar Channel Cycle and Breaching into North Cove

Since 1930, five North Cove breaches have been mapped or photographed. Over this same period, there have been six complete cycles of sediment circulation at the outer entrance to Willapa Bay. Figure 2.2.48 shows these six sediment cycles bounded by vertical, dashed bars. Each began with the initiation of a new bar channel on the northern portion of the ebb delta. The bar channel grew wider and rotated counterclockwise as part of a large-scale sediment recirculation pattern described earlier and shown in Figure 2.2.47. Each cycle ended with the initiation of the next new bar channel. The dashed bars are 1-year wide because the date the cycle began within that year is unknown.

Vertical solid lines indicate the five times between 1930 and 2004 when mapped or photographed inlets opened into North Cove through Graveyard Spit or one of its associated islands.

Figure 2.2.48 also shows coincidences of spit breaches (width of blue bars indicating uncertainty of date), initiation of new bar channels (dashed bars), and El Niños as indicated by the modified Quinn index (short red bar for weak and larger bars for moderate and strong events).

In spite of North Cove's proximity to the massive sediment recirculation pattern at the Willapa Bay entrance, there is nothing in the timing of five documented breaches to support any direct relationship with the sediment recirculation cycle. The simultaneous occurrence of a new bar channel and an island breach in 1954 is reasonable, attributable to chance. Treating the two phenomena as independent random events, having return periods suggested by their occurrences in the 72-year record, the coincidence of both events in a given year would be less than a 1 (0.6) percent chance. The chance, however, that both would occur in the same year at least once over a 72-year interval is about 34 percent. Because null hypotheses are customarily rejected (effectively deciding the data are insufficient to support acceptance of a real connection) unless there is only a small chance (customarily 1, 5, or 10 percent) probability that the coincidence could have arisen by chance, the hypothesized connection is rejected. Assuming that the coincidence in 1954 arose by simply out of chance is therefore consistent with standard statistical testing.

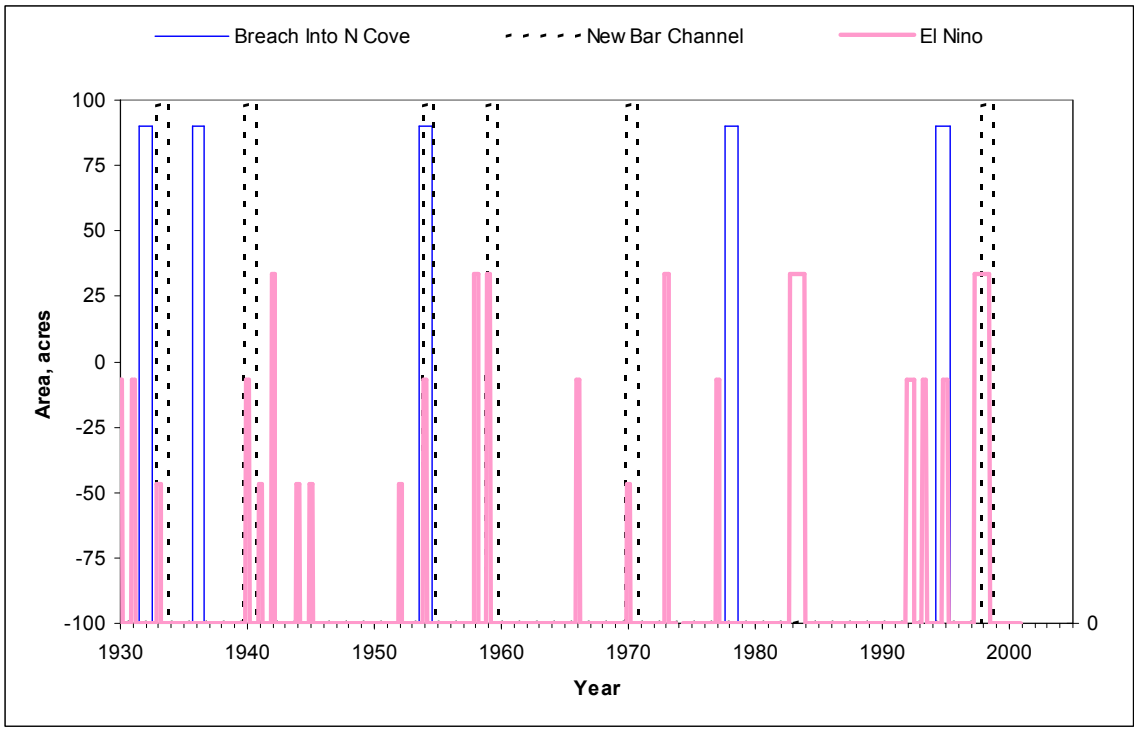

Figure 2.2. 48. Timing of breaches into North Cove, ebb delta sediment cycles, and El Niño.

Land Changes, and Breaching into North Cove

The correlation of North Cove breaches with the El Niños is substantially higher than the two bar channel/breach coincidences discussed in the previous paragraph. Four of the five breaches are linked to El Niños. In fact, only one breach (in 1935) did not occur within a year of an equatorially defined El Niño. That breach occurred when Graveyard spit had reached what is still its record length. If cove breaching were independent of El Niños, it would be logical to assign less than a one percent chance to four breaches following within a year of an El Niño. Because this is so unlikely, breaches into North Cove seem to be strongly dependent on some process promoted by El Niños.

Spit and Island Areas

Years of abrupt island growth always occurred when Graveyard Spit lost substantial area (Figure 2.2.49). This connection is, however, more definitional rather than causal. Breaches through the spit, if lasting, convert spit land, by definition, into islands or submerged shoals as described under the preceding section entitled "Geomorphic Cycles, Events, and Phases".

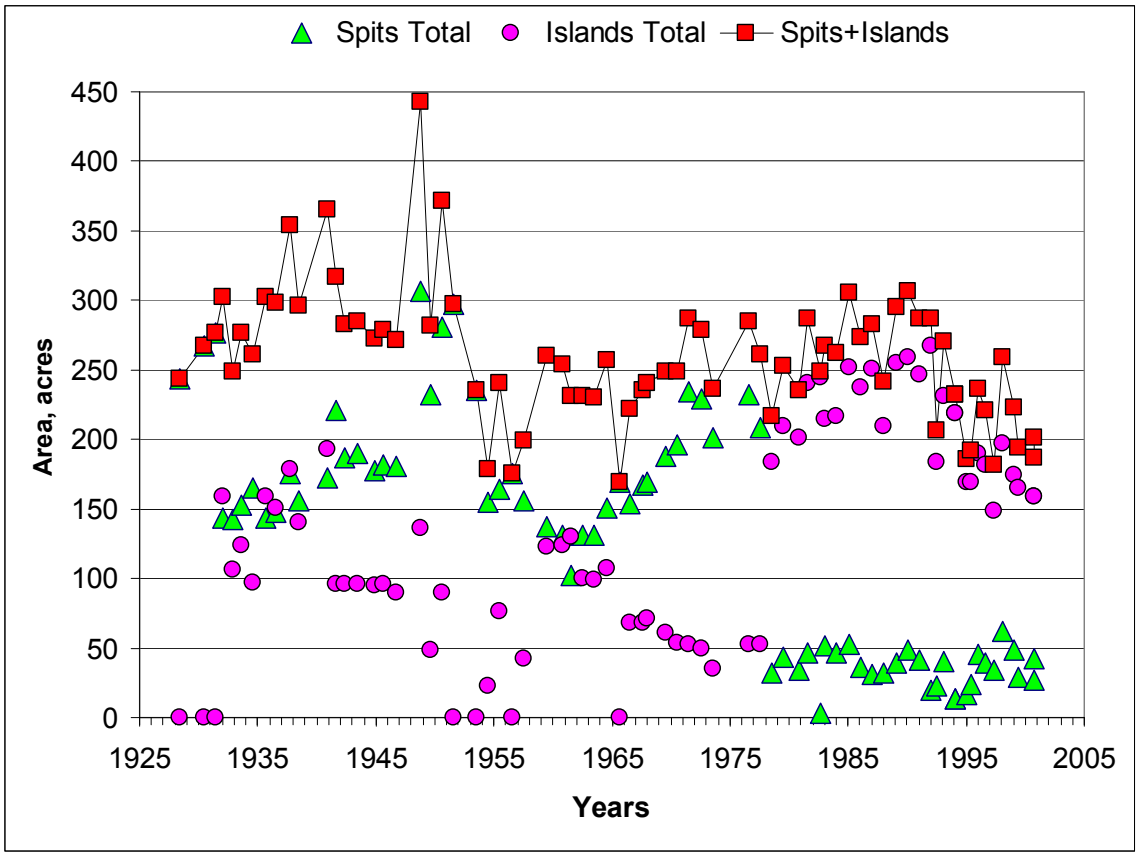

Figure 2.2. 49. Time series of land area changes.

North and Middle Channels Changes

Trends in North Channel depths were presented in Table 2.2.9. Based on measurements along the same ranges, a remarkably consistent pattern of lateral migration can be seen in Figure 2.2.50. The lower panel of Figure 2.2.50 shows the 19 range lines at which elevations were extracted from digital terrain surfaces based on 36 USACE annual surveys. These maximum depths are connected with straight lines in the upper panel. The lines are not intended to follow the channel between ranges, nor to track multiple channels – only the deepest depths along each of the 19 ranges. There are other methods to plot the data, but this display clearly divides the data into sets by survey date, indicates the chronology of each set, and highlights trends and their disruption. Progressively warmer colors are associated with the lines going from blue in 1928 to crimson in 2002.

Focusing first on the Bay entrance, in the western half of the plot, the channel migrated consistently northward. Lines spread evenly except for jumps after 1928 and 1978. These jumps reflect 12- and 15-year breaks in the sequence of otherwise nearly annual surveying. Rates of migration in the entrance were thus remarkably consistent over this 74-year record.

Moving eastward, toward the interior, rates of northward channel migration gradually diminish. Opposite North Cove, the pattern of persistent northward migration is disrupted. After the mid 1960s, northward channel movement essentially ceased in this reach. Then the channel reversed direction and moved slowly south until 1972. During the following year, the channel jumped farther south than it had ever moved in previously recorded years. Thus, in 1973, this section of the channel was at in its most southerly position in 55 years. Northward migration resumed the following year (1974) and continues

still, but at ever-slower rates. The channel position (in the reach south of North Cove) is now aligned along a path previous occupied in the 1960s. No explanation could be found in the climate data for why the 1972 path was the farthest north. Without modeling and subsurface sampling, it is not clear whether the cessation of northward migration in 1972 was related to impingement of the channel against more cohesive sediments or was strictly an improvement in bay-wide hydraulic efficiency in response to persistent widening of the entrance and the evolving basin shape. Whatever the cause, these changes in long-term channel behavior correlate with trends and perturbations in the primary geomorphic time series and suggest non-climate links to North Cove losses.

In 1971 (the year the channel reversed its direction of migration and began slowly moving south):

- The only significant period of increase in Cove area began. The spit and island's north shore moved south to accommodate a bigger lagoon. This unique period of minor, but significant, increase in Cove area lasted for 8 years.

In 1978 (the year prior to the huge shift southward):

- The phase of rapid island area loss, which had persisted for 18 years, ended.
- A long phase of rapid spit growth and slow total land area growth also ended.
- A 26-year period of spit area stability began that persists to the present day.

In 1993 the deepest portions of the channel south and east of North Cove resumed migration northward at rates that declined to the present time. In this latest phase of channel migration:

- The formerly stable-to-slowly growing area of sand south of North Cove began a period of rapid loss.

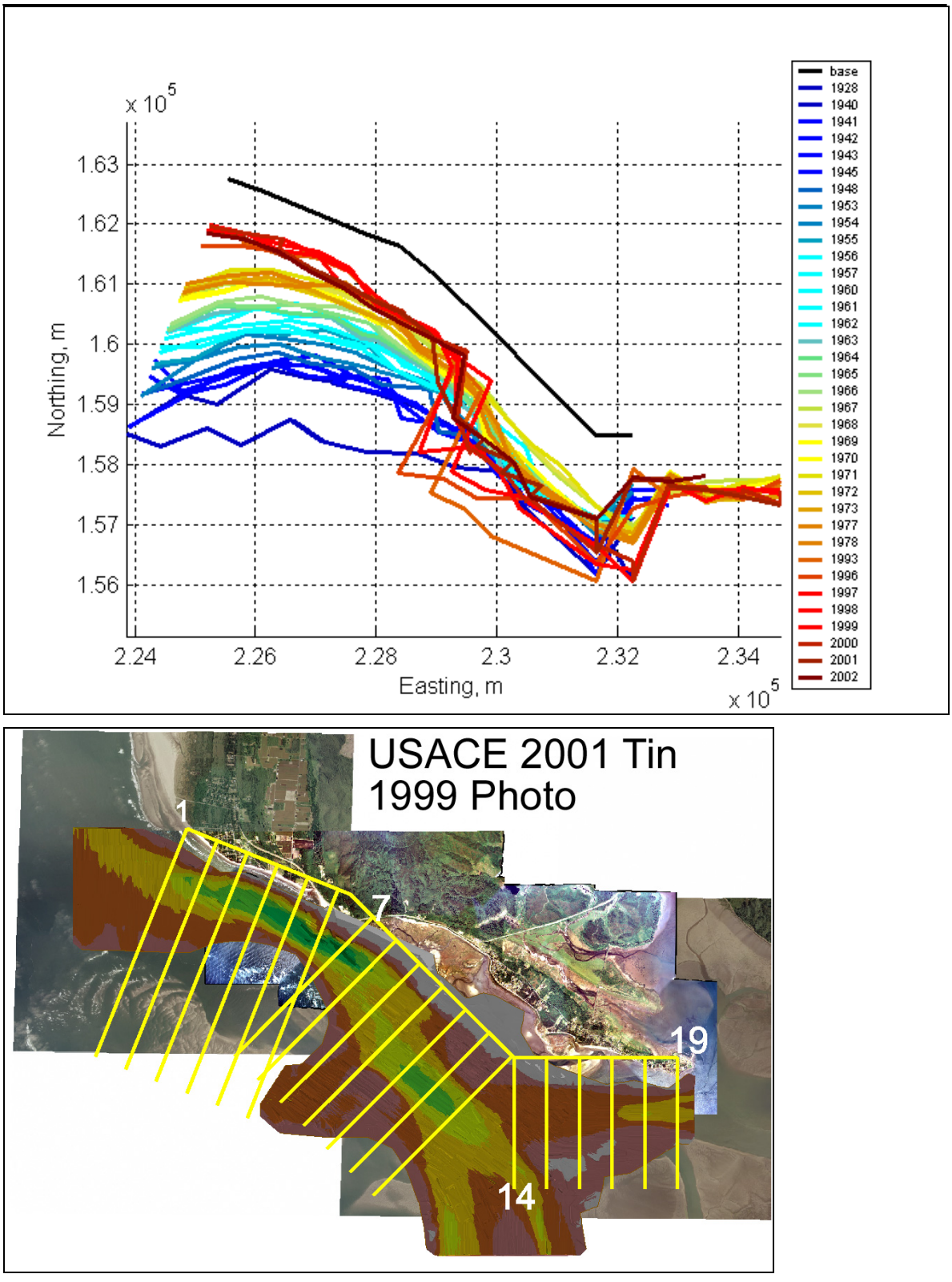

Figure 2.2. 50. Position of thalweg at 19 ranges (shown in lower panel) were determined from each of 36 USACE-survey-based surfaces and connected by lines in upper panel.

Climate Linked to Geomorphic Loss

Land Area Trends

As seen in Figure 2.2.49, the area of emergent land near North Cove displayed several strong trends:

- Early long-term gain: 1927 - 1937
- Large sustained rates of losses: late-1940s to 1950
- Slow gains in area: 1950 to 1988
- Persistent losses: late 1980's to present

The only suggestive link between climate and any of these trends is the onset of more frequent El Niños in the 1990s coincident with the land area switching from slow expansion over the previous 35 years to a period of rapid loss (compare Figures 2.2.48 and 2.2.49). During the 1990s, the magnitude of El Niños increased (Figure 2.2.45) and La Niña magnitudes declined. Based on a comprehensive analysis of sea surface temperature and atmospheric pressure records, Trenberth and Hoar (1997) and Trenberth, Brainard, and Hoar (1997) emphasized the unprecedented nature of a prolonged and intense warm period after 1976 and especially from 1990 to 1997. Even stronger evidence that the 1990s were atypical would have resulted if their analysis could have included the peak of the record-breaking El Niño of 1997-98. The atmospheric pressure record makes the 1990s appear more unusual than the equatorial temperature record, which is very similar to the anomalies calculated here (Figure 2.2.45). Trenberth's conclusion, that the climate of the 1990s cannot be accounted for solely by natural variability, may be questionable, but his identification of this period as highly unusual seems well-grounded.

Land and Cove Area Variations

Because spit and island areas are strongly correlated by the operational definition, the links examined next are between the sum of spit plus island series (total land area) and climate factors. Figures 2.2.51 and 2.2.52 fail to reveal any strong direct correlation of total land area with three climate indices. Climate parameters not shown in these two figures had even less correlation to these primary geomorphic changes. Though not strong, there are some indications of possible links.

Figure 2.2.51 compares changes in cove area with those of land area. Somewhat surprisingly, there is no sign of any connection among these area changes. Ocean-facing barrier islands often experience simultaneous losses of land and back barrier wetland areas. Storm induced erosion can cut away parts of barriers, while overwash and landward barrier migration reduce the area of the receiving lagoon. A further connection can arise afterwards when the lagoon areas emerge at accelerated rates due to sedimentation on storm-built shoals. The fact that these types of relationships have not been important at North Cove seems to be because the Cove has shrunk in area and the land migrated northward relatively continuously. As a consequence, increases in land erosion or cove reduction have been small in comparison to the cumulative effect of the continual changes. Instances were documented when enlargement of the openings between the islands were accompanied by formation of large flood shoals that reduced the area of the Cove (e.g., 1996 and 1998), but these brief couplings leave no lasting impact, due to the chronic long-term retreat of the spit. Thus, island breaching is of minor factor in land loss. It is a major factor in interior flooding, but that is discussed elsewhere.

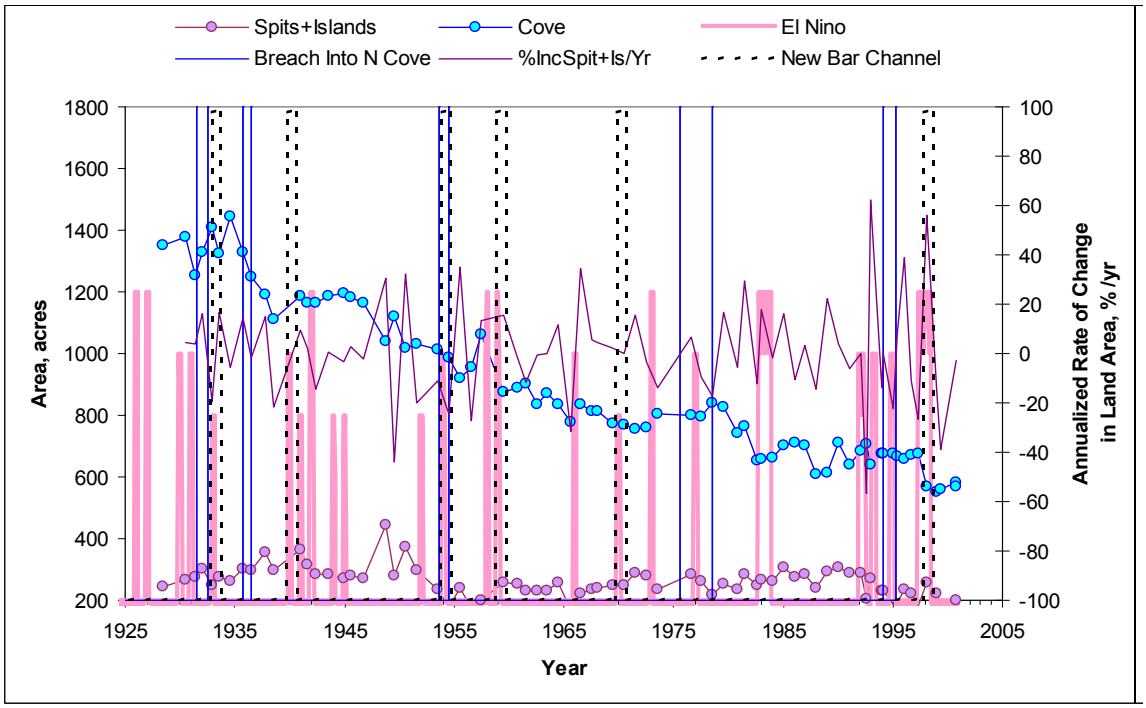

Figure 2.2. 51. History of land and cove loss and annualized percent loss of land compared to El Niño phases, ebb delta cycles and breaches into North Cove.

Annualized Percent Changes in Land Area

Land and Cove areas are represented in Figure 2.2.51 with circular symbols. Though no relationship was obvious between either of the areas and any climate parameter, some coincidences occur between the annualized relative rate of change of land area (shown as a percent change by the bare line) and both El Niño and the ebb delta cycle. For example the annualized rates of loss are extremely low (and sometimes the islands grow) during the years just before a new bar channel forms and losses often peak in the years following El Niño-synchronized bar channel initiation. These tendencies can be seen in Figure 2.2.52 by noting the behavior of the land area annualized relative rate of change (bare line) before and after El Niños (shown by vertical dashed bars). The line rises across the bars and returns below zero (signifying renewed accretion a few years later). These correspondences are, however weaker than the connections between bar cycles and El Niños and the breach episodes and El Niño. Note by comparison that the land area/bar cycle does show a stronger correlation, however, that varies widely between the years of bar channel formation. So, at best, bar channel dynamics are but one of perhaps many independent processes synchronized with erosion and accretion cycles near North Cove.

Pacific Decadal Oscillation (PDO)

The PDO is another widely reported index to Pacific climate changes. Only one cool PDO phase is pertinent to our study. This cool regime prevailed between1947-1976 and was preceded and followed by warm regimes that continued through the rest of our study period (Mantua et al. 1997, Minobe 1997). No close links exist between any of the geomorphic time series and PDO fluctuations. This lack of correlation contrasts with the apparent links between area changes and El Niños. Contrasting the two indices, the definition of PDO depends on a greater number of independent oceanographic phenomena (El Niños are defined strictly by temperature anomalies) and the measurement sites for this larger set of PDO-

defining variables are closer to the study site Willapa Bay (the region where El Niño temperatures are measured lies along the equator). PDO events (lasting for 20 to 30 years) are also much more persistent than El Niño events (strong anomalies typically lasting 6- to 12 months). Therefore the definition and character of the PDO lend it more to correlations with processes in the North Pacific and the continental Northwest. North Cove losses correlated better, however, with El Niño.

El Niños Processes Apparently Promoted Breaching

Though there is surprisingly little land loss associated with breaching of the spit and islands, the dates of breaching (to the extent that could be documented with charts and photographs) tended to occur during El Niño phases of the ENSO. A plausible physical explanation would be that sustained high water during winter El Niños makes breaching more likely. Ocean waves are so filtered by tide-modulated entrance shoals that ocean-transmitted forces are relatively less important than the conditions that elevate mean water surface.

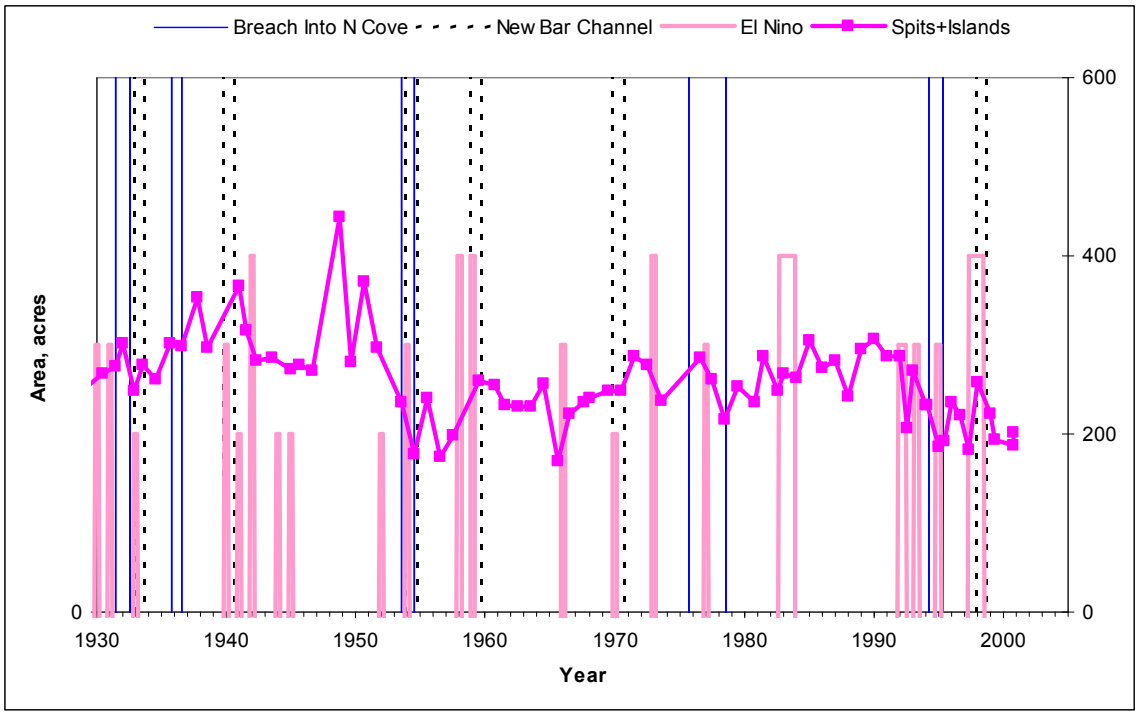

Figure 2.2. 52. Time history of loss of land area compared to other geomorphic cycles and to El Niño phases of the ENSO climate.

Conclusions

This analysis identified modest links between area losses and two climate time series: El Niño and monthly extreme water levels. No links were found to the PDO. This unexpected result suggests that phase shifts between strong decadal trends (Figure 2.2.49) in area losses are more related to sustained high water levels, the dynamics of North Channel migration, and the even longer-term evolution in the shape of Willapa Bay basin than they are to oceanographic variability.

This study uncovered other modest climate links to changes at North Cove. Breaches into North Cove correlate with times of sustained high water. Most of these high water conditions occur during El Niño winters. Annual rates of land area change peak during, or immediately after, transitions from one ebb delta cycle to the next. Rates of land loss rise at the end of one cycle and then typically decline below normal in the following year or the land area may even increase. Because above-average rates of loss are followed by below-average rates and both extremes are superimposed on a substantial persistent loss, climate is not a dominate long-term factor like channel dynamics and basin shape.

Both island and wetland loss rates sometimes peak briefly in association with breaching during El Niños. These climate-moderated perturbations are, however, relatively minor, certainly not controlling factors. Breach-related increases in Cove loss tend to be either compensated for by reduced losses the following year or overridden by the persistence of long-term losses. Except for the period between ebb delta cycles, changes in land area change rates are minor compared to a relatively steady rate of either gain or loss during most of ebb delta cycle. Either erosion or accretion may prevail over the cycle for reasons apparently unrelated to climate or the examined event cycles. In contrast with continual shrinkage of in the area of North Cove, land changes abruptly switch from decades of loss to decades of gain. Erosion dominated from 1948 to 1956 and from 1990 to present. At other times, accretion has been rapid (e.g., 1928-48) or gradual (1956-90). The early phase of rapid gain (1928-48) was probably fed by erosion of large spits to the south that were mapped as continual shrinking from 1887 to 1932. The reason for using the plural term, *areas of spits*, was to acknowledge inclusion at the beginning of the time series of the last emergent vestige of these former spits that wrapped into the Bay entrance from Cape Shoalwater (Figure 2.2.49). Continued erosion of shallow remnants of these formerly huge spits was the probable source for sands that accreted south of North Cove from 1948 to 1956.

For all but possibly the first seven years of record, North Cove has been shrinking. The cove is now less than half the size it was in 1928. A remarkably smooth rate of Cove loss shows no perturbations or transitions related to climate, alternate phases of land loss/gain along its southern boundary, or the 5- to 27-year ebb delta cycles. This long record of unrelenting shrinkage has also been characterized by a smoothly decreasing rate of interannual change. By extrapolation it should take another 30 to 80 years for the cove to shrink again by half. Linear extrapolation over just the most recent decade suggests the shorter (30 year) half-life. Assuming the rate of loss continues slowing as it has historically, an exponential extrapolation provides the more optimistic (80 year) estimate of half-life.

As the Middle Channel's bar shoaled in the 1990s, the inner portion of this record-sized secondary inlet began reshaping of the tidal exchange between the North Channel and South Bay. Earlier, the portion of South Bay flow that did not connect to the ocean elsewhere across the wide entrance joined the Willapa River to the east and then moved along the north shore in the North Channel. The new addition of flow into the North Channel after Middle Channel shoaling in the late 1980s occurred south of Graveyard Spit. As tidal volumes increased in this region, North Channel deepened and its southern bank cut away as the thalweg moved away from the reservation. This realignment of flow may explain why the deepening of the North Channel thalweg and the recent northward migration of the -36 ft contour occurred on all nine seaward ranges (Figure 2.2.50, Table 2.2.9), but not near North Cove.

Short-term accelerations in land area loss correlate with the El Niño-trigged sediment and channel cycles on the ebb delta. But the long-term land and cove losses seem to be driven by northward migration of North Channel. Chronically shrinking land areas briefly expanded when the North Channel made an unusual shift to the south in the late 1960s and again in 1993. Therefore, the relative stability of this critical section of the channel, opposite North Cove, from 1998 to present may appear to offer hope of future low rates of land and cove loss. The history and scale of scale of geomorphic changes, however, suggest the opposite. The first reason for caution is that southward channel displacement was probably influenced by the shoaling of the former large Middle Channel. If so, this influence is now essentially over. There is no known reason for the main channel to move farther away from North Cove or even not to resume soon its customary northward migration. Formation and shoaling of a new large Middle

Channel is not expected for another 50 years assuming it develops as the previous one did. A second and more important reason for caution is that the main channel began expanding southward at about the time the islands switched from a 25-year episode of slow accretion to the present one of rapid erosion. Notice in Figure 2.2.47 that Middle Channel shoaling and the latest phase of land loss occurred at the same time and in spite of the simultaneous movement of North Channel away from North Cove.

The fact that the latest phase of accelerated land loss occurred simultaneously with shoaling of the Middle Channel following a 50-yr trend of increasing cross-section taking more of the tidal flow away from the North Channel could be an ominous sign for North Cove. The most hydraulically efficient location for the main tidal channel through the ever widening entrance to Willapa Bay, the erodability of strata under North Cove, and effects on North Cove of a possible continued southward movement of the channel are all unknowns. With more data and further study theses factors might become clearer, but the more important conclusion, detailed elsewhere in this report, is that even high-cost engineering options like channel training structures designed to modify Channel evolution offer little assurance of success.

Suggestions

Based on the increase in land losses since 1990, even if the critical section of North Channel opposite North Cove does not resume northward migration, erosion of spit and island areas should be expected along with continued loss of lagoon area. Judging from past behavior, North Cove will continue shrinking and for the foreseeable future, tidal flow will continue to remove sand from this formerly accreting area. The relatively consistent past history of Cove loss gives confidence that the future without project half-life of North Cove is about 30 to 80 years. However, the history of land loss, with steady trends abruptly changing every few decades, emphasizes the unreliability of estimates that attempt to predict of the rate of land loss.

Fortunately, land loss is amenable to mitigation. Nourishment of dunes along Graveyard Spit and the island to the east could compensate for some future loss of property. Logs and other debris have reducing North Cove's tidal prism. Removal of debris that washed into the lagoon over the low eroded island might be considered. Placing and planting sand berms could reduce future land area loss, overwash into North Cove, upland flooding, as well as enhancing the ecology and esthetics of North Cove. Periodic replenishment would be required to compensate for continual transport of sand down North Channel. Rates of sand and area loss will fluctuate, being worse during El Niño events, during other periods of sustained high water, and at times of major channel migration. Aerial photography, on-site inspections, and reference to water level and weather data would be an efficient way to assess coming nourishment needs.

Summary

This chapter investigated the timing of events to identify processes that may have affected erosion at North Cove. The physics of erosion was largely ignored. Focus, instead, was on circumstantial evidence that suggested which processes are most likely important and which are not. Support for several links surfaced. Some may warrant further study or monitoring to validate or refute the circumstantial connections presented here. For example, the observed coincidence between El Niño and the breaching into North Cove is so strong that it is highly unlikely that there is not some real physical connection. The connection probably involves processes that elevate the mean surface of the Bay because the tidal record has a correlation to breaching that is just as strong as the correlation to El Niño events. Too many time series were examined to include plots and correlations for them all in this chapter. Evidence of the moderate to strong links was presented. Other processes were described without presenting the lack of correlation or negative results so that they could be dismissed from further consideration.

Amongst the linked processes, degrees of correlation indicate relative likelihood that they arose by chance. For example, the coincidence between breaching into North Cove and the circulation pattern on the ebb delta could easily have arisen by pure chance. The probability that the water level link arose by chance is almost negligible. The link between El Niño and the ebb delta cycle is, however, even stronger. In the absence of data that might show repeated cycles of channel migration, coincidences between channel movement and Cove losses cannot be evaluated statistically. Given the otherwise unexplainable changes in area losses, however, and the understandable role of the channel as a sediment transport mechanism, it seems reasonable that past and future movements will be the main factor determining the fate of north shore property.

The history of geomorphic changes clearly indicates that the land area near North Cove responds to processes we do not understood. Reliable predictions are impossible with present knowledge. Attempts to mitigate the problem must therefore be flexible and responsive to abrupt changes. In contrast, the loss of Cove area over the last 75 years has been relatively smooth. Therefore, predictions for its future by extrapolation are reliable. No evidence could be found to support allegations that engineering works, like the SR-105 dike or channel dredging, played a role in loss of either land or cove areas.

References

Andrews, R. S. (1965). "Modern sediments of Willapa Bay, Washington: a coastal plain estuary," University of Washington Oceanography Technical Report 118. University of Washington, Seattle, WA.

Bjerknes, J. 1972. "El Niño study based on analyses of ocean surface temperatures 1935-1957." *Bull. Inter-Amer. Trop. Tuna Comm.*, 5, 217-303.

Chavez, F.P., J. Ryan, S.E. Lluch-Cota and M. Ñiquen. 2003. "From anchovies to sardines and back: multidecadal change in the Pacific Ocean," *Science*, 299: 217-221.

Ebbesmeyer, C. C., and Coomes, C. A. 1989. "Strong, low frequency (decadal) environmental fluctuations during the 20th century in the North Pacific Ocean, on the Washington coast, and in Puget Sound," *Proceedings, Oceans '89,* IEEE, 242-246.

Ebbesmeyer, C. C., Coomes, C. A., and Tangborn, W. V. 1993. "Interdisciplinary environmental information synthesis: examples of jumps, cycles, and trends in the North Pacific climate, 1930-1990," *Proceedings, Oceans '93,* IEEE, 202-206.

Hands, E. B. 2000b. "ENSO-Related Hydrodynamics off the Coast of Southwest Washington, USA," *EOS, Transactions AGU*, 81(48), Fall Meet., Abstract F659 at http://www.agu.org/meetings/waisfm00.html.

Hands, E. B. 2000c. "Linking Equatorial SST and Hydrodynamics off Southwest Washington, USA," *Proceedings of the 5th Southwest Washington Coastal Erosion Study Workshop in Olympia, Washington*, 15-17 Nov 2000, Washington Department of Ecology, Olympia, WA.

Hands, E. B. 2000a. "Geomorphology." Chapter 3 in "Study of Navigation Channel Feasibility, Willapa Bay, Washington." N. C. Kraus, ed., ERDC/CHL TR-00-6, Vicksburg, MS.

Hare, S. R. and N. J. Mantua, 2000. "Empirical evidence for North Pacific regime shifts in 1977 and 1989," *Progress in Oceanography*, 47(2-4): 103-146

Inman, D. L., Jenkins, S. A., and Elwany, M. H. S. 1996. "Wave climate cycles and coastal engineering practice," *Proceedings, 25th International Conference on Coastal Engineering*. B. L. Edge, ed., American Society of Civil Engineers, New York, 314-327.

Komar, P. D. 1986. "The 1982-83 El Niño and erosion on the coast of Oregon," Shore and Beach 54(2), 3-12.

Komar, P. D. 1997. *The Pacific Northwest Coast: Living with the shores of Oregon and Washington.* Duke University Press, Durham, NC.

Komar, P. D. 1998. "The 1997-98 El Niño and erosion on the Oregon coast," Shore and Beach 66(3), 33-41.

Kraus, N. C. (ed.). 2000. "Study of Navigation Channel Feasibility, Willapa Bay, Washington." Technical Report ERDC/CHL TR-00-6, Vicksburg, MS.

Lowell, S. M. 1997. "Geological study of the North Channel of Willapa Bay – Vicinity of North Cove, Washington," Contract Report, Washington State Department of Transportation, Olympia, WA.

Mantua, N.J., S.R. Hare, Y. Zhang, J.M. Wallace, and R.C. Francis. 1997. A Pacific decadal climate oscillation with impacts on salmon. Bulletin of the American Meteorological Society, Vol. 78, pp 1069-1079.

Minobe, S. 1997. A 50-70 year climatic oscillation over the North Pacific and North America. Geophysical Research Letters, Vol 24, pp 683-686.

Quinn, W. H., Zopf, D. O., Short, K. S., Yang, R. T. W. K. 1978. "Historical trends and statistics of the Southern Oscillation, El Niño, and Indonesian droughts," *Fishery Bulletin* 76, 663-378.

Richey, E. P., Dean, R. G., Ekse, M. I., and Kent, J. C. 1966. "Considerations for the temporary arresting of the erosion at Cape Shoalwater, Washington," State of Washington, Department of Conservation, Olympia, WA.

Seymour, R. J. 1998). "Effects of El Niños on the west coast wave climate," Shore and Beach, 66(3), 3-6.

Shepsis, V., Hosey, H., and Phillips, S. 1996. "The use of dredged material for erosion control at North Cove, Washington," *Proceedings, 15th World Dredging Congress*. B.L. Edge ed., Western Dredging Association, Center for Dredging Studies, College Station, TX, 811-819.
Terich, T., and Levenseller, T. 1986. "The severe erosion of Cape Shoalwater, Washington," *Journal of Coastal Research* 2(4), 465-477.
Trenberth, K. E. and Hoar,T. J. 1996. "The 1990-1995 El Niño-Southern Oscillation Event: Longest on Record," *Geophysical Res Letters*, 23, 57-60.
Trenberth, K. E. and Hurrell. 1994. Decadal atmosphere-ocean variations in the Pacific. Climate Dynamics 9, 303.
Trenberth, K. E., Brainard, R., and Hoar, T. J. 1997. "El Niño and climate change," *Geophysical Res Letters*, 24 3057-3060.
Trenberth, K.E. 1997. "The definition of El Niño," *Bulletin-American Meteorological Society*, 78(12): 2771-2778.
Wooster, W. 1960. "El Niño." Rep. California Op. Ocean Invest., 7, 43-45.
Wyrki, K. 1973. "Telecommunication in the Equatorial Pacific Ocean." *Science*, 180, 66-68.

2.3 Conclusions on Shoreline Evolution[7]

2.3.1 Channel Migration

1. From the 1870's to 1980, the Willapa Bay main channel moved northwards at a greater rate in the west part of the study area (Cross-section lines D-west, D-east, 1, and 2) than further to the east. This retreat most affected Empire Spit and the mainland shore.
2. Further to the east, there is a rotation or anchor point near cross-lines 6 and 7, south of the present opening between Islands 2 and 3. To the west, the channel thalweg traced a slow clockwise rotation from due east-west to the present northwest-southeast. This rotation occurred over 150 years.
3. The channel coming from the Willapa River has followed a stable path for 150 years.
4. From the mid-1980's to the present, the slope of the north bank of the main channel has been constant and has remained in a fixed position (see figures 2.2.35, 2.2.37, and 2.2.39). This indicates that the channel encountered hard strata that are resistant to erosion, probably the very dense, brown Pleistocene terrace unit that was recovered in borings made by the Washington State Department of Transportation.

2.3.2 Spit and Island Morphology

1. Historically, retreat rate was much greater in the west (Graveyard Spit) than further east. At cross-section line D-west, the retreat rate from 1945 to 2003 averaged 28 m/year (93 ft/year).
2. After 1985, Graveyard Spit stabilized, but the sand islands to the east retreated due to loss of sand supply
3. Although the overall retreat has essentially stopped since the 1990's, the spit and islands are narrower and lower, and are therefore and more subject to storm overwash.
4. The opening between Islands 2 and 3, which formed in 1995, is getting wider, which allows more waves to enter from the bay during storm surges.
5. Thalweg and shoreline retreat rates were almost identical during the 20th century.
6. Graveyard Spit and the islands are unlikely to move further north unless the deep channel can move. This will require eroding the channel's north bank into the Pleistocene terrace unit.

[7] Written by Andrew Morang, Ph.D., U.S. Army Engineer Research and Development Center, Coastal and Hydraulics Laboratory, Vicksburg, MS.

3.0 Present Day Littoral Processes

3.1 Tidal Circulation[8]

Tidal circulation study within Willapa Bay is discussed in two sections, with the first, 3.1.1, describing the field data collection effort. Section 3.1.2 provides: a description of the governing equations and algorithm contained in the ADvanced CIRCulation (ADCIRC) numerical model used in evaluating training structures for deflecting the current away from the Shoalwater Bay Indian Reservation (Shoalwater Reservation); an overview of model development, which includes generating the numerical grid was well as the forcing mechanisms used in driving the model; a description the calibration procedure for ensuring the model accurately depicts water-surface elevations and currents in the study area; the evaluation of the training structures effectiveness on modifying the current ; and a summary of study results.

3.1.1 Field Data Collection Program

The USGS with Evans-Hamilton, Inc. conducted a field data collection program for measuring currents and waves at five locations within Willapa Bay. Two measurement periods or deployments were conducted from November 2002 through January 2003. Figure 3.1.1 (Note: figures 3.1.1 through 3.1.31 are located at the end of this section) denotes the approximate locations where measurements were collected, and Tables 3.1.1 and 3.1.2 provide the dates of deployment and recovery of these instruments.

Names given to the sites are based on the general location of each site. Those sites located on the shelf off of Empire Spit are designated as Site ES. Site WR is located where the north channel is carved by the Willapa River. Site NE is located in the eastern Nahcotta channel, whereas Site NW resides in the western Nahcotta channel. Site MC is located in the main channel.

A summary of the current meters deployed during the field data program includes: a bottom-mounted RDI acoustic Doppler current profiler at Site ES; SonTec acoustic Doppler Velocitmeter Ocean Hydra (ADVO) system, which includes a Paroscientific pressure sensor and an optical backscatter sensor; a SonTek acoustic Doppler current profiler (ADCP) with in an internal pressure sensor at Site MC; an ADCP and an ADVO at Site NE; and, an ADCP and ADVO at Site WR. Instruments deployed at Site NW malfunctioned during the field data program.

[8] Written by David Mark, U.S. Army Engineer Research and Development Center, Coastal and Hydraulics Laboratory, Vicksburg, MS.

Table 3.1.1
Summary of instrument deployment 1

Site	Longitude	Latitude	Depth	Deployment	Recovery
ES tripod	124 01.191	46 42.185	7.5	04 Nov 02	04 Dec 02
ES bottom	124 01.204	46 42.194	6.5	04 Nov 02	04 Dec 02
WR	123 58.093	46 41.872	13.5	04 Nov 02	04 Dec 02
NW	124 01.371	46 40.047	17.5	03 Nov 02	04 Dec 02
NE tripod	123 59.720	46 39.335	17.5	03 Nov 02	04 Dec 02
NE mooring	123 59.783	46 39.309	18.5	04 Nov 02	04 Dec 02
MC	124 02.535	46 43.016	19.0	04 Nov 02	04 Dec 02

Table 3.1.2
Summary of instrument deployment 2

Site	Longitude	Latitude	Depth	Deployment	Recovery
ES tripod	124 01.191	46 42.185	7.5	06 Dec 02	19 Jan 03
ES bottom	124 01.204	46 42.194	6.5	03 Dec 02	19 Jan 03
WR	123 58.093	46 41.872	13.5	04 Dec 02	19 Jan 03
NW	124 01.371	46 40.047	17.5	03 Dec 02	19 Jan 03
NE tripod	123 59.720	46 39.335	17.5	03 Dec 02	19 Jan 03
NE mooring	123 59.783	46 39.309	18.5	03 Dec 02	19 Jan 03
MC	124 02.535	46 43.016	19.0	04 Dec 02	19 Jan 03

3.1.2 Description of Tidal Circulation Model

The ADCIRC numerical model was chosen for simulating the long-wave hydrodynamic processes in Willapa Bay. Imposing wind fields extracted from the National Center for Environmental Prediction database, the ADCIRC model can accurately replicate tidally-driven currents and storm-surge levels induced by winter storms. The ADCIRC model was developed in the USACE Dredging Research Program (DRP) as a family of two- and three-dimensional finite element-based models (Luettich, Westerink, and Scheffner 1992; Westerink et al. 1992). Model attributes include the following capabilities:

a. Simulating tidal circulation and storm-surge propagation over very large computational domains while simultaneously providing high resolution in areas of complex shoreline configuration and bathymetry. The targeted areas of interest include continental shelves, nearshore areas, and estuaries.

b. Representing properly all pertinent physics of the three-dimensional equations of motion. These include tidal potential, Coriolis, and all nonlinear terms of the governing equations.

c. Providing accurate and efficient computations over time periods ranging from months to years.

In two dimensions, the model is formulated using the depth-averaged shallow water equations for conservation of mass and momentum. Furthermore, the formulation assumes that the water is incompressible, that hydrostatic pressure conditions exist, and that the Boussinesq approximation is valid. Using the standard quadratic parameterization for bottom stress and neglecting baroclinic terms and lateral diffusion/dispersion effects, the following set of conservation equations in primitive,

nonconservative form, and expressed in a spherical coordinate system, are incorporated in the model (Flather 1988; Kolar et al. 1993):

$$\frac{\partial U}{\partial t} + \frac{1}{r\cos\phi} U \frac{\partial U}{\partial \lambda} + \frac{1}{R} V \frac{\partial U}{\partial \phi} - \left[\frac{\tan\phi}{R} U + f \right] V =$$

$$- \frac{1}{R\cos\phi} \frac{\partial}{\partial \lambda} \left[\frac{p_s}{\rho_0} + g(\zeta - \eta) \right] + \frac{\tau_{s\lambda}}{\rho_0 H} - \tau_* U \tag{1}$$

$$\frac{\partial V}{\partial t} + \frac{1}{r\cos\phi} U \frac{\partial V}{\partial \lambda} + \frac{1}{R} V \frac{\partial V}{\partial \phi} - \left[\frac{\tan\phi}{R} U + f \right] U = \tag{2}$$

$$- \frac{1}{R} \frac{\partial}{\partial \phi} \left[\frac{p_s}{\rho_0} + g(\zeta - \eta) \right] + \frac{\tau_{s\lambda}}{\rho_0 H} - \tau_* V$$

$$\frac{\partial \zeta}{\partial t} + \frac{1}{R\cos\phi} \left[\frac{\partial UH}{\partial \lambda} + \frac{\partial (UV\cos\phi}{\partial \phi} \right] \tag{3}$$

where

t = time

λ and φ = degrees longitude (east of Greenwich is taken positive) and degrees latitude (north of the equator is taken positive)

ζ = free surface elevation relative to the geoid

U and V = depth-averaged horizontal velocities in the longitudinal and latitudinal directions, respectively

R = the radius of the Earth

$H = \zeta + h$ = total water column depth

h = bathymetric depth relative to the geoid

$f = 2\Omega \sin\varphi$ = Coriolis parameter

Ω = angular speed of the Earth

p_s = atmospheric pressure at free surface

g = acceleration due to gravity

η = effective Newtonian equilibrium tide-generating potential parameter

ρ_0 = reference density of water

$\tau_{s\lambda}$ and $\tau_{s\varphi}$ = applied free surface stresses in the longitudinal and latitudinal directions, respectively

τ = bottom shear stress and is given by the expression $C_f(U^2 + V^2)^{1/2} /H$ where C_f = the bottom friction coefficient

The momentum equations (Equations 1 and 2) are differentiated with respect to λ and τ and substituted into the time differentiated continuity equation (Equation 3) to develop the following Generalized Wave Continuity Equation (GWCE):

$$\frac{\partial^2\zeta}{\partial t^2} + \tau_0\frac{\partial\zeta}{\partial t} - \frac{1}{R\cos\phi}\frac{\partial}{\partial\lambda}\left[\frac{1}{R\cos\phi}\left(\frac{\partial HUU}{\partial\lambda} + \frac{\partial(HUV\cos\phi}{\partial\phi}\right) - UVH\frac{\tan\phi}{R}\right]\right.$$

$$\left[-2\omega\sin\phi\, HV + \frac{H}{R\cos\phi}\frac{\partial}{\partial\lambda}\left(g(\zeta - \alpha\eta) + \frac{p_5}{\rho}p_0\right) + \tau_* HU - \tau_0 HU - \tau_{s\lambda}\right]$$

$$-\frac{1}{R}\frac{\partial}{\partial\phi}\left[\frac{1}{R\cos\phi}\left(\frac{\partial HVV}{\partial\lambda} + \frac{\partial HVV\cos\phi}{\partial\phi}\right) + UUH\frac{\tan\phi}{R} + 2\omega\sin\phi\, HU\right] \qquad (4)$$

$$+\frac{H}{R}\frac{\partial}{\partial\phi}\left(g(\zeta - alfa\eta) + \frac{p_s}{\rho_0}\right) + \tau_* - \tau_0 HV - \frac{\tau_{s\lambda}}{\rho_0}]$$

$$-\frac{\partial}{\partial t}[\frac{VH}{R}\tan\phi] - \tau_0[\frac{VH}{R}\tan\phi] = 0$$

The ADCIRC-2DDI model solves the GWCE in conjunction with the primitive momentum equations given in Equations 1 and 2. The GWCE-based solution scheme eliminates several problems associated with finite-element programs that solve the primitive forms of the continuity and momentum equations, including spurious modes of oscillation and artificial damping of the tidal signal. Forcing functions include time-varying water-surface elevations, wind shear stresses, atmospheric pressure gradients, and the Coriolis effect. Also, the study area can be described in ADCIRC using either a Cartesian (i.e., flat earth) or spherical coordinate system.

The ADCIRC model uses a finite-element algorithm in solving the defined governing equations over complicated bathymetry encompassed by irregular sea/ shore boundaries. This algorithm allows for extremely flexible spatial discretizations over the entire computational domain and has demonstrated excellent stability characteristics. The advantage of this flexibility in developing a computational grid is that larger elements can be used in open-ocean regions where less resolution is needed, whereas smaller elements can be applied in the nearshore and estuary areas where finer resolution is required to resolve hydrodynamic details.

3.1.3 Model Development

The grid used for this study was adapted from the grid developed for the Willapa Bay Navigation Study (Kraus et al. 2000), and this grid is displayed in Figure 3.1.2. As shown in the figure, the northern grid limit resides at 56 deg 45 min north latitude, or 157 miles north of Queen Charlotte Islands, British Columbia; its southern limit is located at 34 deg 30 min north latitude, or Point Arguello, California. The western boundary resides at 138 deg west longitude, or approximately 660 miles west of Willapa Bay.

Figure 3.1.3 displays the grid along the western coast of Washington, whereas Figures 3.1.4 and 3.1.5 show the grid in the vicinity of northern Willapa Bay and the North Cove, respectively. The grid encloses the Willapa Bay entirely and the Willapa River extends to Raymond, Washington, which is approximately the head-of-tides. This grid consists of 40,844 nodes and 76,034 elements. The largest elements reside in the eastern North Pacific Ocean, having nodal spacing of about 30.6 miles, whereas the smallest elements resolve the channels within the North Cove, where the nodal spacing is about 150 feet. The Willapa River is represented in the grid as having a "V" shape (in cross-section) with a line of nodes, running its entire length, positioned along its centerline together with a line of nodes along both channel banks. Nodal spacing along the channel bottom is approximately 200 feet.

For areas outside of the United States, the grid boundary is aligned with the shoreline depicted on nautical charts produced by the U.S. National Imaging and Mapping Agency (NIMA). These charts are referenced to the World Geodetic System (WGS) 1984 horizontal datum, which is equivalent to the North American Datum (NAD) 1983 coordinate system used by United States governmental agencies. For areas within the United States, shoreline positions are based on nautical charts produced by the National Ocean Survey (NOS). All charts are referenced to the NAD 1983 datum.

Bathymetry specified in the grid was obtained from three sources. For regions outside of Willapa Bay, depths are based on digitized soundings and contour lines displayed on NIMA and NOS nautical charts. Soundings were extracted from the NIMA Digital Nautical Chart database, and they correspond, with respect to location and depth, to those printed on NOS and NIMA charts. Contour depths were digitized from the nautical charts and then converted from fathoms or feet, depending on the chart, to meters, and their vertical datums were adjusted to mean-tide-level (mtl).

The second source of bathymetric data is a database generated from surveys conducted by the USGS and USACE Seattle District. Surveys incorporated into the model include the USGS-sponsored surveys of August 2000 and May 2001, together with the USACE-sponsored surveys of September 2000, March 2001, July 2001, and March 2002. Data collected during these surveys were incorporated into a single database, and data extracted from older surveys that overlapped more recent ones were omitted from the database. The third data source is NOS Chart 18504; bathymetry obtained from this chart provided water depths for southern and eastern regions of Willapa Bay that were not surveyed.

Assigning depths to the grid nodes were performed by first assembling data from each source into a single database. Nodal depths were computed using a distance-weighted algorithm that weights each sounding or data point inversely proportional to its distance from that node. After completing the interpolation task, coastline nodes were assigned depths equal to 1 m (3.0 feet) over the majority of the grid. Within Willapa Bay, the grid limits extend to -3 m (3 m above mean tide level).

3.1.4 Model Calibration

During the process of establishing a numerical model to represent the study area, calibration was performed to ensure it adequately predicted hydrodynamic conditions. Accuracy of a model is influenced by the accuracy of the forcing functions specified at open-water boundaries, representation of the

geometry of the study area (i.e., bathymetry and shoreline), and to values of certain model parameters, principally the bottom friction coefficient. A satisfactory comparison between calculations and measurements in the calibration procedure provides confidence that the model adequately replicates hydrodynamic processes.

Calibration exercises for the present study were conducted in two phases: In the first phase, the model was simulated under solely astronomical forcing, whereas both astronomical and meteorological forcings are imposed in the second phase. Performing the calibration in this fashion permitted evaluating model accuracy with respect to each forcing mechanism, identifying sources of error. Because tidal constituents used as forcing functions are synthesized from long-term time-series of measured tides and currents, they implicitly contain the attenuation of tide and current induced by bottom friction.

Forcing mechanisms specified in the model include tide, tide-generating potential, Willapa River discharge, and the Coriolis effect. Time-varying tidal elevations specified at nodes along the open ocean boundaries were synthesized using the following eight tidal constituents: M_2, S_2, N_2, K_1, O_1, Q_1, P_1, and K_2. Constituent information was extracted from a database developed by LeProvost and Poncet (1987). Because the model domain is of sufficient size that celestial attraction induces tide within the grid proper, tide-generating potential functions were included in the simulation calculations, and these functions incorporated the above listed eight tidal constituents.

Astronomical Calibration

The ADCIRC model was calibrated by adjusting the bottom friction and the lateral eddy diffusivity coefficients so that model-generated water-surface elevation time-series compare favorably to those reconstructed from NOS-published tidal constituents, which were obtained from the worldwide web site maintained by the NOS.

Calibration simulations were conducted for equilibrium tidal conditions (i.e., all eight constituents mentioned previously begin the simulation in phase), which depicts spring tide. A 3-second time-step was used in each simulation, and the bottom friction and eddy diffusivity coefficients were specified globally throughout the model domain.

The optimum values of the global bottom friction and eddy diffusivity coefficients were found to be 0.003 and 1.0 m^2/s, respectively. Comparisons of model- and constituent-generated water-surface elevations for the Nahcotta, South Bend, and Tokeland gauges are presented in Figures 3.1.6 through 3.1.8.

A harmonic analysis was conducted of the model-generated time-series of water-surface elevations for determining the amplitudes and phases of the eight tidal constituents. Comparison of model-generated and NOS-published constituent amplitudes and phases for the Tokeland station are presented in Figures 3.1.9 and 3.1.10, respectively. A line is drawn diagonally across these plots to aid in interpreting comparisons; a symbol lying on this line signifies perfect agreement between the model-generated and NOS-published constituents. A symbol falling to the right or below the line indicates that the model over predicted the published amplitude (in Figure 3.1.9) or phase (in Figure 3.1.10). Conversely, a symbol falling to the left or above the line indicates that the model under predicted the published amplitude or the phase.

For the study area, the M_2, S_2, K_1, and O_1 constituents are the most dominant constituents, accounting for nearly 73 percent of the spring tide signal. This difference in accuracy may be due to the duration of the simulation (i.e., 60 days) used in the harmonic analysis; amplitudes of the diurnal constituents are generally smaller than for the semi-diurnal constituents, suggesting that a greater number of tidal cycles may be necessary for extracting these constituents from the harmonic analysis.

3.1.5 Alternative Training Structures

The Shoalwater Bay Indian Tribe proposed that training structures, or dikes, be investigated as a possible remedy for controlling the extreme erosion along the North Cove shoreline. The purpose for these structures is to deflect the high current away from the shore, or to divert the flow in the Willapa North Channel such that it opens and maintains the Willapa Middle Channel to the open ocean. As shown in Figure 3.1.11, seven locations for training dikes were proposed. However, only four of these locations were evaluated with the ADCIRC model, and they are alternatives 1, 3, 4, and 6. These four locations were selected for analysis because they are the closest to the tribal lands, thereby having the greatest potential to deflect the current away from the shore than the remaining alternatives.

The base or existing-condition grid was adapted for each alternative by adjusting the nodal positions and adding nodes so that each alternative is highly resolved in the grid. In all cases, the structure protrudes the water surface and no water overtopping of the structure was permitted. Each alternative was tested under spring tide conditions, and no wind forcing was imposed in the simulation. Furthermore, the yearly mean river inflow was specified at the upstream boundary of the Willapa River. Peak spring ebb and flood currents were extracted from each simulation and analyzed as to their effectiveness.

Training Structure Alternative 1

Displayed in Figure 3.1.12, Alternative 1 is located west of the Shoalwater Reservation at Toke Point, and extends 2,050 feet into the channel. Peak spring ebb current in the vicinity of the North Cove for the base and with-alternative conditions are presented in Figures 3.1.13 and 3.1.14, respectively. (To facilitate comparison between existing and with-structure conditions, the barrier islands are delineated in Figure 3.1.14 with a heavy red line.) Peak spring ebb current along then shoreline of North Cove is, for both cases, approximately 0.7 m/s (2.3 ft/s). Consequently, Alternative 1 at its given length will have a minimal impact on current in the vicinity of the Shoalwater Reservation, and therefore will have minimal impact on preventing shoreline erosion along the North Cove.

Training Structure Alternative 4

This alternative is displayed in Figure 3.1.15, and is located at the same position as the SR 105 dike. The structure extends 2,350 feet into the channel, or approximately to the center of the channel thalweg. Peak spring flood current in the vicinity of the North Cove for the base and with-structure conditions are presented in Figures 3.1.16 and 3.1.17, respectively. The structure reduces the peak flood current along the western extent of the cove, but a minimal change in current is noted along the eastern end of Empire Spit. Because the dike resides to the west of the North Cove, current in the vicinity of the Cove was not affected during ebb.

A consequence of constructing a structure is the increased current caused by reducing the conveyance of water flowing past the dike. This increased current, in turn, can induce the formation of a scour hole at the toe of the dike. To determine whether scouring is a possibility, a short-term simulation was conducted where sediment transport was computed for depicting change in the bottom depth at the structure. Figure 3.1.18 presents the change in bottom topography at the conclusion of this simulation. As shown in this figure, a scour hole measuring 0.5 m (1.6 ft) formed at the completion of the 15-day simulation. This suggests that over a longer period of time, a scour hole will form, potentially requiring regular maintenance of the dike to prevent it from slumping into the scour hole.

A second experiment was conducted with this alternative being lengthened to 3,000 feet to determine the structure length necessary for deflecting the current away from the shoreline (Figure 3.1.19). As shown in Figure 3.1.20, a reduction in current is found along the western extent of the study area, but the dike had a minimal impact on current along the eastern extent of the spit.

Training Structure Alternative 6

Displayed in Figure 3.1.21, Alternative 6 is situated along the northern reach of the Nachotta Channel, and is oriented so that the ebb current is deflected in a westerly trajectory, away from the shoreline. Initial testing showed strong current flowing around the eastward end of the dike, raising the potential for the strong current to scour a new channel across the Ellen Sands and also to undermine the foundation of the structure. Consequently, subsequent testing was conducted with the structure extending across low-lying Ellen Sands to high ground. The structure has an overall length of 16,200 feet, and extends 950 feet into the channel. Peak spring ebb current in the vicinity of the North Cove for the existing and with-project conditions are presented in Figures 3.1.22 and 3.1.23, respectively. Peak spring ebb current along the shore of the North Cove for both conditions is approximately 0.7 m/s (2.3 ft/s). At its present length, Alternative 6 would have minimal impact on current along the spit.

This alternative was extended such that it extended completely across the channel and terminated on a sandbar. Total length for this dike was 19,000 feet (Figure 3-1-24). Figure 3.1.25 shows a minimal effect in the vicinity of the North Cove.

Training Structure Alternative 3

This alternative is displayed in Figure 3.1.26, and extends directly across the North Cove and into the channel. The structure length is 12,800 feet and extends 7,800 feet into the channel. Peak spring ebb current in the vicinity of the North Cove for the base and with-alternative conditions are presented in Figures 3.1.27 and 3.1.28, respectively. The structure reduces the peak ebb current along the western extent of Empire Spit, and, to a lesser extent, at the eastern end of the spit. Current along the eastern end of the Spit is reduced during flood tide, whereas a small reduction in current is found to the west (Figure 3.1.29).

Two consequences of training structures is the creation of gyres, a circular or spiraling current, on the lee-side of the structure, and impediment of sediment transported along the shore. Although the gyres are weaker than the main current, the spiraling gyre will still suspend the sediment along the shore, and transport it into deeper water; with the structure preventing movement of sediment along the shore, the area being eroded by the gyre is not replenished, leading to a loss in land. This same process can be see by comparing aerial photographs of the shore before and after the SR-105 dike was constructed (Figures 3.1.30 and 3.1.31).

3.1.6 Summary of Training Structure Modeling Results

This investigation found that flow modifications caused by a training structure are localized, and if a structure is constructed, it must be in close proximity to the North Cove to have an impact on the current. Furthermore, the structure must be massive in size to divert or deflect the strong current away for the shoreline. For example, alternative 3 measured 12,800 feet in length, and extended into the channel to

a depth of about 70 feet. To have an appreciable impact on current, the remaining structures must block a significant portion of the channel in order to reduce the current speed along the shoreline.

Each training structure would also reduce the conveyance of flow within the channel. As such, the current increases as it flows past the structure. As shown in the numerical experiments, as well as the experience with the SR-105 dike, the increase in current would induce the formation of a scour hole at the toe of the structure. To prevent potential failure of the structure, regular maintenance would be required to prevent toe from sliding into the hole.

Historical measurements show that the rate of shoreline erosion has decreased over the past decade, suggesting that the bathymetry in the Bay system is reaching an equilibrium condition. Potentially, constructing a training structure may change this condition, resulting in an unintended adverse effect on the rate of shoreline, spit and/or island erosion.

References

Flather, R. A. (1988). "A numerical model investigation of tides and diurnal-period continental shelf waves along Vancouver Island," *Journal of Physical Oceanography* 18, 115-139.

Garratt, J. R. (1977). "Review of drag coefficients over oceans and continents," *Monthly Weather Review 105*, 915-929.

Hagen, S. C., Westerink, J. J., Kolar, R. L., and Horstmann, O. (2001). "Two-dimensional, unstructured mesh generation for tidal models," *International Journal for Numerical Methods in Fluids* 35, 669-686.

Kolar, R. L., Gray, W. G., Westerink, J. J., and Luettich, R. A. (1993). "Shallow water modeling in spherical coordinates: Equation formulation, numerical implementation, and application," *Journal of Hydraulic Research*.

Kraus, N. C., Editor, (2000). "Study of Navigation Channel Feasibility, Willapa Bay, Washington," Technical Report ERDC/CHL TR-00-6, U.S. Army Engineer Waterways Experiment Station, Vicksburg, MS.

Luettich, R. A., Jr., Westerink, J. J., and Scheffner, N. W. (1992). "ADCIRC: An advanced three-dimensional circulation model for shelves, coasts, and estuaries," Technical Report DRP-92-6, U.S. Army Engineer Waterways Experiment Station, Vicksburg, MS.

LeProvost, C., and Poncet, A. (1987). "Finite Element Method for Spectral Modeling of Tides." *Int. J. Num. Methods Eng.,* 12, 853-871.

Westerink, J. J., Luettich, R. A., Jr., Baptista, A. M., Scheffner, N. W., and Farrar, P. (1992). "Tide and storm surge predictions using finite element model," *Journal of Hydraulic Engineering,* American Society of Civil Engineers, 118(10), 1373-1390.

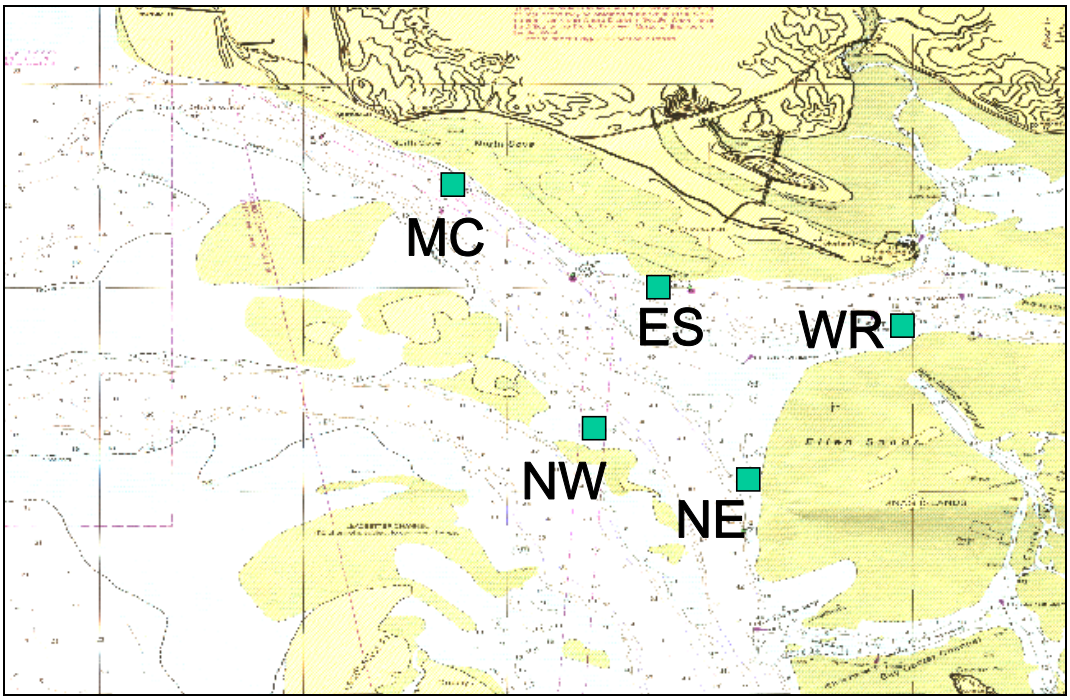

Figure 3.1.1. Position of current meters.

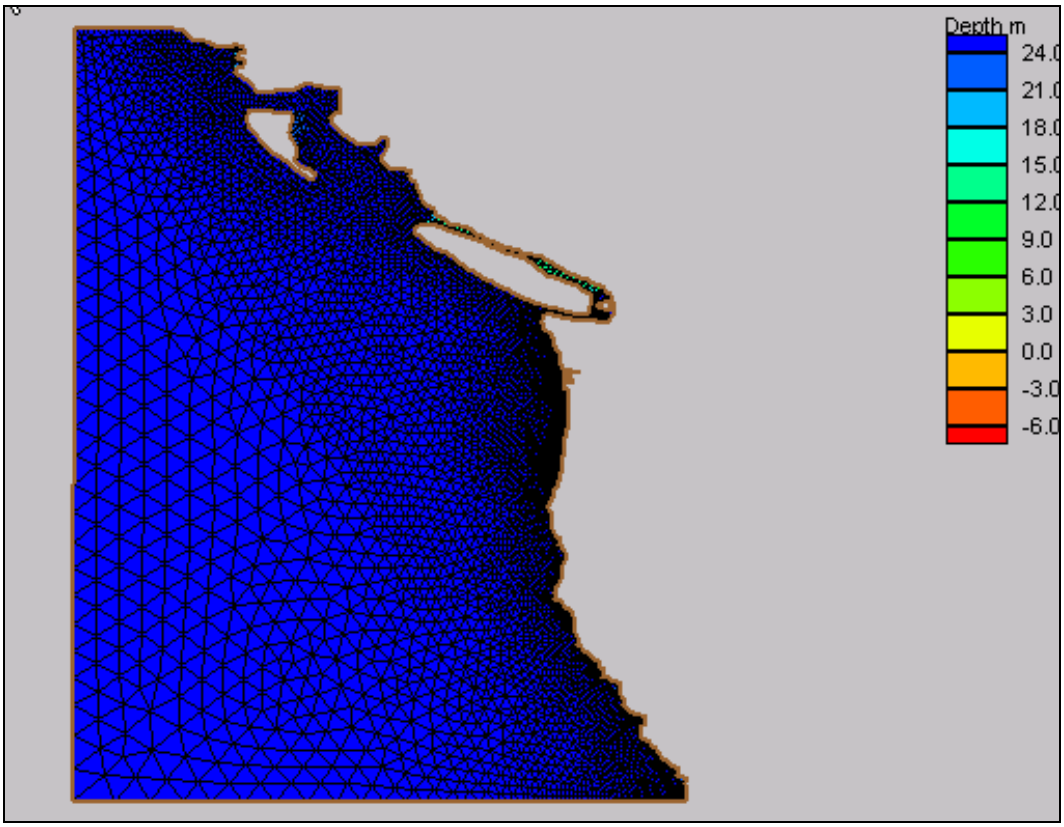

Figure 3.1.2. Numerical grid.

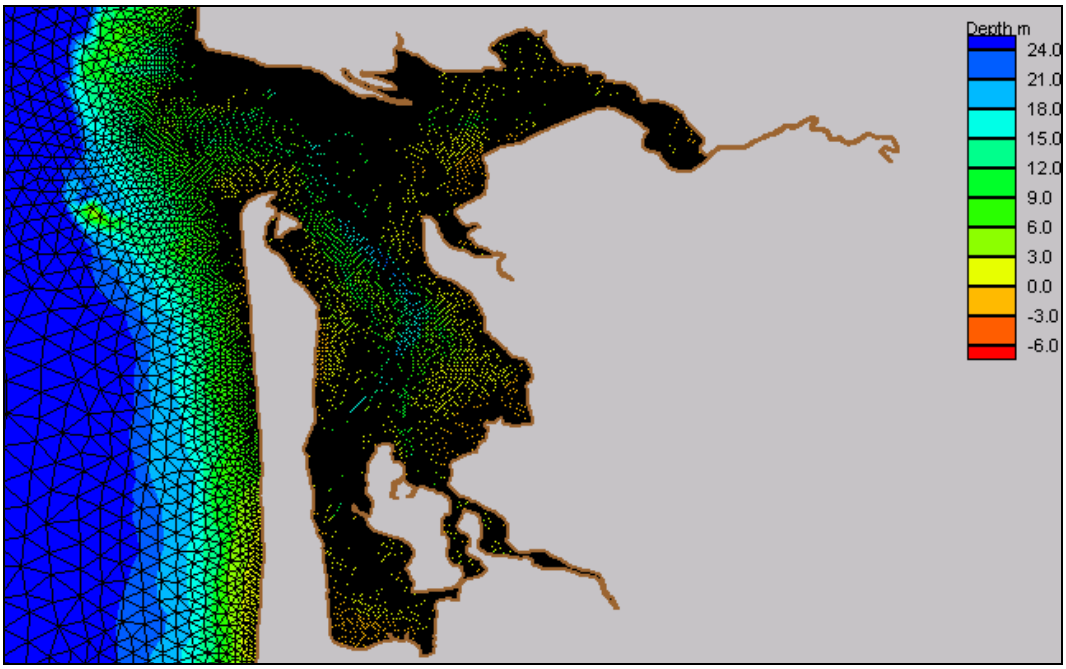

Figure 3.1.3. Grid detail for Willapa Bay.

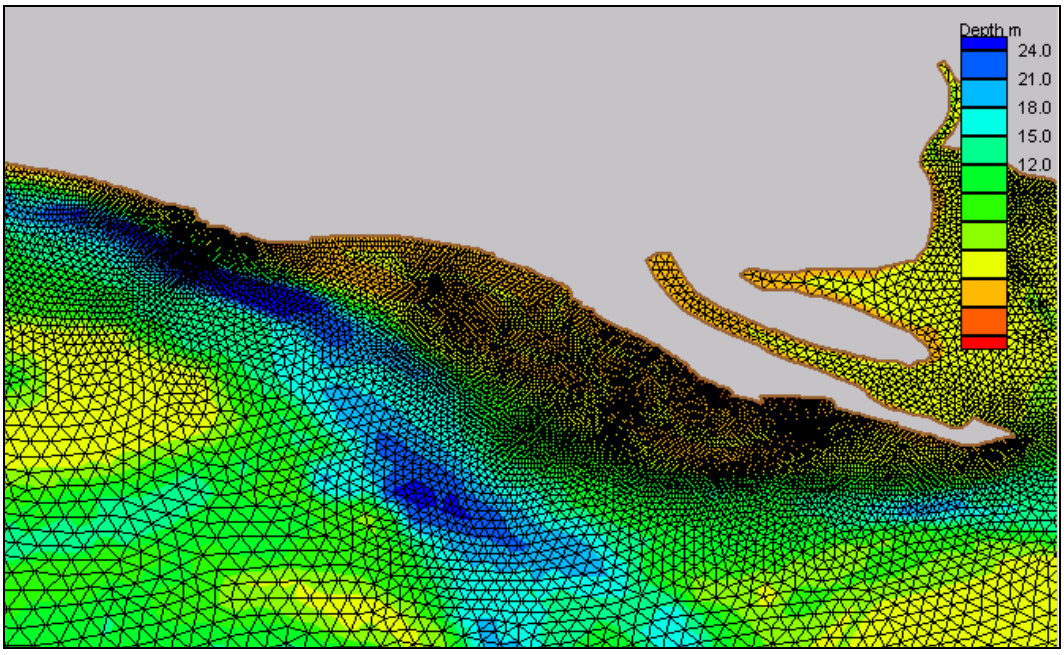

Figure 3.1.4. Grid detail for northern Willapa Bay.

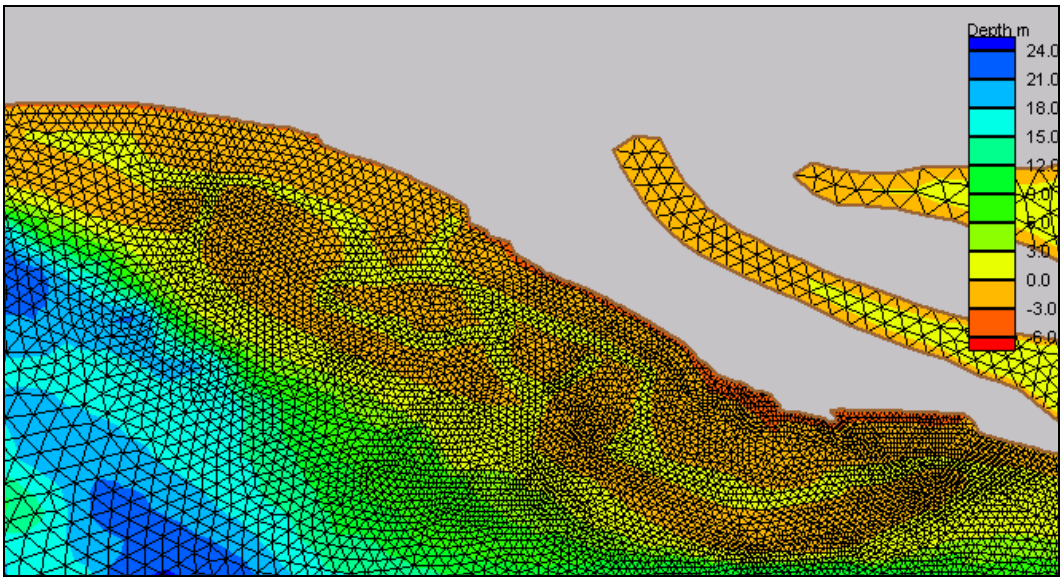

Figure 3.1.5. Grid detail for North Cove.

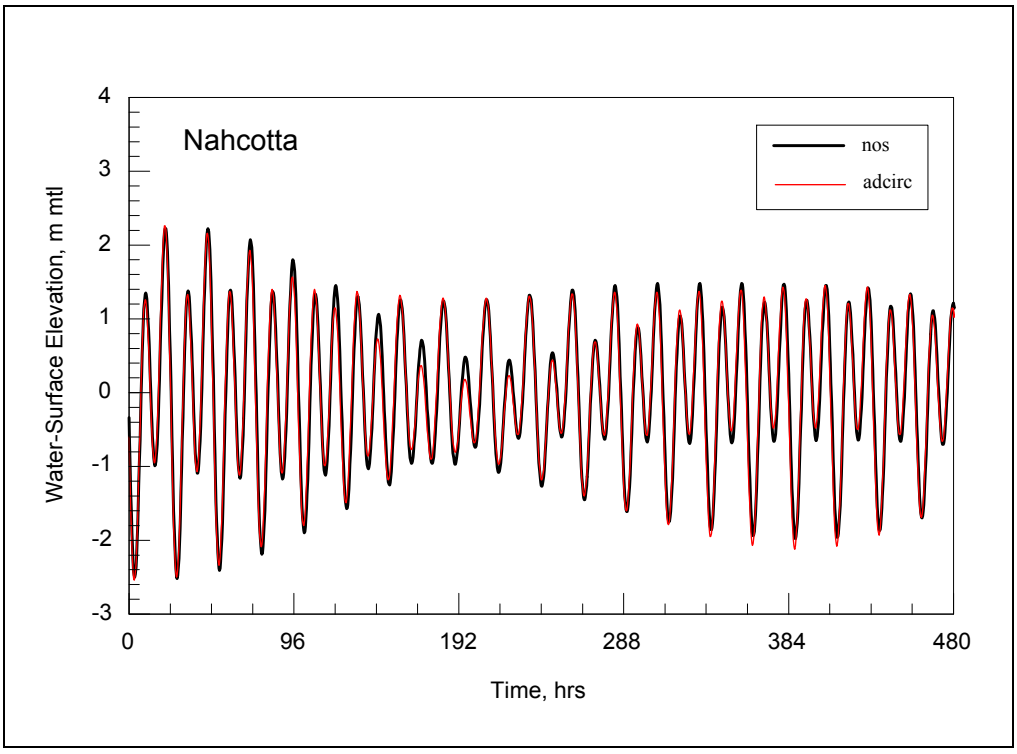

Figure 3.1.6. Comparison of time-series of water-surface elevations synthesized from tidal constituents; Nahcotta gauge.

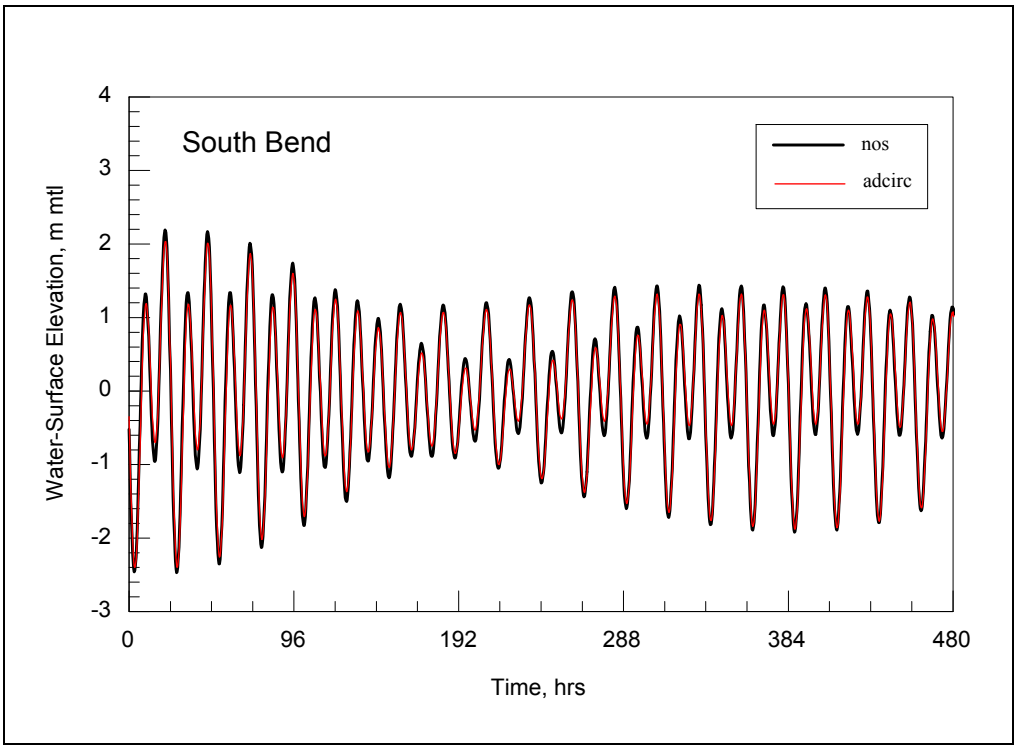

Figure 3.1.7. Comparison of time-series of water-surface elevations synthesized from tidal constituents; South Bend gauge.

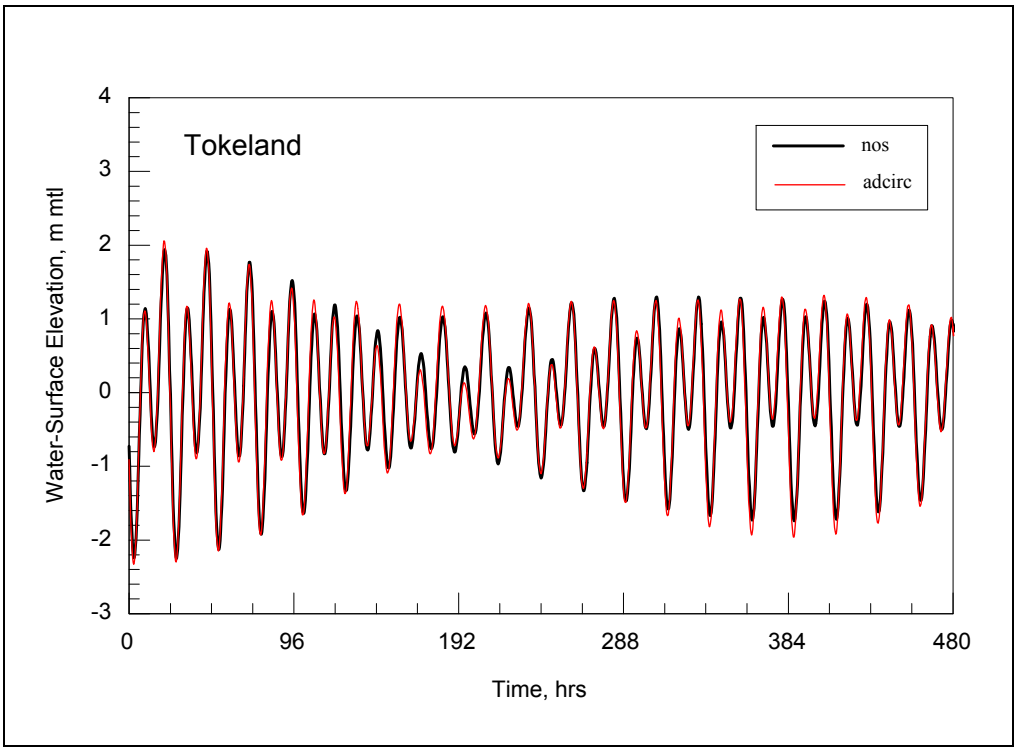

Figure 3.1.8. Comparison of time-series of water-surface elevations synthesized from tidal constituents; Toke Point gauge.

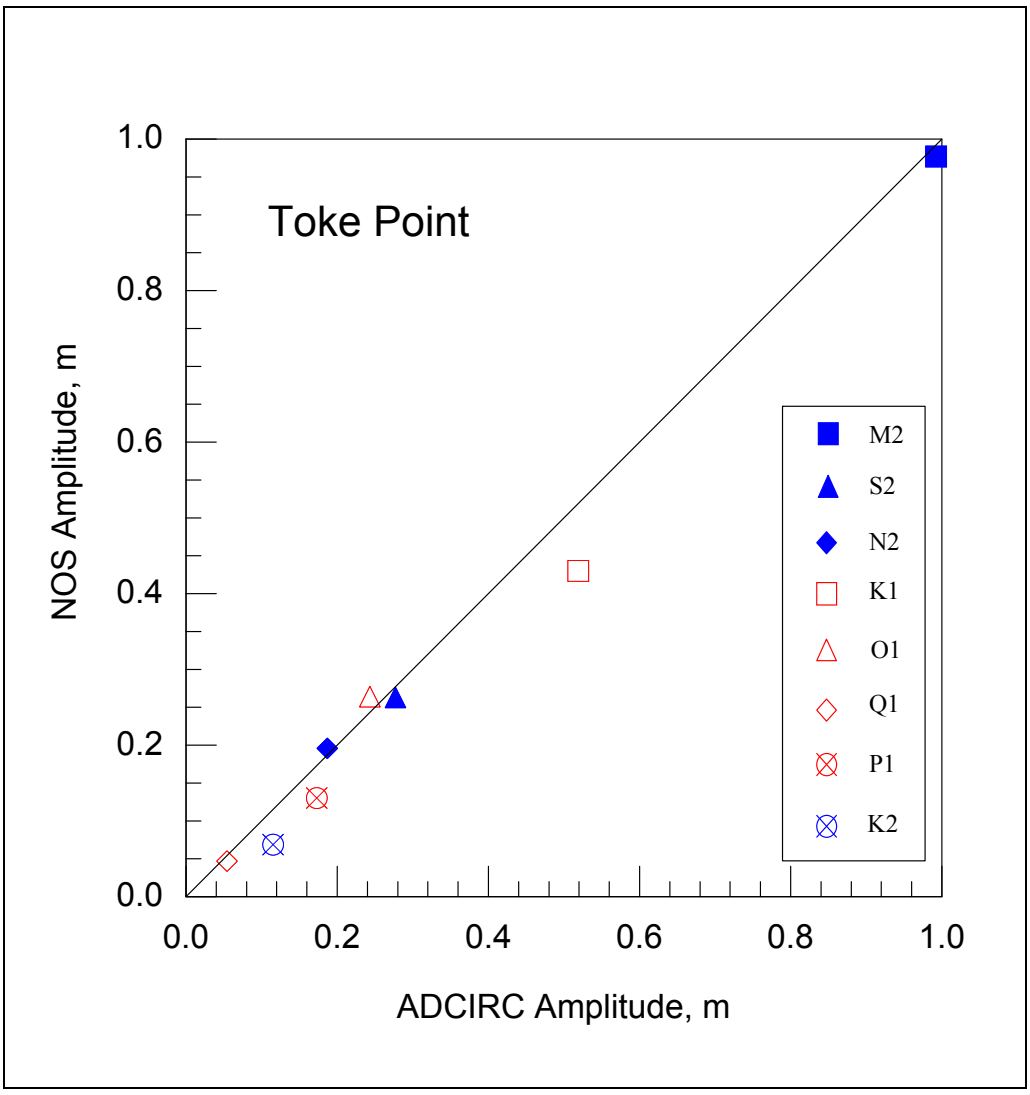

Figure 3.1.9. Comparison of ADCIRC-generated constituent amplitude with NOS-published constituent amplitude for Toke Point gauge.

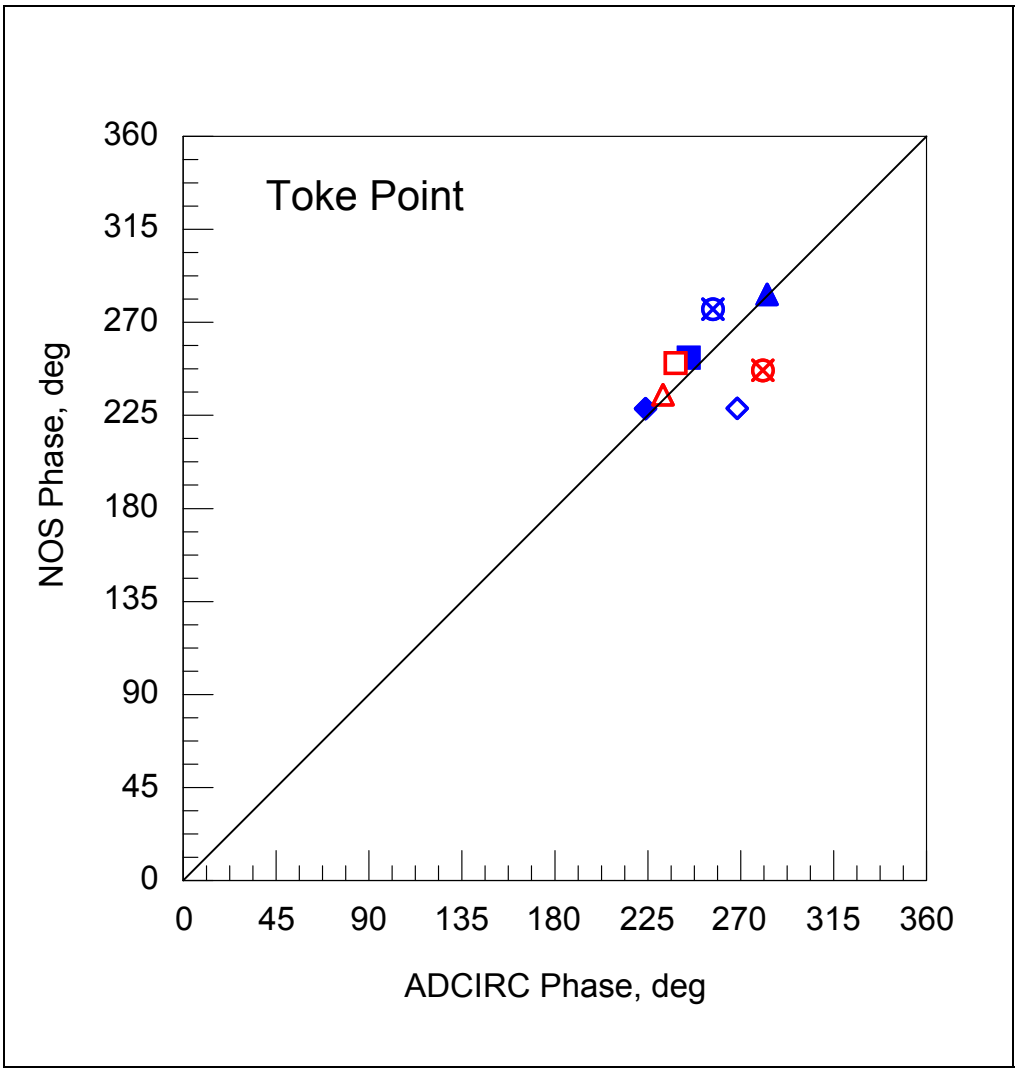

Figure 3.1.10. Comparison of ADCIRC-generated constituent phase with NOS-published constituent phase for Toke Point gauge.

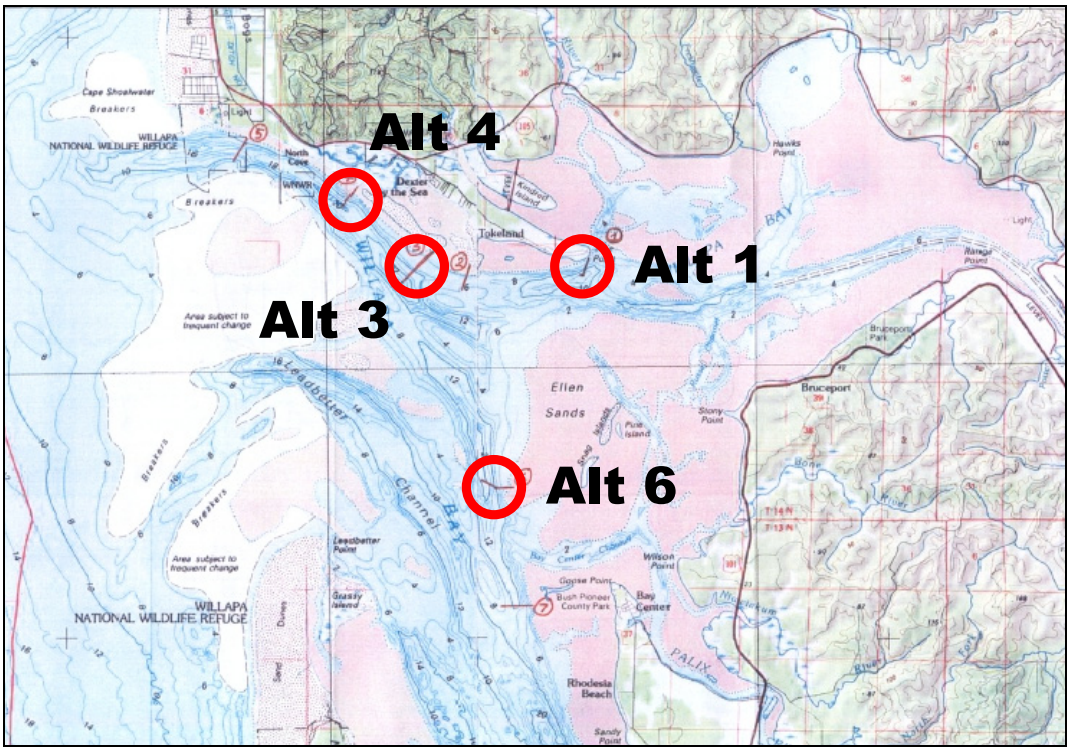

Figure 3.1.11. Proposed locations for training dikes.

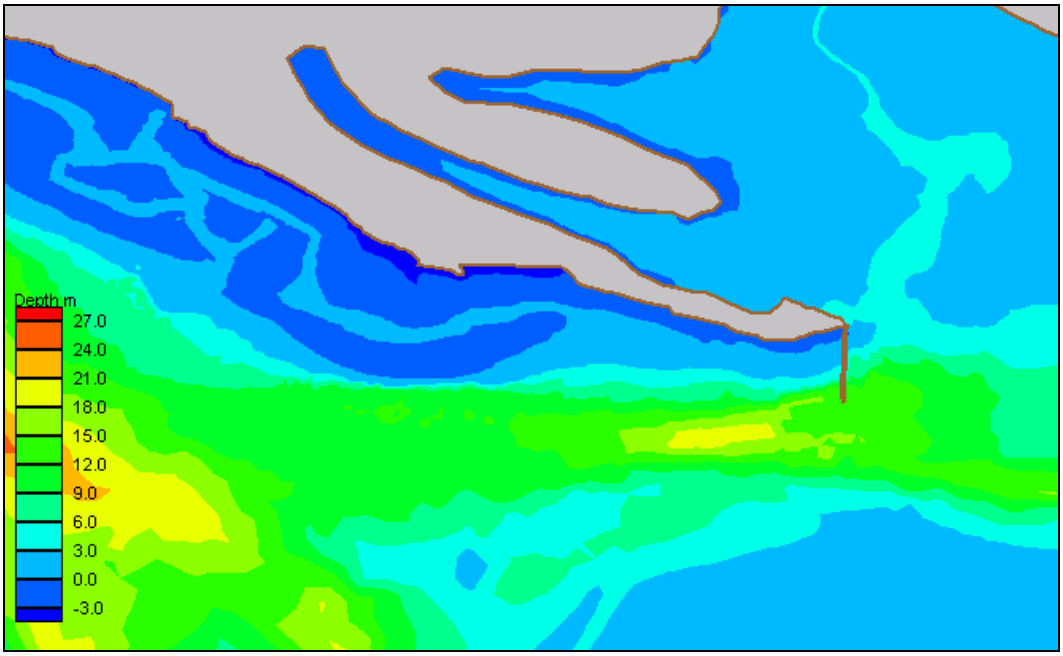

Figure 3.1.12. Location of training dike alternative 1.

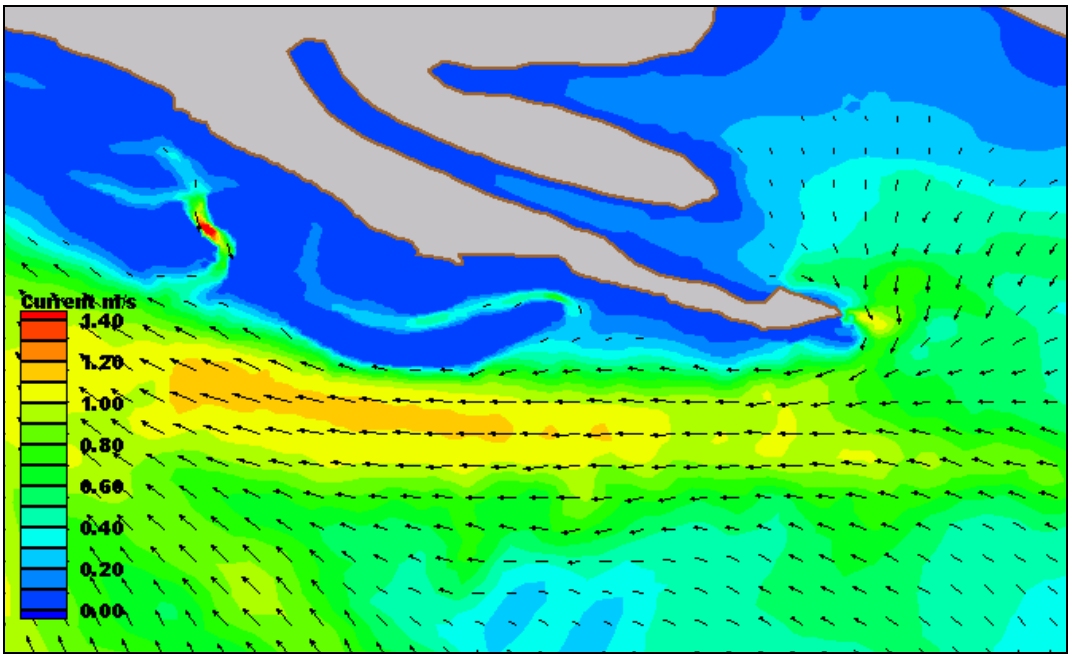

Figure 3.1.13. Peak spring ebb current under existing condition.

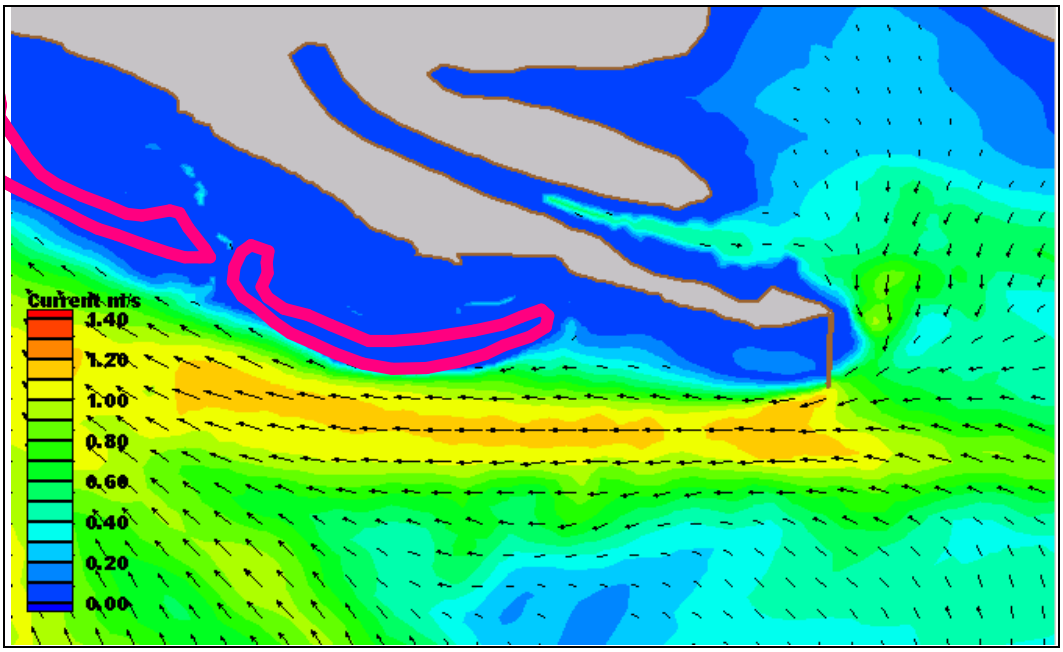

Figure 3.1.14. Peak spring ebb current with training dike alternative 1 in place.

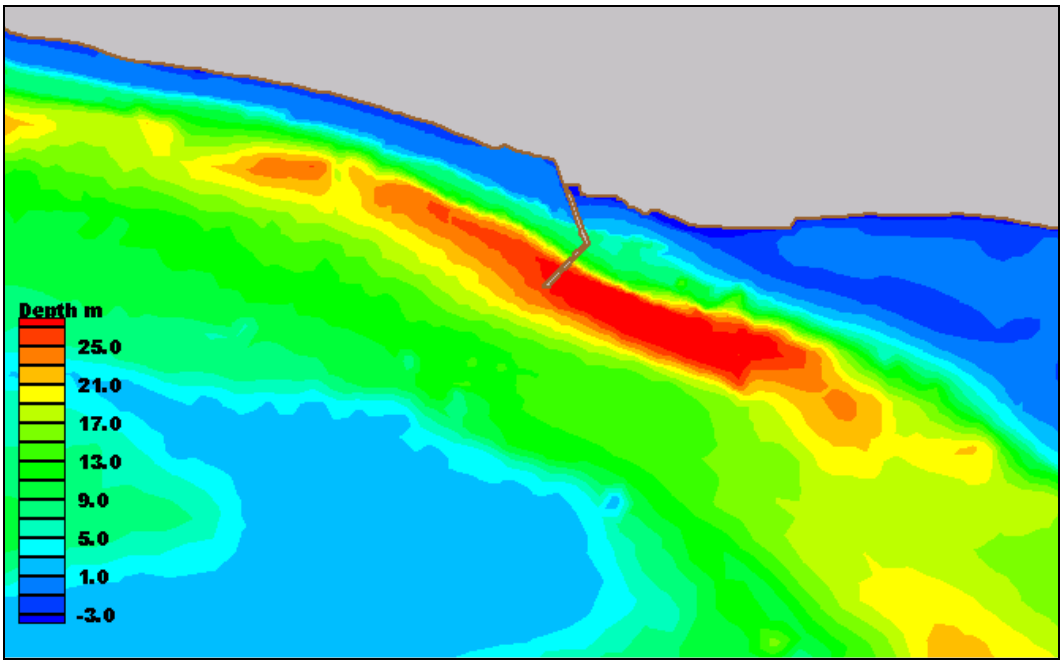

Figure 3.1.15. Location of training dike alternative 4.

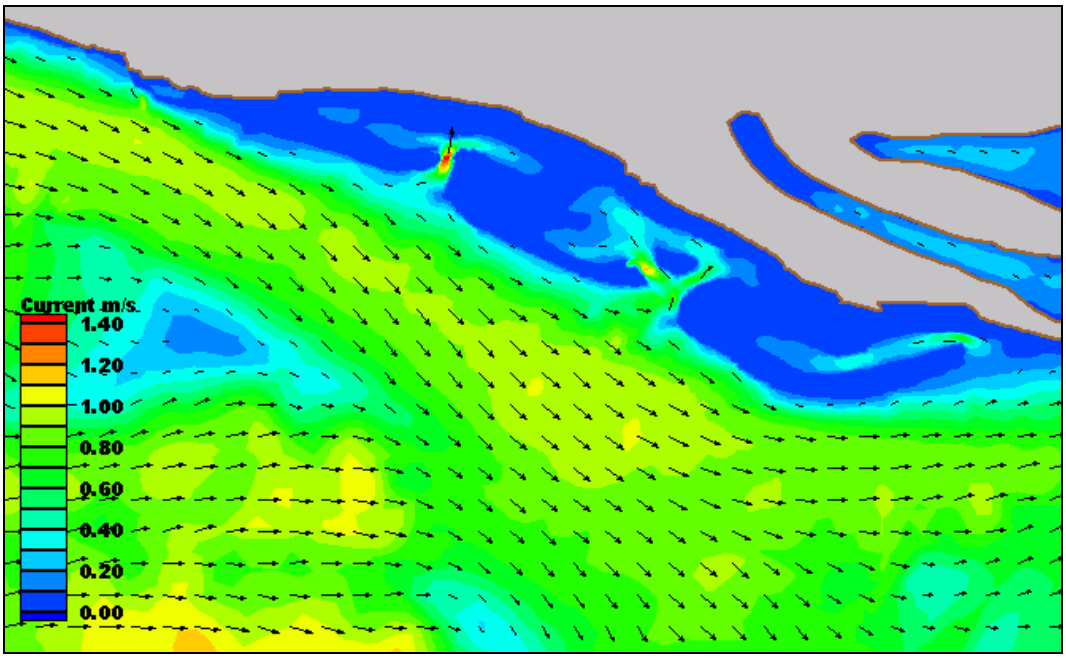

Figure 3.1.16. Peak spring flood current under existing condition.

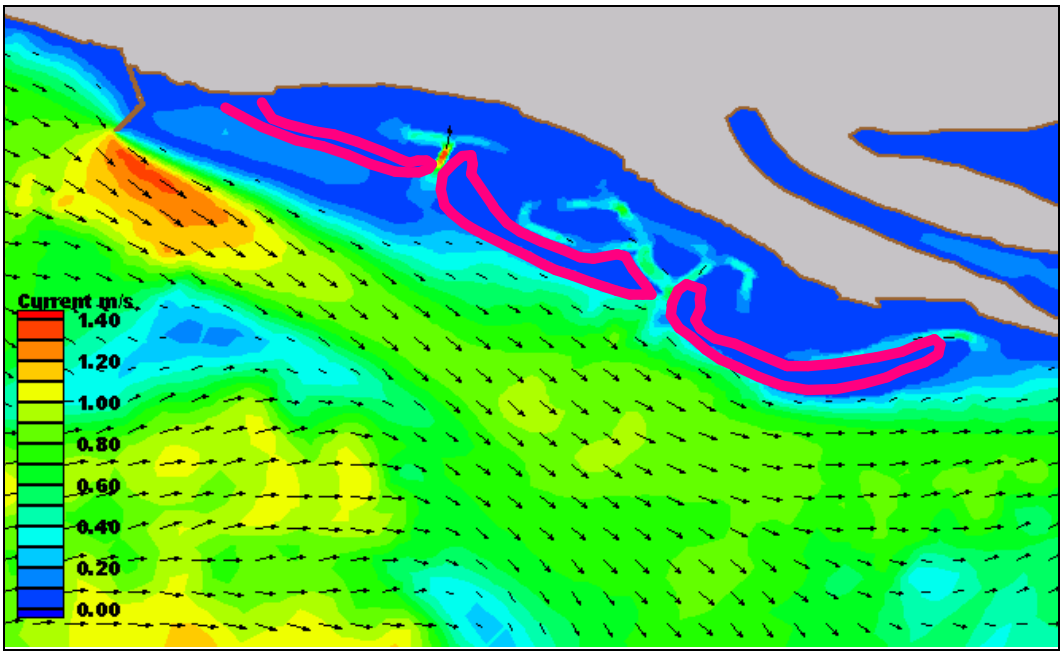

Figure 3.1.17. Peak spring flood current with training dike alternative 4 in place.

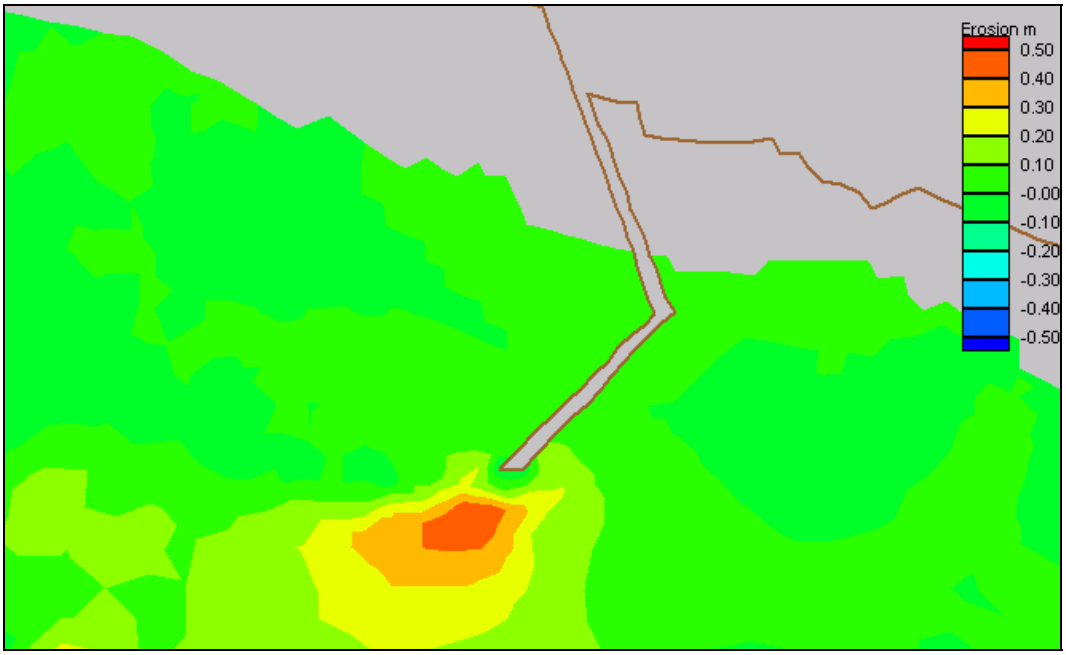

Figure 3.1.18. Model-predicted development of a scour hole due to constructing alternative 4.

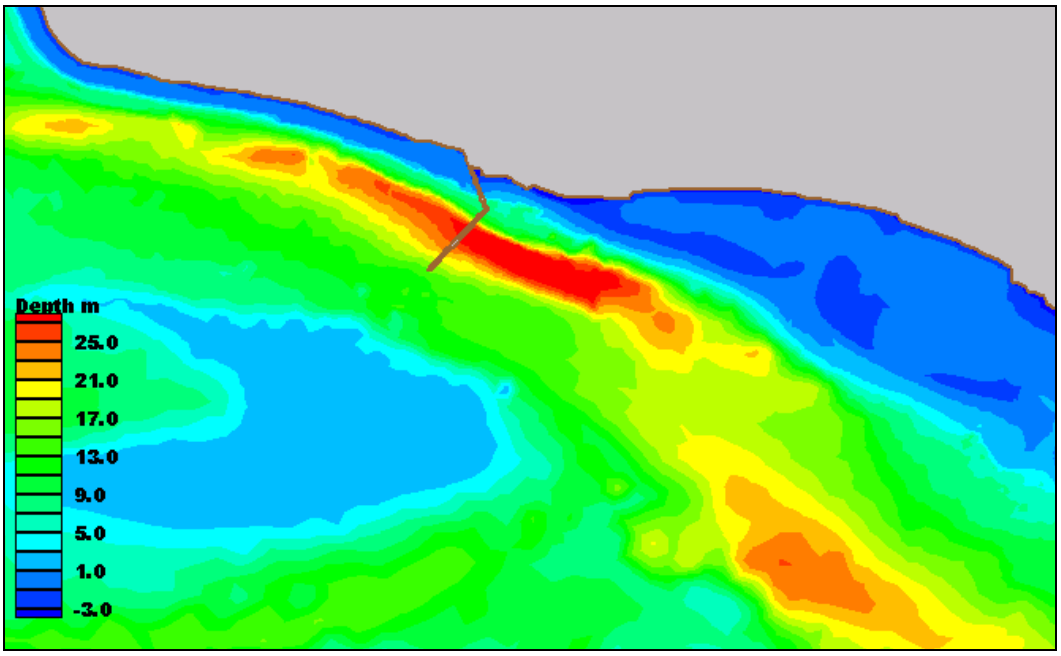

Figure 3.1.19. Location of training dike alternative 4B.

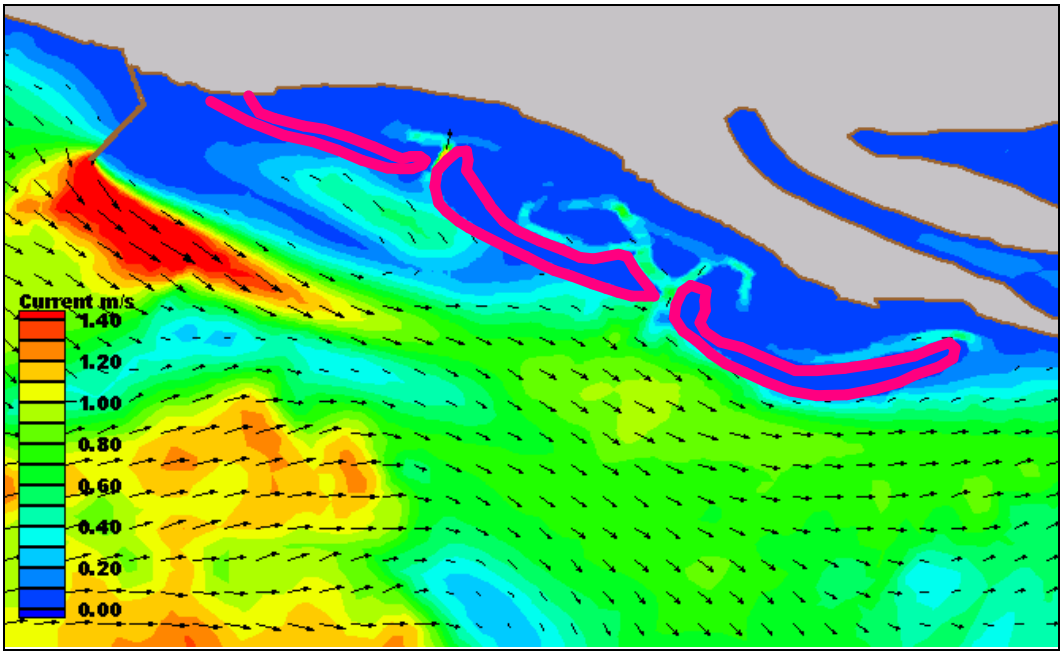

Figure 3.1.20. Peak spring flood current with training dike alternative 4B in place.

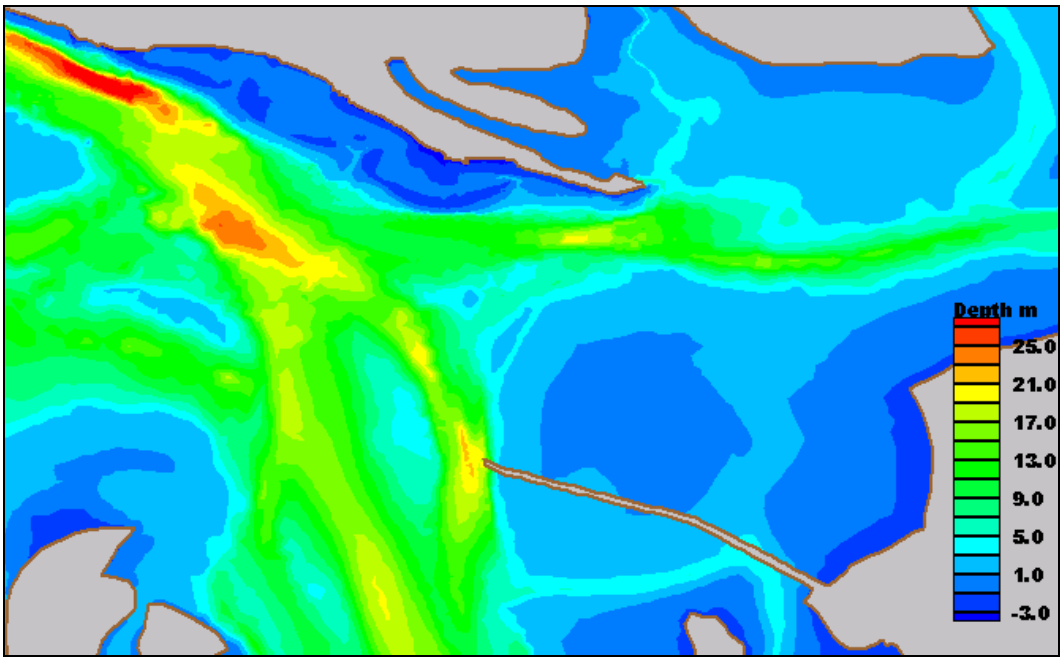

Figure 3.1.21. Location of training dike alternative 6.

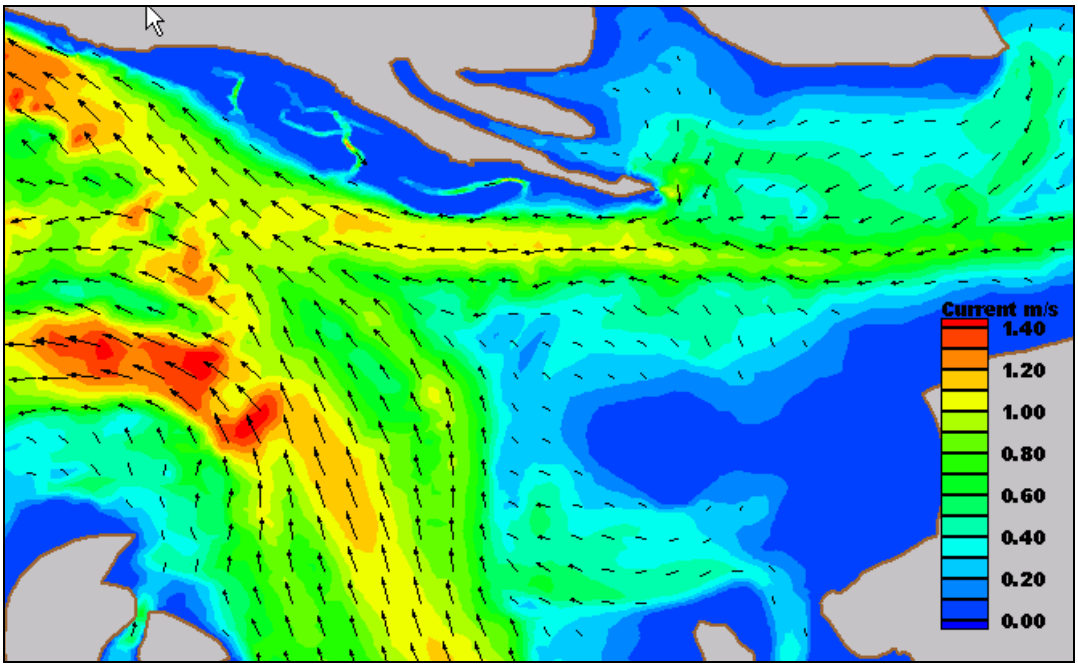

Figure 3.1.22. Peak spring ebb current under existing condition.

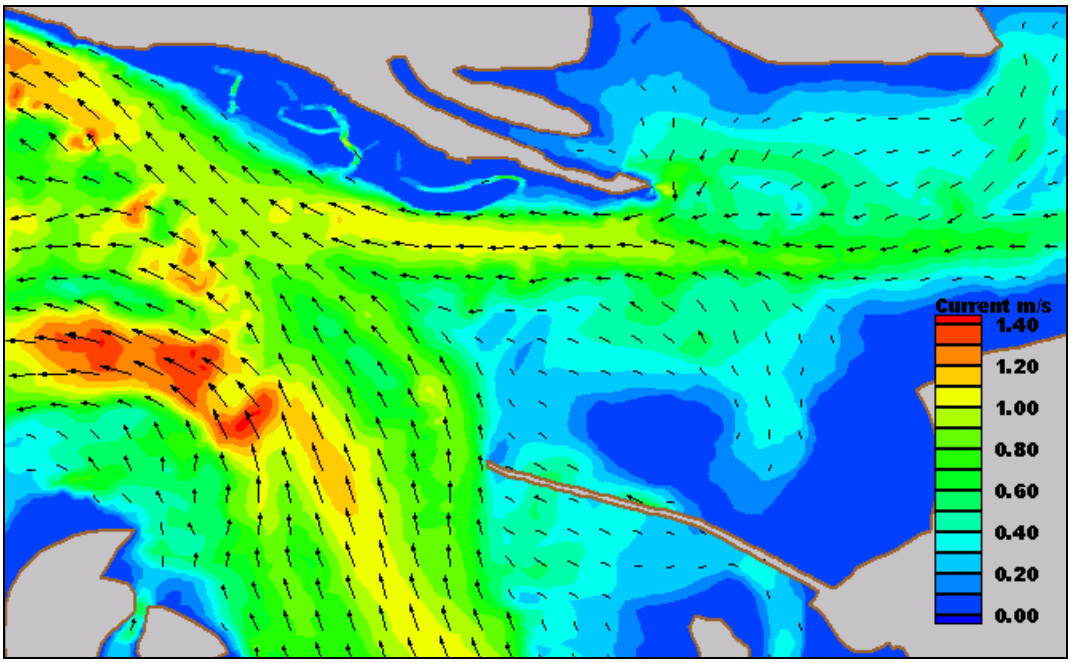

Figure 3.1.23. Peak spring ebb current with training dike alternative 6 in place.

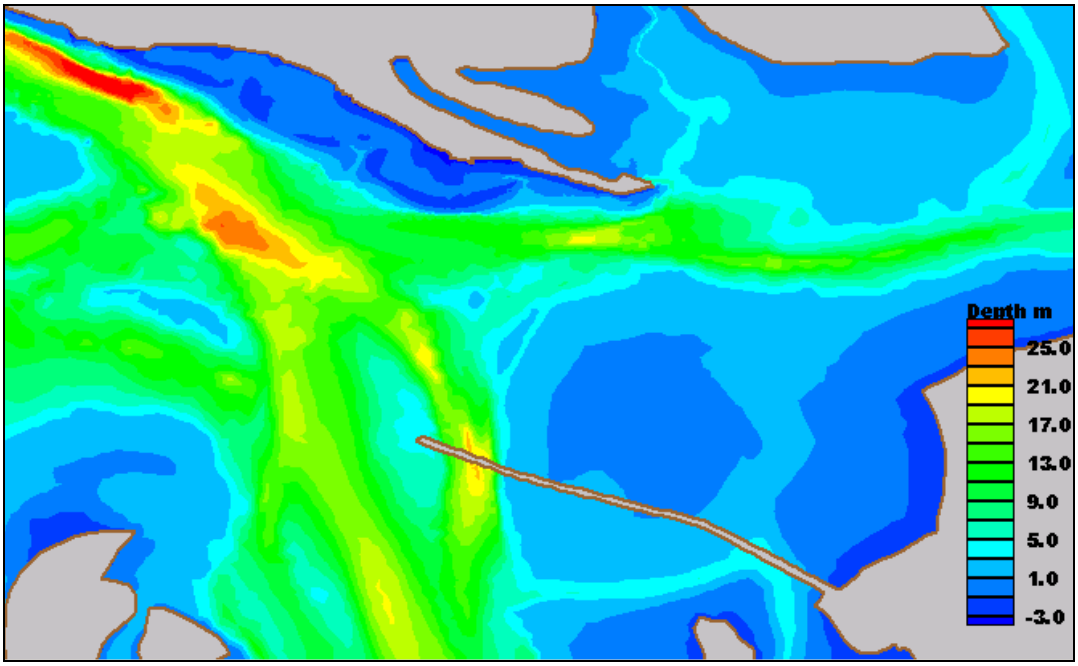

Figure 3.1.24. Location of training dike alternative 6B.

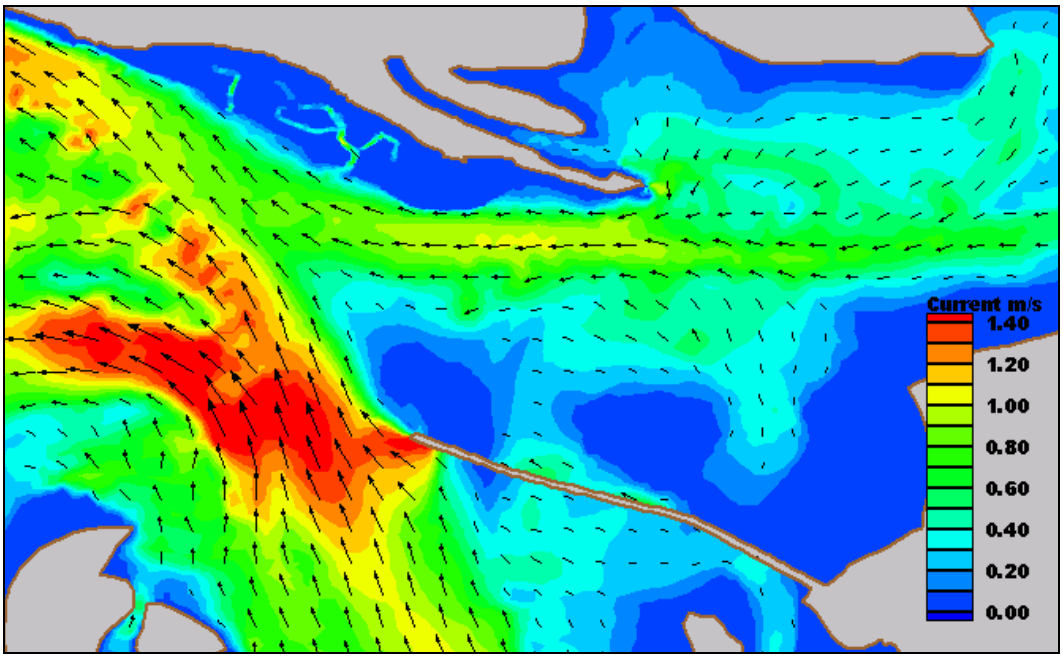

Figure 3.1.25. Peak spring ebb current with training dike alternative 6B in place.

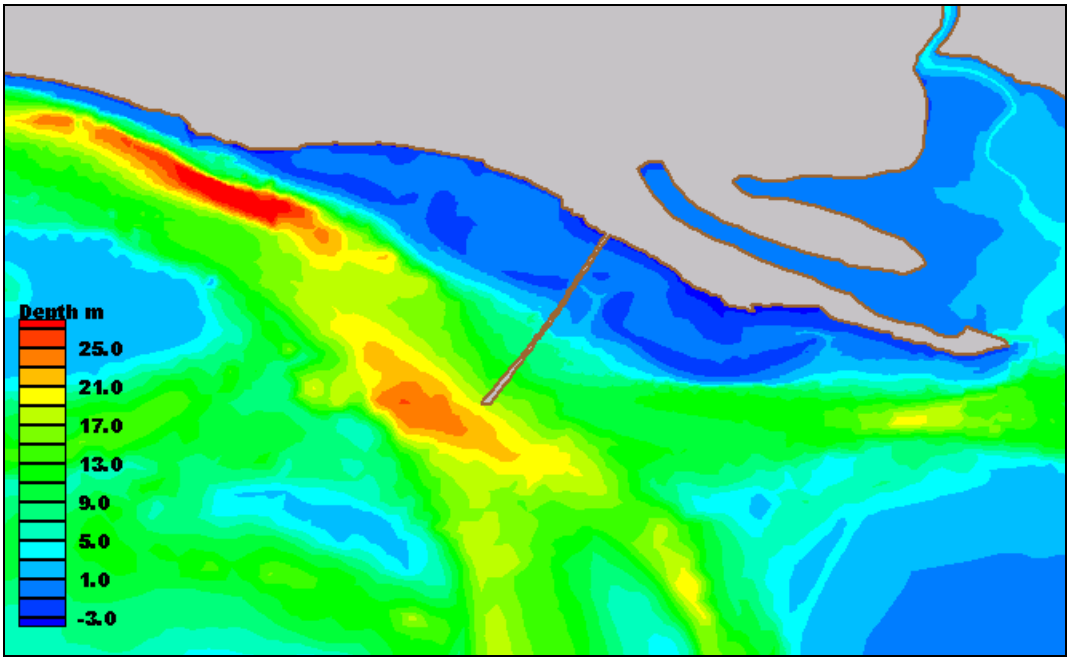

Figure 3.1.26. Location of training dike alternative 3.

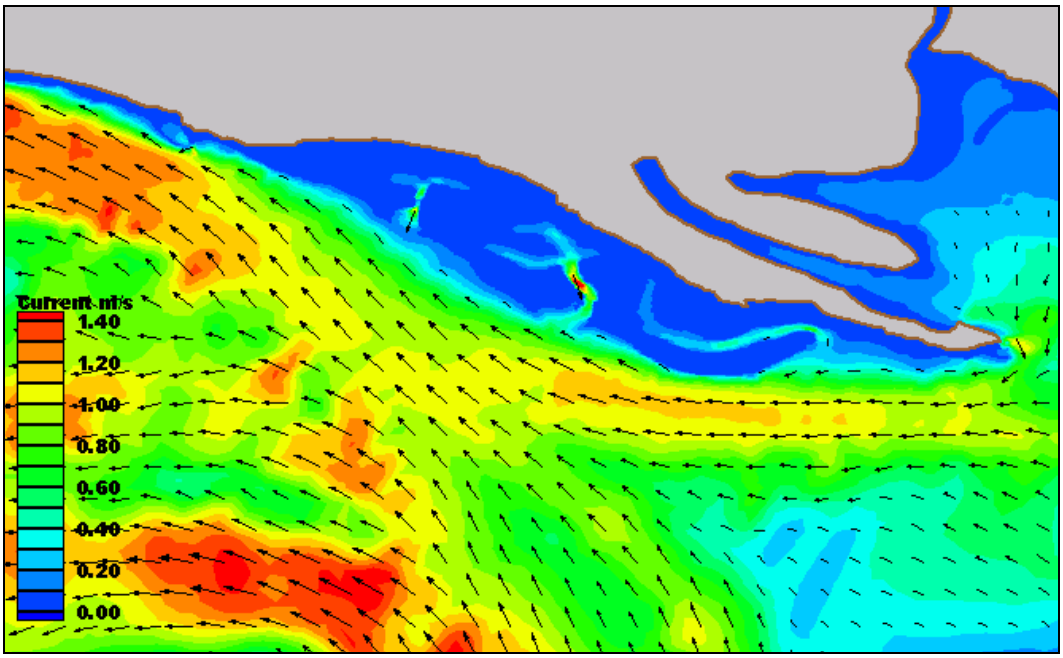

Figure 3.1.27. Peak spring ebb current under existing condition.

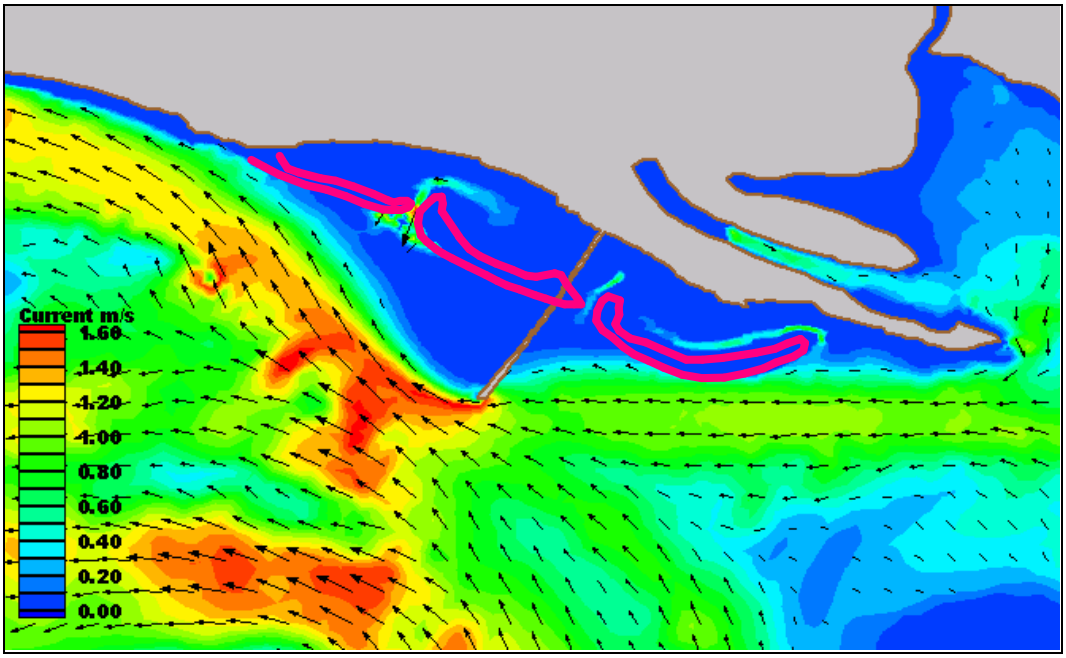

Figure 3.1.28. Peak spring ebb current with training dike alternative 3 in place.

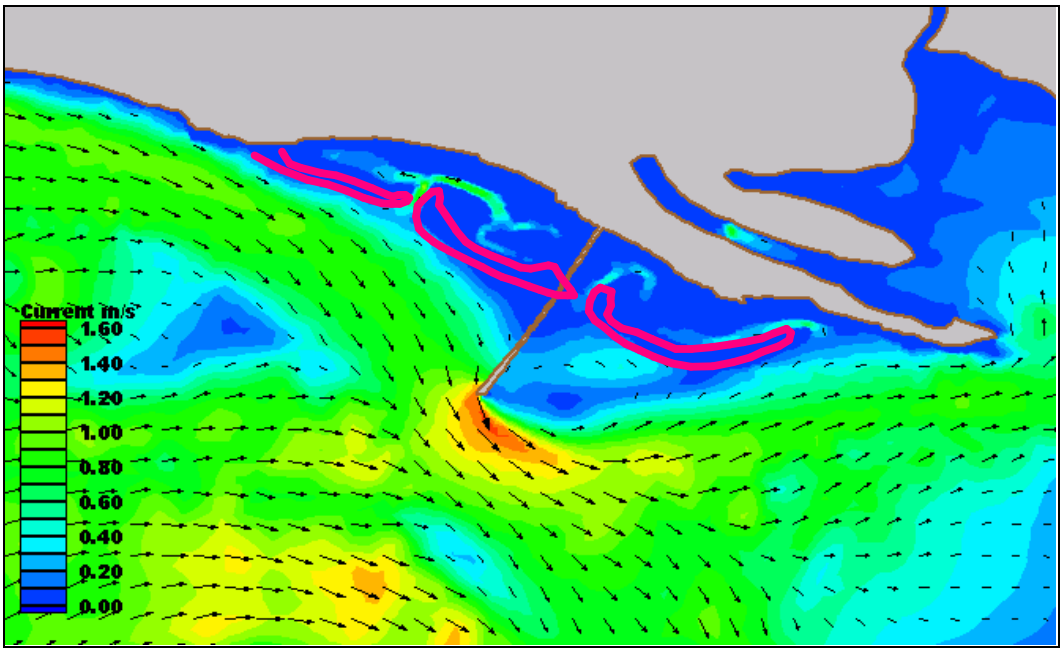

Figure 3.1.29. Peak spring flood current with training dike alternative 3 in place.

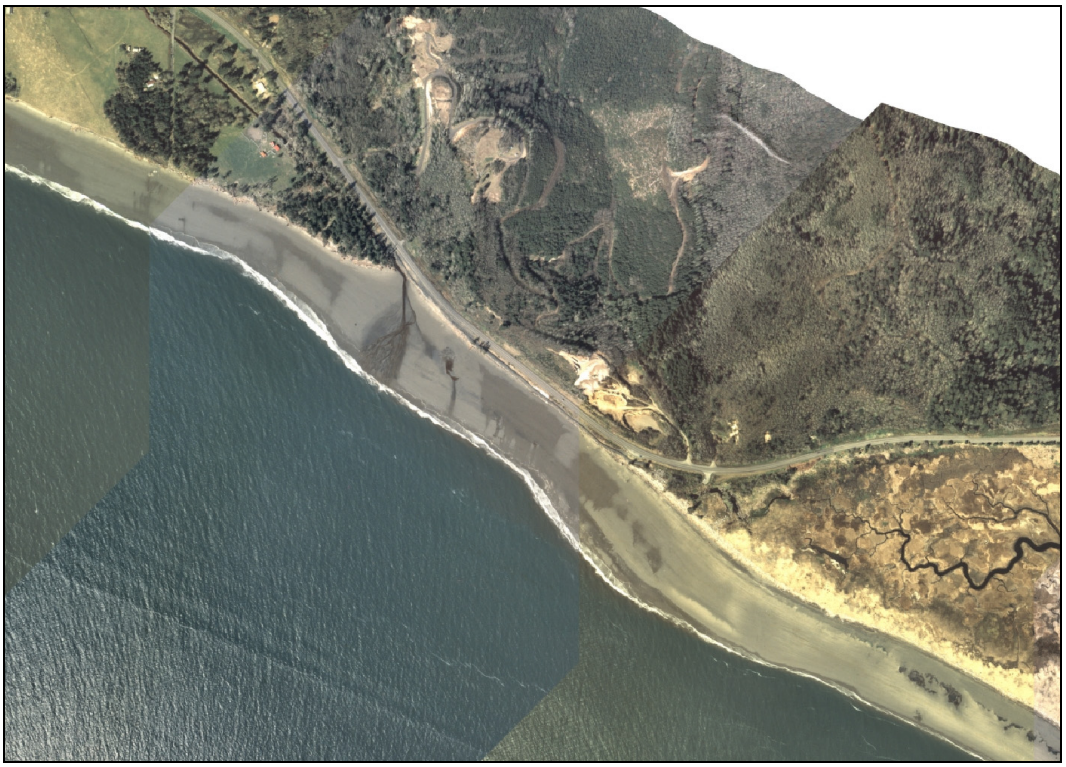

Figure 3.1.30. Northern Willapa Bay shoreline prior to SR 105 dike construction (dated 1997).

Figure 3.1.31. Northern Willapa Bay shoreline after SR 105 dike construction (dated 1999).

3.2 Wave Analysis[9]

Sediment transport and shoreline erosion are driven by a combination of waves and currents. The purpose of this section is to analyze wave conditions that influence sediment transport at Graveyard Spit and northern Willapa Bay and provide wave information required for the design of engineering alternatives. The wave analysis consists of field measurements of waves taken in Willapa Bay and numerical modeling of wave transformation and generation. The field measurements are used to validate the wave model and investigate the role of local wave generation within Willapa Bay. The numerical model is used to simulate historical storms (forced by offshore waves and local winds and modified by tides and currents). The wave model results are used in the sediment transport calculations discussed in Section 3.3 and in the development of the design alternatives.

Smith and Ebersole (2000) measured and modeled waves in Willapa Bay in a previous study. The focus of this previous study was to evaluate the feasibility of modifying the Willapa Bay entrance channel to improve navigation. Results from the navigation study included:

- The incident wave climate at Willapa Bay is severe, with storm wave heights exceeding 7 m (as measured by the Gray Harbor Buoy, Station 03601).
- The shoals extending north from Leadbetter Point substantially attenuate incident waves. The tide level modulates waves within the bay, with more wave energy penetrating the bay at high tide levels and less at low tide levels.
- Field measurements were used to validate the wave transformation model STWAVE for wave transformation and attenuation across the shoals and into the bay.
- The STWAVE model demonstrated that wave-current interaction is significant in the outer Willapa entrance channel where currents can exceed 2 m/sec, but is relatively insignificant in the interior channels.

This previous study provides much of the background information required for the present study: incident wave climate, numerical model validation, and understanding of the large-scale wave transformation from offshore into Willapa Bay. Building on this previous work, the present study additionally requires wave conditions at the Graveyard Spit shoreline for designing alternatives, waves in the interior of North Cove for sediment transport estimation and evaluation of alternatives, quantification of the impact of wave generation within Willapa Bay on the project area, and analysis of the impact of the Graveyard Spit and island dunes on reducing wave heights along the Tokeland Peninsula shoreline.

3.2.1 Field Data

Field measurements of waves at the project site were required to verify the numerical wave model and to confirm the importance of locally generated waves within Willapa Bay, south of the project. The wave measurements were part of an integrated field measurement deployment that included waves, currents, water levels, and sediment concentration. The deployment, recovery, and initial data analysis was performed by Evans-Hamilton, Inc (EHI). The wave gauge used for this study was an RD Instruments workhorse Acoustic Doppler Current Profiler (ADCP). The wave gauge was deployed 4 November – 4 December 2002 and then redeployed 6 December 2002 – 20 January 2003. The gauge was deployed at 46.7032 deg N, 124.0201 deg W in a depth of approximately 6.5 m MTL (Station 1a). Waves were sampled hourly (starting at the top of the hour) for 20 min at a rate of 2 Hz. The bin width was 0.35 cm. During the first deployment, the wave gauge was buried approximately 40 percent of the

[9] Written by Jane McKee Smith, Ph.D., Barbara A. Tracy, and Ann R. Sherlock, U.S. Army Engineer Research and Development Center, Coastal and Hydraulics Laboratory, Vicksburg, MS.

time due to the active sediment transport in the area and the tripod design (depth change were over 0.5 m), so these data were not used. Data recovery from the second deployment was good, and it included a storm with offshore wave heights exceeding 5 m during 13-16 December 2002. The peak offshore wave height during the storm was 7.9 m with a peak period of 13 sec. Figure 3.2.1 shows the incident offshore waves from the Grays Harbor Buoy and the nearshore Cape Shoalwater wave and water level measurements for the period 6-31 December 2002. Note the event with incident waves exceeding 5 m during 13-16 December 2002 (Julian days 347 through 350). Similar to the previous study, these data show the same trend that waves within Willapa Bay are strongly attenuated across the shoals and are modulated by the tide elevation.

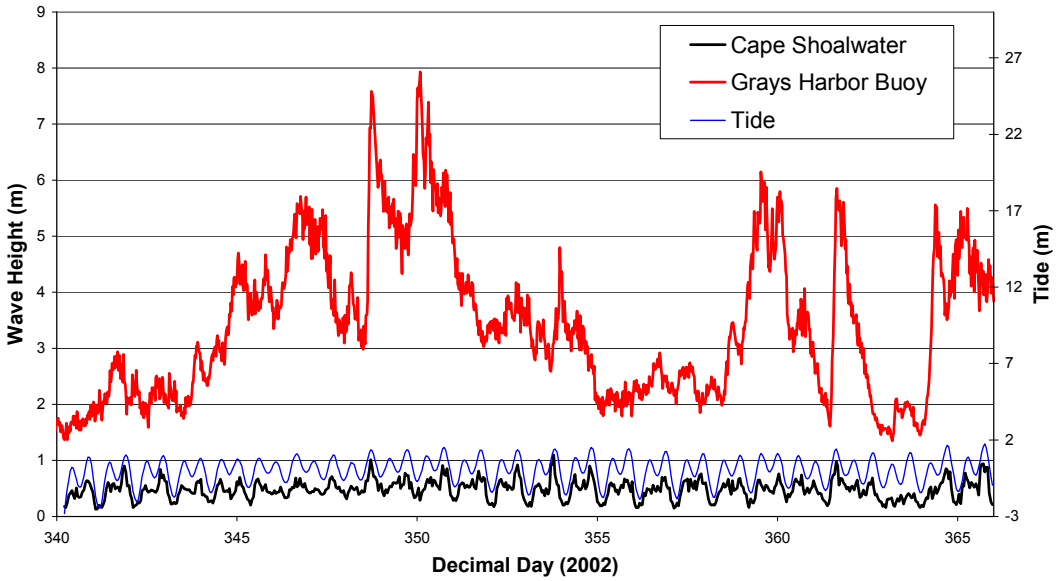

Figure 3.2.1. Measured waves and water levels.

The bottom-mounted ADCP measures waves using three methods: pressure, ranging to the surface along each of the four acoustic beams, and velocity profiles along the four beams. Wave direction and directional wave spectra are estimated using a virtual array of 12 velocity measurements (three in each of the four beams) near the surface. During the Willapa deployment, the three methods used to estimate wave energy did not always agree. The pressure measurement gave results generally much lower than the velocity or surface measurement. The problem appeared to be with the calibration, so the pressure measurements were not used. The velocity and surface measurements agreed for approximately 50 percent of the measurements. Close inspection of individual wave spectra showed the velocity measurements were most representative of field wave spectra, so the velocity measurements were used for data comparisons. The standard data analysis performed by EHI included a high-frequency cutoff of 0.2 Hz. The locally generated waves from the south bay generally fall in the peak frequency range of 0.33-0.2 Hz (3-5 sec), so the waves of interest were neglected in the analysis. Thus, the data were reanalyzed with a cutoff of 0.35 Hz. Increasing the cutoff required that each spectrum be examined for data quality (the higher frequency data are susceptible to amplified noise). It was found that the data tended to be poor for very strong currents and at the reversal from ebb to flood current. Any questionable measurements were eliminated. The reanalysis of the wave measurements increased wave heights by 0.4-0.7 m during strong winds from the south (Figure 3.2.2). Peak wave directions and peak periods also shifted for cases when the locally generated waves dominated. The reanalyzed wave parameters for 12

December 2002 are used for wave modeling verification because strong southerly winds occurred during that day.

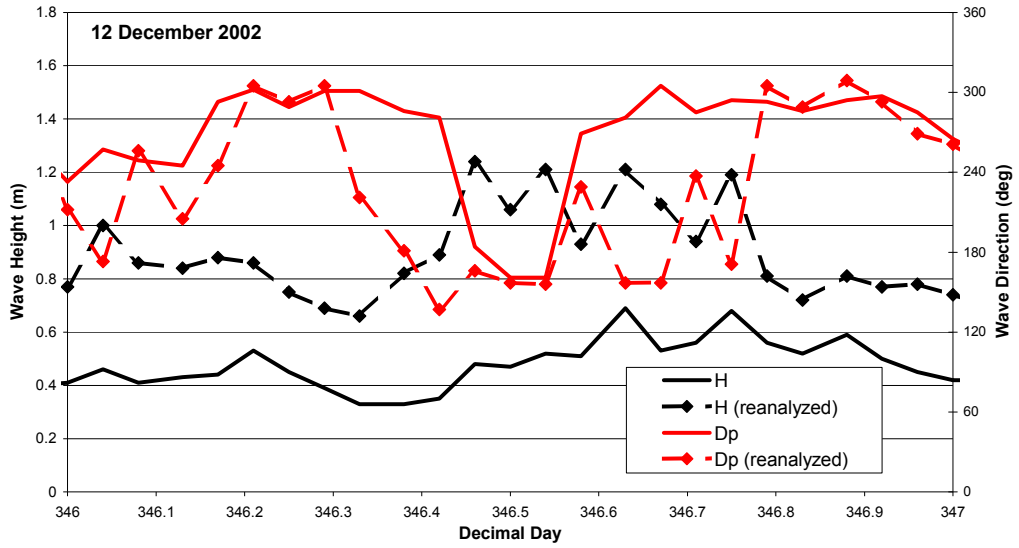

Figure 3.2.2. Reanalyzed wave heights (H) and peak directions (D_p) for 12 December 2002.

3.2.2 STWAVE Model

Numerical model simulations of waves in Willapa Bay were required for this study because field measurements cannot provide the spatial and temporal coverage required to evaluate engineering alternatives. The Steady-state spectral wave (STWAVE) model used in the previous Willapa Bay study was selected for the wave simulations. This section describes the STWAVE model and simulations for Graveyard Spit. STWAVE was forced with directional wave spectra and wind vectors from nearby field measurements for three storms. The simulations include tide input, which is required to simulate wave dissipation across the shoals. The STWAVE simulations transformed waves resulting from these Pacific Ocean wave conditions to locations within Willapa Bay, adjacent to Graveyard Spit. Three storms were selected for model simulations. The model was verified with measurements for December 2002, including strong winds from the south and local wave generation within Willapa Bay. The impact of wave-current interaction was evaluated for the area adjacent to the project. Wave-current interaction was relatively small at the project site, so additional STWAVE runs for each alternative were not required, because waves would not change from the base condition (only currents). Finally, a nested-grid was developed to simulate wave transformation across the Graveyard Spit dunes and North Cove to the Tokeland Peninsula for elevated water levels. Simulations were made to compare wave penetration with and within the dunes in place.

STWAVE Model Description

The numerical model STWAVE (Smith, Sherlock, and Resio 2001) was used to transform waves into Willapa Bay for evaluation of alternatives. STWAVE numerically solves the steady-state conservation of spectral action balance along backward-traced wave rays:

$$(C_{ga})_x \frac{\partial}{\partial x} \frac{C_a C_{ga} \cos(\mu - \alpha) E(f,\alpha)}{\omega_r} + (C_{ga})_y \frac{\partial}{\partial y} \frac{C_a C_{ga} \cos(\mu - \alpha) E(f,\alpha)}{\omega_r} = \sum \frac{S}{\omega_r} \qquad (1)$$

where

C_{ga} = absolute wave group celerity

x,y = spatial coordinates, subscripts indicate x and y components

C_a = absolute wave celerity

μ = current direction

α = propagation direction of spectral component

E = spectral energy density

f = frequency of spectral component

ω_r = relative angular frequency (frequency relative to the current)

S = energy source/sink terms

The source terms include wind input, nonlinear wave-wave interactions, dissipation within the wave field, and surf-zone breaking. The terms on the left-hand side of Equation 1 represent wave propagation (refraction and shoaling), and the source terms on the right-hand side of the equation represent energy growth or decay in the spectrum.

The assumptions made in STWAVE are as follows:

a. Mild bottom slope and negligible wave reflection.

b. Spatially homogeneous offshore wave conditions.

c. Steady waves, currents, and winds.

d. Linear refraction and shoaling.

e. Depth-uniform current.

f. Negligible bottom friction.

STWAVE is a half-plane model, meaning that only waves propagating toward the coast are represented. Waves reflected from the coast or waves generated by winds blowing offshore are neglected. Wave breaking in the surf zone limits the maximum wave height based on the local water depth and wave steepness:

$$H_{mo_{\max}} = 0.1L \tanh kd$$

where

H_{mo} = zero-moment wave height

L = wavelength

k = wave number

d = water depth

STWAVE is a finite-difference model and calculates wave spectra on a rectangular grid with square grid cells. The model outputs zero-moment wave height, peak wave period (T_p), and mean wave direction (α_m) at all grid points and two-dimensional spectra at selected grid points.

Wave Model Inputs

The inputs required to execute STWAVE are as follows:

a. Bathymetry grid (including shoreline position and grid size and resolution).

b. Incident frequency-direction wave spectrum on the offshore grid boundary.

c. Current field (optional).

d. Tide elevation, wind speed, and wind direction (optional).

Bathymetry Grid

Figure 3.2.3 shows a contour plot of the bathymetry for the Willapa STWAVE grid. The grid origin is at Universal Trans Mercator (UTM) 5,136,069 m North and 407,546 m East. The grid has 511 rows (south to north, along shore) and 301 columns (west to east, cross-shore), and grid spacing is 100 m. The grid orientation is 0 deg meaning that the x-axis points due East. Depths are relative to mean tide level (MTL). Note that Willapa Bay has a majority of areas with depths less than 10 m (see Figure 3.2.3) indicating a very shallow environment. Initial grid bathymetry came from the STWAVE grid system that was developed for the Willapa Bay Channel Feasibility study (Smith and Ebersole 2000). Survey data collected in 2002 were used to update the bathymetry.

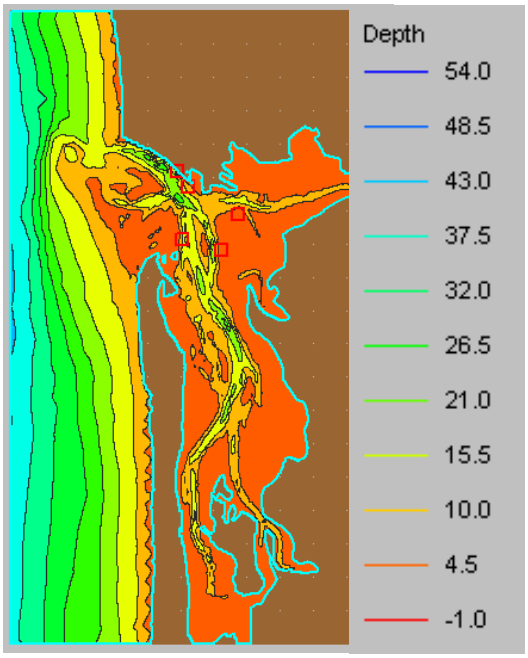

Figure 3.2.3. STWAVE bathymetry grid for Willapa Bay (depths in meters). Land area is shown in brown.

Input Wave Spectra

Input wave spectra forcing for the wave model on the western (Pacific Ocean) grid boundary: the input wave spectra provide the distribution of wave energy as a function of frequency and direction. For this project, the input spectra were generated based on the one-dimensional frequency spectra from the Grays Harbor buoy, when available. The Columbia River Buoy (NDBC[10] 46029) was used to supplement missing data at Grays Harbor. The directional distributions measured at the buoy lack sufficient resolution to drive the model, so a theoretical distribution of the form $\cos^{nn}(\alpha-\alpha_m)$ was applied, where *nn* is the spreading coefficient, and α_m is the mean wave direction. The values used for *nn* are given in Table 3.2.1 (Thompson et al. 1996). Large values of *nn* indicate a narrow directional distribution (swell waves), and small values represent a wide distribution (sea waves). The value of *nn* for the peak of the spectrum (Table 3.2.1) was applied for the peak and lower frequencies. For frequencies higher than the peak, the values in Table 3.2.1 were applied. The input spectra have 30 frequencies, starting with 0.04 Hz and incrementing by 0.01 Hz. The directional resolution is 5 deg.

Table 3.2.1 Values of *nn* used for input wave spectra

***F*, Hz**	≤ 0.04	0.045	0.05	0.055	0.06	0.08	≥ 0.1
nn	38	36	30	26	22	10	4

Current Fields

For applications where wave-current interaction significantly alters the wave height, or blocks the waves, current fields are needed as an input to the model. Wave height generally increases on strong ebb currents and decreases on strong flood currents. Currents also alter wave direction. The current modifies waves with higher frequencies (shorter periods) more than waves with lower frequencies. In addition to shoaling and refraction by currents, wave breaking is also changed by an opposing or following current (*L* and *k* change in Equation 2). Wave breaking is enhanced on an opposing current (ebb) and reduced on a following current (flood). If the ebb current is strong, waves with short periods cannot propagate against it, and wave energy is blocked and dissipated.

For Willapa Bay, model runs with and without a current were made to assess the sensitivity of the wave transformation at the study site to wave-current interaction. For the sensitivity analysis, a storm 1-5 March 1999 was simulated with and without wave-current interaction. Figure 3.2.4 shows the differences in wave heights for simulations with and without currents for a location near the Graveyard Spit shoreline (same location as the nearshore wave measurement Station 1a described in section 3.2.1). The maximum difference in wave height is approximately 10 percent. The differences are relatively small because the currents in this interior region are generally significantly less than the strong (ebb) currents in the entrance channel. Smith and Ebersole (2000) also showed that the effects of wave-current interaction in the interior bay are relatively small (their Figures 5-3 and 5-4).

[10] National Data Buoy Center.

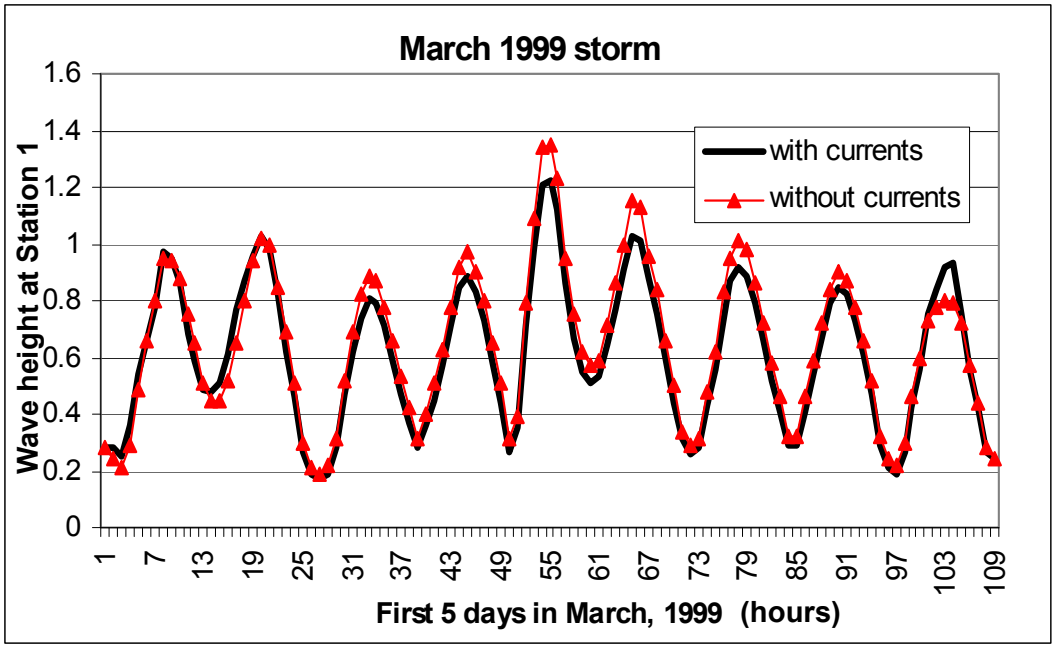

Figure 3.2.4. Comparison of STWAVE results with and without wave-current interaction for 1-5 March 1999 storm. Wave height is in meters

Water Level and Wind

Water level variations are a combination of tide, storm surge, and wave setup. Water level is applied in STWAVE as constant water depth change over the entire grid. Within the Willapa grid domain, the tide elevation does vary spatially, but the influence of this variation on wave transformation is small. Water level for wave runs is specified from measurements at the NOS Toke Point gauge. Because the grid depths are specified relative to MTL, water level fluctuations are also specified relative to MTL. Water level is critical for Willapa wave transformation because it controls the amount of wave energy dissipated on the shoals or dunes.

Wind input in STWAVE creates wave growth across the grid domain. Wave measurements at the Grays Harbor buoy reflect most of the local wave-generation processes for the ocean waves. During meetings with representatives of the Shoalwater Bay Indian Tribe, the issue of waves generated within Willapa Bay due to winds from the south was raised. These locally generated waves are not included in the STWAVE simulation because they are generally outside the half-plane generation included in the model. These waves are independent of the waves propagating from offshore, thus, the generation of these local bay waves was calculated outside the numerical model. The calculation process and validation of results is presented in the next section. Wind data used in this study was the Toke Point gauge (when available) or from the Columbia River Buoy (NDBC buoy 46029).

Selection of Storms

Three storms were selected for simulation of storm wave conditions. The first storm of record was 1-5 March 1999, and was suggested by Eric Nelson, Seattle District. This storm strengthened by 43 mb in 24 hrs and was termed a "bomb" by Mariner's Weather Log (Bancroft 1999). Winds reached hurricane force off the north Oregon coast and generated phenomenal seas in coastal waters and rapid building of sea conditions as the storm approached. This event produced 14 m waves at NDBC 46050 (37 km west

of Newport, Oregon); this was more than twice the 6.5 m wave height reported only 6 hours earlier (Bancroft 1999). Wave and wind information available for this event is available from NDBC buoy 46029 (Columbia River Bar, 144 km south southwest of Aberdeen, Washington). NDBC tables for this location show 26 m/sec on 3 March 1999 at 0500 as the maximum wind over the period of record (March 1984 - December 2001). This same table notes the maximum significant wave height over the period of record as 12.8 m on 3 March 1999 at 0800. Figure 3.2.5 shows the locations of these measurement sites relative to the project site. Table 3.2.2 gives locations of NDBC measurement sites in latitude and longitude. Figure 3.2.6 shows the wind conditions for 1-5 March 1999, from NDBC 46029. Note the classic direction swing and maximum wind conditions in excess of 25 m/sec. Figure 3.2.7 shows a wave rose from the Coastal Data Information Program (CDIP) buoy at Gray's Harbor for 1-5 March 1999. The Gray's Harbor buoy is located at 46.85665deg N, 124.24455deg W. Note that 6-7 m waves are coming in from 202.5-270 deg (Meteorological convention where 270 deg refers to waves coming from due West). Some measured wave results at Gray's Harbor were missing for 3 March 1999, so the maximum conditions may not be shown in this plot. Gray's Harbor does not report wind information so wind and wave measurements from NDBC 46029 were used in the STWAVE storm simulation for March 1999. Figure 3.2.8 shows the measured wave height and peak period results at NDBC 46029 for 1-5 March 1-5 1999. The 12.8 m maximum wave height occurred on 3 March 1999. Measurements close to Cape Shoalwater were not available for this historic event, but the simulation results evaluate site conditions during this event of record.

Figure 3.2.5. Cape Shoalwater location on the coast of Washington state at the entrance to Willapa Bay. Gray's Harbor buoy, part of the Coastal Data Information Program (CDIP), is shown by a blue dot. Red dots show sites of previous CDIP measurement locations. Orange squares show locations of NDBC 46041 (Cape Elizabeth), 46029 (Columbia River Bar), and 46050 (Stonewall Banks).

Table 3.2.2 NDBC buoys near Willapa Bay

NDBC Identifier	Name	Latitude (deg N)	Longitude (deg W)
46041	Cape Elizabeth	47.34	124.75
46029	Columbia River Bar	46.12	124.51
46050	Stonewall Banks	44.62	124.53

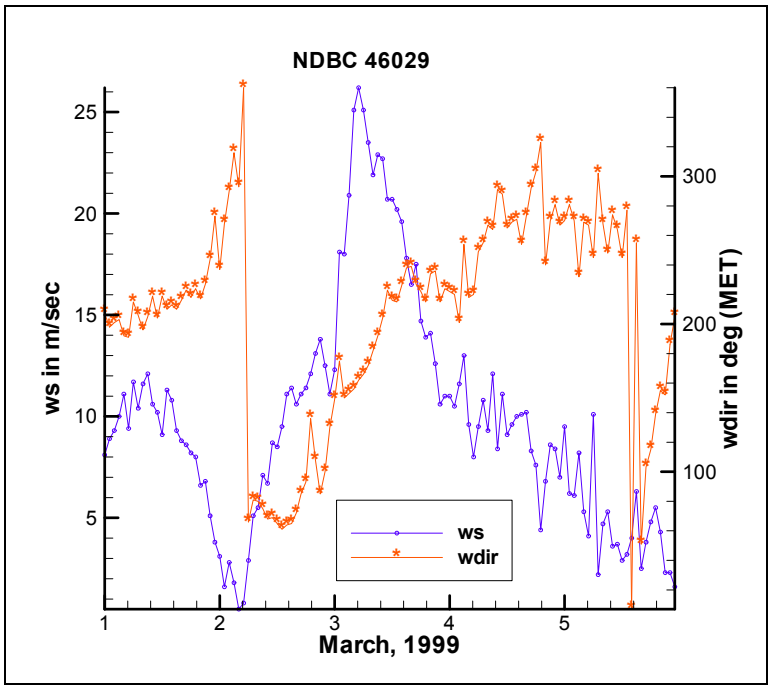

Figure 3.2.6. Wind speed and wind direction information for 1-5 March 1999, at NDBC 46029 (Columbia River Bar).

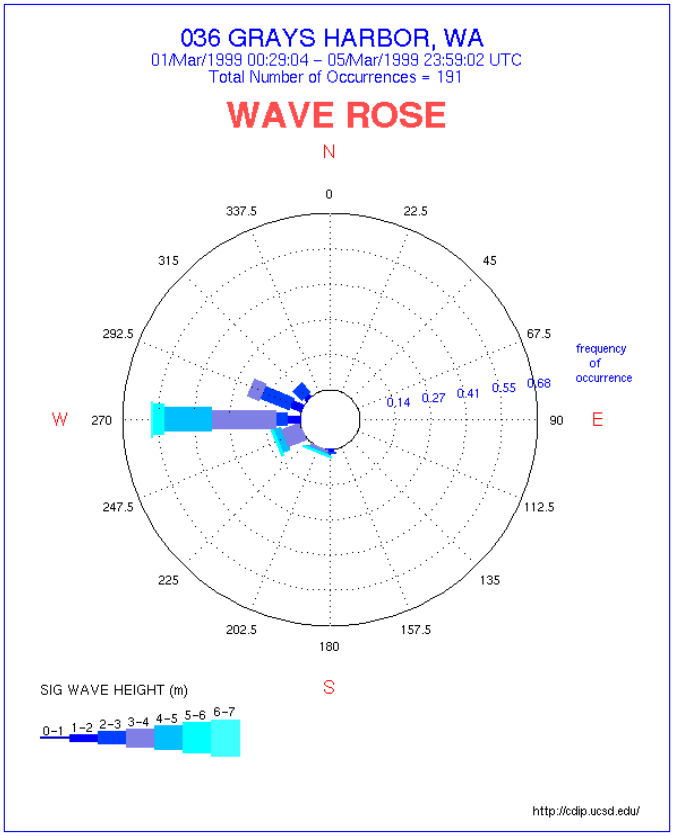

Figure 3.2.7. Wave rose plot for the storm of 1-5 March 1999 at Grays Harbor.

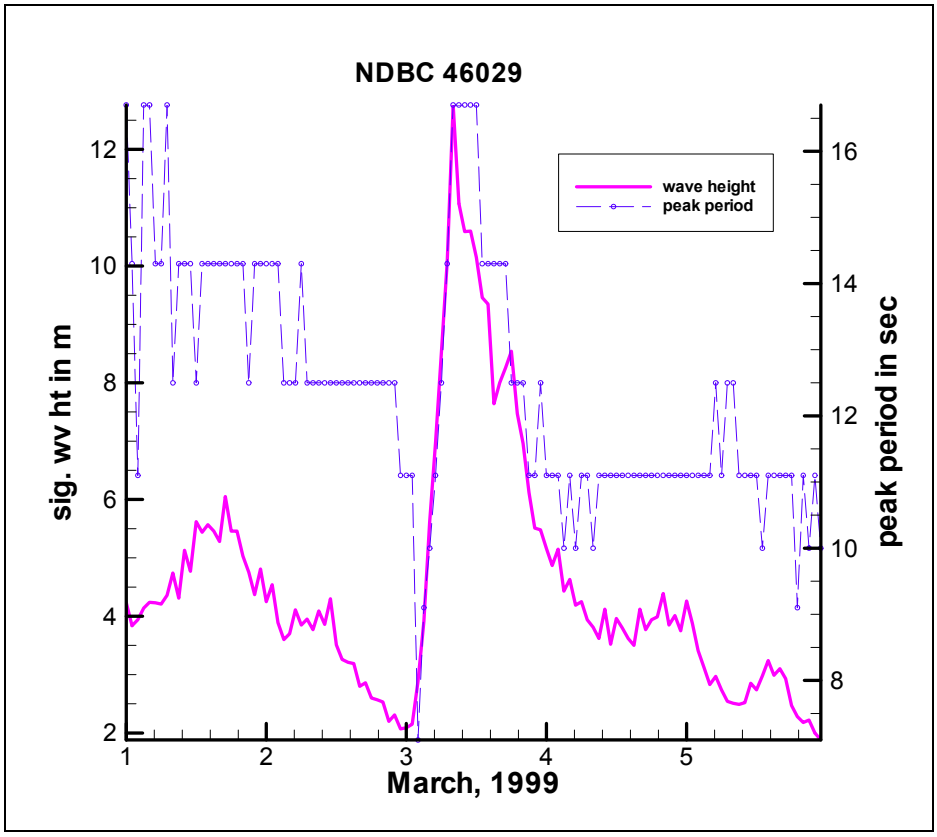

Figure 3.2.8. Significant wave height and peak period for storm of 1-5 March 1999 at NDBC 46029.

Two additional recent storm events were chosen to coincide with the measurements taken for this project. Information from NOAA web pages was used to select these recent events. The first event, November 6-11, 2002, was a flooding event that produced almost 8 m waves at the Gray's Harbor buoy. Coastal flooding damaged a restaurant and roads in Gray's Harbor area. Figure 3.2.9 shows a wave rose plot for November 6-11, 2002 at the Gray's Harbor buoy. The storm produced 7-8 m waves incident from 270 and 247.5 deg and 4-5 m waves incident from 225 deg. Figure 3.2.10 shows the measured wave height and peak period at Cape Elizabeth (NDBC 46041) for November 2002. Note the occurrence of waves in excess of 7 m on November 9. The second storm on December 14-18, 2002 was characterized as a high wind event. This storm also created 8 m waves at Gray's Harbor buoy and produced a high-wind warning in Pacific county with 27 m/sec. Figure 3.2.11 shows a wave rose for the Grays Harbor buoy for December 14-18, 2002. The storm produced 7-8 m waves incident from both 225 and 247.5 deg. Figure 3.2.12 shows wave height and peak period at the Cape Elizabeth buoy (NDBC 46041) for December 10-20, 2002. Waves exceeded 7 m on December 14-16. Figure 3.2.13 shows the wind speed and wind direction for December 10-20, 2002 at Cape Elizabeth. Note the extended period of wind from the south-southwest on December 12. Information at Columbia River Bar was not available for these storms. Both these storms are large events. Unfortunately, wave data are not available for the November storm (as discussed in section 3.1.2), but data are available for the December storm.

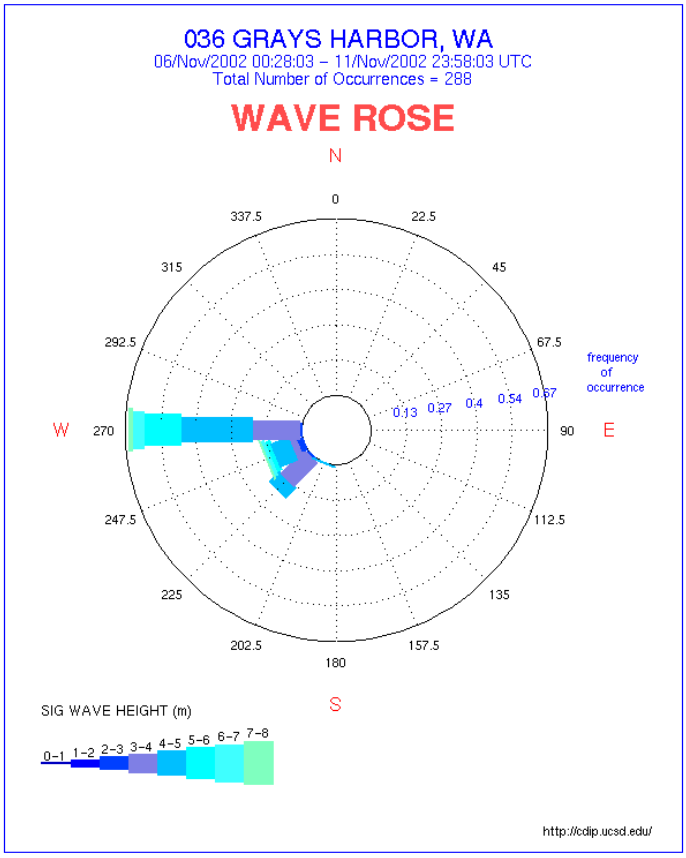

Figure 3.2.9. Wave rose plot for the storm of 6-11 November 2002.

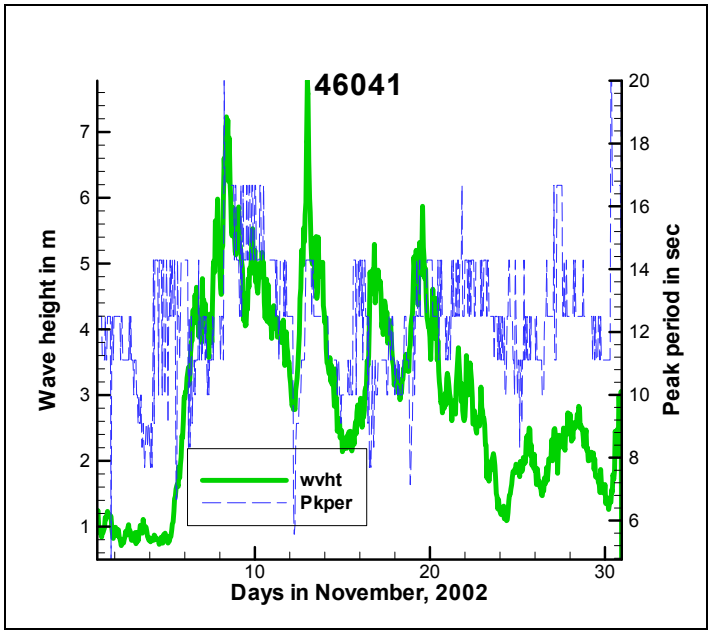

Figure 3.2.10. Significant wave height in green and peak period in blue for NDBC buoy 46041 for November 2002.

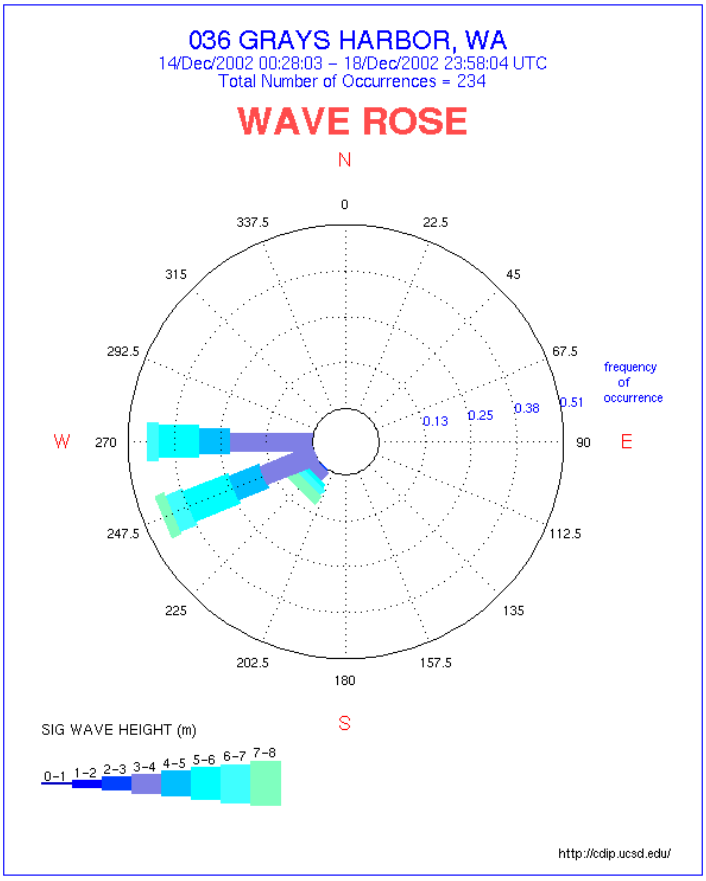

Figure 3.2.11. Wave rose plot for the storm of 14-18 December 2002.

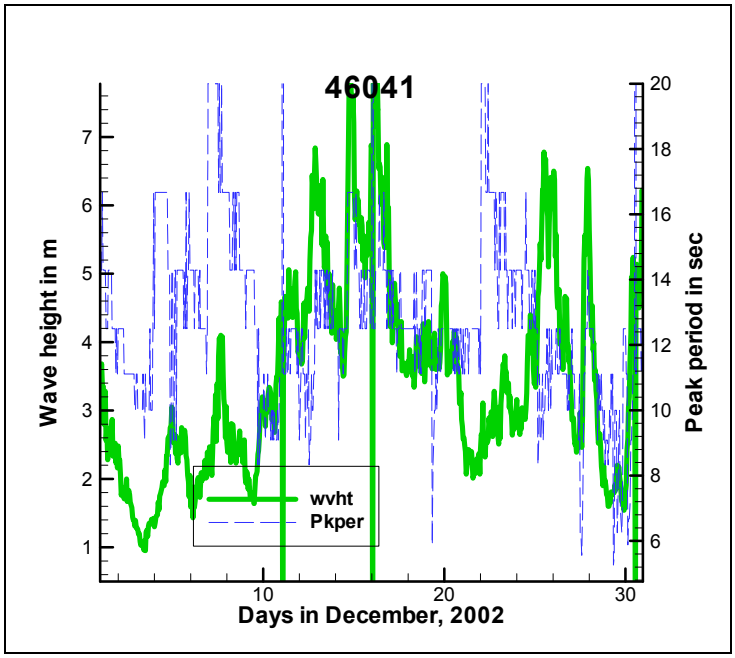

Figure 3.2.12. Significant wave height in green and peak period in blue for NDBC buoy 46041 for December 2002.

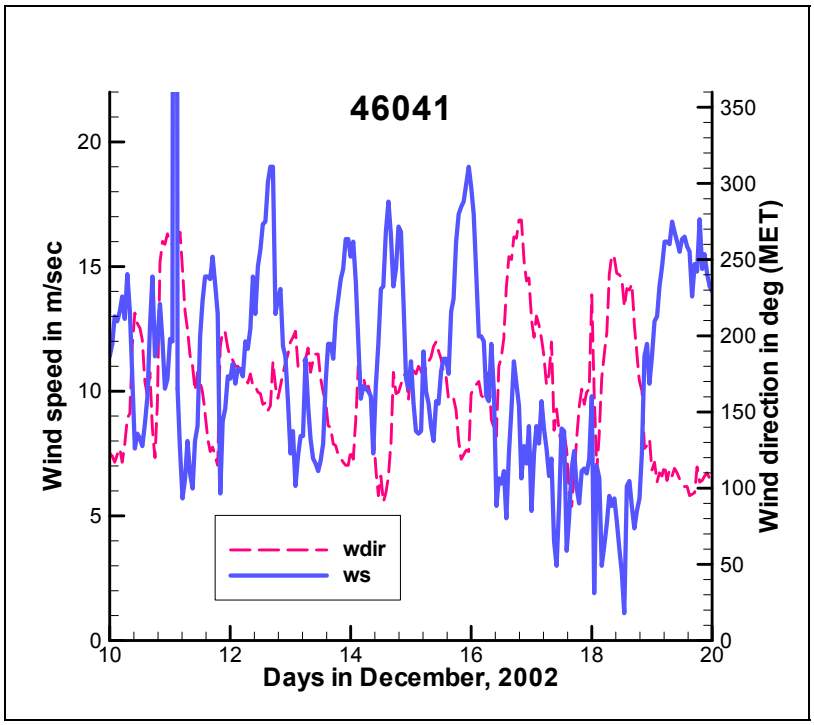

Figure 3.2.13. Wind speed in blue and wind direction in red at NDBC 46041 for 10-20 December 2002.

Model Verification for Local Generation -- 12 December 2002

The Willapa Bay navigation study (Smith and Ebersole 2000) included verification of STWAVE for transformation of ocean waves into Willapa Bay. This verification did not include measurements in areas that would capture local generation in Willapa Bay. The field measurements collected in December 2002 are directly adjacent to the shoreline of Graveyard Spit and do include local generation in the south bay. Inspection and analysis of the measured directional spectra for 12 December 2002 showed significant energy from southerly directions at relatively high frequencies, indicating local generation within Willapa Bay. Wind information available at offshore buoys indicated that winds were blowing from the south, and local wave generation in Willapa Bay was added to the wave energy propagating into the bay from the ocean.

The STWAVE application only considers wave growth and transformation on a half plane centered on wind and wave energy coming from 270 deg. The additional wave energy generated in the south bay was calculated from available winds for 12 December 2002 and fetches calculated from the bay geometry. The additional generated wave energy was added to the STWAVE results at the measurements site (Station 1a). Cape Elizabeth showed over-water wind speeds in excess of 15 m/sec coming from due south or slightly south-southwest on December 12. Wave growth was estimated using the wind-stress factor U_A defined in the Shore Protection Manual (SPM 1984). The SPM 3 m (chosen because Willapa Bay is very shallow) shallow-water wave forecasting charts were used with a maximum fetch of 17 km to produce the additional 0.5 m wave height that was added to the STWAVE results. Figure 3.2.14 shows initial STWAVE wave results (in red) at Station 1a (without wave energy from the south bay) compared to initial measurement results (in green) at Station 1a (high-frequency cut off of 0.2 Hz) for 12 December 2002. This figure also shows the reanalyzed measurements in black (0.35 Hz cutoff) and the STWAVE results with estimated wind-wave enhancement in purple. This procedure provided a reasonable match between the measured wave results and the enhanced STWAVE results.

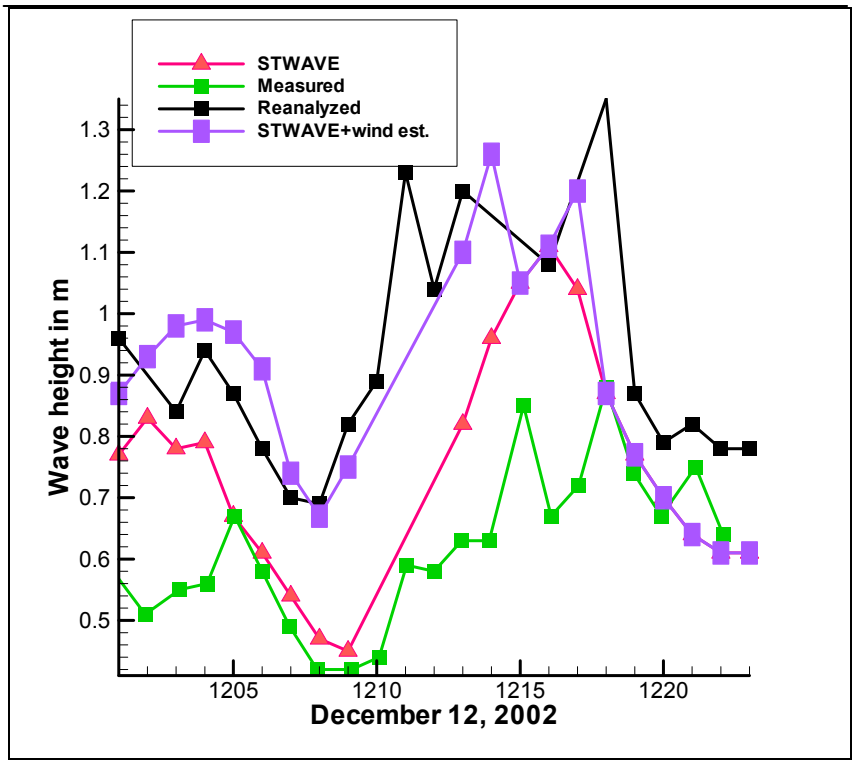

Figure 3.2.14. STWAVE results (red) compared to initial measurement results (green) and reanalyzed measurement results (black) for 12 December 2002. Winds during this time were coming from the south over Willapa Bay, and STWAVE results (in purple) were enhanced with wave energy contributions from the south.

3.2.3 Model Results

March 1999 Storm

The storm of record is 1-5 March 1999. Measurements were not available in Willapa Bay, but results from the STWAVE simulations are used to quantify waves for this severe event. Figure 3.2.15 shows wave results at a station close to the project site at Cape Shoalwater (Station 1a). The figure shows the offshore wave heights used to drive STWAVE, the tide elevation, and the nearshore wave heights. The March 1999 STWAVE runs used directional wave spectral input and wind vector information from Columbia River Bar because the Grays Harbor buoy was not operational for the full storm. The maximum nearshore wave height was approximately 1.65 m on 3 March. Local winds from southern Willapa Bay contributed to the maximum height. Figure 3.2.16 shows a contour plot of the STWAVE wave results for 3 March 1999 at 0800. The figure shows waves in excess of 11 m offshore and indicates 1.5 m wave heights at Station 1a near the Shoalwater project site. Wave vectors show the offshore storm waves are coming in from the southwest. The March 1999 storm was used to evaluate the alternatives selected for the Shoalwater site. The wave heights near the project site are strongly modulated by the water level as illustrated in Figure 3.2.17. Figure 3.2.17 shows a nearly linear relation between water level and interior bay wave height. Thus, during storm events with elevated water levels, more wave energy penetrates into Willapa Bay. The elevated water levels also mean that the waves attack higher elevations on the dunes and shorelines.

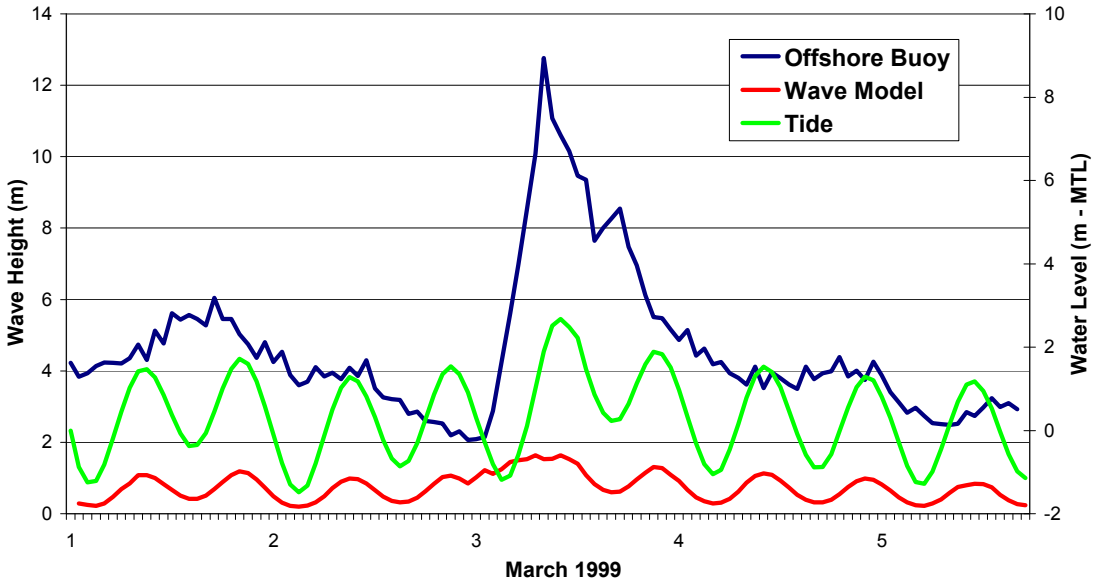

Figure 3.2.15. Time history of March 1999 storm: measured wave height offshore, measured tide, and simulated wave height nearshore.

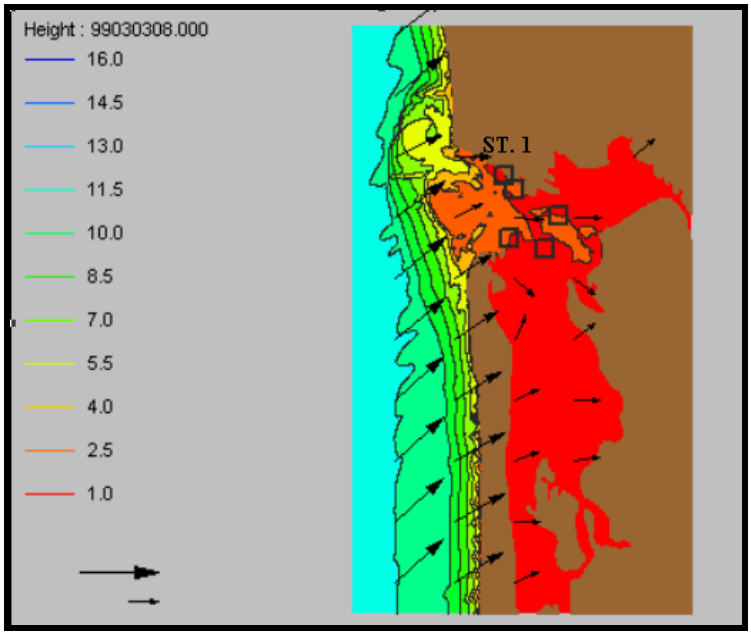

Figure 3.2.16. Contoured wave height diagram of Willapa Bay for the 8th hour on 3 March 1999. The large arrow in the legend indicates 12 m maximum wave height and the smaller legend arrow indicates 0 m wave height. Station 1 is located near the project site.

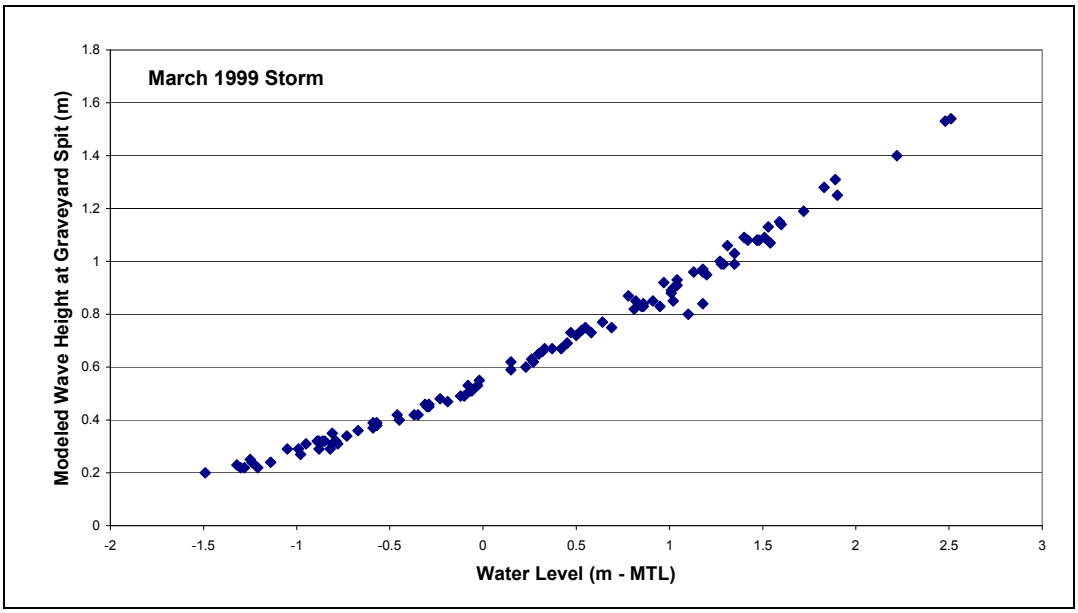

Figure 3.2.17. Relationship of modeled wave heights and water levels at Station 1 for March 1999 storm.

November 2002 Storm

STWAVE results for the November 2002 storm are summarized in Figure 3.2.18. The offshore wave heights exceeded 7 m, but the nearshore wave heights ranged from 0.1 to 1.4 m. An example contour plot of the wave height for 9 November 2002 at 1500 is shown in Figure 3.2.19. The figure shows the strong dissipation of wave energy over the Willapa shoals.

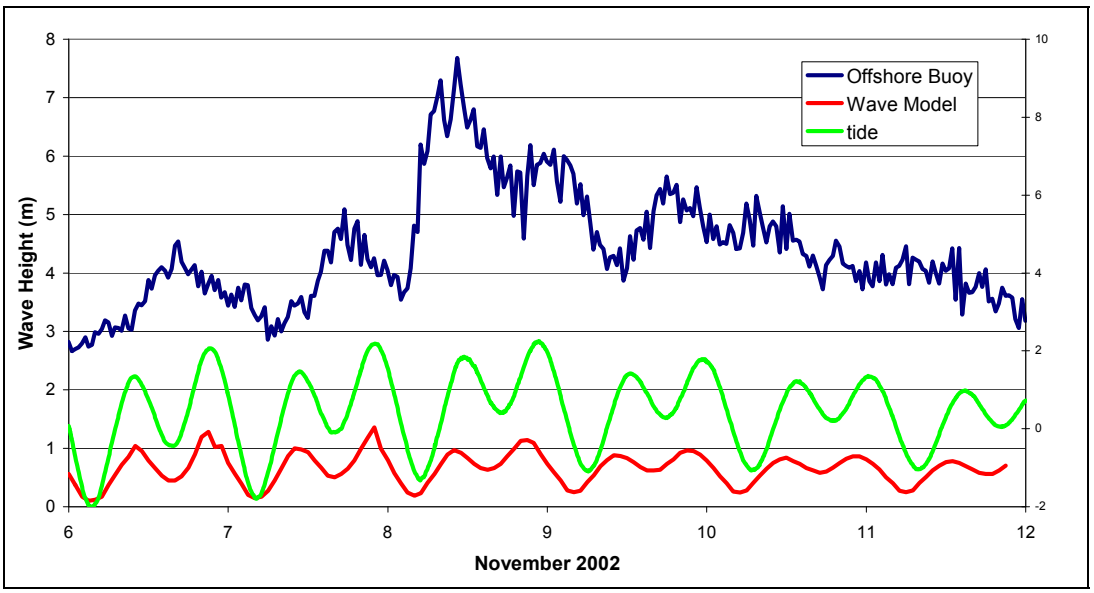

Figure 3.2.18. Time history of November 2002 storm: measured wave height offshore, measured tide, and simulated nearshore wave height.

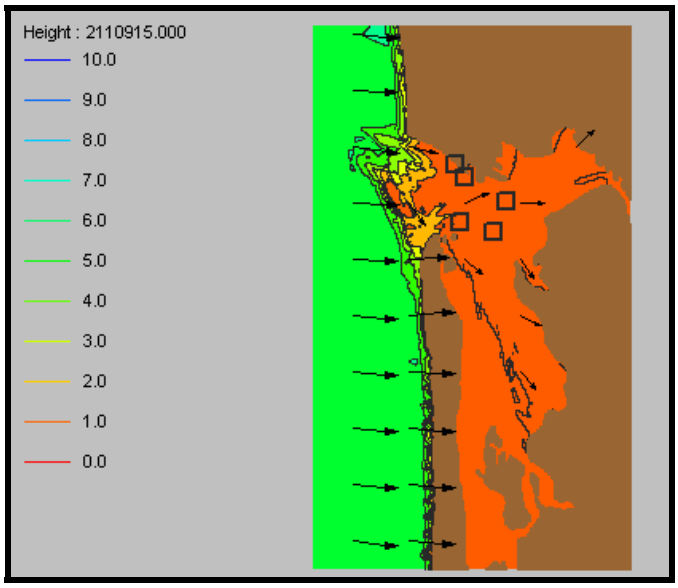

Figure 3.2.19. Wave height contour plot of the STWAVE grid for the Willapa Bay area shows wave conditions on the 15th hour on 9 November 2002. Offshore waves were in excess of 5 m, from due west.

December 2002 Storm

STWAVE results for the December 2002 storm are summarized in Figure 3.2.20. The maximum offshore wave height was approximately 8 m, and the nearshore wave heights ranged from 0.5 to 1.2 m.

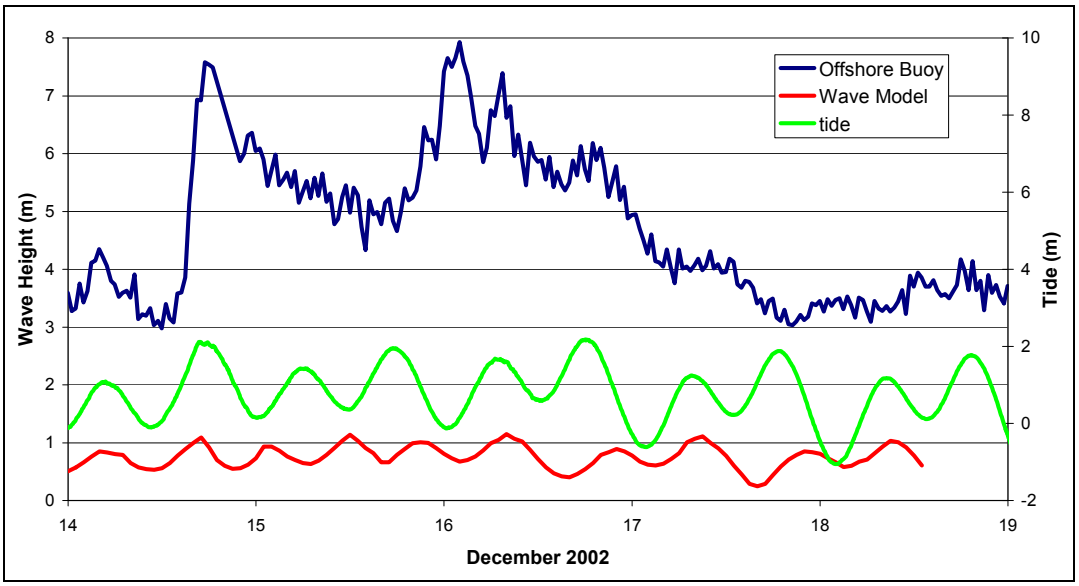

Figure 3.2.20. Time history of December 2002 storm: measured wave height offshore, measured tide, and simulated nearshore wave height.

3.2.4 North Cove Waves With and Without Protective Dunes

Other sections of this study showed that the channel migration and shoreline erosion rates within Willapa Bay have slowed over recent years. But, degradation of the barrier dunes protecting the Shoalwater Tribe shoreline indicate continued erosion of the dunes and flooding of tribal land during storms with elevated water levels. To investigate the protection from wave attack provided by the dunes, additional, refined STWAVE runs were made to compare waves at the shoreline with and without the barrier dunes in place.

A nested grid of the dune and shoreline area was developed with a resolution of 30 m. This grid nested into the larger Willapa Bay grid and focuses on the North Cove area. The grid origin is at UTM 5171170 m North and 422,330 m East. The grid has 160 rows and 115 columns. The grid orientation (x-axis) is 35 deg north of east. Two versions of the grid were developed: one with the dunes as they exist based on 2002 bathymetry, and one with the barrier dune elevations above mean high water removed (Figure 3.2.21). The existing condition is referred to as the 'with dune' case and the altered bathymetry as the 'without dune' case. The offshore boundary conditions for the nested grid runs are taken directly from the larger-scale STWAVE simulations, including local generation in southern Willapa Bay.

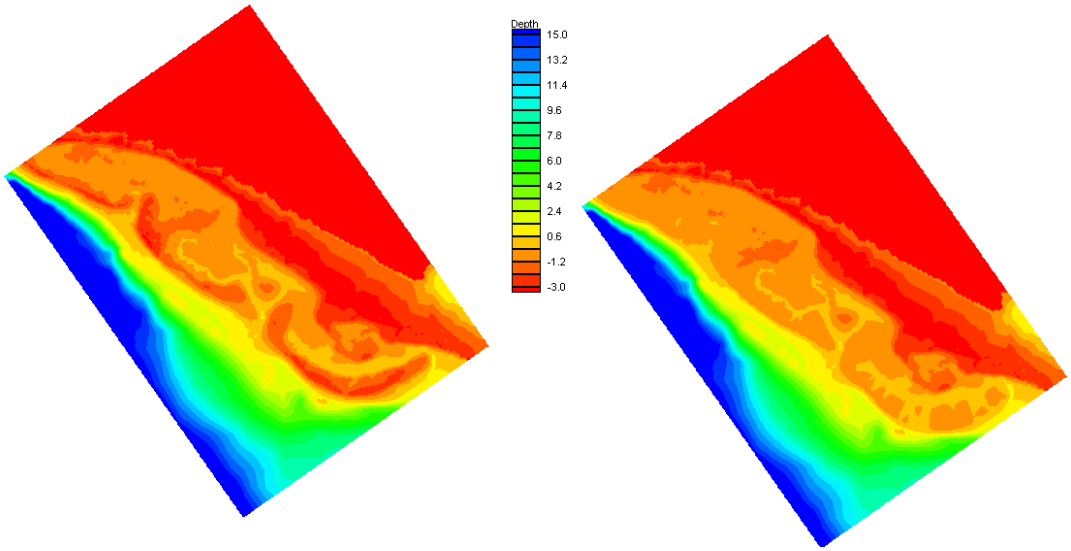

Figure 3.2.21. Bathymetry grids for nested grid simulations with and without dunes (with dunes on left and without dunes on right).

The March 1999 storm was selected to simulate the with and without dune cases. The results are shown in a series of figures. Figures 3.2.22 and 3.2.23 show a snap shot of the wave heights for the with and without dune cases, respectively, for 3 March at 0900. The warmer colors (orange to green) indicate larger wave heights and the blues indicate lower heights. These plots are representative of the storm. The orange regions represent where waves shoal and break as they propagate up the slope to the dune. In the with dune case (Figure 3.2.22), waves continue to break up to the crest of the dune. Wave energy also passes through some gaps in the dune line. In the without dune case (Figure 3.2.23), waves exceeding 1 m in height pass over the lowered dunes and impact the shoreline. Eight station locations are indicated in Figures 3.2.22 and 3.2.23, with Station 1 being the furthest to the northwest and station 8 to the southeast. Figure 3.2.24 shows the wave height for the 8 alongshore stations at the peak of the March 1999 storm (same hour as Figures 3.2.22 and 3.2.23) for the with and without dune simulations. The wave height is

significantly reduced at the shoreline for the with dune case for all stations except station 6, which is behind a gap in the dune line. Wave heights for these 8 stations are plotted in Figure 3.2.25 for the duration of the March 1999 storm. The filled symbols indicate simulations with the dunes and open symbols indicate without the dunes. Wave height is plotted as a function of water level (similar to Figure 3.2.17, which showed waves seaward of the dunes). The figure shows quantitatively, the protection provided by the dunes. With the dunes in place (existing condition), wave heights at the shoreline are generally less than 0.6 m, but without the dunes, wave heights are approximately twice as large. The existing dunes provide significant protection to the shoreline. Loss of the dunes would increase wave heights at the shoreline (increases storm damage) and increase overwash into North Cove.

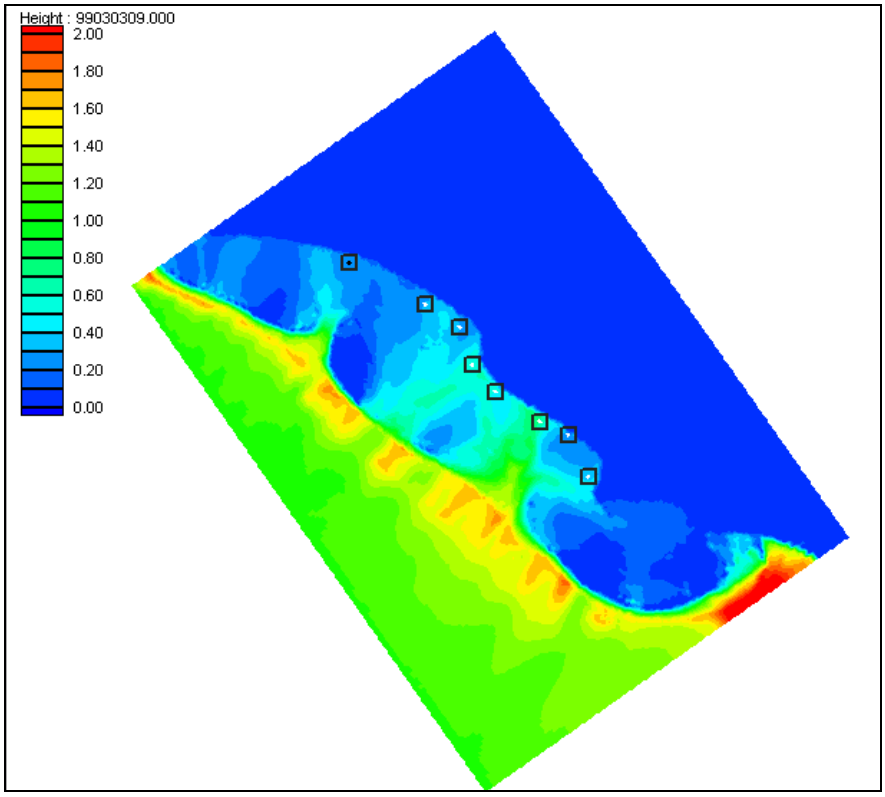

Figure 3.2.22. Contour plot of wave height with dunes for 3 March 1999 at 0900.

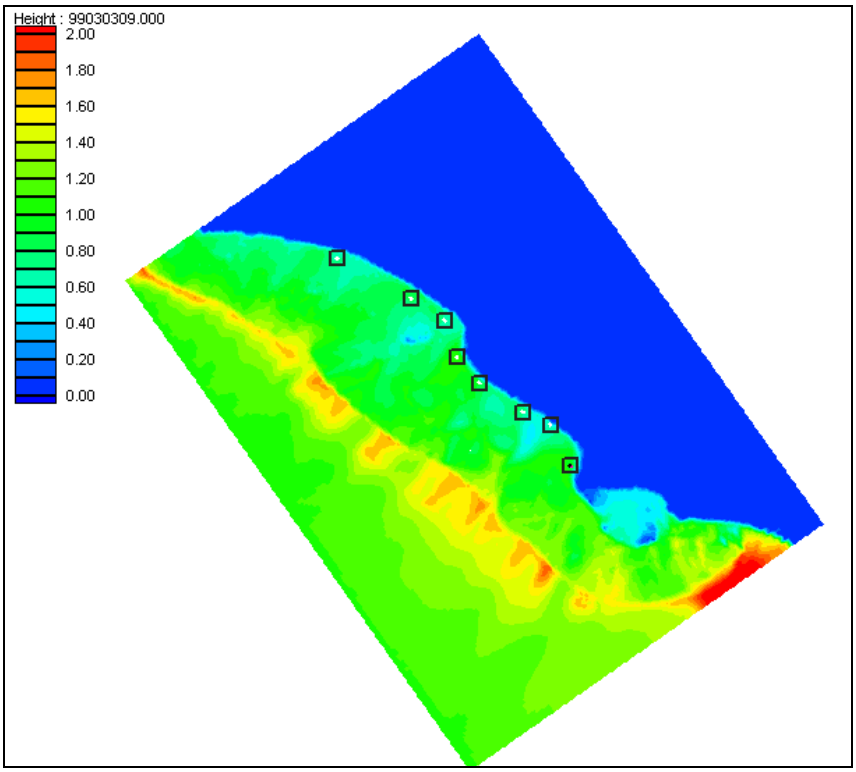

Figure 3.2.23. Contour plot of wave height without dunes for 3 March 1999 at 0900.

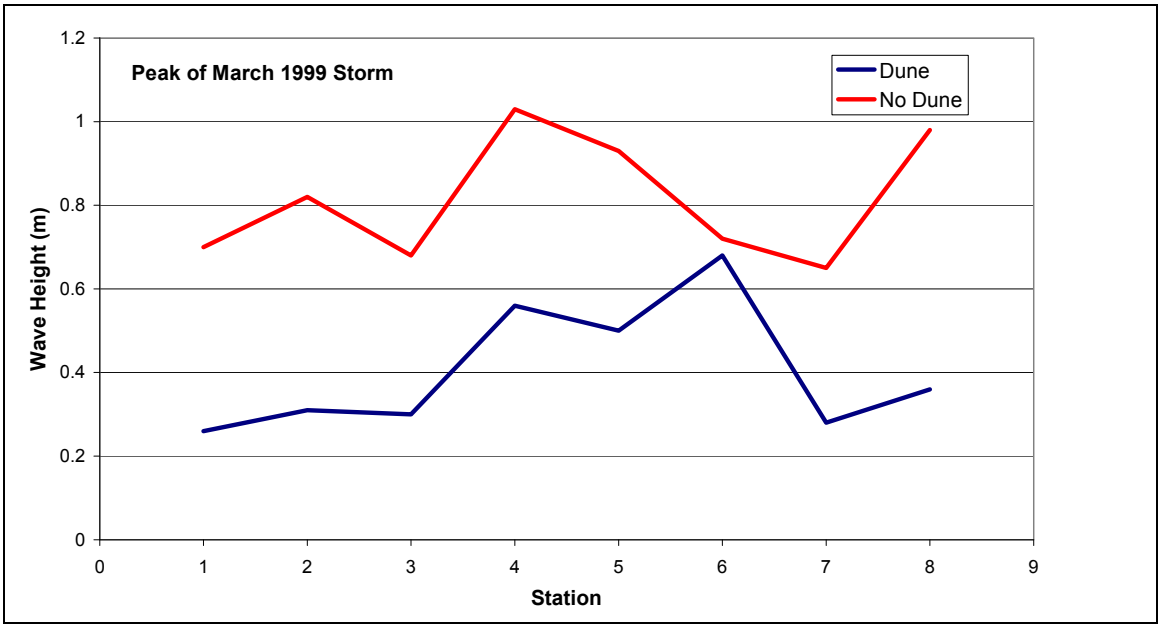

Figure 3.2.24. North Cove alongshore distribution of wave heights with and without dunes for 3 March 1999 at 0900.

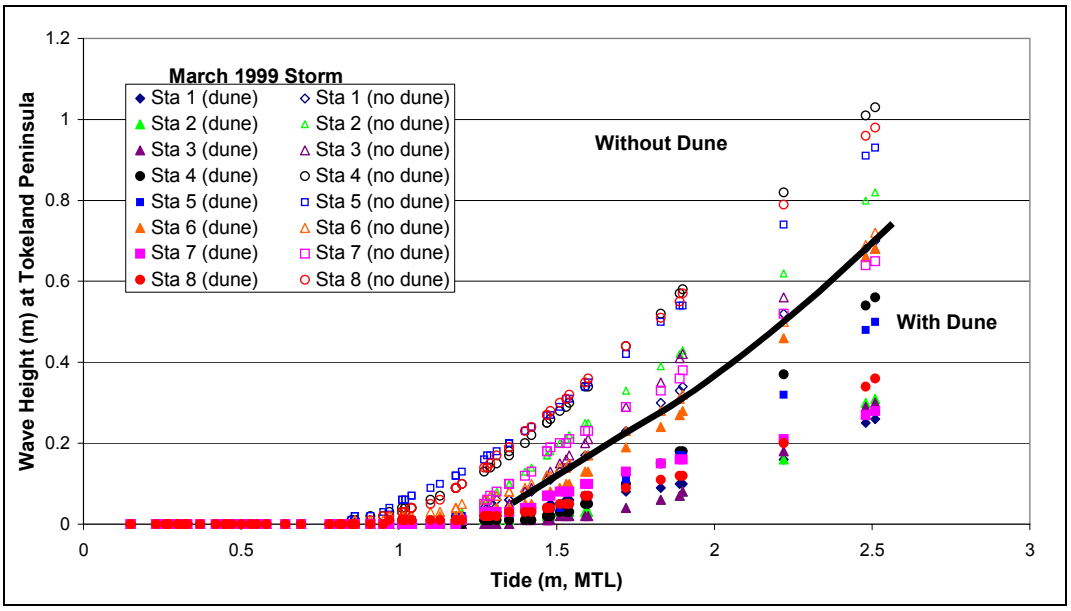

Figure 3.2.25. North Cove wave heights with and without dunes for 3 March 1999.

3.2.5 Summary of Study Results

Waves are attenuated across the shoals at the mouth of Willapa Bay. The water level over the shoals is the critical limiting parameter. Offshore-generated waves reaching Graveyard Spit are generally in the range of 0.3 to 1.0 m. During storms, water levels are elevated across the shoals and the larger wave heights occur. Also during storms, local winds from the south generate waves in southern Willapa Bay. The total wave heights (offshore plus local generation) at the project site are potentially in the range of 1.5 to 2.0 m. The wave heights simulated for the March 1999 storm peaked at 1.6 m along the spit. Even as the overall shoreline erosion rate is reduced by reduction in the Willapa channel migration, waves will continue to act on the barrier spit during storm events (surge and southerly winds). This will result in continued flooding, overwash, and loss of dune elevation. Model results showed that the existing dunes provide significant protection to the shoreline, and further loss of dune elevation will exacerbate flooding and storm damage.

References

Bancroft, G. P. 1999. "Marine Weather Review, North Pacific Area, December 1998 through March 1999," *Mariner's Weather Log,* NWS/NOAA, 43 (2), August 1999, p36-42.

Smith, J. M., and Ebersole, B. A. 2000. "Modeling and Analysis of Short Waves," Chapter 5 in "Study of Navigation Channel Feasibility, Willapa Bay, Washington." Technical Report ERDC/CHL-00-6, N. C. Kraus, ed., U.S. Army Engineer Research and Development Center, Vicksburg, MS, 23 pp.

Smith, J. M., Sherlock, A. R. and Resio, D. T. 2001. "STWAVE: Steady-State Spectral Wave Model User's Manual for STWAVE, Version 3.0," ERDC/CHL SR-01-1, US Army Corps of Engineers Engineer Research and Development Center, Vicksburg, MS.

Shore Protection Manual, 1984. Coastal Engineering Research Center, Department of the Army, U.S. Army Corps of Engineers, Washington, D.C.

Thompson, E. F., Hadley, L. L., Brandon, W. A., McGehee, D. D., and Hubertz, J. M. (1996). "Wave response of Kahului Harbor, Maui, Hawaii." Technical Report CERC-96-11, U.S. Army Engineer Waterways Experiment Station, Vicksburg, MS.

3.3 Waves, Currents, and Sediment Transport[11]

Waves and currents in northern Willapa Bay have eroded the Cape Shoalwater shoreline at rates exceeding 100 feet/year during the past 147 years (Kraus 2000). Historically, the Bay had extensive shoals residing at its mouth dating back to at least 1871 (see Figure 2.2.26), the date of the first chart of the area contained in the USACE archive. The most pronounced change at the western end of the Bay is the disappearance of Cape Shoalwater and the massive spit extending across the mouth. The severe erosion of the spit and Cape has opened the mouth, suggesting that the tidal prism of the bay has increased, thereby permitting stronger current through its entrance and into the bay.

Kraus (2000) notes the shoreline has receded in a clockwise direction around a pivot point near the North Cove. The shoreline to the west of the pivot point has receded at a fairly constant rate, but this rate has been declining since the 1980s. Lowell (1997) notes that the receding shoreline is encountering increasingly older, higher and more consolidated sediments that are more resistant to erosion. Similar sediments may exist similar to those in the area behind the North Cove lagoon, which are relatively more stable.

Conceptually, sediment transport is a function of wave orbital velocity and current, where the wave orbital velocity will entrain a sediment particle from the bed, suspending the particle in the water column, after which it can be carried or transported down-drift by the current. Discussed in Section 3.2, the significant wave height seaward of the bay entrance can exceed 7.0 m; the shoals at the Bay mouth dramatically attenuate the significant wave heights within the bay to about of 0.3 m to 1 m (depending on the tide elevation). Although the wave attack may have played a significant role in eroding the entrance spit, the relatively small wave heights within the Bay suggest that current is the dominate mechanism in causing the severe erosion along the northern shore of the Bay.

To demonstrate the impact of changing landform geometry and bathymetry over time, the ADCIRC model was applied simulating 1928, 1941, and 2002 conditions. The numerical grid discussed in Section 3.1.3 was used for simulating the 2002 conditions. This grid was adapted to 1928 and 1941 conditions using bathymetry obtained from USACE navigation charts of the Willapa Bay entrance. Bathymetry in areas beyond the domain of the charts remained unchanged from 2002 conditions. Each period was tested under spring tide conditions, and no wind forcing was imposed in the simulation. The yearly mean river inflow was specified at the upstream boundary of the Willapa River. Peak spring ebb and flood currents were extracted from each simulation for characterizing the current in that particular year.

Figure 3.3.1 presents the 1928 navigation chart of the Willapa Bay entrance. As shown, the spit extends approximately 5,000 m (16,400 ft) westward from Cape Shoalwater. The average depth of the North Channel is 20 m (65 ft) (south of the North Cove), and its width is approximately 1,100 m (3,600 ft). Figures 3.3.2 and 3.3.3 display the peak spring ebb and flood current, respectively. Peak ebb current at the confluence of the North and East Nachotta Channels is about 1 m/s (3.3 ft/s). Proceeding west of the confluence, the current strengthens to 1.7 m/s (5.6 ft/s) in the vicinity of the North Cove, and reaches a maximum current of about 2 m/s (6.6 ft/s) as the channel reaches the spit.

Between 1928 and 1941, the entrance spit extending from Cape Shoalwater greatly diminished, from 5,000 m (16,000 ft) to about 1,200 m (4,000 ft), and the northern Bay shore receded about 850 m (2,800 ft) (Figure 3.3.4). Average depth of the North Channel is 20 m (65 ft) and its width is about 1,250 m (4,100 ft). The convex curvature of the North Channel has flattened since 1928, where in 1941 its orientation is more east-west in direction. The changing landform resulted in weakening the current at

[11] Written by David Mark and Jane McKee Smith, Ph.D., U.S. Army Engineer Research and Development Center, Coastal and Hydraulics Laboratory, Vicksburg, MS.

the Bay entrance, while the current strengthened directly south of the North Cove. During peak ebb, peak current at the entrance is about 1 m/s (3.2 ft/s) versus 2 m/s (6.6 ft/s) south of the Cove (Figure 3.3.5). As shown in Figure 3.3.6, current magnitudes during peak flood are approximately the same as during peak ebb.

From 1941 to 2002, the northern shore receded about 1,700 m (5,500 ft) and the spit extending from the Cape has narrowed and shortened (Figure 3.3.7). The North Channel both deepened, to 24 m (80 ft), and widened by approximately 340 m (1,100 ft) over the 61-year period. As shown in Figure 3.3.8, the peak spring ebb current weakened along the North Cove shoreline compared to 1941 to approximately 1.2 m/s (3.9 ft/s). The strongest ebb current occurred at the entrance spit and is 1.7 m/s (5.6 ft/s). Peak spring flood current is approximately 0.8 m/s (2.6 ft/s) (Figure 3.3.9). In general, the tidal currents at the study area are weaker in the 2002 simulation than in those predicted in the 1941 simulation.

In addition to the more consolidated material along the western end of the north shore, the declining shoreline erosion rate may also contribute to the change in channel orientation and increase in cross-sectional area of the channel. Over the past 75 years, the channel at and to the west of the North Cove has migrated from a predominately east-west direction to a more northwesterly direction. During this 75-year period, the position of the North Channel east of North Cove as well as the Eastern Nachotta Channel remained fairly stable. During ebb, water discharging from the Nachotta Channel had a trajectory directed towards the North Cove, where it then turns towards the west and flows seaward; with the shoreline receding, the trajectory becomes straighter, which is more hydraulically efficient than the predominately east-west channel alignment.

Furthermore, from 1993 through 2003, bathymetric surveys show that the North Channel west of the North Cove has widened and deepened. Therefore, the cross-sectional area has increased, enhancing the conveyance of flow through the channel. Assuming a constant volume of water flowing through the channel, increasing the cross-sectional area of the channel results in weakening the current and thereby reducing current-induced erosion.

Kraus (2000) noted that the entrance spit undergoes periods of elongation and retraction, with a single period ranging from 10 to 15 years, and that channel migration is interrupted by periods when the North Channel breaches the spit, allowing the ebb current to flow directly to the open ocean (eleven such cycles can be documented between 1887 and 1987.) Breaching, or dissection, of the spit always begins with a notch eroding on the landward side of the spit. Breaching may occur at several locations along the spit, leading to multiple outlets. Typically, the notch or notches will widen and extend oceanward for several years until the depth across the entire spit reaches 18 feet, at which point the distal end of the spit is detached from the spit proper and begins migrating to the southeast. The new outlet captures the majority of the North Channel discharge and the other outlets gradually fill. The shoal eventually merges with others in the middle portion of the bay entrance.

The evolution of the geometry of the entrance to Willapa Bay has resulted in a substantial change in the tidal flow through the North Channel. In 1928, prior to the erosion of the entrance spit, the peak spring flood current in the vicinity of the North Cove was about 1.7 m/s (5.6 ft/s), whereas, in 1941, the peak spring flood current was 2 m/s (6.6 ft/s) at the same location. In 2002, the peak spring flood current weakened to 0.8 m/s (2.6 ft/s). The weaker current is attributed to channel widening.

References

Kraus, N. C., Editor, (2000). "Study of Navigation Channel Feasibility, Willapa Bay, Washington," Technical Report ERDC/CHL TR-00-6, U.S. Army Engineer Waterways Experiment Station, Vicksburg, MS.

Lowell, S. M., (1997). "Geological Study of the North Channel of Willapa Bay – Vicinity of Cove, Washington," Contract Report, Washington State Department of Transportation, Olympia, WA.

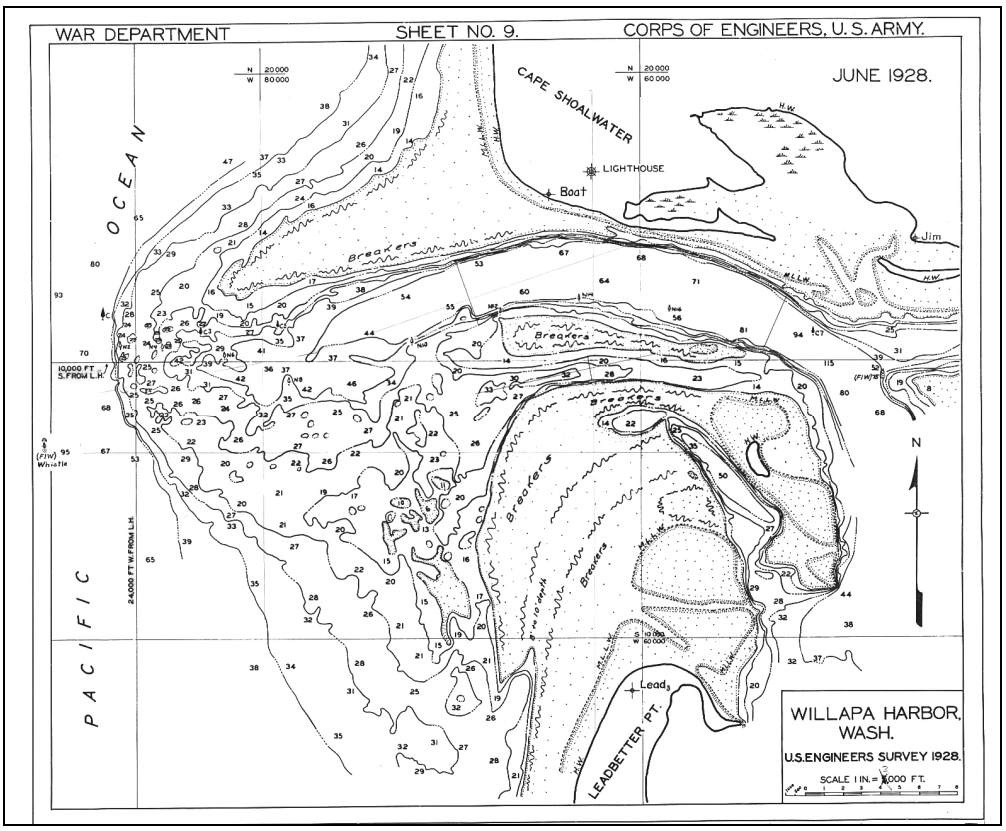

Figure 3.3.1. Navigation chart of Willapa Bay, circa 1928.

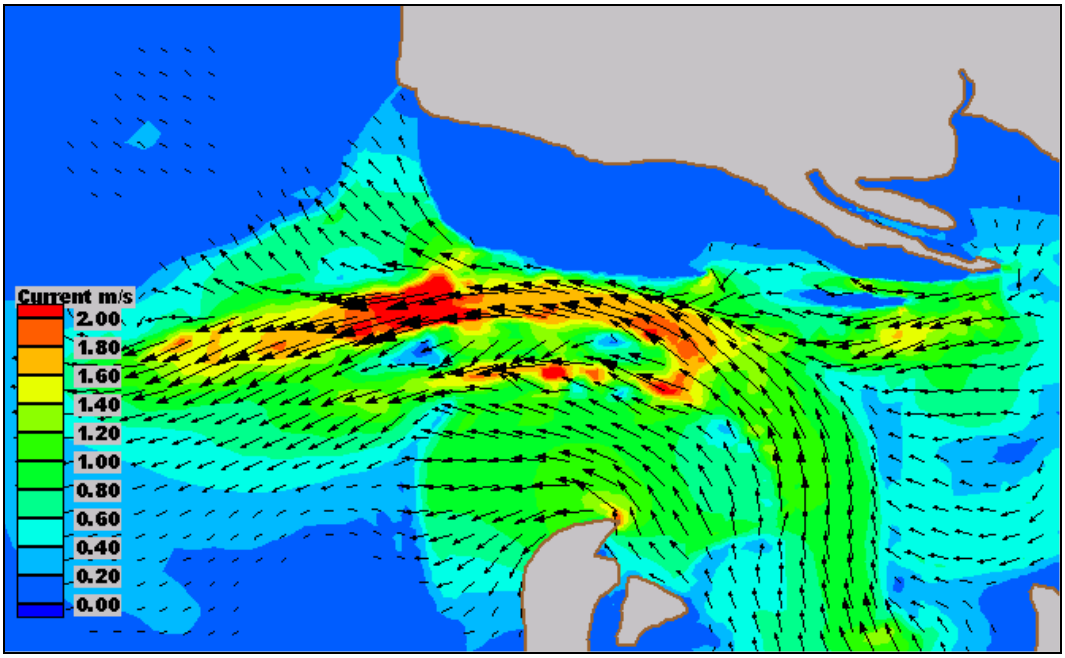

Figure 3.3.2. Peak spring ebb tide under 1928 North Channel configuration.

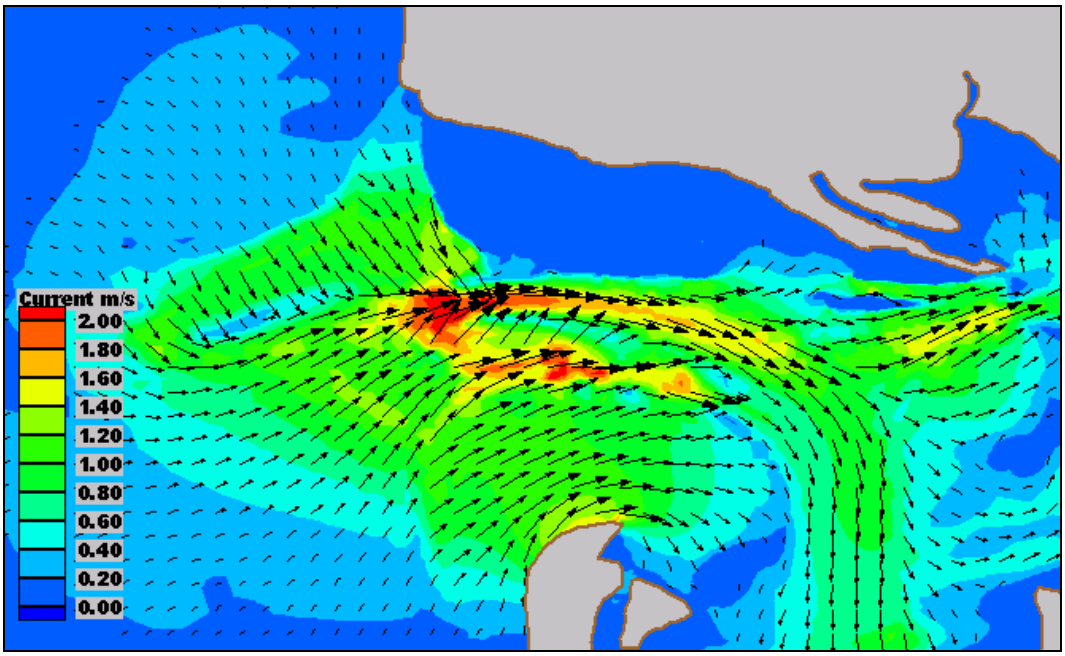

Figure 3.3.3. Peak spring flood tide under 1928 North Channel configuration.

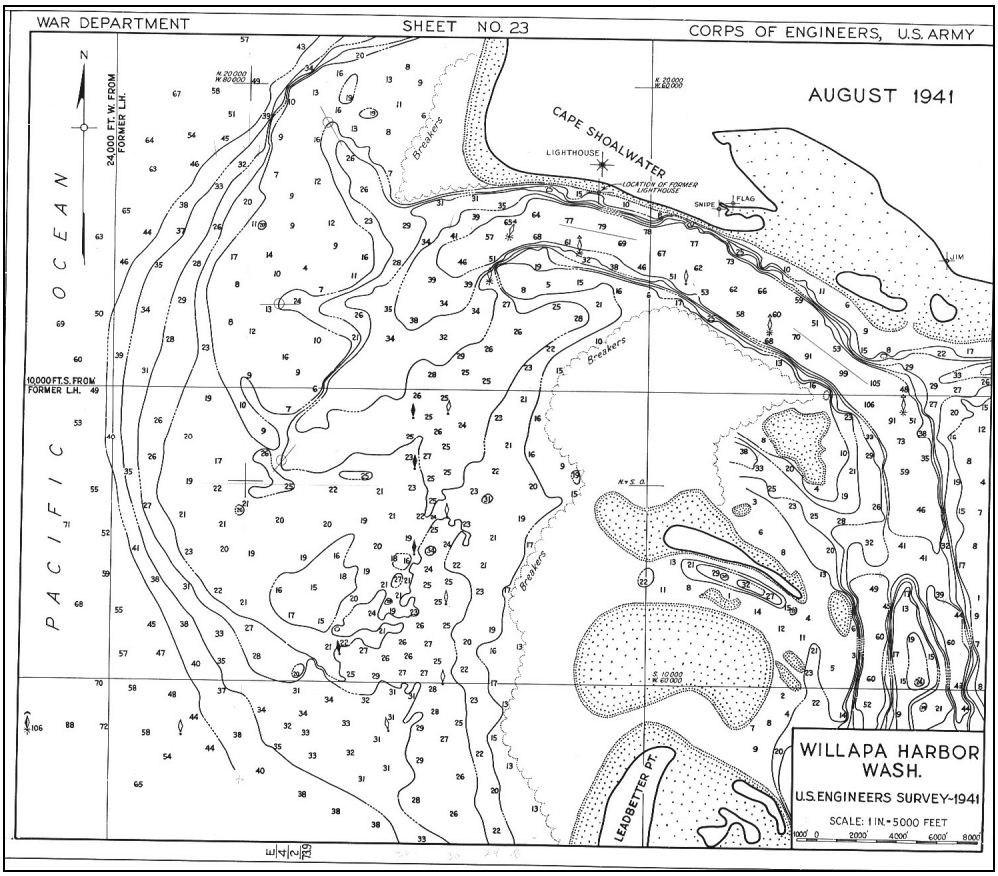

Figure 3.3.4. Navigation chart of Willapa Bay, circa 1941.

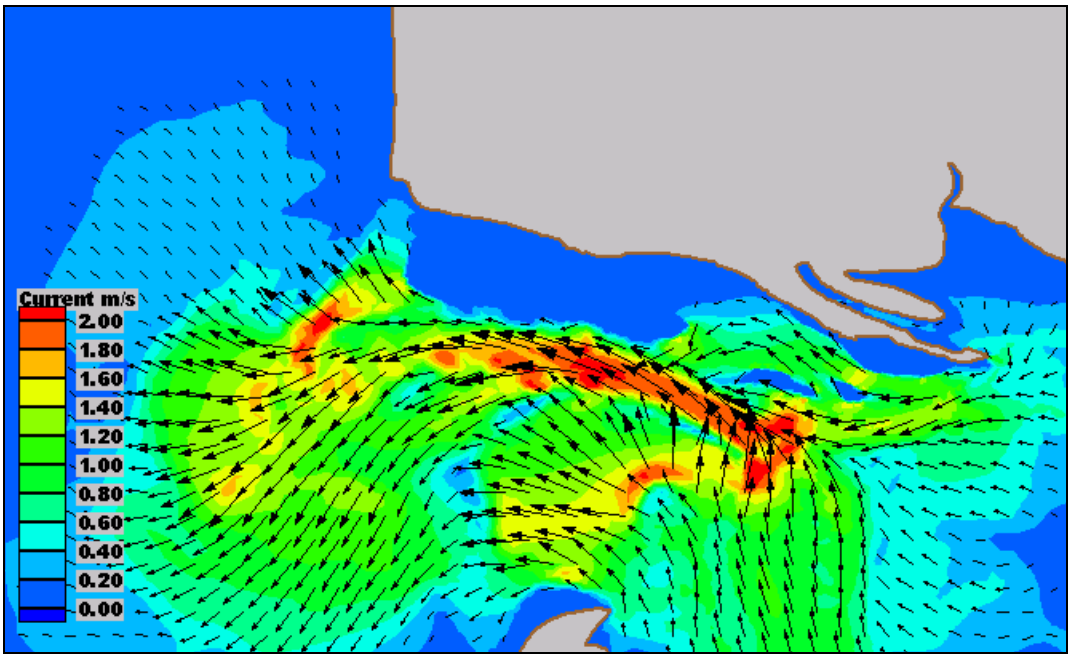

Figure 3.3.5. Peak spring ebb tide under 1941 North Channel configuration.

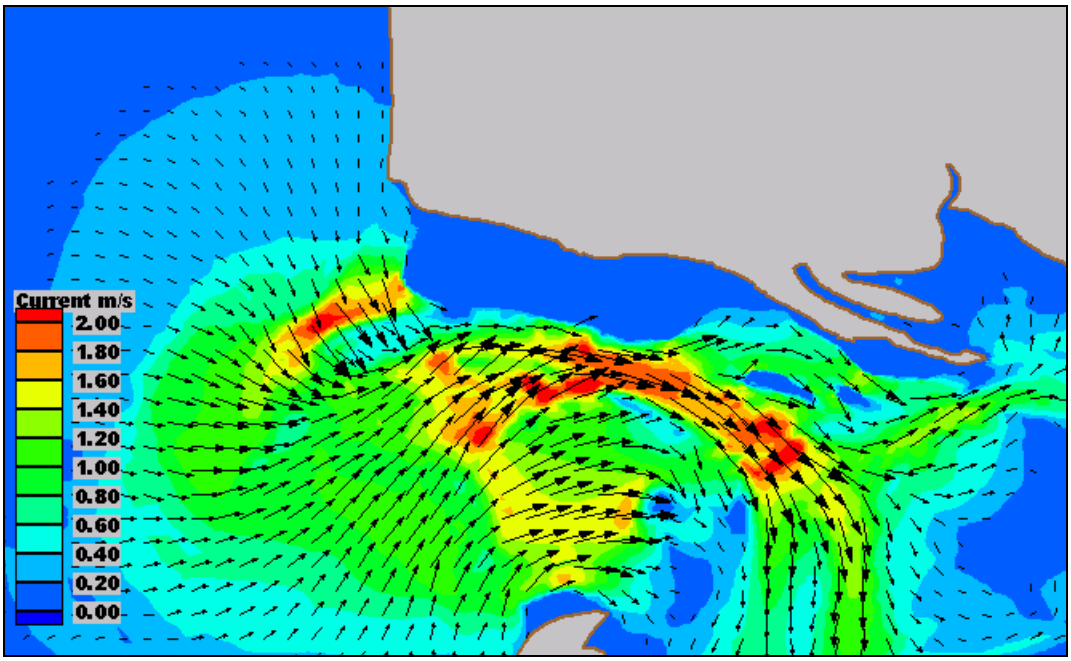

Figure 3.3.6. Peak spring flood tide under 1941 North Channel configuration.

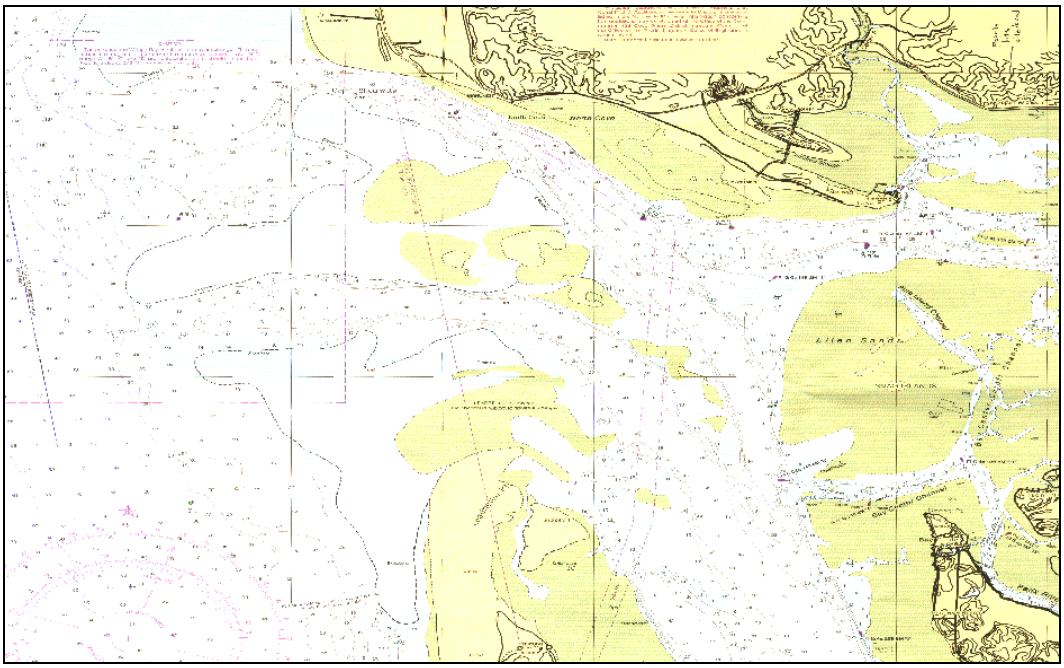

Figure 3.3.7. Navigation chart of Willapa Bay, circa 2002.

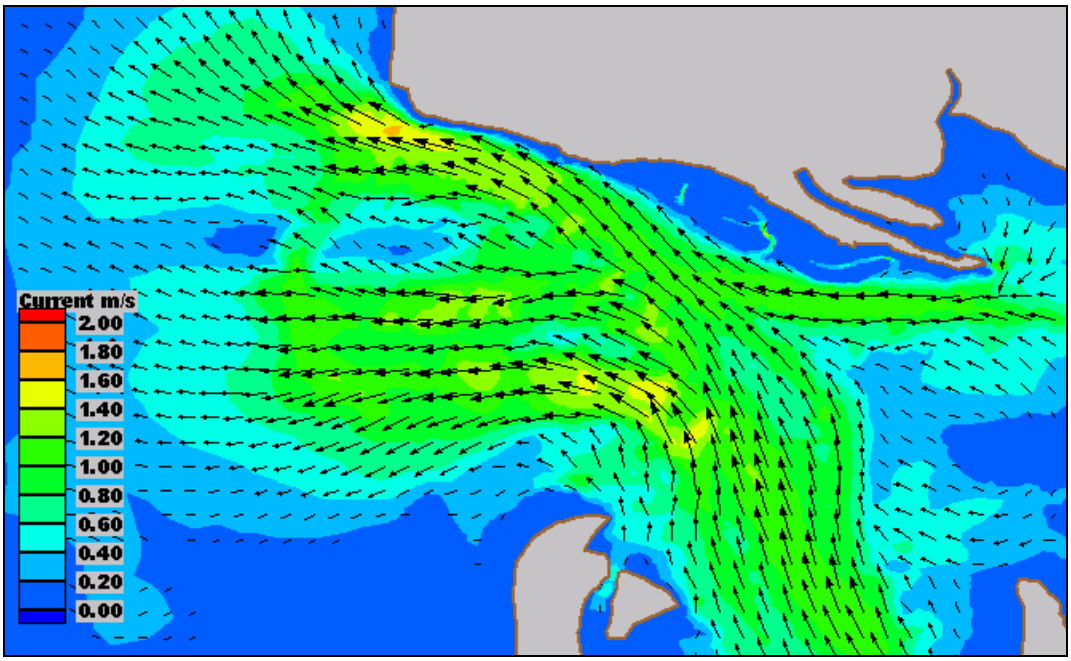

Figure 3.3.8. Peak spring ebb tide under 2002 North Channel configuration.

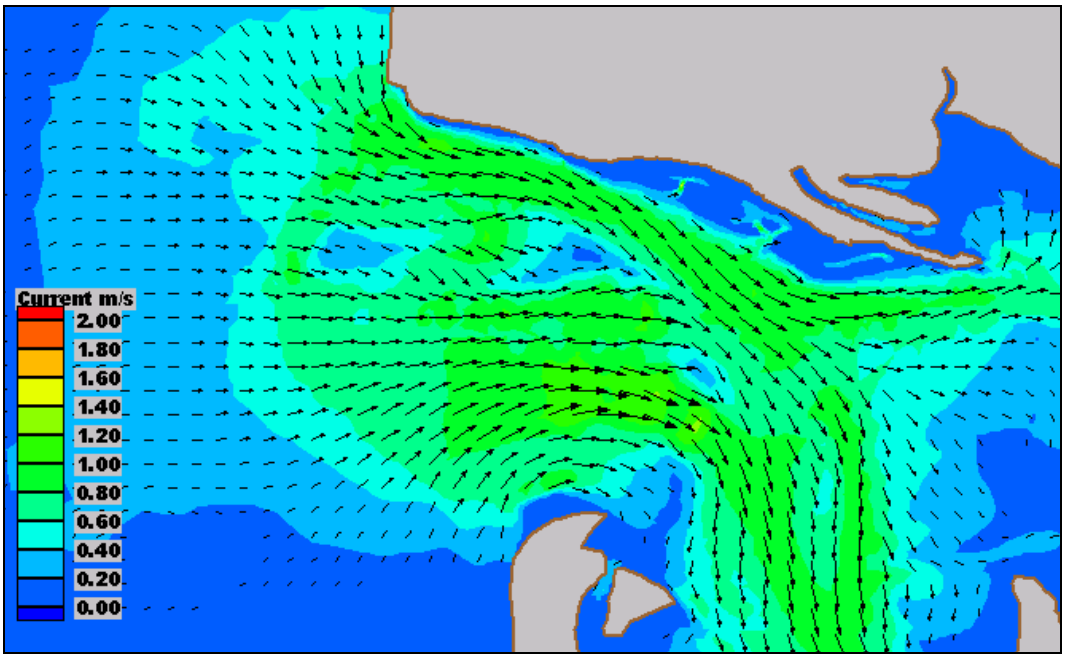

Figure 3.3.9. Peak spring flood tide under 2002 North Channel configuration.

3.4 Recent Bathymetric Changes

3.4.1 Bathymetric Surveys

The Corps of Engineers has conducted hundreds of hydrographic surveys of Willapa Bay in the last 100 years. The advent of digital surveying techniques has automated the methods of collecting and analyzing bathymetric survey data, but surveying the rapidly changing bar and entrance to Willapa Bay remains a difficult and dangerous challenge. The Corps began collecting survey data digitally in 1987, and the first digital map of Willapa Bay was produced in 1993. Hydrographic surveys of the bar and entrance to Willapa Bay were made in 1993, 1996, and annually since 1996. Figures 3.4.1 through 3.4.10 show the tracklines of the Corps' survey vessel, for the annual condition surveys that were made between 1993 and 2003. The density of data and the orientation and spacing of survey tracklines has varied over this period of time. Coverage was most consistent between 1998 and 2003, and these surveys were used in this study to assess recent bathymetric changes.

3.4.2 Bathymetric Changes, 1998 – 2003

Figures 3.4.11 through 3.4.15 show the bathymetric changes that took place annually between 1998 and 2003. The figures all show a similar pattern of erosion (yellow and red) and accretion (blue and purple). Areas of erosion are obvious on the north side of the entrance, west of the SR-105 project dike. Areas of persistent accretion are apparent on the bar and in several discrete locations on both sides of the entrance channel. The volumes involved in these changes are enormous. Based on the 1998 – 2003 survey data, the average annual rate of erosion, in the accessible portions of the entrance channel, was 23 million cy/year. The annual accretion volume exceeded 30 million cy/year. The scale of the sediment movement is so large that attempting to alter the natural evolution of the entrance appears to be far beyond the scope of this project. However, understanding and quantifying these changes allows the anticipated effects of the proposed alternatives to be appropriately weighed in relation to the ongoing processes.

3.4.3 Effect of SR-105 Dike and Groin on Adjacent Shoreline[12]

In 1997 – 1998, the Washington State Department of Transportation constructed a rock groin and dike as part of the SR-105 Emergency Stabilization Project. The purpose of the project was to "Plug…the North Channel in order to slow or stop the northerly channel migration…" (Environmental Assessment, SR-105 Emergency Stabilization Project, April 1997). The morphology patterns and bathymetry changes discussed in the previous sections of this report were used to evaluate the influence of the rock dike and groin on the coastal processes at Graveyard Spit and the associated islands, and in the channel in the vicinity of the Shoalwater Reservation.

Based on the available data, there is no evidence that the SR-105 dike has had any effect on the morphology or migration patterns of spit and islands. Graveyard spit stabilized around 1985, 13 years before construction of the dike. At all the cross-section lines, the deepest portion of the channel – the

[12] Written by Andrew Morang, Ph.D., and David Mark, U.S. Army Engineer Research and Development Center, Coastal and Hydraulics Laboratory, Vicksburg, MS.

thalweg – stabilized and began moving south in the early 1990s as the overall channel widened. Again, this began before construction of the dike (see figures 2.2.35 to 2.2.39). As discussed in Section 3.3, the widening of the channel may have been caused by the northward migration of the former middle channel, which added water volume to the main (northernmost) Willapa channel.

The SR-105 dike has caused local channel scour at the dike toe. A zone of scour has spread along the channel greater than about 600 m (2,000 ft) from the toe. At Cross-line 1, in 2003, the bottom was about 10 m (30 ft) deeper than in 1998. However, the cross-section plots show that as the channel scoured, it became wider to the south. The north (landward) bank has not been affected, probably because of outcrops of hard Pleistocene terrace deposits (see Jackson, Allen, and Lowell 1997).

The surface area of Graveyard Spit and the adjacent islands have been getting smaller since about 1992. Furthermore, the dunes have lowered since the late 1990's. This indicates that the supply of sediment that formerly came from a source to the northwest (erosion of Cape Shoalwater or offshore shoals) diminished during the early 1990's, before the dike was built.

The presence of outcrops of hard strata (the very dense, brown Pleistocene Terrace unit cored by and described by the Washington State DOT geologists) is a far more fundamental factor affecting northward movement of the Willapa Bay channel than the SR-105 dike.

A geological or morphological signal on the Shoalwater Reservation spit and islands as a result of the dike is masked by the strong flow of tidal currents, by wind-driven waves, and by the underlying geology.

The effective zone of influence of a dike, defined as that distance where the dike has an appreciable effect on the flow of current, is 2 to 3 times the length of the structure itself. The SR-105 dike had a design length of about 360 m (1,200 ft), measured from mean tide level. As such, its effective zone of influence ranges from 730 m (2,400 ft) to 1,100 m (3,600 ft). The alongshore distance from the dike to the northern limit of the North Cove is about 300 m (1,000 ft), and the distance from the dike to the Shoalwater Reservation lands is about 900 m (3,000 ft), suggesting that the dike influences the flood current along the North Cove shoreline. However, the effective zone of influence of the dike is diminished because of several factors. First, the estimated effective zone of influence provided above assumes that the top of the structure is above water, whereas the SR-105 dike is submerged, resulting in a smaller zone of influence because it does not completely block the current. Second, because of difficulties in constructing the dike in a strong current environment, project funds were exhausted prior to its completion; consequently, the as-built length of the SR-105 dike is shorter than the design length. Third, scouring at its toe has resulted in the structure slumping into the scour hole, further reducing its ability to block or divert the current. Because of the above factors, the effective length of the dike is probably much shorter than 2 to 3 times its length, and, therefore, the SR-105 dike has only minimal impact on current along the North Cove shore.

References

Jackson, D., Allen, T.M., and Lowell, S. M. 1997. SR-105: Geological Study of the North Channel of Willapa Bay – Vicinity of north Cove, Washington. Geotechnical Report, Willapa Bat Channel Restoration Project, C.S. 2532, OL- 2431, Washington Department of Transportation, Olympia, WA.

Federal Highway Administration and Washington Department of Transportation, 1997. Environmental Assessment, SR 105 Emergency Stabilization Project, North Cove, Washington.

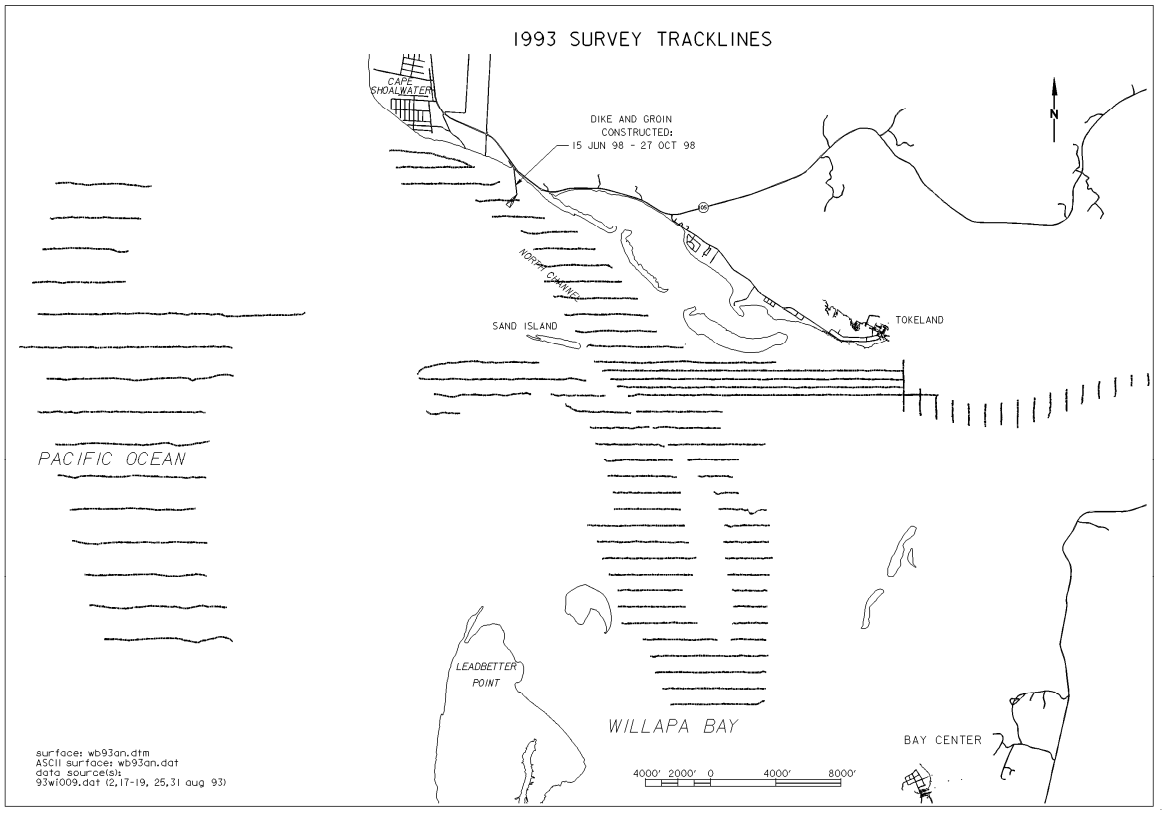

Figure 3.4.1 Willapa Bay 1993 annual condition survey tracklines.

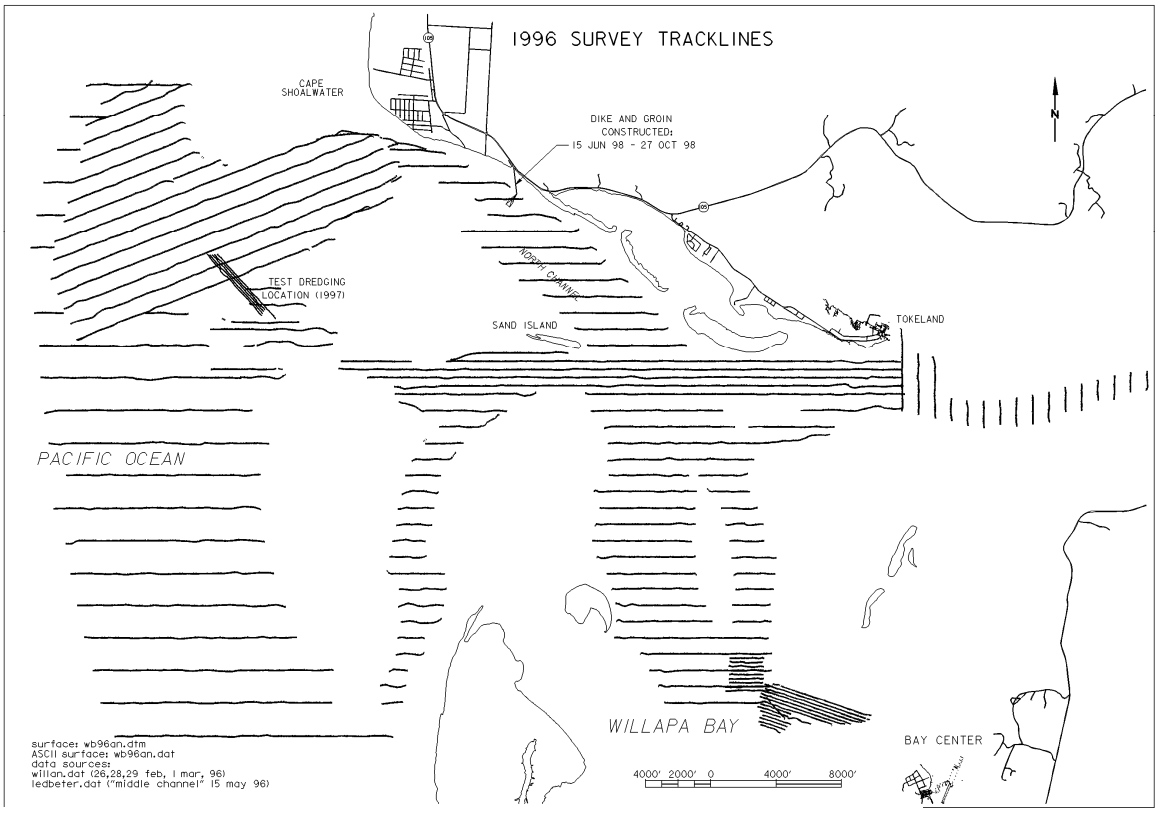

Figure 3.4.2 Willapa Bay 1996 annual condition survey tracklines.

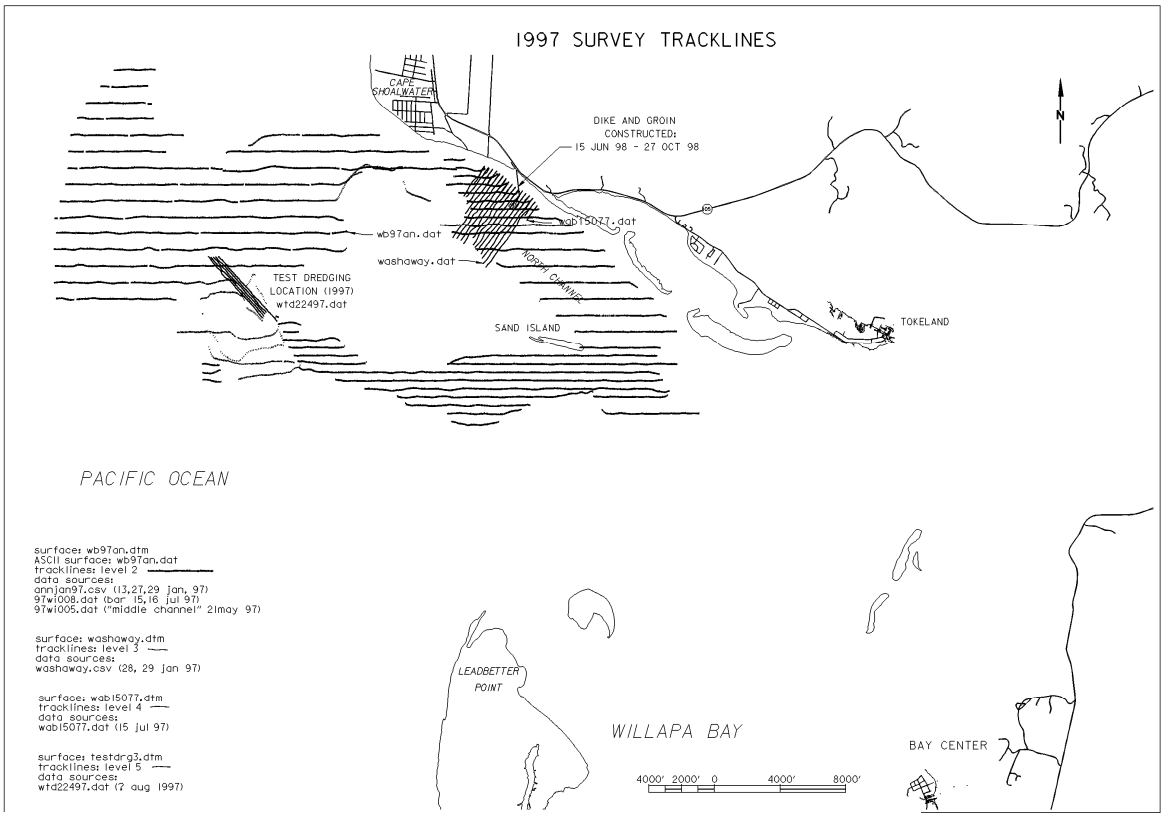

Figure 3.4.3 Willapa Bay 1997 annual condition survey tracklines.

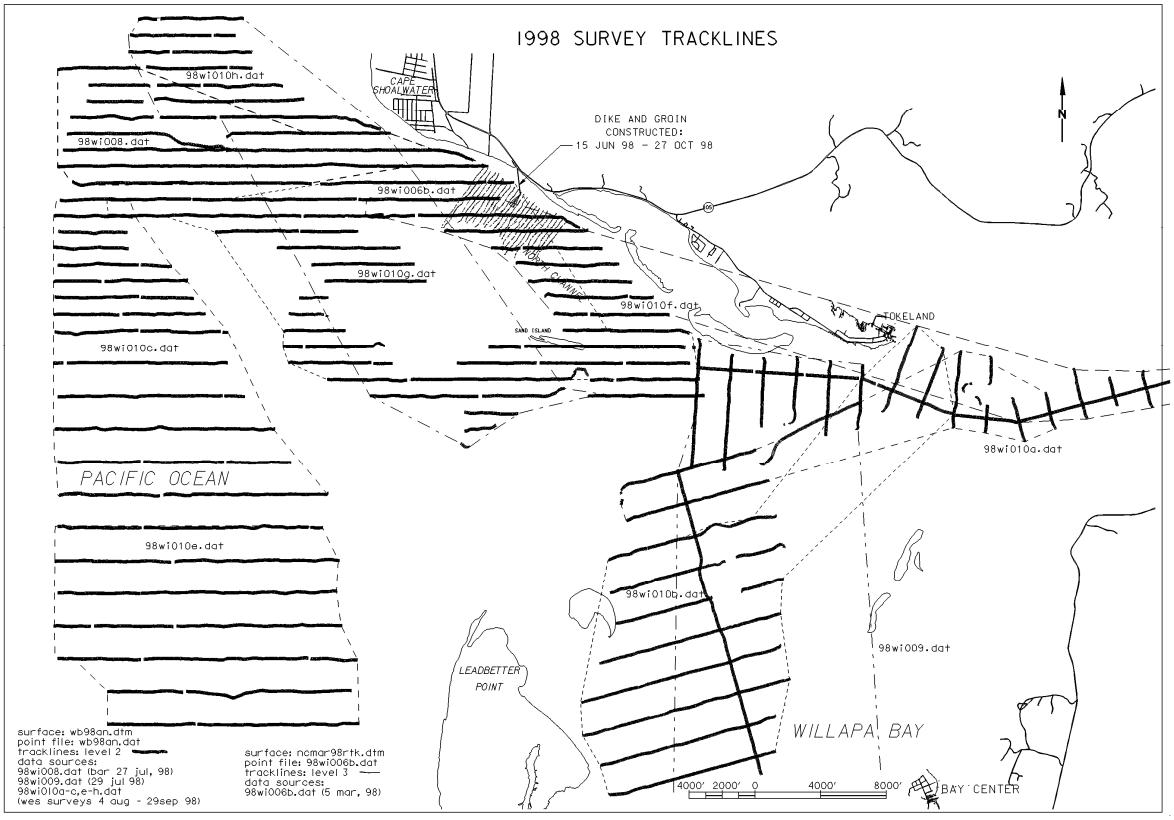

Figure 3.4.4 Willapa Bay 1998 annual condition survey tracklines.

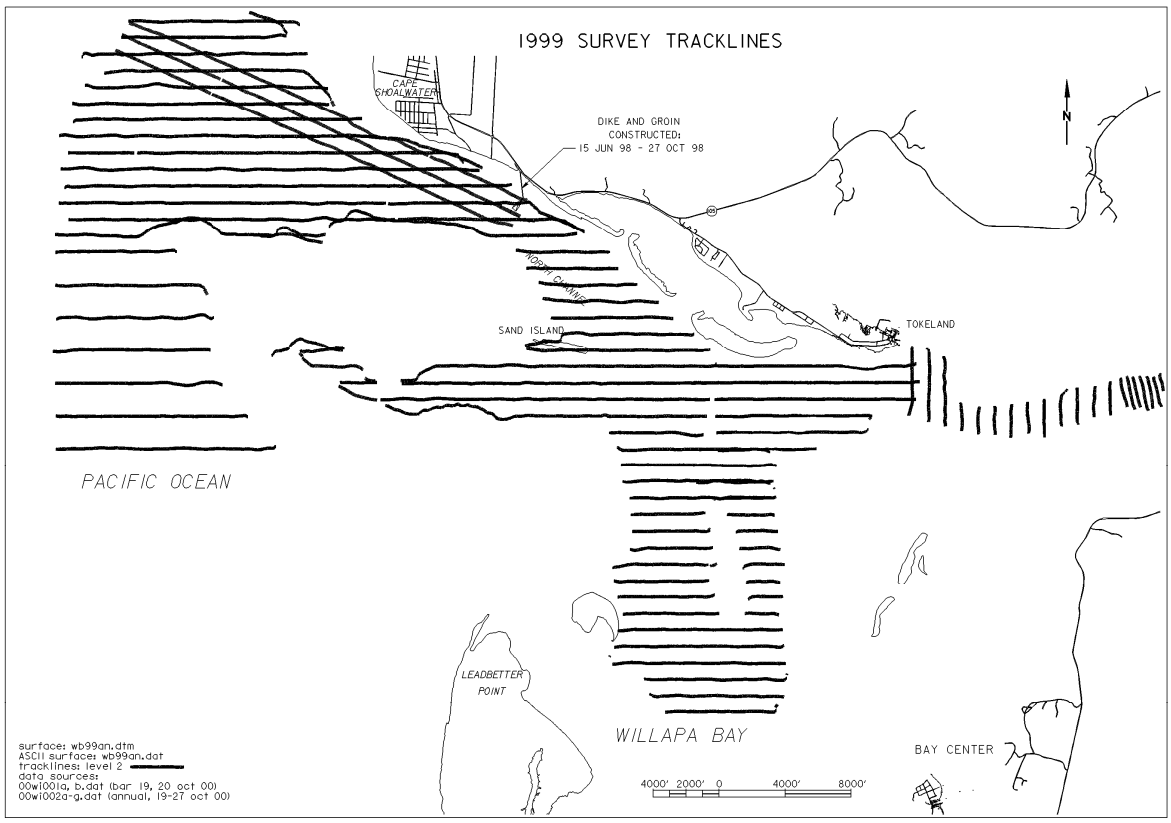

Figure 3.4.5 Willapa Bay 1999 annual condition survey tracklines.

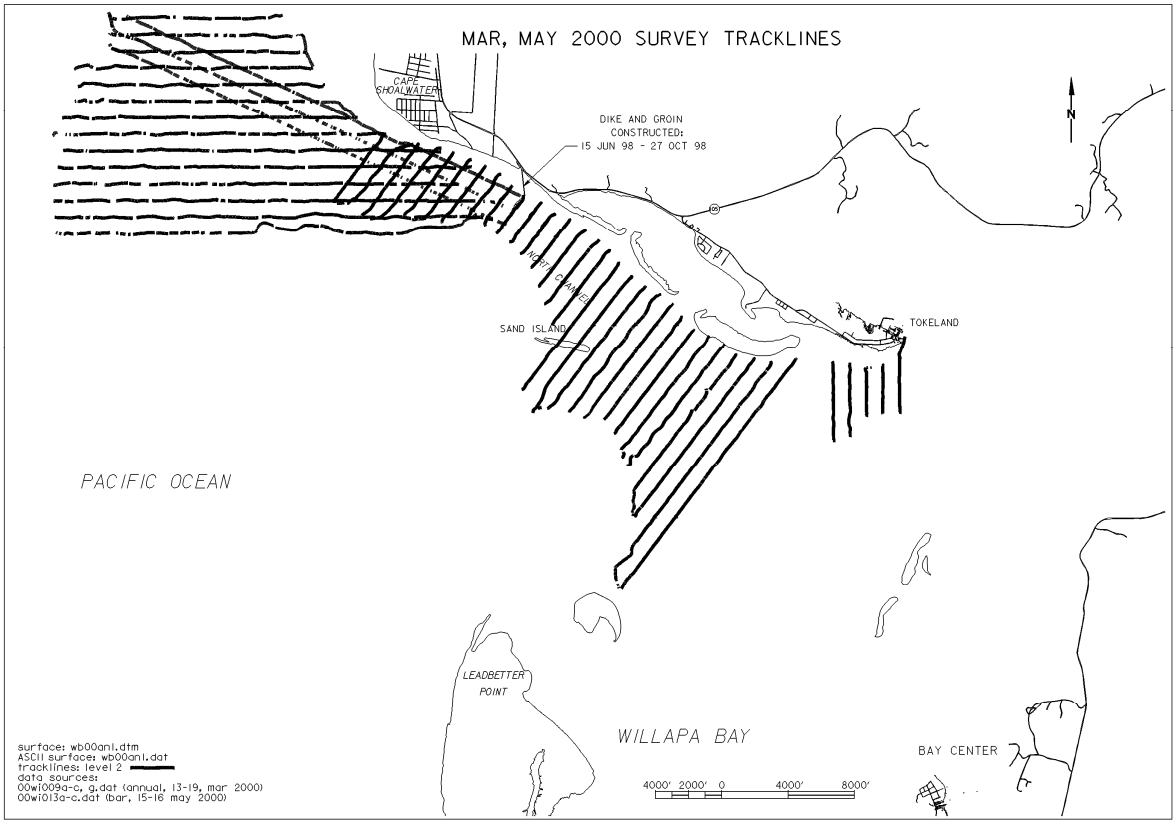

Figure 3.4.6 Willapa Bay March – May 2000 condition survey tracklines.

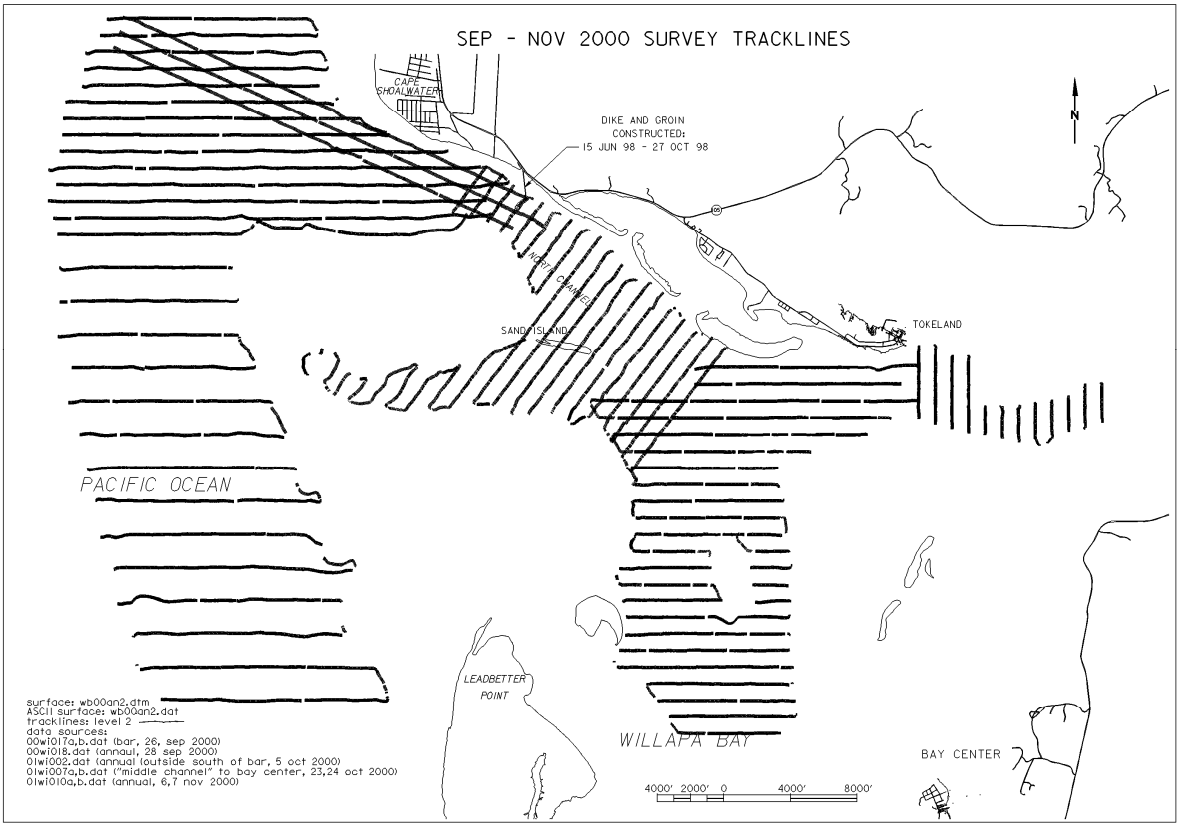

Figure 3.4.7 Willapa Bay September – November 2000 condition survey tracklines.

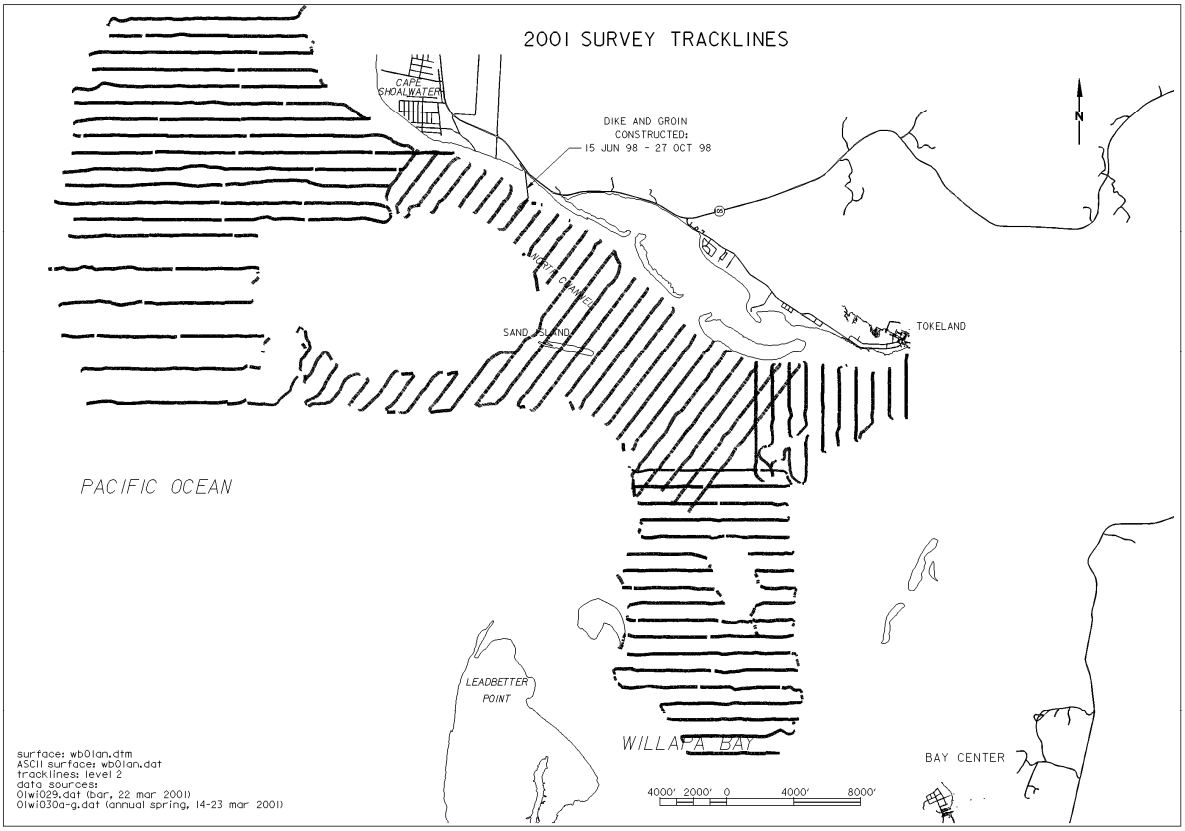

Figure 3.4.8 Willapa Bay 2001 annual condition survey tracklines.

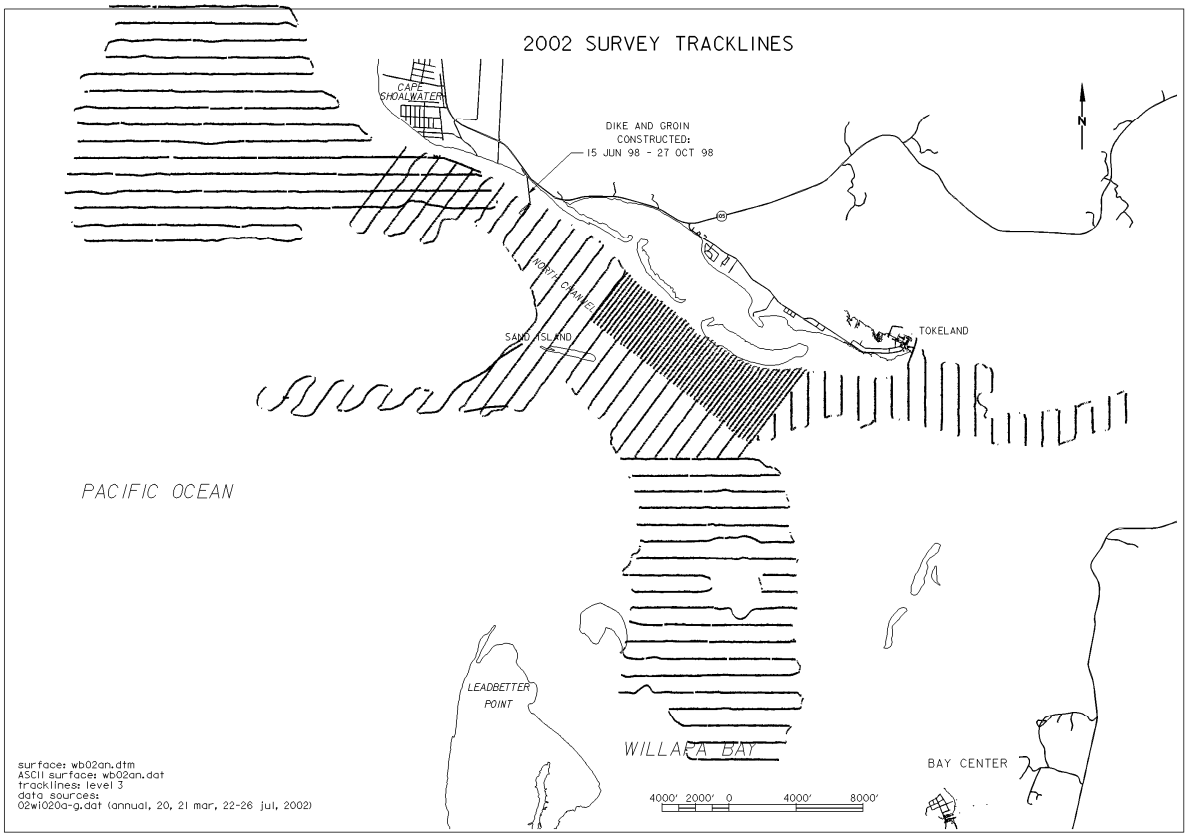

Figure 3.4.9 Willapa Bay 2002 annual condition survey tracklines.

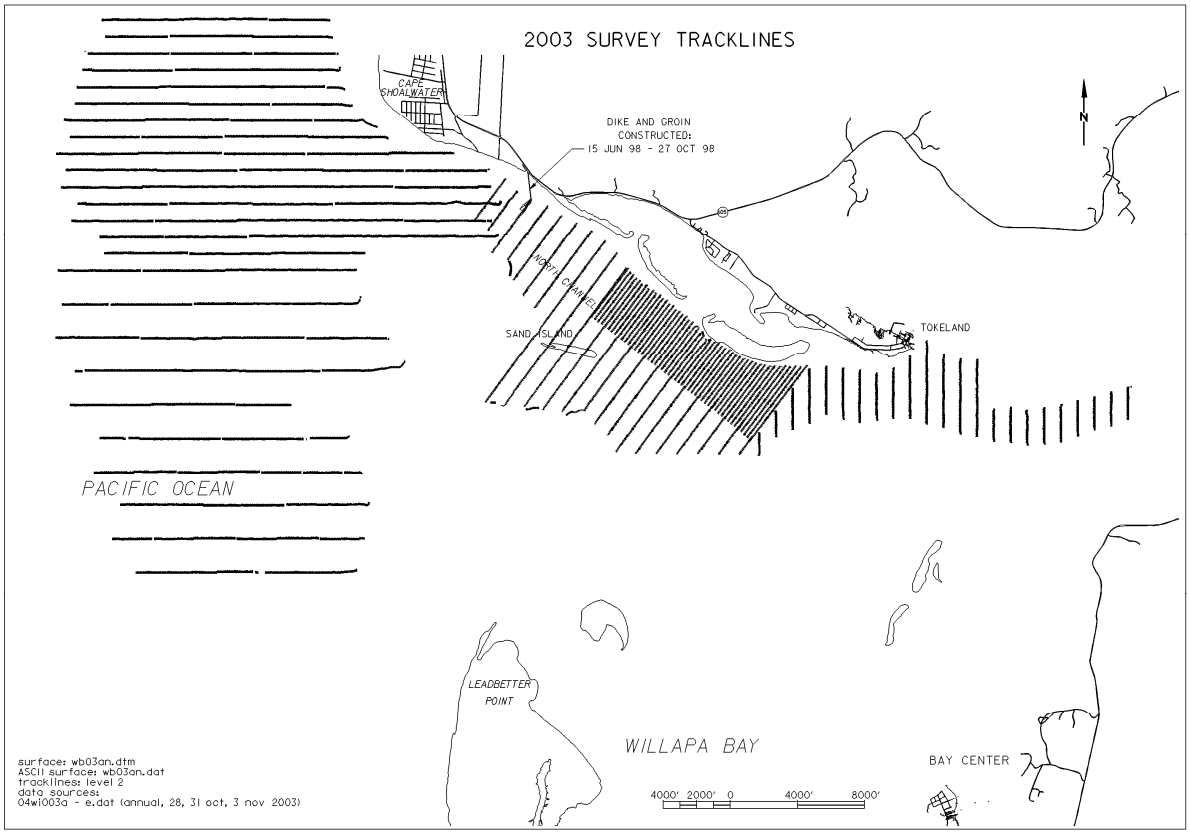

Figure 3.4.10 Willapa Bay 2003 annual condition survey tracklines.

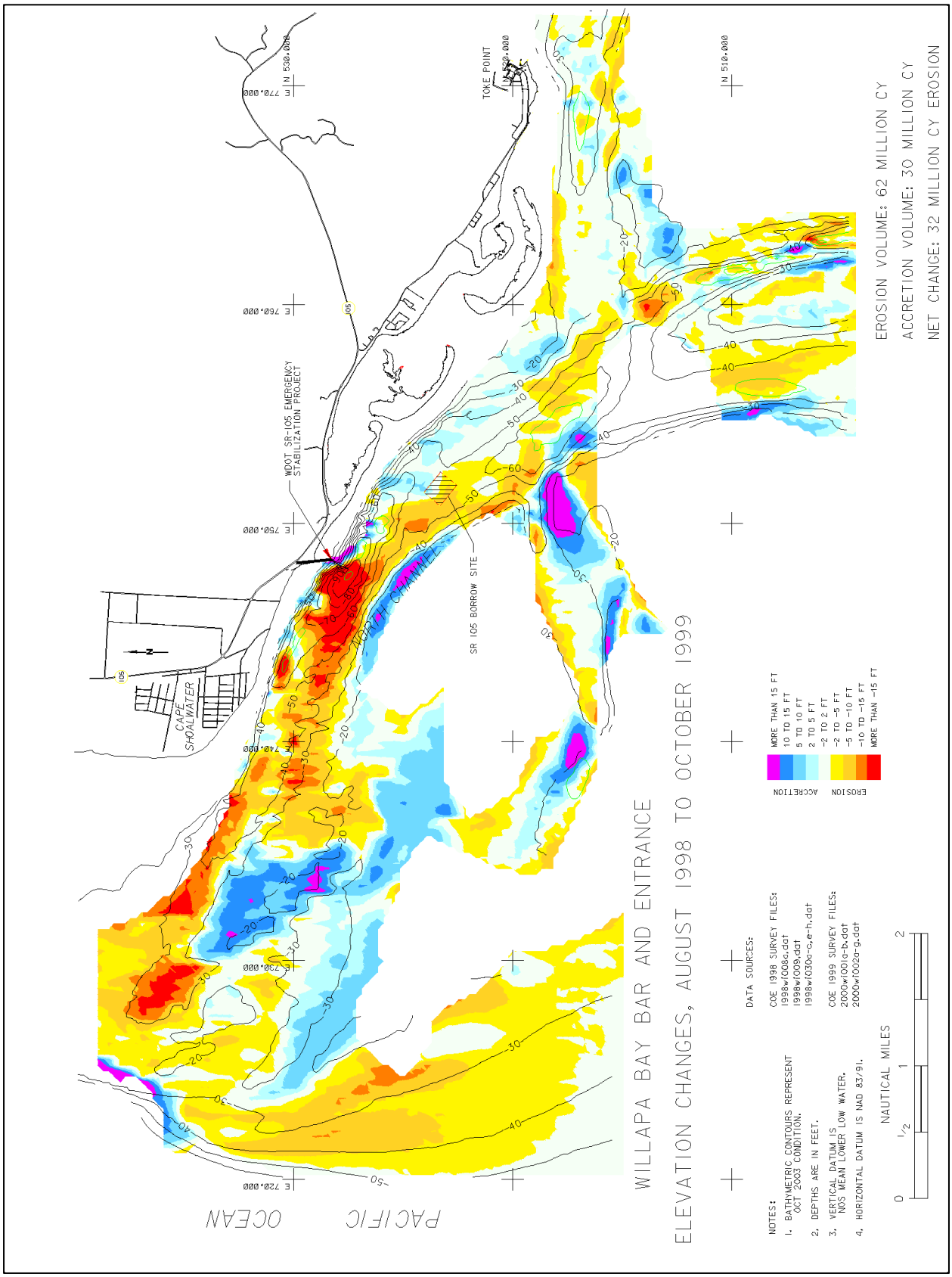

Figure 3.4.11 Willapa Bay Bar and Entrance elevation changes, August 1998 to October 1999.

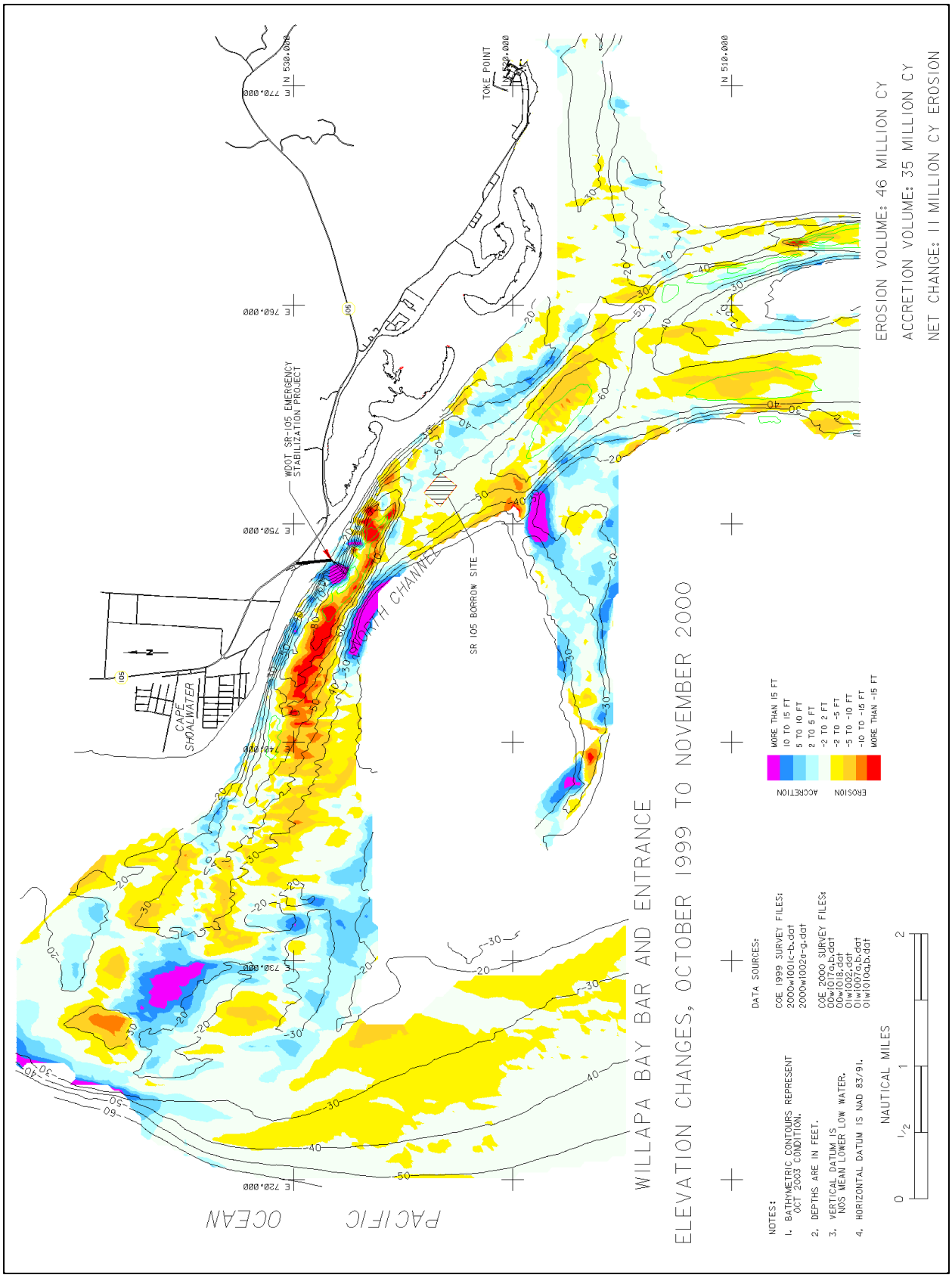

Figure 3.4.12 Willapa Bay Bar and Entrance elevation changes, October 1999 to November 2000.

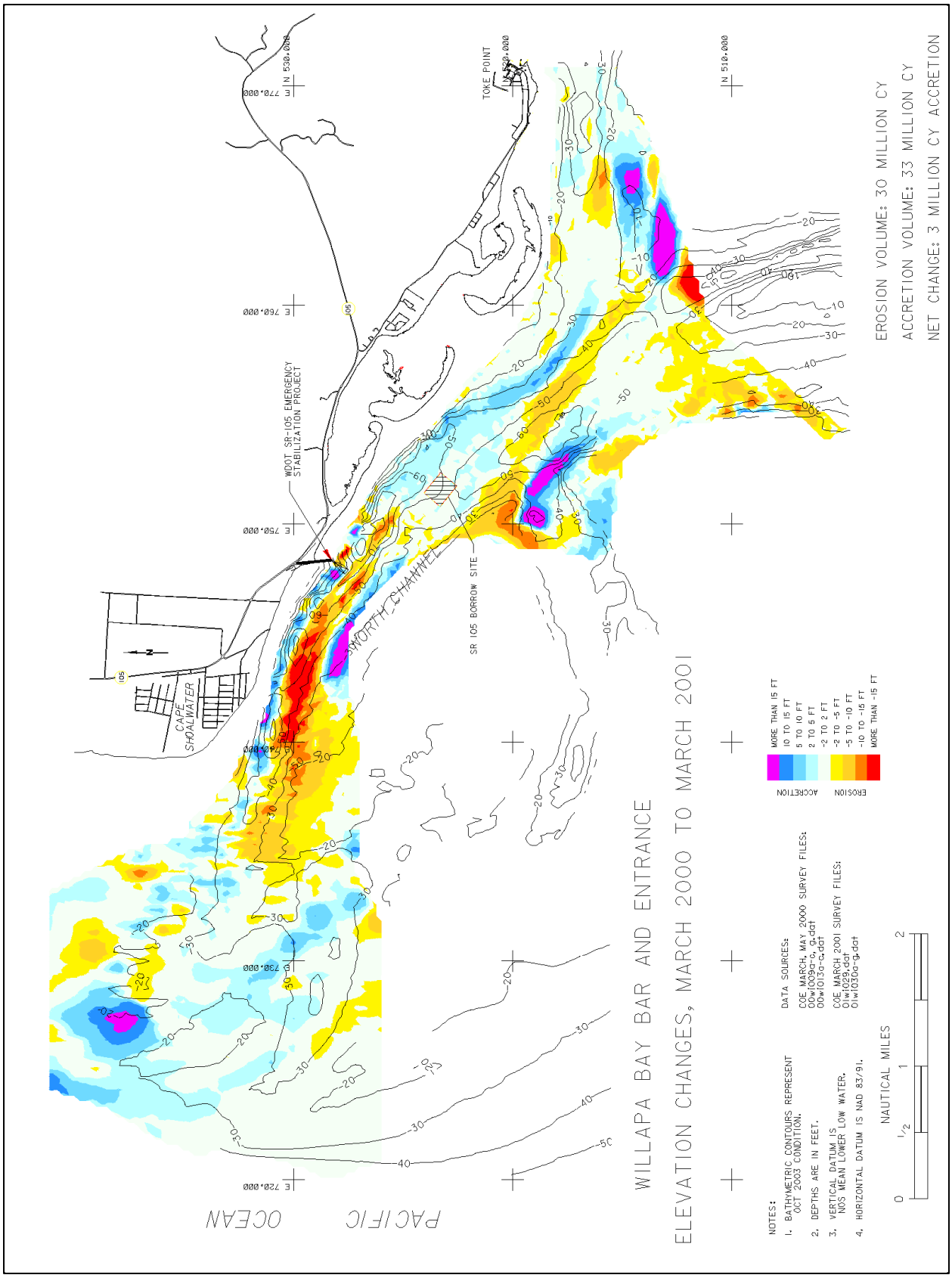

Figure 3.4.13 Willapa Bay Bar and Entrance elevation changes, March 2000 to March 2001.

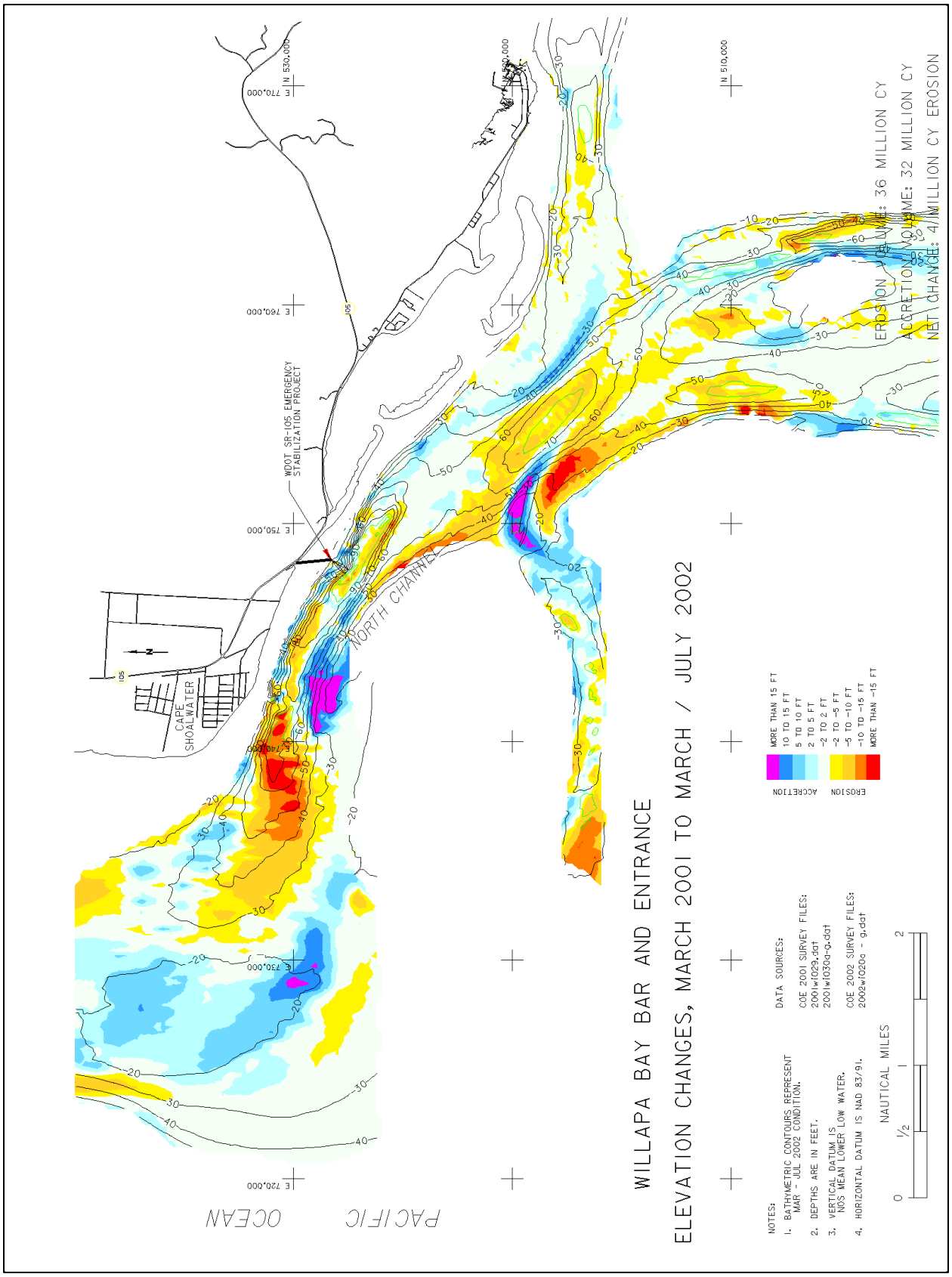

Figure 3.4.14 Willapa Bay Bar and Entrance elevation changes, March 2001 to March/July 2002.

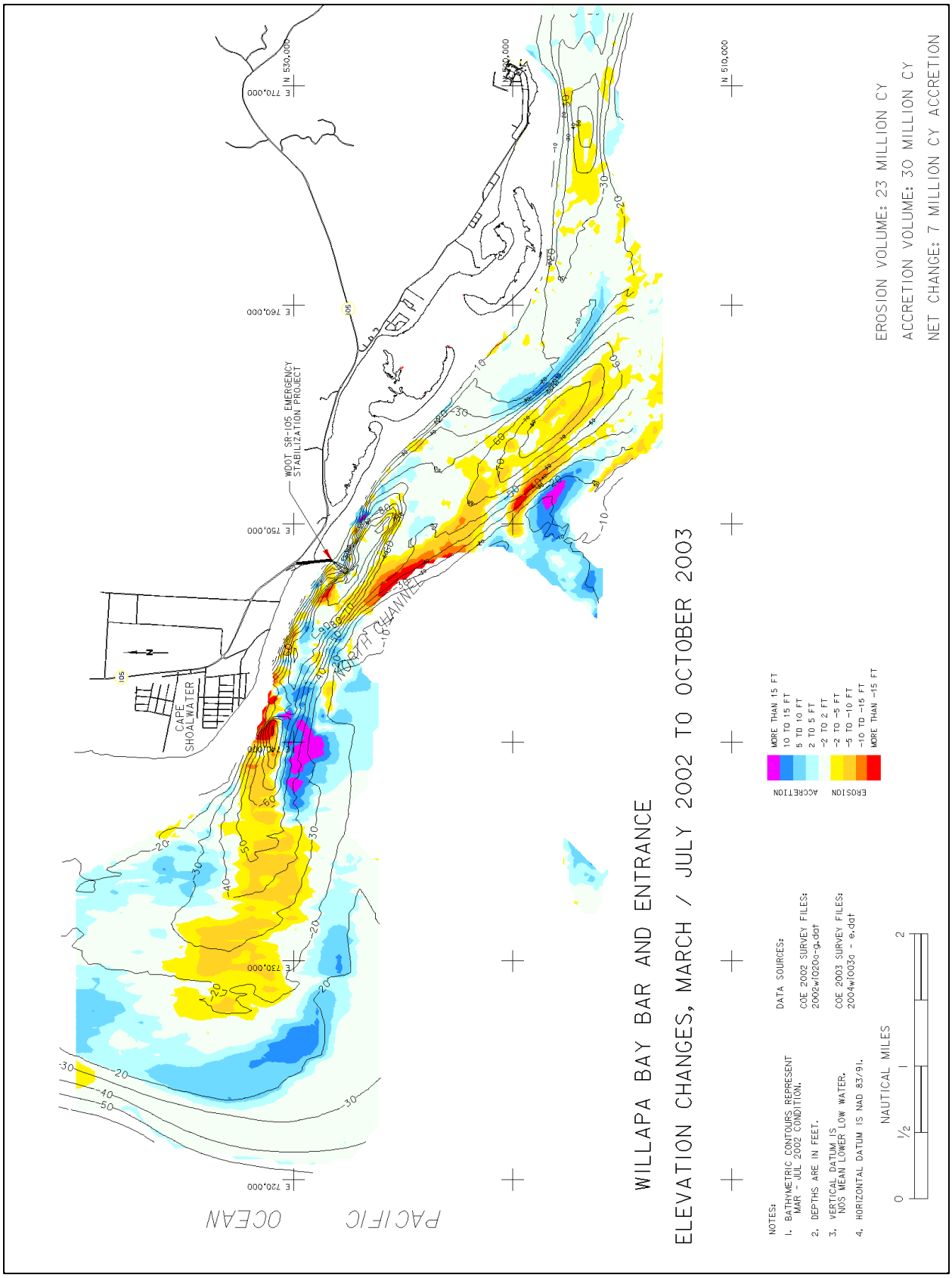

Figure 3.4.15 Willapa Bay Bar and Entrance elevation changes, March/July 2002 to October 2003.

3.5 Shoreline and Dune Erosion - SBEACH Analysis[13]

SBEACH Model Description

The Storm induced BEAch CHange model – SBEACH (Larson and Kraus 1989) simulates beach profile change, including the formation and movement of major morphologic features such as longshore bars, troughs, and berms under varying storm waves and water levels. The present study incorporates recent model updates including the hard bottom feature (Larson and Kraus 1998) to address non erodedible features located in the beach profile and overwash transport over barrier dunes (Larson et al. 2004).

Erosion Model Inputs

The inputs required to execute SBEACH are as follows:

a. Bathymetric survey (profile data).
b. Sediment characteristics (grain size, angle of repose, hard bottom areas, sediment transport parameters).
c. Incident wave conditions at offshore boundary (wave height, wave period, wave direction, water surface elevation).

Bathymetric Data

The merged hydrographic and topographic bathymetric survey data from 2002 is used to generate the beach profile transects. Profiles 1, 3, and 5 displayed in Figures 3.5.1(a) and (b) are cut normal to the Shoalwater Reservation shoreline and extend offshore beyond Graveyard Spit.

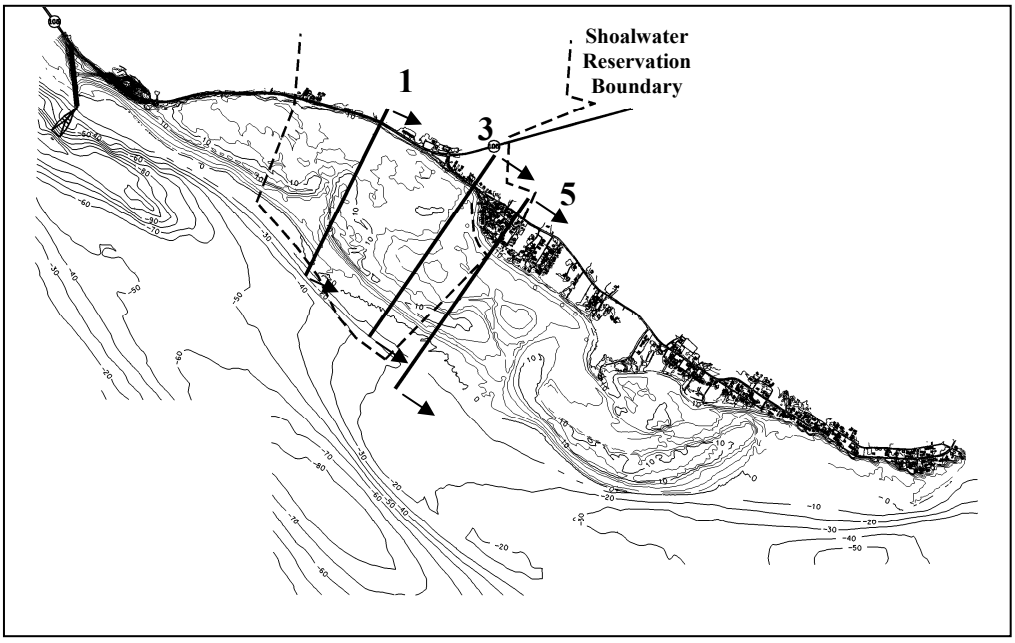

Figure 3.5.1 (a) SBEACH profiles relative to 2002 survey

[13]Written by David Michalsen, U.S. Army Corps of Engineers, Seattle District

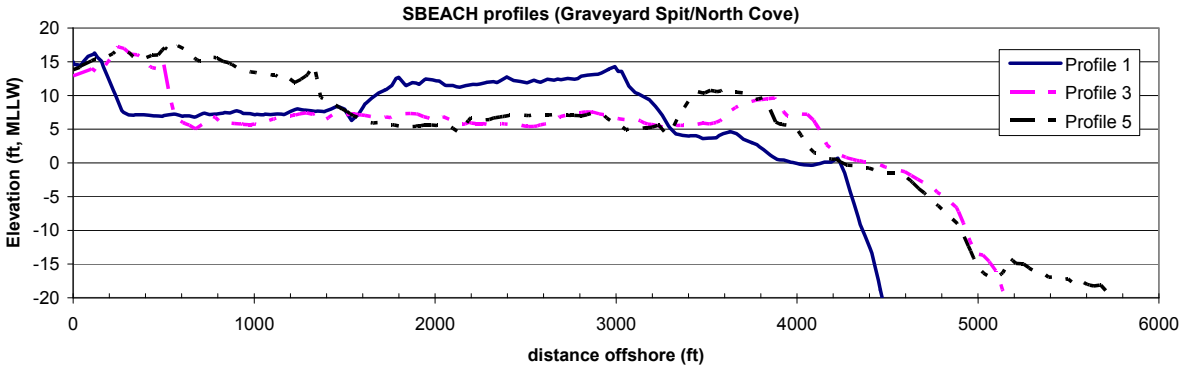

Figure 3.5.1 (b) Profile of SBEACH profiles

Sediment characteristics

The sediment in North Cove is described as fine sand to silty material (Morton et al 2002). The median grain size specified in SBEACH is d_{50} = 0.15 mm. The hard bottom feature in SBEACH is utilized on Profile 3 which includes the existing stone revetment (i.e., flood berm) on the shoreline at elevations ranging from +6 to +16 ft MLLW.

Table 3.5.1. List of peak storm surges at Toke Point 1988-2007

Date	elevation (m)	Duration[1] (hr)	Spring tide elevation ratio[2]
December 3, 2007	1.619	58	0.79
March 3, 1999	1.562	32	0.86
February 4, 2006	1.334	25	0.91
January 1, 1997	1.265	124	0.77
November 23, 1998	1.226	103	0.82
December 1, 2001	1.151	45	0.96
January 17, 1998	1	108	0.79
January 2, 2003	0.99	96	1.01
January 1, 2006	0.961	97	1.01
January 29, 1999	0.866	32	0.89
December 1, 1998	0.832	114	0.97
November 8, 2002	0.828	80	0.98

[1] duration defined as time above threshold elevation shown in Fig. 3.5.2
[2] metric to describe the tidal phase during the surge event relative to the spring tide elevation

Incident wave conditions

The historic storm hydrographs displayed in Figure 3.5.2 are used to drive the SBEACH numerical model. Table 3.5.1 lists the peak storm surge and duration recorded at the Toke Point tide gage in the past 20 years. The astronomical tide elevation relative to the spring tide elevation is included to show the impact of the storm surge on the total water elevation. Values near one indicate surges occurring during extreme high tides.

Wave heights immediately offshore of Graveyard Spit are modulated by the water surface elevation as described in Section 3.2. Therefore, the largest waves occur during the highest tide

plus storm surge. The relationship between wave height and water levels provided in Figure 3.2.17 is used to calculate the incident wave height time series driving the SBEACH model. The wave period is specified using the CDIP buoy 036 offshore of Grays Harbor, WA (46 51.58 N 124 14.69 W). Wave direction is assumed to act normally incident along the beach profile.

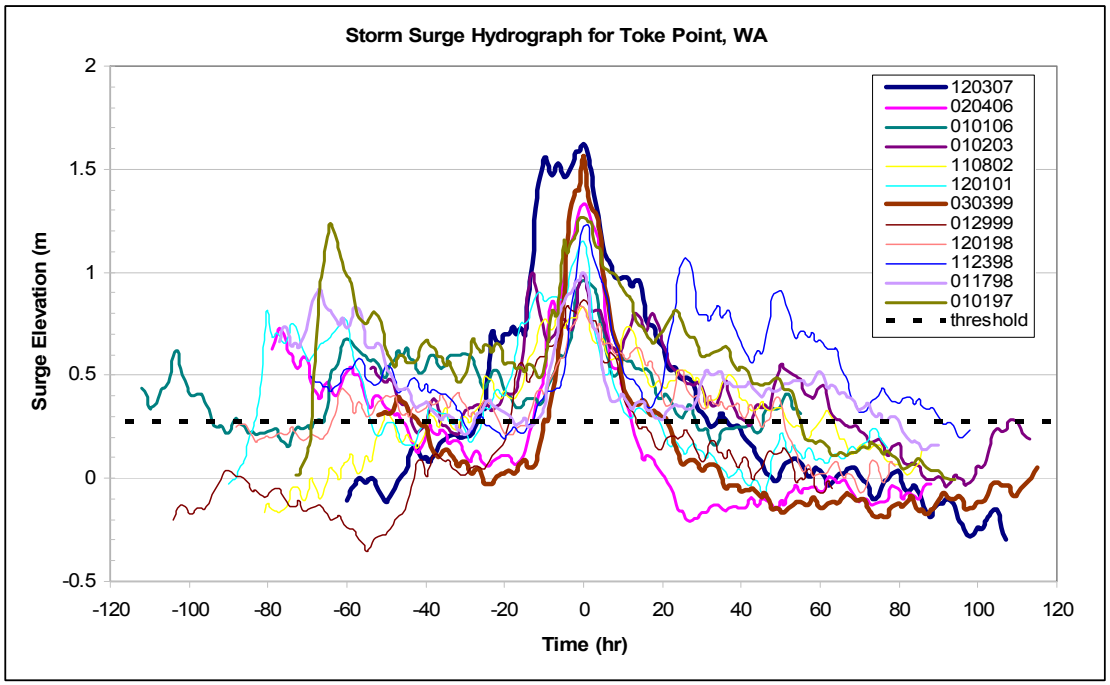

Figure 3.5.2. Largest storm surge hydrographs recorded at Toke Point gage 1988-2007 centered about peak surge elevation

3.5.1 Without Protective Dunes – Erosion to Shoalwater Reservation Shoreline

The erosion on the Shoalwater Reservation is computed using the SBEACH model for each storm hydrograph. For the without dunes condition it is assumed that the dune crest elevation has been allowed to erode to an elevation of mean high water. As described in Section 3.2.4, the wave heights acting on the shoreline are approximately twice as large without the protective dunes. Figure 3.5.3 display the SBEACH results for storm related erosion on the shoreline for the March 3, 1999 storm condition time series shown in Figure 3.2.15. Profile 5, the southwest portion of the shoreline, shows the largest potential for erosion. The area of the profile eroded is computed in SBEACH and is listed in Table 3.5.2 for each storm condition modeled. The model computes an area of 131 ft^2 per linear foot of shoreline eroded during the March 3, 1999 storm. This portion of shoreline is susceptible to erosion due to a low and narrow back shore berm (height less than +16 ft MLLW). This allows waves to run-up and overtop the back shore berm, thereby eroding the berm shoreward.

Empirical Simulation Technique

In order to estimate the amount of erosion for a specific storm return interval, the Empirical Simulation Technique (Scheffner et al 1999) is employed. The Empirical Simulation Technique

(EST) is a bootstrap-based statistical procedure for simulating multiple time sequences of non-deterministic multi-parameter systems. Results of the multiple repetitions are subsequently analyzed to compute frequency-of-occurrence relationships for storm effects. Because multiple life-cycle scenarios are simulated through the EST, mean value frequencies are computed along with error estimates of deviation about the mean.

The input vectors describing the extratropical storm used are wave height, wave period, tide phase, maximum storm surge, and storm duration. The response vector is the area per linear foot of shoreline eroded above the mean high water line.

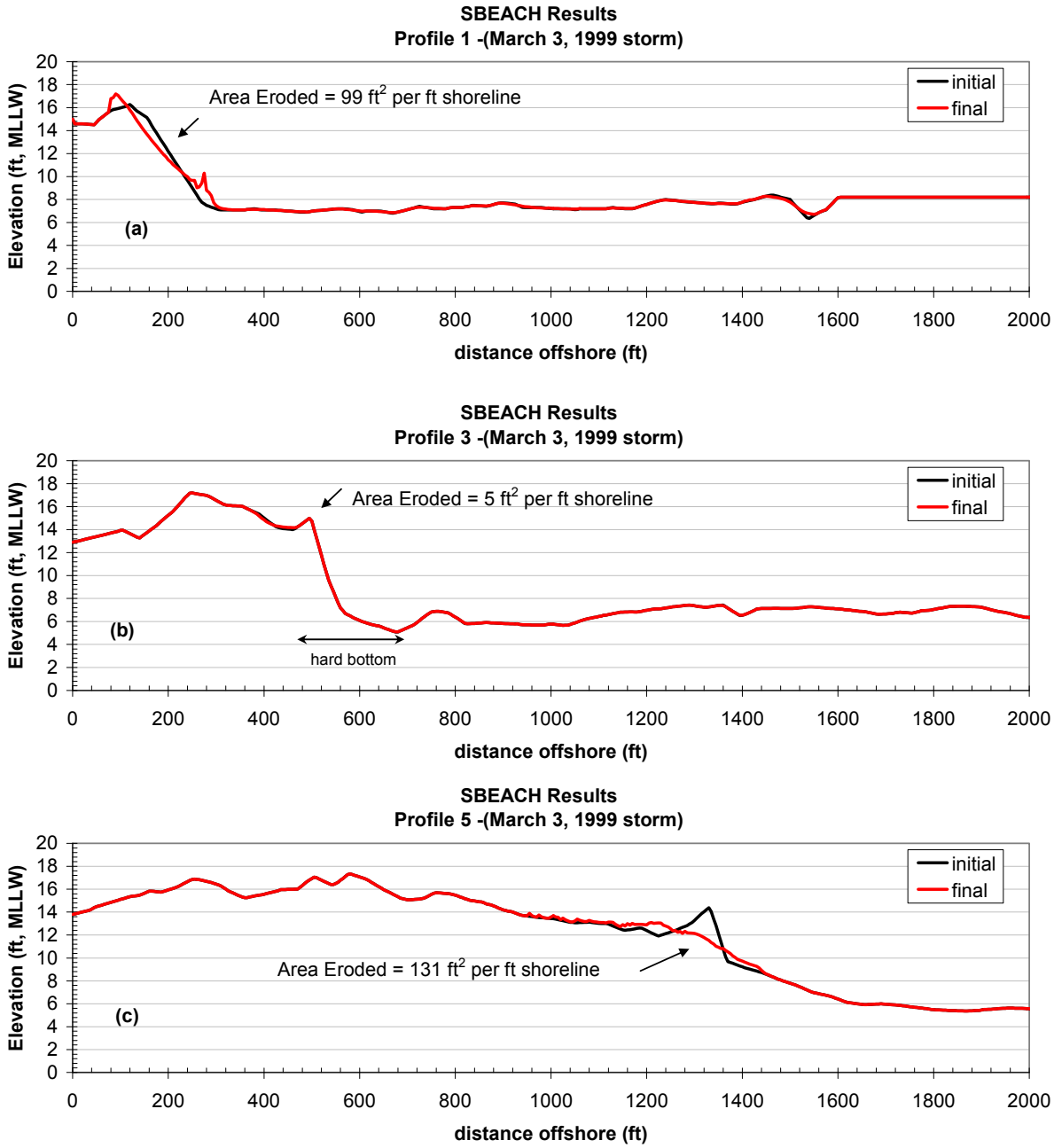

Figure 3.5.3 Predicted erosion on Shoalwater Reservation shoreline for without dune condition during the March 3, 1999 storm. (a) Profile 1 (b) Profile 3 (c) Profile 5

Table 3.5.2. SBEACH results for shoreline erosion for select storms

Date	Profile 1 Area (ft2 – ft)	Profile 3 Area (ft2 – ft)	Profile 5 Area (ft2 – ft)
December 3, 2007	117	7	140
February 4, 2006	152	11	133
January 1, 2006	178	6	174
January 2, 2003	151	3	152
November 8, 2002	80	0	113
December 1, 2001	102	3	128
March 3, 1999	99	5	131
January 29, 1999	68	1	131
December 1, 1998	108	0	160
November 23, 1998	44	0	18
January 17, 1998	127	0	135
January 1, 1997	70	0	38

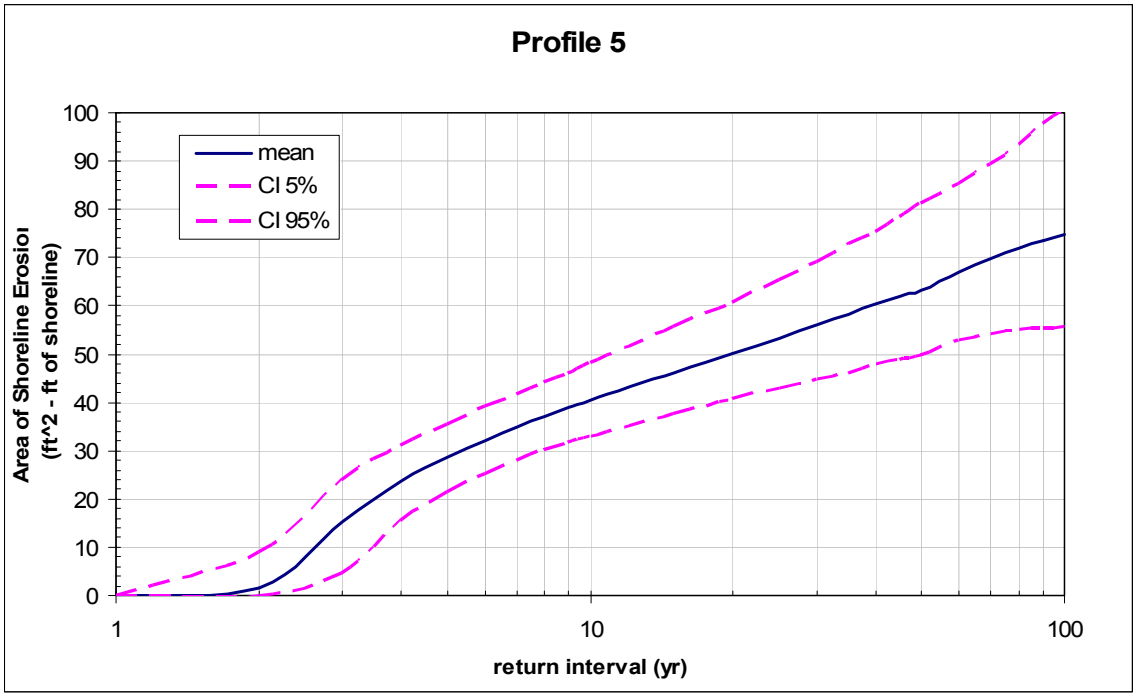

Figure 3.5.4. Return period of shoreline erosion on Profile 5 computed using the Empirical Simulation Technique

Figure 3.5.4 displays the mean and the 5% and 95% confidence intervals of shoreline erosion area for various storm return intervals. The mean 2, 5, 50, and 100 year events for shoreline erosion area on profile 5 are 2 ft^2, 29 ft^2, 63 ft^2, and 75 ft^2 per linear foot of shoreline respectively.

3.5.2 SBEACH Analysis of Barrier Dune Performance

The SBEACH model is used to analyze project performance for the barrier dune restoration alternative. Reliability of the dune against erosion is a function of the storm characteristics such as storm duration, surge height, and tidal amplitude and the dune geometry (Hallermeier and Rhodes 1998, Kriebel and Dean 1993, Judge et al. 2003).

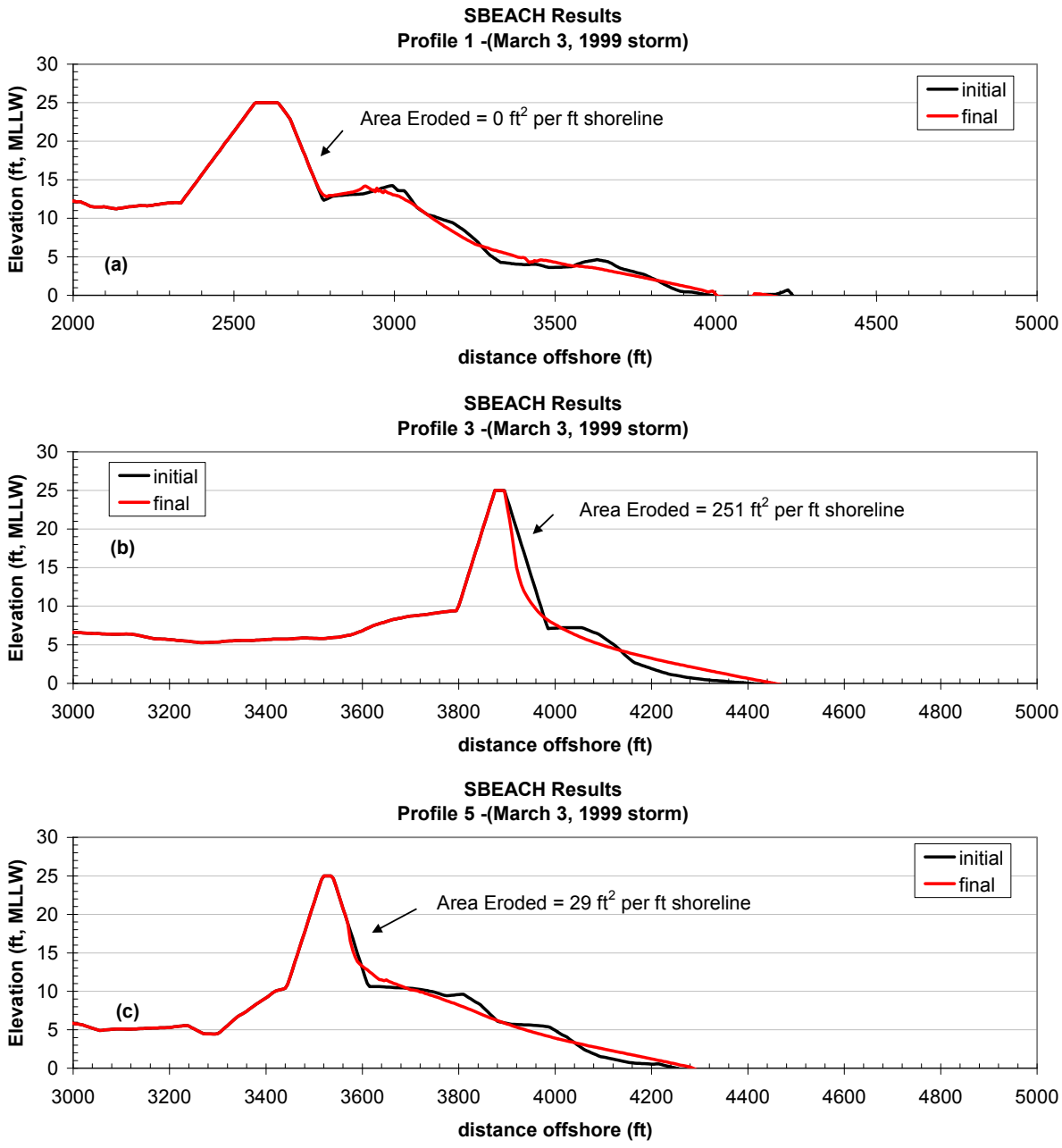

Figure 3.5.5 Predicted erosion restored dune alternative during the March 3, 1999 storm. (a) Profile 1 (b) Profile 3 (c) Profile 5

The restored barrier dune would have a crest height of +25 ft MLLW, a crest width of 20 ft and side slopes of 1:5. The dune would be placed on the existing footprint of the barrier dune which ranges in elevation from +5 to +12 ft MLLW. The design dune cross-section is shown in Figure 3.5.5 on each existing profile. The total cross-sectional area of the dune above mean high water would be 1785 ft^2.

Figure 3.5.5 displays the SBEACH results for storm related erosion on the restored dune for the March 3, 1999 storm condition time series. The dune cross-section located on Profile 3, shows the largest potential for erosion. The area of the profile eroded is computed in SBEACH and is listed in Table 3.5.3 for each storm condition modeled. The model computes an area of 251 ft^2 per linear foot of restored dune eroded during the March 3, 1999 storm. This represents roughly 14% of the cross-sectional area of dune above mean high water. This portion of dune is susceptible to erosion due to a narrow shoreline fronting the dune and a fairly steep profile offshore as a result of the North Willapa Bay Entrance Channel paralleling the barrier dune.

Empirical Simulation Technique

The same input vectors are as in the previous section. However in this case the response vector is the area per linear foot of dune eroded above mean high water. Figure 3.5.6 displays the mean and the 5% and 95% confidence intervals of dune erosion area for various storm return intervals. The mean 2, 5, 50, and 100 year events for dune erosion on profile 3 are 0 ft^2, 336 ft^2, 484 ft^2, and 519 ft^2 per linear foot of shoreline respectively.

The results confirm periodic nourishment of the barrier dune would be needed to sustain a reasonable level of protection over the entire life cycle of the project given that there would be multiple storms events over this time. However, the analysis also indicates that the dune would be able to withstand a 100 year event (1% annual chance of occurrence) with a reasonable degree of confidence. It is computed that the maximum area eroded from a dune cross-section for the 100 year return interval would fall in between 630 - 800 ft^2, or approximately 35 – 45% of the original cross-section.

Table 3.5.3. SBEACH results for erosion to restored dune for select storms

Date	Profile 1 Area (ft2 – ft)	Profile 3 Area (ft2 – ft)	Profile 5 Area (ft2 – ft)
December 3, 2007	0	289	42
February 4, 2006	0	311	37
January 1, 2006	0	475	35
January 2, 2003	0	416	24
November 8, 2002	0	315	4
December 1, 2001	0	378	26
March 3, 1999	0	251	29
January 29, 1999	0	297	13
December 1, 1998	0	377	12
November 23, 1998	0	300	0
January 17, 1998	0	317	16
January 1, 1997	0	338	0

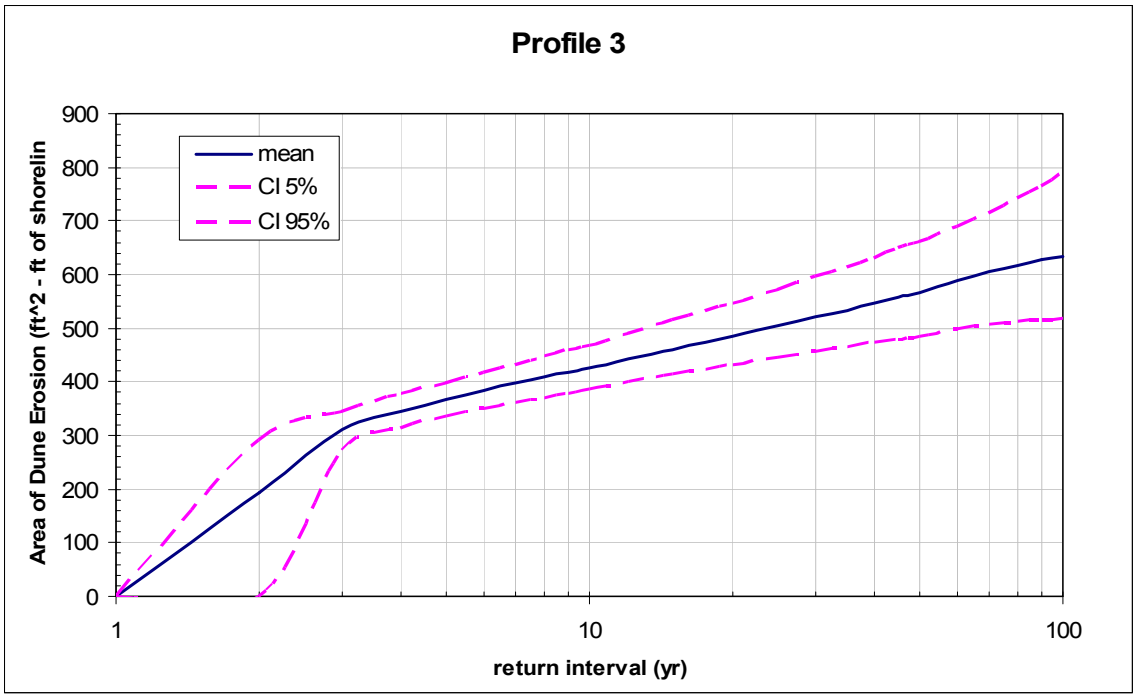

Figure 3.5.6. Return period of restored dune erosion on Profile 3 computed using the Empirical Simulation Technique.

References

Hallermeier, R. J., and Rhodes, P. E. 1988. Generic treatment of dune erosion for 100-year event. *Proc., 21st Int. Conf. on Coastal Engineering*, ASCE, New York, 1197–1211.

Judge, E.K. Overton, M.F., and fisher, J.F., 2003. Vulnerability indicators for coastal dunes. *J. Waterw., Port, Coastal, Ocean Eng.,* 129(6), 270–278.

Kriebel, D. L., and Dean, R. G. 1993. Convolution method for time dependent beach-profile response. *J. Waterw., Port, Coastal, Ocean Eng.,* 119(2), 204–226.

Larson, M., and Kraus, N. C. 1989. *SBEACH: numerical model for simulating storm-induced beach change, report 1: Empirical formulation and model development*, U.S. Army Engineer Waterways Experimentation Station, Vicksburg, Miss.

Larson, M., and Kraus, N. C. 1998. SBEACH: Numerical model for simulating storm-induced beach change. Report 5. Representation of nonerodible (hard) bottoms, Technical Report CERC-89-9, U.S. Army Engineer Waterways Experiment Station, Vicksburg, MS.

Larson, M., Wise, R. A., and Kraus, N. C. 2004. Coastal Overwash. Part 2: Upgrade to SBEACH, Regional Sediment Management Demonstration Technical Note, ERDC/RSM-TN-15, U.S. Army Engineer Research and Development Center, Vicksburg, MS.

Morton, R.A., Purcell, N.A., and Peterson, R.L. 2002. Large-scale cycles of Holocene deposition and erosion at the entrance to Willapa Bay, Washington. U.S. Geological Survey Open File Report 02-46.

Sheffner, N.W., Clausner, J.E., Militello, A., Borgman, L.E., Edge, B.L., Grace, Peter, J. 1999. Use and Application of the Empirical Simulation Technique: User Guide. Technical Report CHL-99-21, U.S. Army Engineer Waterways Experiment Station, Vicksburg, MS.

3.6 Storm Inundation Analysis[14]

3.6.1 Statistical analysis

Hourly water level data are reported at the Toke Point NOAA/NOS tidal station #9440910 starting in 1979. Extreme water levels are a combination of astronomical tide and storm surge. The tide component can be considered a deterministic event. Storm surge is a stochastic event and must be analyzed statistically using observed data to determine the frequency of occurrence of various surge elevations. In this analysis, storm surge is simply computed as the difference between the predicted astronomical tide and the observed tide. Figure 3.6.1 shows the joint distribution of tides and storm surge at the tide gage from 1980 to 2007. Figure 3.6.2 displays the cumulative density function of tide and storm surge. The most frequent events occur near mean tide level and a zero magnitude surge. However, the coincidence of high tides and extreme storm surges is evident by the data populated in the upper right hand corner of the figure.

Frequency of high water levels can be computed from the joint distribution using the convolution method originally described by Pugh and Vassie (1978), assuming the surge and tides are statistically independent of one another. In shallow water areas extending a large distance inland such as Willapa Bay, the enhanced depth associated with the tide can affect the propagation and transformation of the storm surge. This would suggest the two parameters are dependent and the convolution method would be invalid. Instead, a more conservative approach is utilized to develop the extreme water levels simulated in the inundation model. Representative tidal elevations of mean higher high water (MHHW) and maximum astronomical tide (MAT) are added to the extreme distribution of storm surge for various frequency intervals. A peak storm surge occurring at MHHW represents a likely occurrence while a peak storm surge coincident with MAT is less likely, but represents an upper limit to the extreme water level.

A peak over threshold analysis is performed to select extreme surges from the Toke Point NOS gage from years 1980 to 2007. Selecting all surge elevations above a threshold of 3.3 ft yielded $N_T = 31$ events, or approximately one extreme event per year. An extreme distribution following a Fisher-Tippet type I (or Gumbel distribution) is fit to the data using the least squares method. The form of the cumulative distribution follows

$$F(x) = \exp\left[-\exp\left(-\frac{x-B}{A}\right)\right] \quad : -\infty \le x < \infty. \tag{1}$$

where parameter A governs the linear scale of x and parameter B fixes the location of the x-axis. The distribution is fit to the data using the unbiased plotting position formula outlined in Goda (2000). Figure 3.6.3 shows the fitted distribution with the 90% confidence intervals. The storm surge return interval (in years) is calculated following the relation

$$R = \frac{1}{\lambda\left[1 - F(x_u)\right]}, \tag{2}$$

[14]Written by David Michalsen, U.S. Army Corps of Engineers, Seattle District

where λ is the ratio of extreme samples to the number of years of data (e.g. $\lambda = N_T/N$), and $F(x_u)$ is the probability that the extreme variate x does not exceed a given value x_u in one year. Table 3.6.1 lists the computed return intervals for storm surge as well as the 90% confidence limits.

Table 3.6.1. Extreme storm surge elevation distribution data

RETURN INTERVAL (YR)	% Annual Occurrence	MEAN (ft, surge)	90% C.I. min (ft, surge)	90% C.I. max (ft, surge)
2	50	3.9	3.7	4.1
50	2	5.5	5.2	5.8
100	1	5.8	5.5	6.2

Model Cases

Table 3.6.2 lists the nine storm cases simulated. Three historical cases are modeled representing the three highest storm surges on record since 1980. Additionally, six hypothetical storms are modeled using wave data from observed storms occurring at different tidal phases. The hypothetical storms represent the 50, 2, and 1% annual storm surge occurrence from Table 3.6.1 occurring at MHHW and MAT. The wave parameters for the hypothetical storms are selected based on observed surge data equal to these occurrence intervals. Figure 3.6.4 demonstrates extreme storm surges are well correlated with wave height, period, and direction as these extreme events are always associated with long period south-southwesterly waves.

Table 3.6.2. Model cases run in CMS-WAVE

Storm Description	Peak Surge elevation (ft)	Total water level (ft, mllw)	Wave height (ft)	Wave period (s)	Wave direction (deg)
3-Mar-99 1000 UTC	5.1	13.6	34.8	16.67	226
3-Dec-07 1700 UTC	5.3	13.4	31.5	16.67	214
4-Feb-06 1300 UTC	4.4	13.9	39.3	15.38	233
2yr @ MHHW	3.9	12.8	26	16.67	226
50yr @ MHHW	5.5	13.4	31.5	16.67	214
100yr @ MHHW	5.8	13.9	39.3	15.38	233
2yr @ MAT	3.9	14.9	26	16.67	226
50yr @ MAT	5.5	16.5	31.5	16.67	214
100yr @ MAT	5.8	16.8	39.3	15.38	233

[1] MHHW = 8.94 ft MLLW
[2] MAT = 11 ft MLLW

3.6.2 Wave Modeling

Extreme water levels combined with large offshore waves result in flooding to the Shoalwater Reservation shoreline. Documented damage to local infrastructure has typically been associated with dynamic flooding due to wave runup, overtopping, and overland wave propagation during these extreme water levels. The feature in the CMS-WAVE (version 1.9) numerical wave model computing inundation depth due to dynamic flooding was determined a useful extension to the previous STWAVE modeling performed in Section 3.2. CMS-WAVE and STWAVE require the same model inputs; therefore the exercise is fairly streamlined.

The intensity of the storm surge, tidal phase, offshore wave height, and topography each affect the magnitude of inundation. In order to help quantify the degree of flooding, results from the statistical analysis are utilized to specify the wave model boundary conditions for each model case.

CMS-WAVE Model description

CMS-Wave, previously called WABED (Wave-Action Balance Equation Diffraction), is a two-dimensional (2D) spectral wave model formulated from a parabolic approximation equation (Mase et al. 2005) with energy dissipation and diffraction terms. It simulates a steady-state spectral transformation of directional random waves co-existing with ambient currents in the coastal zone. The model operates on a coastal half-plane, implying waves can propagate only from the seaward boundary toward shore. It includes features such as wave generation, wave reflection, and bottom frictional dissipation. CMS-WAVE Version 1.9 additionally includes features to investigate storm wave related inundation (Lin et al. 2008). The model utilizes analytical relations to include wave setup, runup, and overtopping to compute inundation depths over low lying backshore regions.

Model inputs

The digital terrain model used to construct the model grid is generated from three sources. Topographic data surveyed in July 2008 is used to generate the most recent Graveyard Spit dune condition and Tokeland Peninsula shoreline. Annual hydrosurvey condition survey data from September 2008 of the North Channel and offshore dune area are utilized for the surrounding bathymetry. Finally, the Taylor et al. (2008) NOAA combined topography and bathymetry tsunami inundation digital elevation model is utilized for coverage outside of the 2008 data. Model grids are constructed relative to the mean tide level (MTL) tidal datum.

The wave modeling is performed using a nested grid approach. A coarser regional scale grid with 200 ft cell spacing is run to output wave information to "nesting cells" located at the offshore boundary of the higher resolution local scale grid. This 40 ft cell spacing grid covers Tokeland Peninsula and the immediate offshore area. The two grids used in the simulations are shown in Figure 3.6.5.

Wave spectra for the cases listed in Table 3.6.2 are collected from the Grays Harbor Coastal Data Information Program (CDIP) 036 buoy and are utilized to specify the offshore wave boundary condition. For the case of the March 3, 1999 storm, there is a gap in the CDIP buoy data; therefore the National Data Buoy Center (NDBC) buoy 46029 offshore the Mouth of the Columbia River wave spectra is used. In this case, the wave spectrum is transformed using

the maximum entropy method to the 130 ft depth, which corresponds to the water depth at the offshore boundary of the regional scale grid.

As in Section 3.2, water level is applied in CMS-WAVE as a constant depth change over the entire model domain. Cells representing land are specified in the *.struct file to compute wave setup and runup. The parameter k = 2 is specified at these cells as discussed in Lin et al. (2008).

Inundation depth and flow velocity computations

Inundation depth is defined as the water depth associated with overland flooding. The maximum water depth can be a result of dynamic (i.e. short time scale) wave runup or inundation by rise in static water levels (i.e. long time scale) due to tide and storm surge. Wave runup is significant for beach erosion as well as wave overtopping rubble mound structures. The total wave runup consists of two components: (a) rise of the mean water level by wave breaking at the shore, known as the wave setup, and (b) swash of incident waves. Wave setup is computed as:

$$\frac{\partial \eta}{\partial x} = -\frac{1}{\rho g h}\left(\frac{\partial S_{xx}}{\partial x} + \frac{\partial S_{xy}}{\partial y}\right) \quad , \quad \frac{\partial \eta}{\partial y} = -\frac{1}{\rho g h}\left(\frac{\partial S_{xy}}{\partial x} + \frac{\partial S_{yy}}{\partial y}\right) \tag{1}$$

where ρ is the water density and S_{xx}, S_{xy}, and S_{yy} are radiation stress components from the excess momentum flux caused by waves. The swash oscillation of incident waves on the shoreline is a random process. The most landward swash excursion corresponds to the maximum wave runup. Wave runup is largest on steep topography such as rubble mound structures. A statistical parameter describing the 2% exceedance of all runups is defined by Komar (1998) as:

$$R2 = 2\eta_{max} \tag{2}$$

In CMS-Wave, *R2* is calculated at the land-water interface and averaged with the local depth to determine if the water can flood the proceeding dry cell. If the wave runup level is higher than the adjacent land cell elevation, CMS-Wave can flood the dry cells and simulate wave overtopping and overwash at them. In areas which have been flooded to allow overland wave propagation, the maximum water level is computed as the wave amplitude plus the wave setup, or, $\eta + 0.5H_{1/3}$, where $H_{1/3}$ is wave height. In low lying regions removed from overland wave propagation, water may flood strictly due to static water level increases by storm surge and tide. Thus, over the entire model domain the maximum flooding depth (dynamic or static) is computed using the following relation:

Maximum flooding depth =
max ($R2$, $\eta + 0.5H_{1/3}$) + tide elevation + surge elevation – land elevation. (3)

In shallow water, the maximum velocity of the wave (or celerity) is only a function of water depth. The velocity of overland wave propagation is

$$V = \sqrt{gh} \tag{4}$$

where g is gravitational acceleration (i.e. 32.2 ft/s^2 or 9.81 m/s^2) and h is the local water depth.

Without project condition

In Section 3.2, the wave analysis is performed using bathymetric and topographic data prior to 2002. Since this time the Graveyard spit dunes have undergone significant erosion and have lowered in crest height to only a few feet above mean high water (MHW) as shown in Figure 3.6.6. The STWAVE modeling performed by CHL modeled the without project condition as a dune with crest elevation equal to mean high water (MHW), or approximately +9 ft MLLW. The analysis found the significant wave height along the shoreline doubled from the 2002 dune condition to increase to a maximum of H_s = 1m or 3.3 ft. Figure 3.6.6 demonstrates the dune has eroded most near the eastern breach. Model results indicate that this breach allows the most wave energy to enter North Cove. A wave height contour plot and alongshore wave height from Stations 1-22 are shown in Figure 3.6.7 for the March 3, 1999 storm scenario. In the dunes current condition, a maximum significant wave height of H_s = 2.8 ft, or 0.85 m is predicted at Station 18 and suggest the dunes are nearing the condition previously modeled by CHL. The increase in wave height brings potential adverse impacts such as larger wave runup on the shoreline and potential for greater storm related flooding.

Damage to structures from coastal flooding is often related to flood depth or velocity of flood waters (FEMA 2005). High velocity flow associated with wave runup, overtopping, and overland wave propagation has the potential of transporting damaging debris. Potential damages associated with flooding can occur to Washington DOT State Route 105, private residences, and property owned by the Shoalwater Indian Reservation. A structure inventory was performed for all property located within the Reservation Boundary and is listed in Tables 3.6.4 to 3.6.7. Flooding depth is a function of the proximity to the shoreline and the structure's first floor elevation and adjacent grade. The threat of flooding is assigned using the following classification (codes in parentheses):

- Low risk (L) = low flooding threat (flood depth less than 0.03 feet).
- Moderate risk (M) = moderate flooding threat; potential for structural and contents damage (flood depth less than one foot).
- High risk (H) = High velocity flow; potential for structural and contents damage from debris due to wave runup, overtopping, and overland wave propagation (flood depths greater than one foot)

A flooding threat to a structure is defined as any classification exceeding a low threat (L). As a validation set, the March 3, 1999 storm resulted in 54% of the structures classified with a flooding threat (inventory listed in Table 3.6.4). Figures 3.6.8 to 3.6.12 show detailed inundation map for the March 3, 1999 storm. Documented damages by local residents during the storm confirm model results to be reasonable at predicting inundation depths.

The same approach is utilized to describe the threat during the 50, 2, and 1% annual storm surge occurrence intervals. Tables 3.6.3(a) and 3.6.3(b) list the flooding risk of Shoalwater Reservation structures for each occurrence interval at MHHW and MAT, respectively. Tables 3.6.5 and 3.6.6 list the maximum flooding depth for each structure

inventoried for the 2% annual storm surge at MHHW and MAT. For a 2% annual storm surge occurring during MAT, 92% of the structures inventoried are classified with a flooding threat.

Table 3.6.3 (a) Percentage of Structures at Flooding Risk for Storm Surge Event Frequency at Mean Higher High Water (MHHW)

Flood and Storm Damage Risk	50% Annual Occurrence	2% Annual Occurrence	1% Annual Occurrence
Low	85	17	12
Medium	7	40	35
High	8	43	53

Table 3.6.3 (b) Percentage of Structures at Flooding Risk for Storm Surge Event Frequency at Maximum Astronomical Tide (MAT)

Flood and Storm Damage Risk	50% Annual Occurrence	2% Annual Occurrence	1% Annual Occurrence
Low	9	8	8
Medium	35	12	12
High	56	80	80

With project condition

In effort to determine the effectiveness of project alternative at mitigating flood threat, the sea dike and dune restoration alternatives are simulated as designed in CMS-WAVE for the same storms listed in Table 3.6.2.

Sea Dike (Alternative 4)

The sea dike structure would have a crest height of +20 ft MLLW, a crest width of 14 ft, and side slopes of 1V:2H. The sea dike will not eliminate flooding caused by extreme water elevations, such as those occurring during MAT. The sea dike is not designed as a flood control structure, since North Cove will continue to be hydraulically connected to the Pacific Ocean through two inlets to the east and west of the sea dike. A sea dike will mitigate structure damage from debris carried inland by high velocity sheet flows near the Reservation Boundary shoreline. However, it was hypothesized during the initial design that terminating the protective sea dike structure at the Reservation boundary might cause adverse impacts to adjacent shorelines left

unprotected. Figure 3.6.13 depicts the change in flood elevation with the sea dike that terminates at the Shoalwater Reservation boundary in place compared to the without project condition. An increase in flooding depth and extent of flooding adjacent shorelines of this sea dike is indicated by the model. The largest impact is found east of the sea dike terminus near the Dexter by the Sea community where flood depths are predicted to increase approximately 1.5 ft. Thus enhanced risk to structures outside the Reservation from high velocity flow may result in addition to residual risk to structures within the Reservation due to overland wave propagation.

Barrier Dune Restoration (Alternative 6)

The restored dune structure would have a crest height of +25 ft MLLW, a crest width of 20 ft, and side slopes of 1V:5H. The dune restoration will not eliminate flooding caused by extreme water elevations, such as those occurring during MAT. The restored dune is not designed as a flood control structure, since North Cove will continue to be hydraulically connected to the Pacific Ocean through two inlets. However, the barrier dune will significantly reduce the frequency and magnitude of dynamic water level flooding due to wave runup and overland wave propagation. Figure 3.6.14 depicts the change in flood elevation with a restored dune versus the without project condition. The figure demonstrates the shoreline leeward of the dune will experience a decrease in flood elevations in areas most prone to overland wave propagation and wave runup. Table 3.6.7 lists that with a restored dune, the threat to the inventoried structures is reduced from 54% (without project – see table 3.6.4) to 7% (with project) during a March 3, 1999 storm condition. The restored dune will mitigate structure damage from debris carried inland by high velocity sheet flows. However, instances of extreme water levels caused by large storm surges occurring at MAT will flood low lying topography (ponding). Thus some residual flooding risk to structures will exist in the with project condition.

References

FEMA 2005. Guidelines for Coastal Flood Hazard Analysis and Mapping for the Pacific Coast of the United States http://www.fema.gov/plan/prevent/fhm/frm_cfham.shtm

Goda, Y. 2000. Random seas and design of maritime structures, World Scientific, Singapore.

Komar, P. D. 1998. Beach processes and sedimentation. 2nd ed. Upper Saddle River, NJ: Prentice-Hall, Inc.

Lin, L.,Demirbilek, Z., Mase, H., Zheng, J. and F. Yamada. 2008. CMS-WAVE: A nearshore spectral wave processes model for coastal inlets and navigation projects. Coastal and Hydraulics Engineering Technical Report ERDC/CHL TR-08-13. Vicksburg, MS: U.S. Army Engineer Research and Development Center.

Mase, H., H. Amamori, and T. Takayama. 2005. Wave prediction model in wave-current coexisting field. *Proceedings 12th Canadian Coastal Conference* (CD-ROM).

Pugh, D.T. and Vassie, J.M. 1978. Extreme sea levels from tide and surge probability. *Proc. 16th Coastal Engineering Conference.* Hamburg, Germany. pp. 911-930

Taylor, L.A., B.W. Eakins, K.S. Carignan, and R.R. Warnken. 2008. Digital Elevation Model for Astoria, Oregon: Procedures, Data Sources and Analysis. Prepared for the Pacific Marine Environmental Laboratory (PMEL) NOAA Center for Tsunami Research by the NOAA National Geophysical Data Center (NGDC). May 30, 2008

Table 3.6.4. Predicted flooding depth and velocity for March 3, 1999 1000 UTC storm (Without project condition)

Inventory	Structure Name / Function	Distance from Shoreline (feet)	i	j	elevation (m, mtl)	elevation (ft, mllw)	Max Flooding depth (m)	Max velocity (m/s)	Flood Risk
1	Tribal Business (Fireworks Stand)	131	136	477	3.11	15.0	0.305	1.730	H
2	Tribal Business (Fireworks Stand)	283	136	485	3.59	16.5	1.016	3.157	H
3	Tribal Business (Convenience Store) / Single Family Residence	334	138	484	3.82	17.3	0.141	1.176	M
5	Single Family Residence	412	140	485	4.35	19.0	-	-	L
7	Tribal Business (Fireworks Stand)	282	140	484	4.19	18.5	0.601	2.428	H
8	Vacant Old Building	343	140	480	3.48	16.2	0.537	2.295	H
9	Vacant Old Building	343	140	480	3.48	16.2	0.537	2.295	H
10	Single Family Residence	220	140	477	3.43	16.0	0.383	1.938	H
11	Single Family Residence	372	144	475	6.48	26.0	-	-	L
12	Mobile Home Residence	220	140	475	3.18	15.2	0.430	2.054	H
13	Tribal Business (Fireworks Stand)	169	149	429	3.56	16.4	1.880	4.295	H
14	Tribal Business (Fireworks Stand)	177	150	426	3.41	16.0	-	-	L
15	Tribal Business (Fireworks Stand)	183	149	421	3.35	15.8	1.556	3.907	H
16	Single Family Residence	225	151	419	3.78	17.2	-	-	L
17	Single Family Residence	220	152	417	3.72	17.0	-	-	L
18	Single Family Residence	220	152	414	3.72	17.0	0.075	0.858	M
19	Single Family Residence	220	151	412	3.72	17.0	0.257	1.588	M
20	Water Treatment, Pump House, Back-up Generator	245	152	407	2.86	14.2	0.296	1.704	M
21	Single Family Residence	397	156	405	2.88	14.2	0.224	1.482	M
23	Single Family Residence	361	156	399	2.79	13.9	-	-	L
24	40 foot shipping container	308	154	397	3.11	15.0	-	-	L
25	40 foot shipping container	328	155	397	2.98	14.5	-	-	L
26	40 foot shipping container	338	155	397	2.98	14.5	-	-	L
27	Tribal Business Storage	287	154	396	3.22	15.3	-	-	L
28	Tribal Business (Convenience Store)	273	154	396	3.22	15.3	-	-	L

Table 3.6.4. Predicted flooding and velocity for March 3, 1999 1000 UTC storm (Without project condition) (continued)

Inventory	Structure Name / Function	Distance from Shoreline	i	j	elevation (m, mtl)	elevation (ft, mllw)	Max Flooding depth (m)	Max velocity (m/s)	Flood Risk
29	Tribal Gaming (Regulators) Office	422	158	395	2.63	13.4	0.056	0.099	M
30	Tribal Casino Administrative Office	418	158	392	3.07	14.8	-	-	L
31	Tribal Casino Administrative Office	435	159	389	3.12	15.0	0.083	0.902	M
32	Tribal Casino and emergency back-up generator	358	157	392	3.08	14.9	-	-	L
33	Bus Shelter	287	152	388	3.6	16.6	0.882	2.941	H
33a	Casino Septic Field	260	153	404	3.06	14.8	0.083	0.902	L
34	Single Family Residence	190	151	380	3.77	17.1	0.546	2.314	H
36	Single Family Residence	277	153	380	3.68	16.8	0.579	2.383	H
37	Single Family Residence	366	155	378	3.14	15.1	0.440	2.078	H
38	Single Family Residence	364	154	376	2.92	14.4	0.255	1.582	M
39	Single Family Residence	272	153	375	3.65	16.7	0.130	1.129	M
40	Single Family Residence	185	150	377	3.28	15.5	0.595	2.416	H
42	Single Family Residence	375	155	374	3.08	14.9	0.111	1.044	M
43	Single Family Residence	501	158	374	2.52	13.0	0.190	0.505	M
44	Tribal Business (Fireworks Stand)	114	147	371	2.81	14.0	0.336	1.816	H
45	Mobile Home Residence	310	152	369	3.39	15.9	-	-	L
47	Single Family Residence	303	153	367	3.4	15.9	-	-	L
49	Mechanical Repairs Building for Tribal Fishing Boats and Gear	388	155	366	3.11	15.0	-	-	L
50	Mobile Home Residence	506	157	366	2.73	13.7	0.065	0.799	M
51	Single Family Residence	154	149	368	3.49	16.2	-	-	L
52	Single Family Residence	151	148	365	3.45	16.1	0.276	1.645	M
54	Mobile Home Residence	306	153	366	3.38	15.9	-	-	L
55	Mobile Home Residence	306	153	365	3.33	15.7	-	-	L
60	Single Family Residence	244	149	357	4.05	18.1	-	-	L
61	Single Family Residence	224	149	360	4.04	18.0	-	-	L
62	Single Family Residence	289	152	361	3.81	17.3	-	-	L

Table 3.6.4. Predicted flooding depth and velocity for March 3, 1999 1000 UTC storm (Without project condition) (continued)

Inventory	Structure Name / Function	Distance from Shoreline	i	j	elevation (m, mtl)	elevation (ft, mllw)	Max Flooding depth (m)	Max velocity (m/s)	Flood Risk
63	Single Family Residence	381	154	359	4.14	18.4	-	-	L
64	Single Family Residence	420	154	356	4.14	18.4	-	-	L
65	Single Family Residence	420	153	353	4.01	17.9	-	-	L
66	Single Family Residence	405	152	352	4.03	18.0	-	-	L
67	Single Family Residence	315	148	352	4.06	18.1	-	-	L
69	Tribal Community Center / Tribal Police	153	144	353	3.54	16.4	0.141	1.176	M
71	Tribal Education Center and Library	260	143	346	3.85	17.4	-	-	L
72	Tribal Court	105	139	350	3.35	15.8	0.615	2.456	H
73	Tribal Social and Family Services	163	139	350	3.35	15.8	0.615	2.456	H
74	Emergency Back-up Generator (Flood-proofed)	163	139	350	3.35	15.8	0.615	2.456	H
75	Tribal Cultural Repository Building	276	136	346	3	14.6	0.452	2.106	H
76	Tribal Counseling / Interview Facility	276	136	345	3	14.6	0.522	2.263	H
83	Tribal Wellness Center	463	144	341	3.42	16.0	-	-	L
83a	Emergency Back-up Generator (Flood-proofed)	460	141	342	3.78	17.2	-	-	L
84	Duplex Family Residence	710	147	338	3.82	17.3	-	-	L
85	Duplex Family Residence	720	150	338	3.87	17.5	-	-	L
86	Tribal Gymnasium and Assembly Hall	707	154	339	3.23	15.4	-	-	L
87	Gymnasium Storage Building	860	153	336	3.24	15.4	-	-	L
88	Duplex Family Residence	1032	155	334	2.67	13.5	0.025	0.221	M
89	Duplex Family Residence	1117	156	331	2.7	13.6	0.040	0.626	M
90	Duplex Family Residence	1213	157	329	2.6	13.3	0.146	0.774	M
91	Duplex Family Residence	1301	158	327	2.49	12.9	0.236	0.611	M
92	Tribal Recreational Vehicle Park & Casino Parking	90	148	390	2.69	13.6	0.390	1.956	H
93	Tribal Cemetery	462	149	346	2.9	14.3	-	-	L
								% Low Risk	**46**
								% Moderate Risk	**25**
								% High Risk	**29**

Table 3.6.5. Predicted flooding depth and velocity for 2% annual surge occurrence interval at Mean Higher High Water (Without project condition)

Inventory	Structure Name / Function	Distance from Shoreline (feet)	i	j	elevation (m, mtl)	elevation (ft, mllw)	Max Flooding depth (m) 2% annual occurrence at MHHW	Max velocity (m/s) 2% annual occurrence	Flood Risk for 2% annual occurrence at MHHW
1	Tribal Business (Fireworks Stand)	131	136	477	3.11	15.0	0.526	1.721	H
2	Tribal Business (Fireworks Stand)	283	136	485	3.59	16.5	0.456	2.115	H
3	Tribal Business (Convenience Store) / Single Family Residence	334	138	484	3.82	17.3	0.312	1.749	H
5	Single Family Residence	412	140	484	4.19	18.5	0.064	0.792	M
7	Tribal Business (Fireworks Stand)	282	138	481	3.3	15.6	0.582	2.389	H
8	Vacant Old Building	343	140	480	3.48	16.2	0.543	2.308	H
9	Vacant Old Building	343	140	480	3.48	16.2	0.543	2.308	H
10	Single Family Residence	220	140	477	3.43	16.0	0.398	1.976	H
11	Single Family Residence	372	144	475	6.48	26.0	-	-	L
12	Mobile Home Residence	220	140	475	3.18	15.2	0.363	1.887	H
13	Tribal Business (Fireworks Stand)	169	150	429	3.5	16.3	0.658	2.541	H
14	Tribal Business (Fireworks Stand)	177	150	426	3.41	16.0	0.626	2.478	H
15	Tribal Business (Fireworks Stand)	183	149	421	3.35	15.8	0.534	2.289	H
16	Single Family Residence	225	151	419	3.78	17.2	0.411	2.008	H
17	Single Family Residence	220	152	417	3.72	17.0	0.103	1.005	M
18	Single Family Residence	220	151	414	3.72	17.0	-	-	L
19	Single Family Residence	220	151	412	3.72	17.0	0.178	1.321	M
20	Water Treatment, Pump House, Back-up Generator	245	152	407	2.86	14.2	0.164	0.852	M
21	Single Family Residence	397	156	405	2.88	14.2	0.127	0.767	M
23	Single Family Residence	361	156	399	2.79	13.9	0.206	0.686	M
24	40 foot shipping container	308	154	397	3.11	15.0	0.484	2.179	H
25	40 foot shipping container	328	155	397	2.98	14.5	0.223	1.479	M
26	40 foot shipping container	338	155	397	2.98	14.5	0.223	1.479	M
27	Tribal Business Storage	287	154	396	3.22	15.3	0.254	1.579	M
28	Tribal Business (Convenience Store)	273	154	396	3.22	15.3	0.254	1.579	M

Table 3.6.5. Predicted flooding depth and velocity for 2% annual surge occurrence interval at Mean Higher High Water (Without project condition) (continued)

Inventory	Structure Name / Function	Distance from Shoreline (feet)	i	j	elevation (m, mtl)	elevation (ft, mllw)	Flooding depth (m)	Max velocity (m/s)	Flood Risk
29	Tribal Gaming (Regulators) Office	422	158	395	2.63	13.4	0.346	0.551	H
30	Tribal Casino Administrative Office	418	158	392	3.07	14.8	0.212	1.442	M
31	Tribal Casino Administrative Office	435	159	390	3.02	14.7	0.092	0.950	M
32	Tribal Casino and emergency back-up generator	358	157	392	3.08	14.9	0.467	2.140	H
33	Bus Shelter	287	152	388	3.6	16.6	0.372	1.910	H
33a	Casino Septic Field	260	156	394	3	14.6	0.051	0.707	M
34	Single Family Residence	190	151	380	3.77	17.1	0.757	1.958	H
36	Single Family Residence	277	153	380	3.68	16.8	0.416	2.020	H
37	Single Family Residence	366	155	378	3.14	15.1	0.228	1.496	M
38	Single Family Residence	364	154	376	2.92	14.4	0.445	2.089	H
39	Single Family Residence	272	153	375	3.65	16.7	0.426	2.044	H
40	Single Family Residence	185	150	377	3.28	15.5	0.653	1.666	H
42	Single Family Residence	375	155	374	3.08	14.9	0.157	1.241	M
43	Single Family Residence	501	158	374	2.52	13.0	0.458	0.586	H
44	Tribal Business (Fireworks Stand)	114	147	371	2.81	14.0	0.202	0.805	M
45	Mobile Home Residence	310	152	369	3.39	15.9	0.242	1.541	M
47	Single Family Residence	303	153	367	3.4	15.9	0.170	1.291	M
49	Mechanical Repairs Building for Tribal Fishing Boats and Gear	388	155	366	3.11	15.0	0.145	1.193	M
50	Mobile Home Residence	506	157	366	2.73	13.7	0.276	0.754	M
51	Single Family Residence	154	149	368	3.49	16.2	-	-	L
52	Single Family Residence	151	148	365	3.45	16.1	0.238	1.528	M
54	Mobile Home Residence	306	153	366	3.38	15.9	0.151	1.217	M
55	Mobile Home Residence	306	153	365	3.33	15.7	0.295	1.701	M
60	Single Family Residence	244	149	357	4.05	18.1	0.057	0.748	M
61	Single Family Residence	224	149	360	4.04	18.0	0.087	0.924	M
62	Single Family Residence	289	152	361	3.81	17.3	0.303	1.724	H

Table 3.6.5. Predicted flooding depth and velocity for 2% annual surge occurrence interval at Mean Higher High Water (Without project condition) (continued)

Inventory	Structure Name / Function	Distance from Shoreline	i	j	elevation (m, mtl)	elevation (ft, mllw)	Flooding depth (m)	Max velocity (m/s)	Flood Risk
63	Single Family Residence	381	154	359	4.14	18.4	0.087	0.924	M
64	Single Family Residence	420	154	356	4.14	18.4	-	-	L
65	Single Family Residence	420	153	353	4.01	17.9	-	-	L
66	Single Family Residence	405	152	352	4.03	18.0	-	-	L
67	Single Family Residence	315	148	352	4.06	18.1	0.141	1.176	M
69	Tribal Community Center / Tribal Police	153	144	353	3.54	16.4	0.576	2.377	H
71	Tribal Education Center and Library	260	143	346	3.85	17.4	-	-	L
72	Tribal Court	105	139	350	3.34	15.7	0.355	1.866	H
73	Tribal Social and Family Services	163	139	350	3.15	15.1	0.355	1.866	H
74	Emergency Back-up Generator (Flood-proofed)	163	139	350	3.15	15.1	0.355	1.866	H
75	Tribal Cultural Repository Building	276	136	346	3	14.6	1.440	1.411	H
76	Tribal Counseling / Interview Facility	276	136	345	3	14.6	0.620	1.579	H
83	Tribal Wellness Center	463	144	341	3.42	16.0	-	-	L
83a	Emergency Back-up Generator (Flood-proofed)	460	141	342	3.78	17.2	-	-	L
84	Duplex Family Residence	710	147	338	3.82	17.3	-	-	L
85	Duplex Family Residence	720	150	338	3.87	17.5	-	-	L
86	Tribal Gymnasium and Assembly Hall	707	154	339	3.23	15.4	-	-	L
87	Gymnasium Storage Building	860	153	336	3.24	15.4	-	-	L
88	Duplex Family Residence	1032	155	334	2.67	13.5	0.280	0.099	M
89	Duplex Family Residence	1117	156	331	2.7	13.6	0.249	0.280	M
90	Duplex Family Residence	1213	157	329	2.6	13.3	0.359	0.371	H
91	Duplex Family Residence	1301	158	327	2.49	12.9	0.472	0.371	H
92	Tribal Recreational Vehicle Park & Casino Parking	90	148	390	2.69	13.6	0.713	2.124	H
93	Tribal Cemetery	462	149	346	2.9	14.3	0.049	-	M
							% Low Risk		**17**
							% Moderate Risk		**40**
							% High Risk		**43**

Table 3.6.6. Predicted flooding depth and velocity for 2% annual surge occurrence interval at Maximum Astronomical Tide (Without project condition)

Inventory	Structure Name / Function	Distance from Shoreline (feet)	i	j	elevation (m, mtl)	elevation (ft, mllw)	Flooding depth (m) 2% annual occurrence at MAT	Max velocity (m/s) 2% annual occurrence	Flood Risk for 2% annual occurrence at MAT
1	Tribal Business (Fireworks Stand)	131	136	477	3.11	15.0	0.785	1.775	H
2	Tribal Business (Fireworks Stand)	283	136	485	3.59	16.5	0.472	2.027	H
3	Tribal Business (Convenience Store) / Single Family Residence	334	138	484	3.82	17.3	0.341	1.369	H
5	Single Family Residence	412	140	485	4.35	19.0	0.061	0.280	M
7	Tribal Business (Fireworks Stand)	282	140	484	4.19	18.5	0.574	1.241	H
8	Vacant Old Building	343	140	480	3.48	16.2	0.490	1.257	H
9	Vacant Old Building	343	140	480	3.48	16.2	0.490	1.257	H
10	Single Family Residence	220	140	477	3.43	16.0	0.369	1.098	H
11	Single Family Residence	372	144	475	6.48	26.0	-	-	L
12	Mobile Home Residence	220	140	475	3.18	15.2	0.479	0.902	H
13	Tribal Business (Fireworks Stand)	169	150	429	3.5	16.3	0.644	1.648	H
14	Tribal Business (Fireworks Stand)	177	150	426	3.41	16.0	0.542	1.217	H
15	Tribal Business (Fireworks Stand)	183	149	421	3.35	15.8	0.510	1.522	H
16	Single Family Residence	225	151	419	3.78	17.2	0.376	0.913	H
17	Single Family Residence	220	152	417	3.72	17.0	0.089	0.198	M
18	Single Family Residence	220	151	414	3.72	17.0	0.075	0.611	M
19	Single Family Residence	220	151	412	3.72	17.0	0.460	1.125	H
20	Water Treatment, Pump House, Back-up Generator	245	152	407	2.86	14.2	0.915	1.383	H
21	Single Family Residence	397	156	405	2.88	14.2	0.832	1.151	H
23	Single Family Residence	361	156	399	2.79	13.9	0.843	0.741	H
24	40 foot shipping container	308	154	397	3.11	15.0	0.522	0.714	H
25	40 foot shipping container	328	155	397	2.98	14.5	0.646	0.707	H
26	40 foot shipping container	338	155	397	2.98	14.5	0.646	0.707	H
27	Tribal Business Storage	287	154	396	3.22	15.3	0.425	0.774	H
28	Tribal Business (Convenience Store)	273	154	396	3.22	15.3	0.425	0.774	H

Table 3.6.6. Predicted flooding depth and velocity for 2% annual surge occurrence interval at Maximum Astronomical Tide (Without project condition) (continued)

Inventory	Structure Name / Function	Distance from Shoreline	i	j	elevation (m, mtl)	elevation (ft, mllw)	Flooding depth (m)	Max velocity (m/s)	Flood Risk
29	Tribal Gaming (Regulators) Office	422	158	395	2.63	13.4	0.979	0.578	H
30	Tribal Casino Administrative Office	418	158	392	3.07	14.8	0.534	0.524	H
31	Tribal Casino Administrative Office	435	159	390	3.02	14.7	0.573	0.408	H
32	Tribal Casino and emergency back-up generator	358	157	392	3.08	14.9	0.529	0.551	H
33	Bus Shelter	287	152	388	3.6	16.6	0.301	1.303	H
33a	Casino Septic Field	260	156	394	3	14.6	0.619	0.611	H
34	Single Family Residence	190	151	380	3.77	17.1	0.341	1.261	H
36	Single Family Residence	277	153	380	3.68	16.8	0.348	0.965	H
37	Single Family Residence	366	155	378	3.14	15.1	0.497	0.761	H
38	Single Family Residence	364	154	376	2.92	14.4	0.301	0.420	H
39	Single Family Residence	272	153	375	3.65	16.7	0.386	0.533	H
40	Single Family Residence	185	150	377	3.28	15.5	0.448	1.217	H
42	Single Family Residence	375	155	374	3.08	14.9	0.521	0.542	H
43	Single Family Residence	501	158	374	2.52	13.0	1.083	0.533	H
44	Tribal Business (Fireworks Stand)	114	147	371	2.81	14.0	1.007	1.534	H
45	Mobile Home Residence	310	152	369	3.39	15.9	0.391	0.792	H
47	Single Family Residence	303	153	367	3.4	15.9	0.331	0.780	H
49	Mechanical Repairs Building for Tribal Fishing Boats and Gear	388	155	366	3.11	15.0	0.517	0.735	H
50	Mobile Home Residence	506	157	366	2.73	13.7	0.894	0.679	H
51	Single Family Residence	154	149	368	3.49	16.2	0.300	1.176	H
52	Single Family Residence	151	148	365	3.45	16.1	0.471	1.837	H
54	Mobile Home Residence	306	153	366	3.38	15.9	0.372	0.817	H
55	Mobile Home Residence	306	153	365	3.33	15.7	0.485	0.880	H
60	Single Family Residence	244	149	357	4.05	18.1	0.036	0.243	M
61	Single Family Residence	224	149	360	4.04	18.0	0.345	0.707	H
62	Single Family Residence	289	152	361	3.81	17.3	0.441	0.505	H

Table 3.6.6. Predicted flooding depth and velocity for 2% annual surge occurrence interval at Maximum Astronomical Tide (Without project condition) (continued)

Inventory	Structure Name / Function	Distance from Shoreline	i	j	elevation (m, mtl)	elevation (ft, mllw)	Flooding depth (m)	Max velocity (m/s)	Flood Risk
63	Single Family Residence	381	154	359	4.14	18.4	0.028	0.099	M
64	Single Family Residence	420	154	356	4.14	18.4	-	-	L
65	Single Family Residence	420	153	353	4.01	17.9	0.036	0.099	M
66	Single Family Residence	405	152	352	4.03	18.0	0.077	0.454	M
67	Single Family Residence	315	148	352	4.06	18.1	0.097	0.560	M
69	Tribal Community Center / Tribal Police	153	144	353	3.54	16.4	0.535	1.112	H
71	Tribal Education Center and Library	260	143	346	3.85	17.4	-	-	L
72	Tribal Court	105	139	350	3.35	15.8	0.421	1.358	H
73	Tribal Social and Family Services	163	139	350	3.35	15.8	0.421	1.358	H
74	Emergency Back-up Generator (Flood-proofed)	163	139	350	3.35	15.8	0.421	1.358	H
75	Tribal Cultural Repository Building	276	136	346	3	14.6	0.802	1.492	H
76	Tribal Counseling / Interview Facility	276	136	345	3	14.6	0.758	1.380	H
83	Tribal Wellness Center	463	144	341	3.42	16.0	0.184	0.515	M
83a	Emergency Back-up Generator (Flood-proofed)	460	141	342	3.78	17.2	0.007	0.262	L
84	Duplex Family Residence	710	147	338	3.82	17.3	0.003	0.172	L
85	Duplex Family Residence	720	150	338	3.87	17.5	0.006	0.243	L
86	Tribal Gymnasium and Assembly Hall	707	154	339	3.23	15.4	0.353	0.262	H
87	Gymnasium Storage Building	860	153	336	3.24	15.4	0.351	0.371	H
88	Duplex Family Residence	1032	155	334	2.67	13.5	0.923	0.357	H
89	Duplex Family Residence	1117	156	331	2.7	13.6	0.887	0.396	H
90	Duplex Family Residence	1213	157	329	2.6	13.3	0.991	0.396	H
91	Duplex Family Residence	1301	158	327	2.49	12.9	1.106	0.420	H
92	Tribal Recreational Vehicle Park & Casino Parking	90	148	390	2.69	13.6	1.211	1.794	H
93	Tribal Cemetery	462	149	346	2.9	14.3	0.854	0.465	H
								% Low Risk	**8**
								% Moderate Risk	**12**
								% High Risk	**80**

Table 3.6.7. Predicted flooding depth and velocity for March 3, 1999 1000 UTC storm (With project condition – dune restoration)

Inventory	Structure Name / Function	Distance from Shoreline (feet)	i	j	elevation (m, mtl)	elevation (ft, mllw)	Max Flooding depth (m)	Max velocity (m/s)	Flood Risk
1	Tribal Business (Fireworks Stand)	131	136	477	3.11	15.0	-	-	L
2	Tribal Business (Fireworks Stand)	283	136	485	3.59	16.5	-	-	L
3	Tribal Business (Convenience Store) / Single Family Residence	334	138	484	3.82	17.3	-	-	L
5	Single Family Residence	412	140	485	4.35	19.0	-	-	L
7	Tribal Business (Fireworks Stand)	282	140	484	4.19	18.5	-	-	L
8	Vacant Old Building	343	140	480	3.48	16.2	-	-	L
9	Vacant Old Building	343	140	480	3.48	16.2	-	-	L
10	Single Family Residence	220	140	477	3.43	16.0	-	-	L
11	Single Family Residence	372	144	475	6.48	26.0	-	-	L
12	Mobile Home Residence	220	140	475	3.18	15.2	-	-	L
13	Tribal Business (Fireworks Stand)	169	150	429	3.5	16.3	-	-	L
14	Tribal Business (Fireworks Stand)	177	150	426	3.41	16.0	-	-	L
15	Tribal Business (Fireworks Stand)	183	149	421	3.35	15.8	-	-	L
16	Single Family Residence	225	151	419	3.78	17.2	-	-	L
17	Single Family Residence	220	152	417	3.72	17.0	-	-	L
18	Single Family Residence	220	151	414	3.72	17.0	-	-	L
19	Single Family Residence	220	151	412	3.72	17.0	-	-	L
20	Water Treatment, Pump House, Back-up Generator	245	152	407	2.86	14.2	-	-	L
21	Single Family Residence	397	156	405	2.88	14.2	-	-	L
23	Single Family Residence	361	156	399	2.79	13.9	-	-	L
24	40 foot shipping container	308	154	397	3.11	15.0	-	-	L
25	40 foot shipping container	328	155	397	2.98	14.5	-	-	L
26	40 foot shipping container	338	155	397	2.98	14.5	-	-	L
27	Tribal Business Storage	287	154	396	3.22	15.3	-	-	L
28	Tribal Business (Convenience Store)	273	154	396	3.22	15.3	-	-	L

Table 3.6.7. Predicted flooding depth and velocity for March 3, 1999 1000 UTC storm (With project condition – dune restoration) (continued)

Inventory	Structure Name / Function	Distance from Shoreline	i	j	elevation (m, mtl)	elevation (ft, mllw)	Max Flooding depth (m)	Max velocity (m/s)	Flood Risk
29	Tribal Gaming (Regulators) Office	422	158	395	2.63	13.4	0.056	0.099	M
30	Tribal Casino Administrative Office	418	158	392	3.07	14.8	-	-	L
31	Tribal Casino Administrative Office	435	159	390	3.02	14.7	-	-	L
32	Tribal Casino and emergency back-up generator	358	157	392	3.08	14.9	-	-	L
33	Bus Shelter	287	152	388	3.6	16.6	-	-	L
33a	Casino Septic Field	260	156	394	3	14.6	-	-	L
34	Single Family Residence	190	151	380	3.77	17.1	-	-	L
36	Single Family Residence	277	153	380	3.68	16.8	-	-	L
37	Single Family Residence	366	155	378	3.14	15.1	-	-	L
38	Single Family Residence	364	154	376	2.92	14.4	-	-	L
39	Single Family Residence	272	153	375	3.65	16.7	-	-	L
40	Single Family Residence	185	150	377	3.28	15.5	-	-	L
42	Single Family Residence	375	155	374	3.08	14.9	-	-	L
43	Single Family Residence	501	158	374	2.52	13.0	0.164	-	M
44	Tribal Business (Fireworks Stand)	114	147	371	2.81	14.0	-	-	L
45	Mobile Home Residence	310	152	369	3.39	15.9	-	-	L
47	Single Family Residence	303	153	367	3.4	15.9	-	-	L
49	Mechanical Repairs Building for Tribal Fishing Boats and Gear	388	155	366	3.11	15.0	-	-	L
50	Mobile Home Residence	506	157	366	2.73	13.7	-	-	L
51	Single Family Residence	154	149	368	3.49	16.2	-	-	L
52	Single Family Residence	151	148	365	3.45	16.1	-	-	L
54	Mobile Home Residence	306	153	366	3.38	15.9	-	-	L
55	Mobile Home Residence	306	153	365	3.33	15.7	-	-	L
60	Single Family Residence	244	149	357	4.05	18.1	-	-	L
61	Single Family Residence	224	149	360	4.04	18.0	-	-	L
62	Single Family Residence	289	152	361	3.81	17.3	-	-	L

Table 3.6.7. Predicted flooding depth and velocity for March 3, 1999 1000 UTC storm (With project condition – dune restoration) (continued)

Inventory	Structure Name / Function	Distance from Shoreline	i	j	elevation (m, mtl)	elevation (ft, mllw)	Max Flooding depth (m)	Max velocity (m/s)	Flood Risk
63	Single Family Residence	381	154	359	4.14	18.4	-	-	L
64	Single Family Residence	420	154	356	4.14	18.4	-	-	L
65	Single Family Residence	420	153	353	4.01	17.9	-	-	L
66	Single Family Residence	405	152	352	4.03	18.0	-	-	L
67	Single Family Residence	315	148	352	4.06	18.1	-	-	L
69	Tribal Community Center / Tribal Police	153	144	353	3.54	16.4	-	-	L
71	Tribal Education Center and Library	260	143	346	3.85	17.4	-	-	L
72	Tribal Court	105	139	350	3.35	15.8	-	-	L
73	Tribal Social and Family Services	163	139	350	3.35	15.8	-	-	L
74	Emergency Back-up Generator (Flood-proofed)	163	139	350	3.35	15.8	-	-	L
75	Tribal Cultural Repository Building	276	136	346	3	14.6	-	-	L
76	Tribal Counseling / Interview Facility	276	136	345	3	14.6	-	-	L
83	Tribal Wellness Center	463	144	341	3.42	16.0	-	-	L
83a	Emergency Back-up Generator (Flood-proofed)	460	141	342	3.78	17.2	-	-	L
84	Duplex Family Residence	710	147	338	3.82	17.3	-	-	L
85	Duplex Family Residence	720	150	338	3.87	17.5	-	-	L
86	Tribal Gymnasium and Assembly Hall	707	154	339	3.23	15.4	-	-	L
87	Gymnasium Storage Building	860	153	336	3.24	15.4	-	-	L
88	Duplex Family Residence	1032	155	334	2.67	13.5	0.020	-	M
89	Duplex Family Residence	1117	156	331	2.7	13.6	-	-	L
90	Duplex Family Residence	1213	157	329	2.6	13.3	0.085	-	M
91	Duplex Family Residence	1301	158	327	2.49	12.9	0.198	-	M
92	Tribal Recreational Vehicle Park & Casino Parking	90	148	390	2.69	13.6	-	-	L
93	Tribal Cemetery	462	149	346	2.9	14.3	-	-	L
								% Low Risk	**93**
								% Moderate Risk	**7**
								% High Risk	**-**

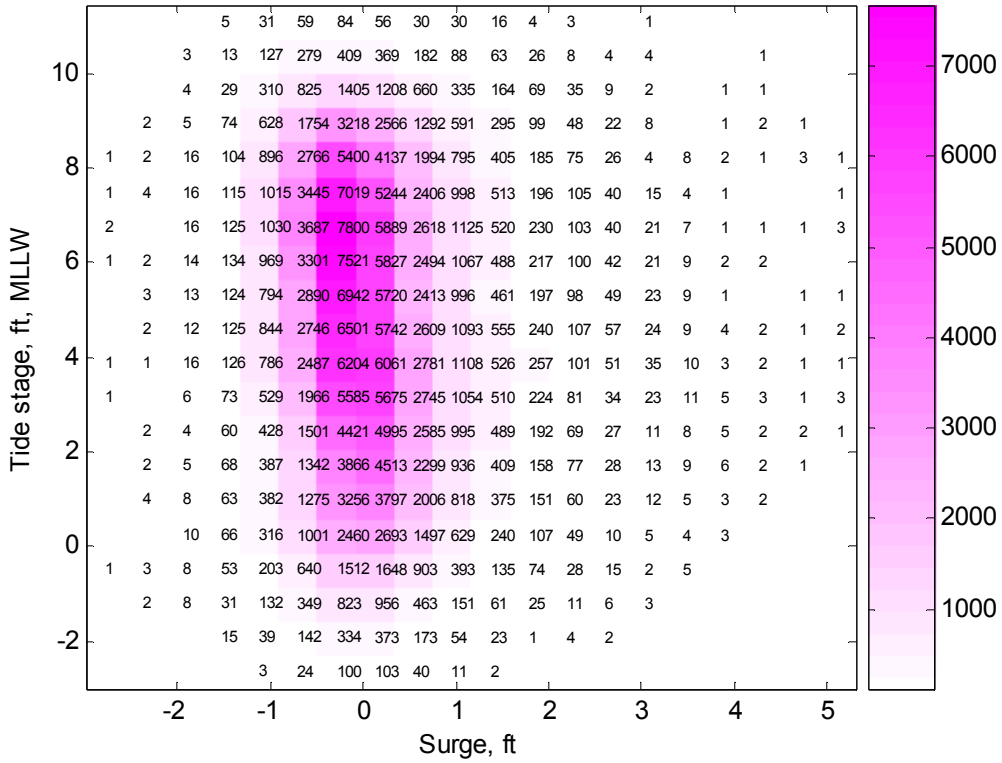

Figure 3.6.1 Toke Point Station #9440910 joint distribution of tide stage (ft, MLLW) and storm surge (ft) from 1980-2007. Numbers indicate number of events over time period

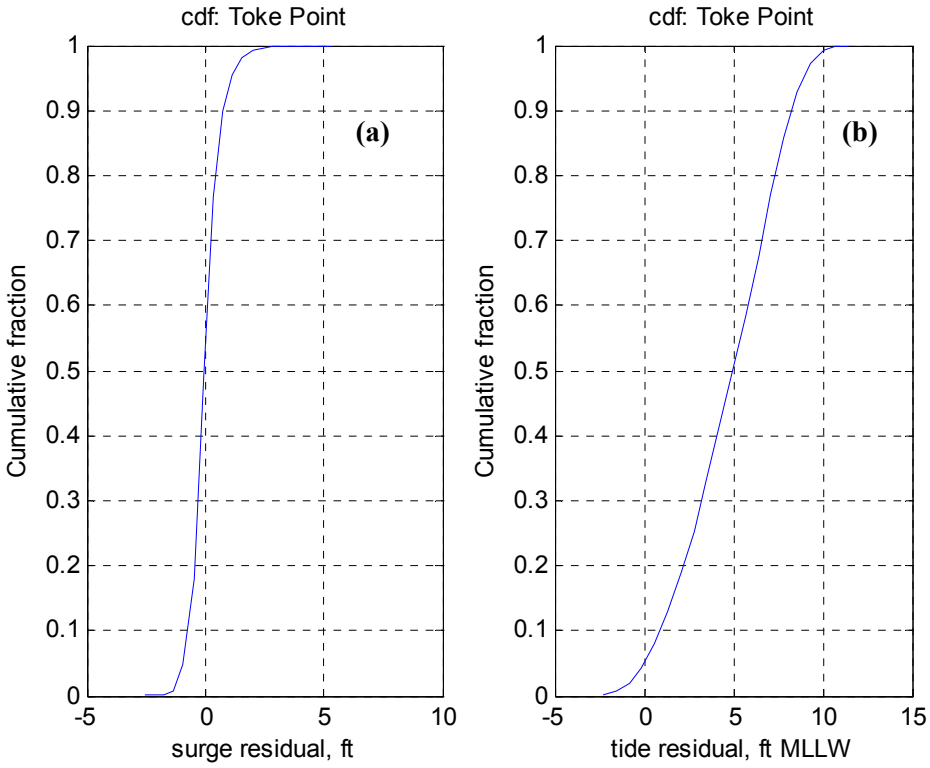

Figure 3.6.2 Toke Point Station #9440910 cumulative density function of (a) surge (b) tide

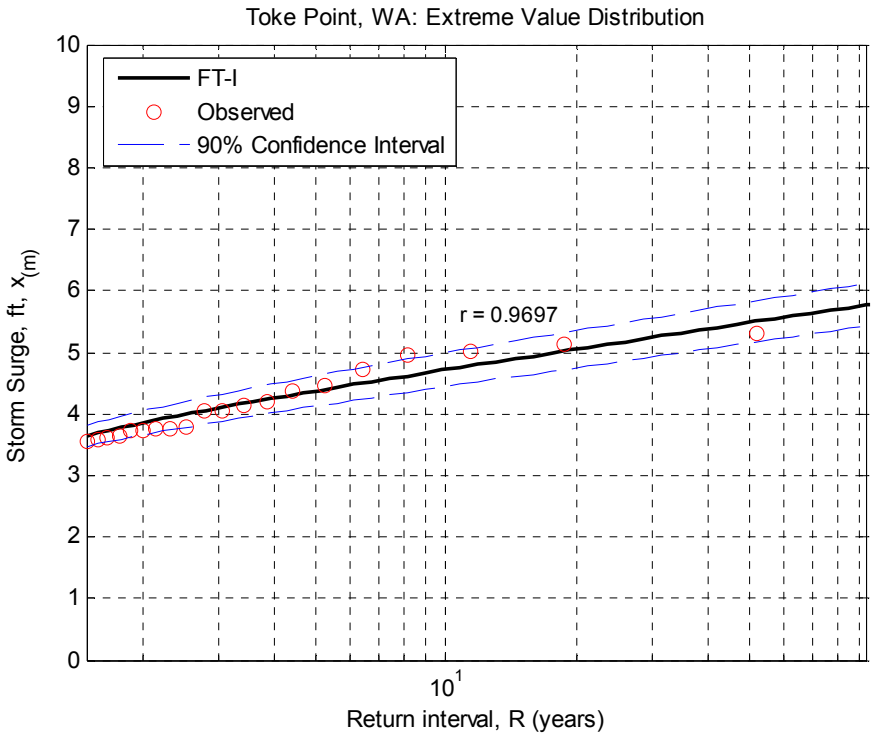

Figure 3.6.3 Storm surge elevation return interval in feet at Toke Point Station #9440910

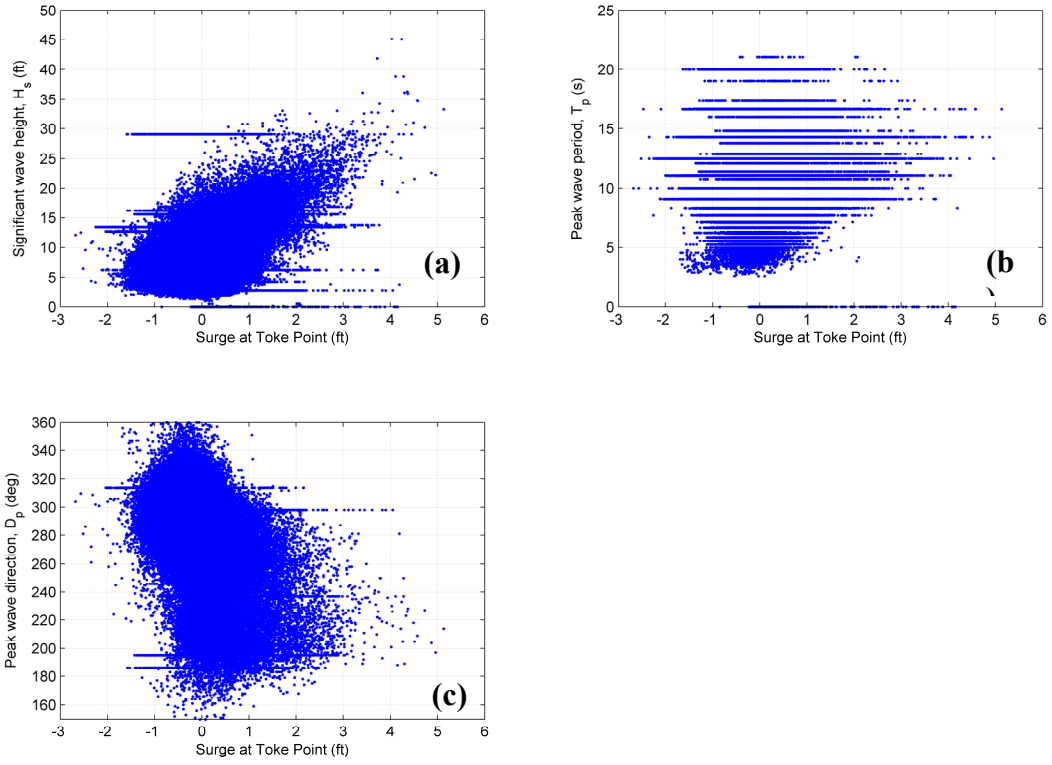

Figure 3.6.4. NDBC 46029 wave parameters versus storm surge computed from Toke Point NOS gage (1984-2007). (a) wave height (b) peak period (c) peak wave direction

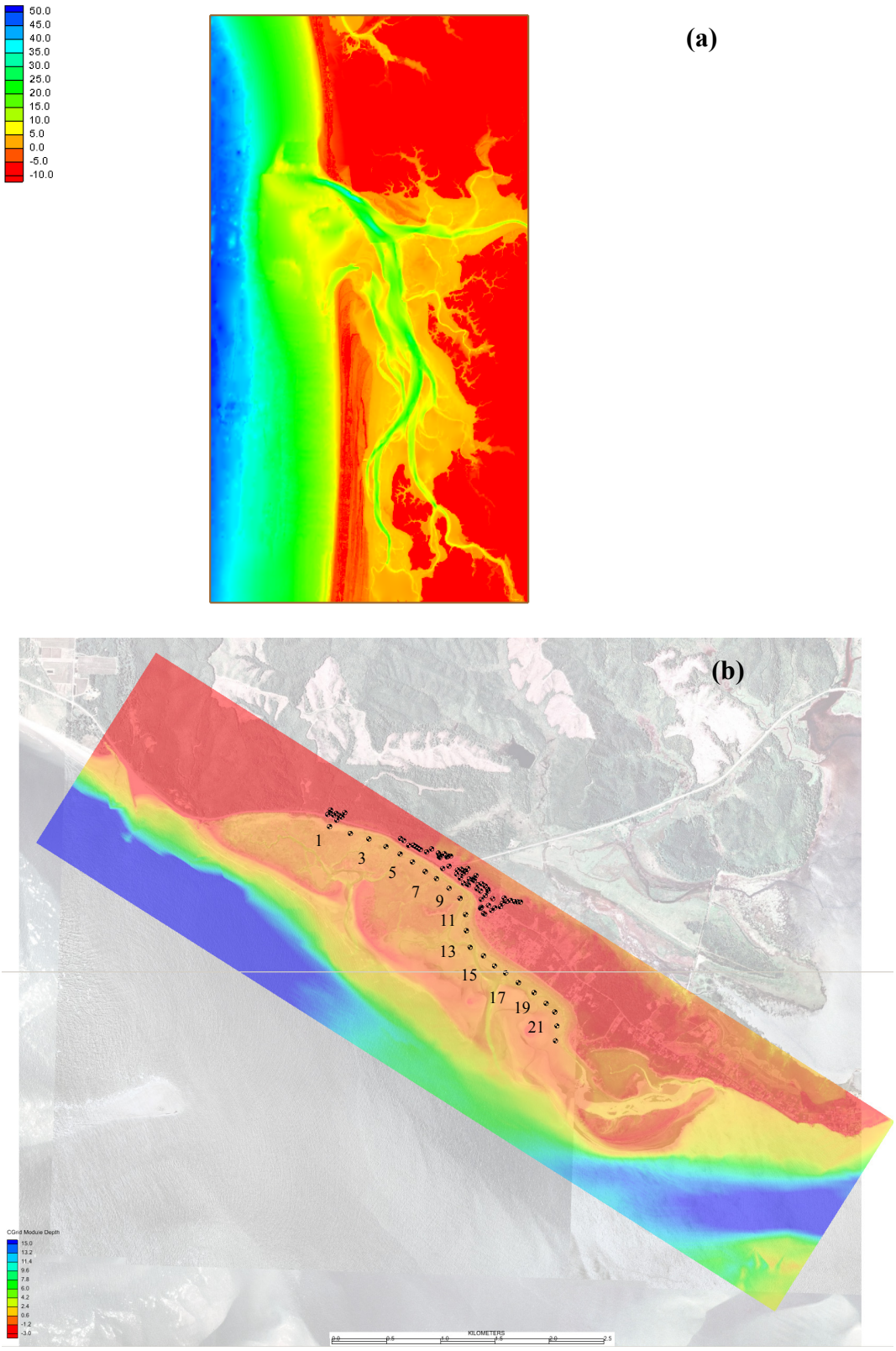

Figure 3.6.5. CMS-WAVE model domain (a) Coarse grid and (b) nested grid with observation cell location (color map represents water depth in m MTL)

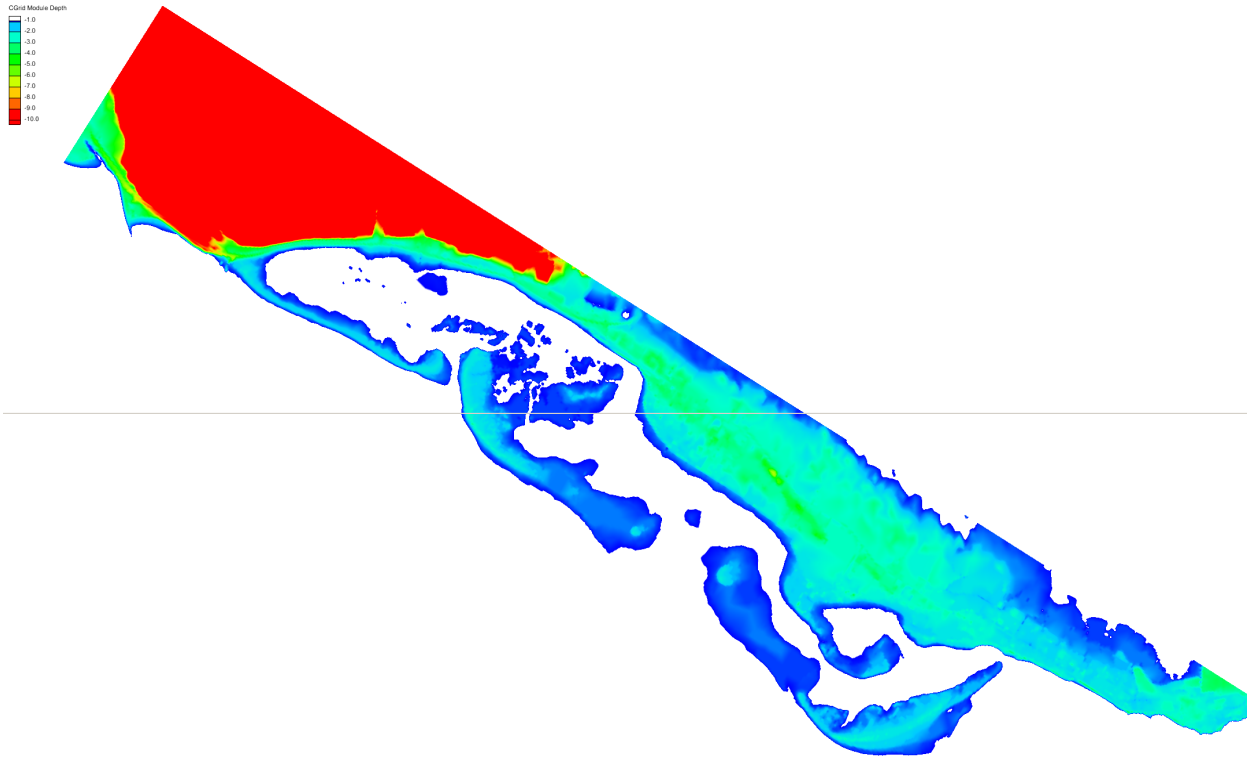

Figure 3.6.6. Elevations above mean high water in meters (note significant dune height reduction near eastern breach since 2002)

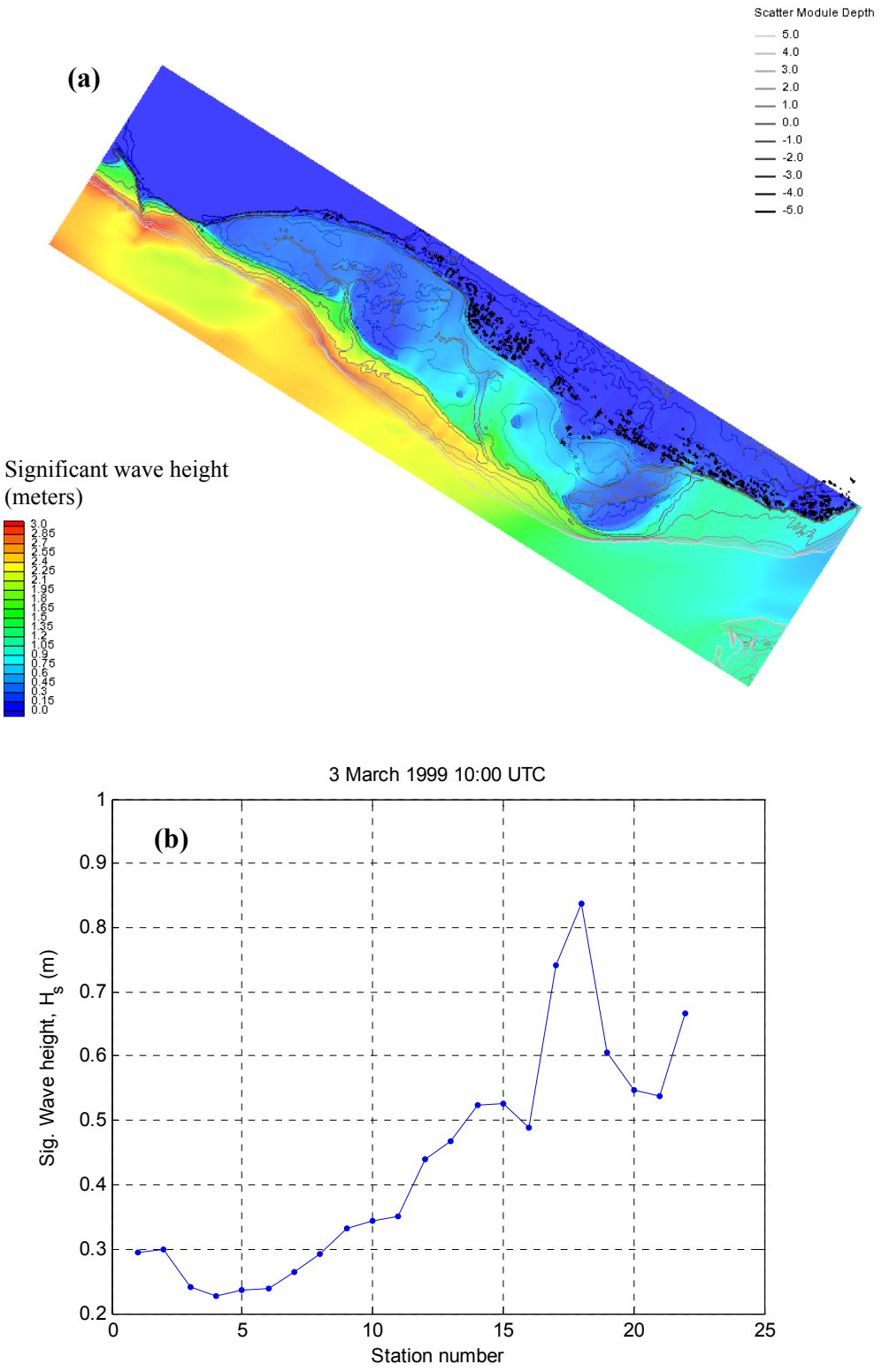

Figure 3.6.7. Predicted wave height in meters for 3 Mar 1999 at 1000 UTC storm (2008 dune condition survey). (a) Wave height contour plot (b) wave height at observation cells

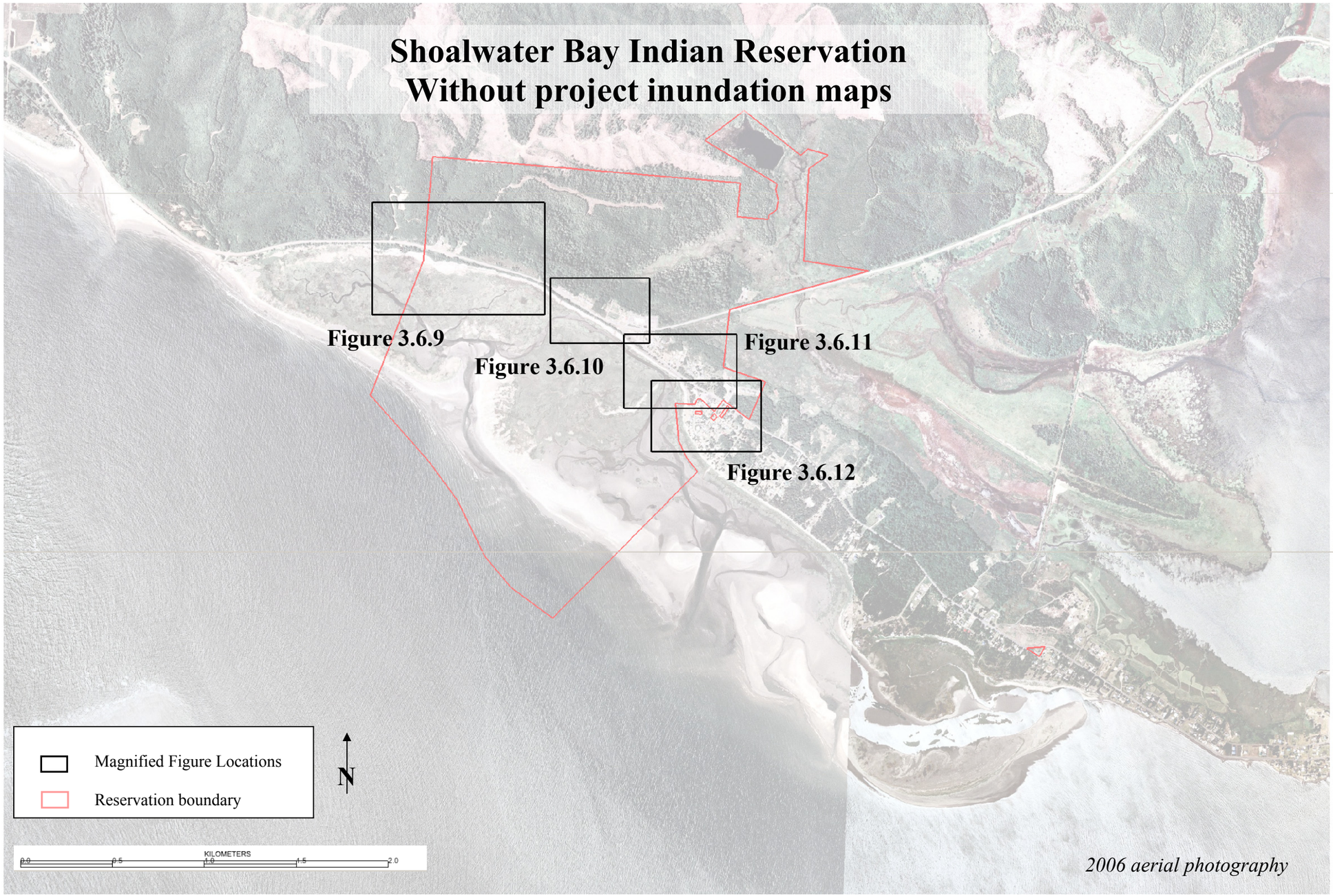

Figure 3.6.8 Shoalwater Reservation and Locations of Detailed Inundation Maps

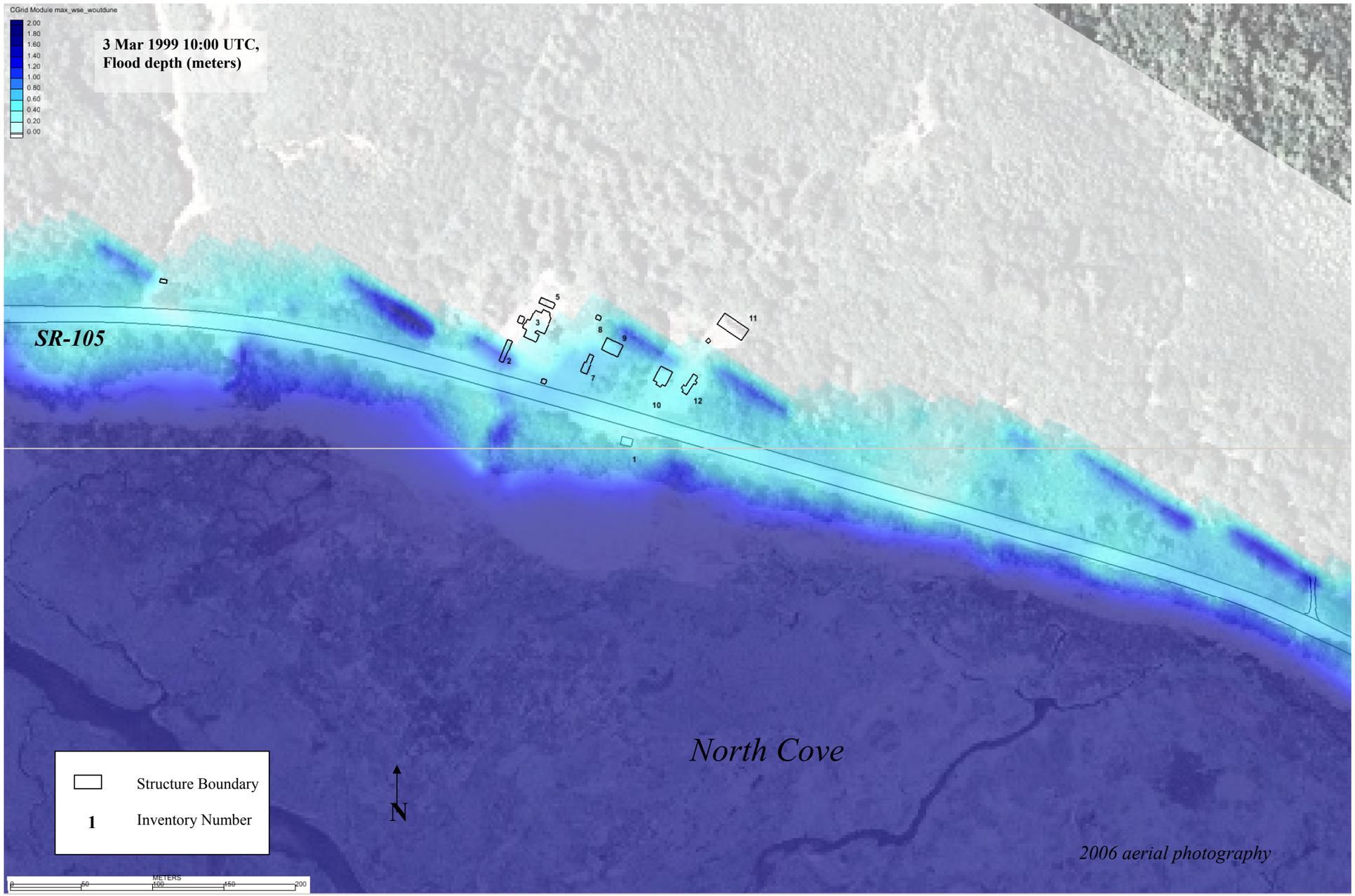

Figure 3.6.9 Shoalwater Reservation Inundation (Map #1) for March 3, 1999 1000 UTC. [Without Project Condition − Inundation (flood depth) in meters]

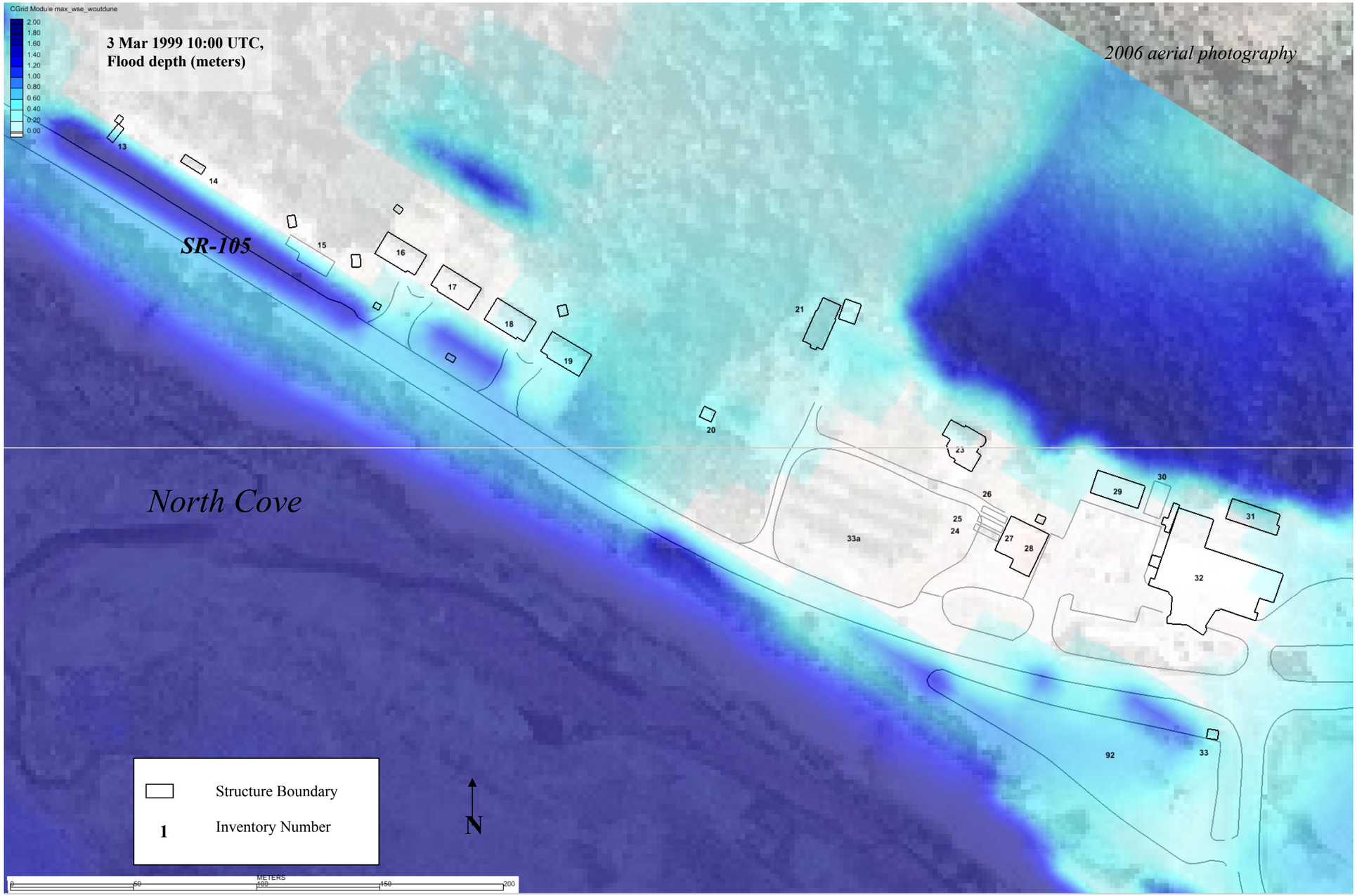

Figure 3.6.10 Shoalwater Reservation Inundation (Map #2) for March 3, 1999 1000 UTC. [Without Project Condition − Inundation (flood depth) in meters]

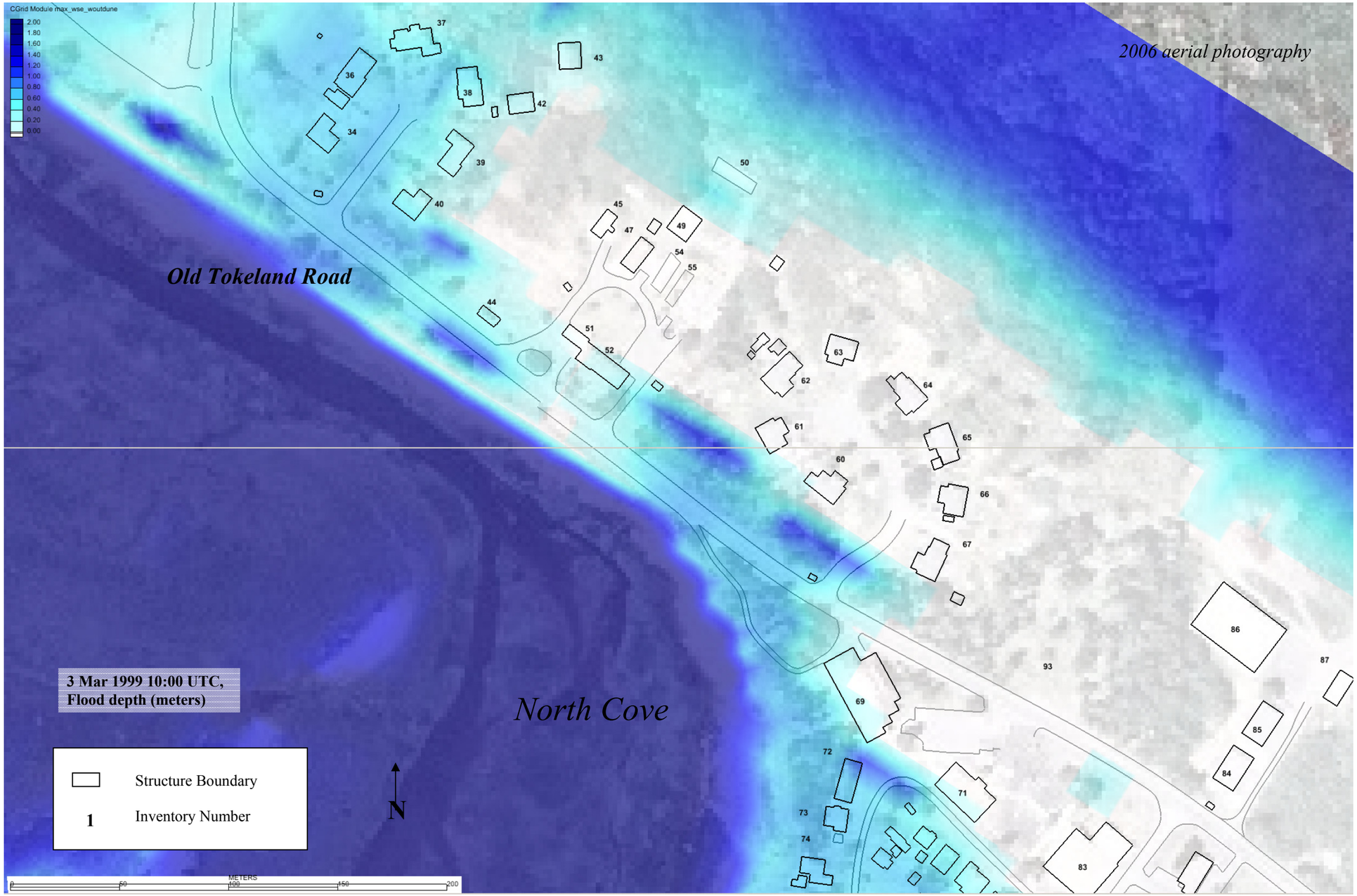

Figure 3.6.11 Shoalwater Reservation Inundation (Map #3) for March 3, 1999 1000 UTC. [Without Project Condition − Inundation (flood depth) in meters]

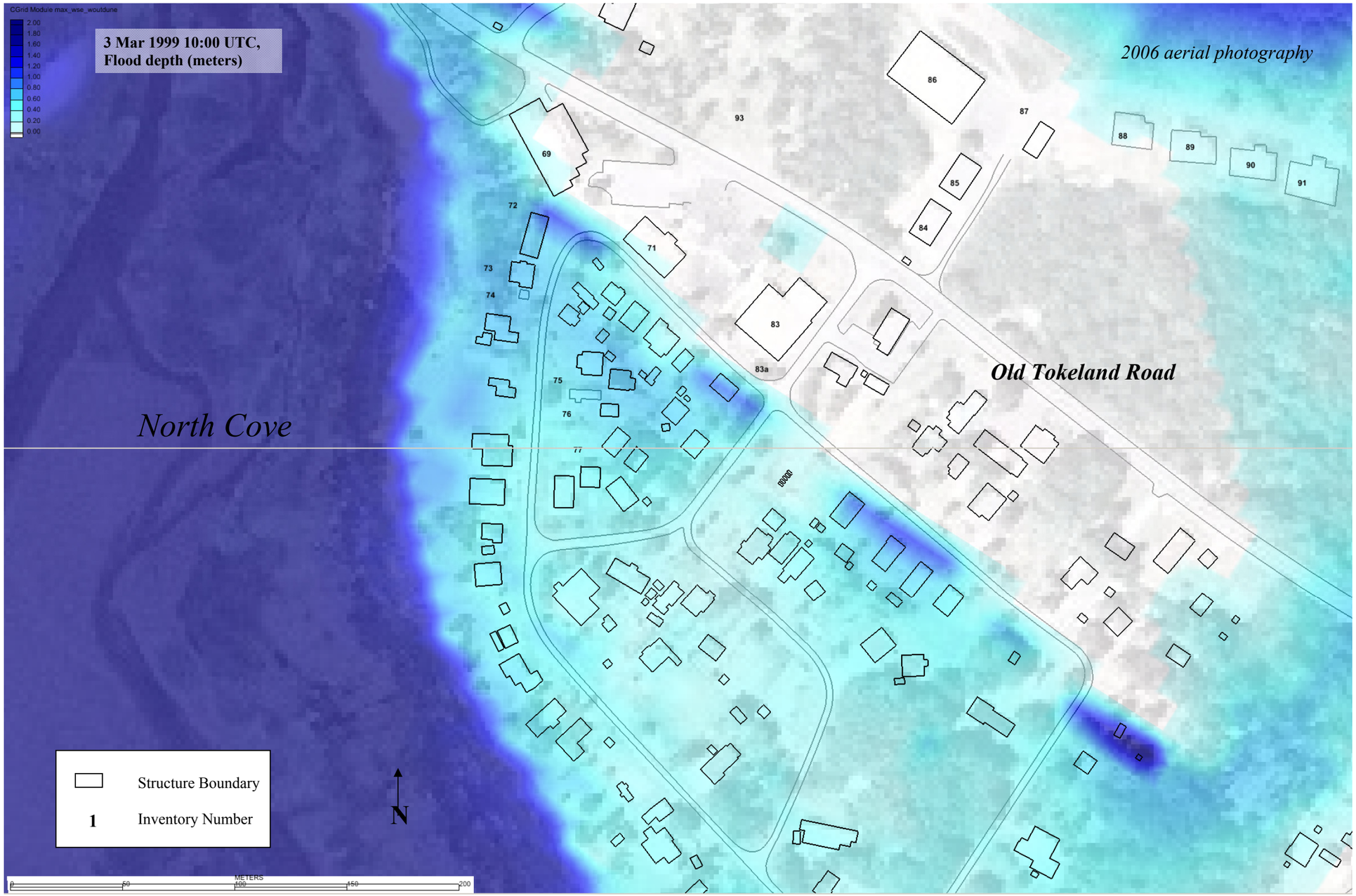

Figure 3.6.12 Shoalwater Reservation Inundation (Map #4) for March 3, 1999 1000 UTC. [Without Project Condition − Inundation (flood depth) in meters]

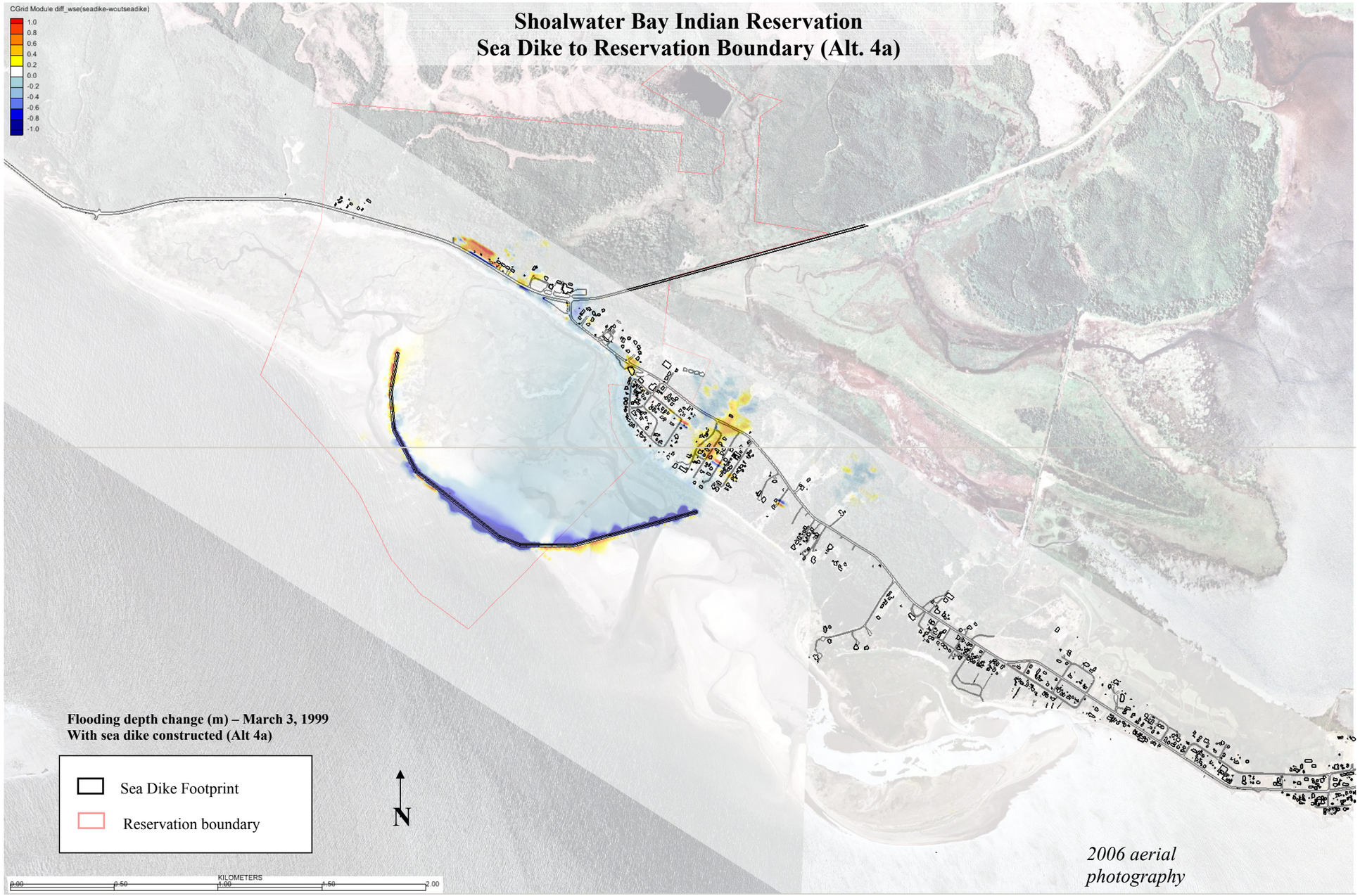

Figure 3.6.13. Flooding depth change (in meters) after sea dike to Reservation boundary is constructed (Alternative 4a). March 3, 1999 storm simulation

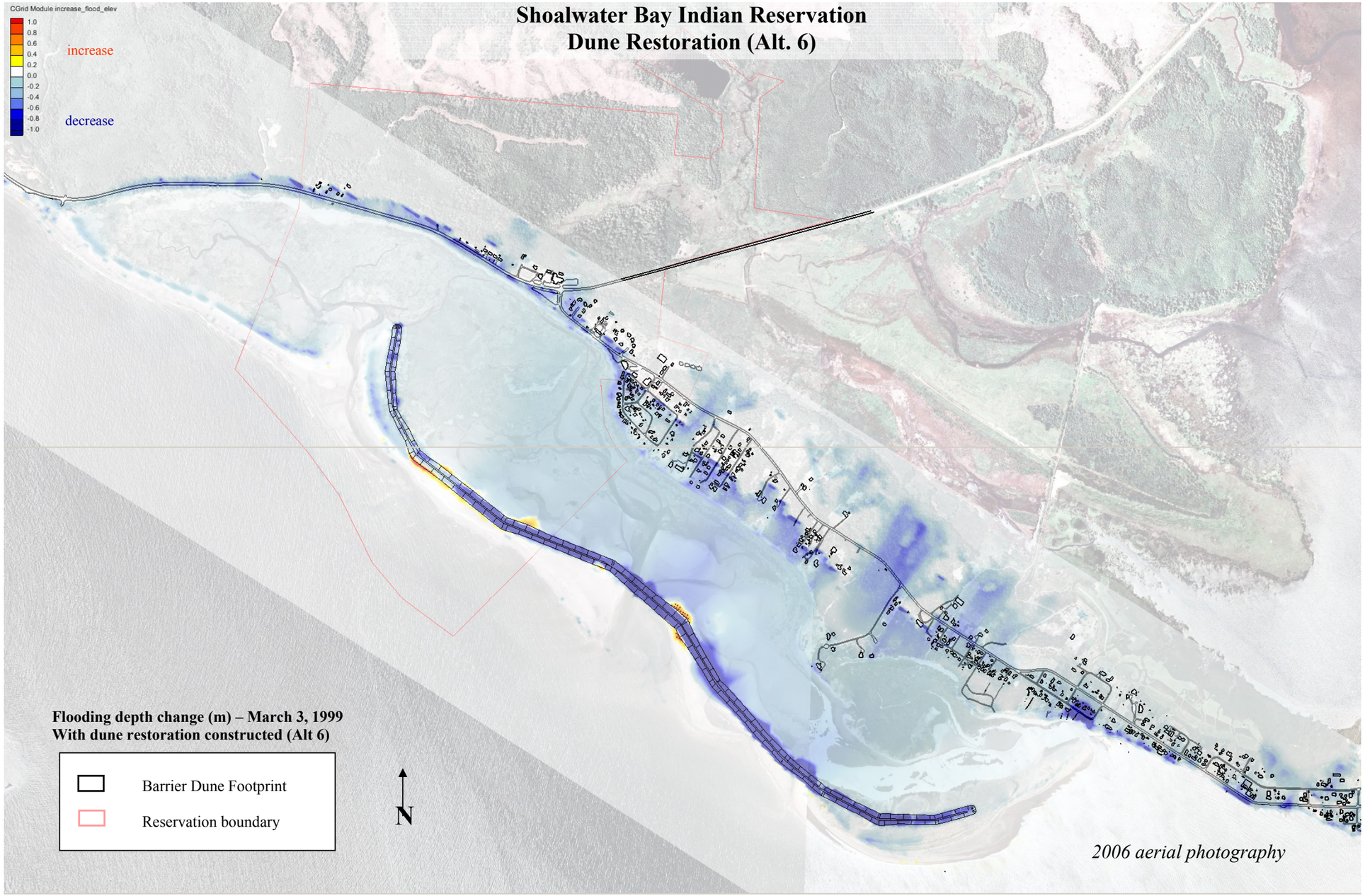

Figure 3.6.14. Flooding depth change (in meters) after dune restoration (Alternative 6). March 3, 1999 storm simulation

4.0 Alternatives Analysis [15]

4.1 No Action

The "No Action" alternative assumes that no measures will be undertaken to address the ongoing erosion of the barrier dunes located on Graveyard Spit fronting the Tokeland Peninsula. This alternative also assumes that, although the northern migration of the North Willapa Channel has halted seaward of the Shoalwater Reservation, tidal currents and – to a greater extent – storm waves associated with extreme water levels will continue to erode the barrier dunes which have afforded protection to the Shoalwater Reservation and Tokeland Peninsula (see Figure 4.1). Bathymetric surveys show that the North Willapa Channel west of North Cove has widened and deepened. The cross-sectional area has increased, enhancing the conveyance of flow through the channel. Assuming a constant volume of water flowing through the channel, increasing the cross-sectional area of the channel results in weakening the current and thereby reducing current-induced erosion. From the mid-1980's to the present, the slope of the north bank of the channel has been constant and has remained in a fixed position, indicating that the channel encountered hard strata that are resistant to erosion. Material that is eroded from the barrier dunes will continue to be carried by wave overtopping into the inter-tidal area behind the dunes, eventually filling in what remains of North Cove tide flat and intertidal habitat. Lowering of the dunes will also expose the Shoalwater Reservation/ Tokeland Peninsula shoreline to increasing levels of flooding due to wave overtopping during periods of extreme water level storms.

The level of wave protection currently provided by the eroded barrier dune was evaluated (see paragraphs 3.4 and 3.6). Tide records are available from a NOAA tide station located at nearby Toke Point. Figure 4.2 presents a listing to the 12 highest tides measured between 1973 and 2007. Figure 4.3 is an exceedance frequency curve for extreme water levels recorded during this period of time. Since the extreme maximum tides are always associated with low atmospheric pressure events, storm extreme water levels are almost always accompanied by storm wave conditions. A numerical model was used to evaluate wave heights along the Shoalwater Reservation/Tokeland Peninsula shoreline for the "with" and "without" dune conditions for a storm and extreme +13.61 feet mean lower low water (MLLW) tide that occurred on March 3, 1999. The model results indicate that the March 1999 storm probably generated waves at the shoreline that were approximately 2 feet high, (0.6 meters).

The numerical model was also used to simulate the storms assuming that the dune was eroded to the elevation of the surrounding land (+8 feet MLLW). Model results indicate that, without the protection of the dune, wave heights at the shoreline would more than double to as much as 3.3 feet. The March 1999 storm caused severe flooding and resulted in the initiation of an "emergency flood protection planning process." As a consequence, in March 2001, the Corps of Engineers constructed a riprap flood berm along 1,700 feet of the Shoalwater Reservation shoreline. While this segment of flood berm provides protection from direct wave attack, the structure fails to address flooding caused by overtopping of the adjacent shoreline areas. Portions of the shoreline that are not protected by the 1,700 foot-long revetment will continue to be overtopped, causing flooding of all the low lying backshore areas of the Shoalwater Reservation with elevations lower than approximately +15 feet MLLW. Figure 4.4 is a topographic survey that illustrates the extent of flooding that can be expected during storm events during which the

[15] Written by Eric Nelson, Steven Babcock, and David Michalsen, U.S. Army Corps of Engineers, Seattle District

tide elevation exceeds approximately +13 feet MLLW. High tides exceeding about +13 feet occurred 12 times in the last 34 years, and tides at or above +13 feet have occurred five times in the last seven years. Even if the frequency of high tides remains constant, erosion and lowering of the barrier dunes due to erosion will continue. The limited wave protection currently afforded by the eroded barrier dune will continue to decrease, and flooding of the Shoalwater Reservation and adjoining lands, with associated shoreline erosion, will occur at increasingly frequent intervals.

4.2 Hydraulic Modification of the Entrance to Willapa Bay

For many years, modifying the tidal ebb flow in Willapa Bay has been proposed as a way to "turn back the clock" and arrest, if not reverse, the northward migration of the main (northernmost) Willapa channel. In 1998, the Washington Department of Transportation (WSDOT) constructed the SR-105 Emergency Stabilization Project. The purpose of the project was to "Plug…the North Channel in order to slow or stop the northerly channel migration…." (WSDOT, *Environmental Assessment, SR 105 Emergency Stabilization Project*, April 1997). While the effect of the SR-105 project on the ebb flow of the northernmost Willapa channel appears to be confined to the immediate vicinity of the structure, (see paragraph 3.4.3), the idea of redirecting the ebb flow of the Willapa entrance was an appealing concept for reducing the threat posed by the encroaching channel.

Four representative flow diversion structures, or training dikes were modeled at the Corps' Coastal and Hydraulics Laboratory, using the ADCIRC hydrodynamic model (see Figure 4.5). The dimensions and orientation of the structures were adjusted until an obvious change in the flow regime of the channel occurred. Whether or not the change was potentially "good" or "bad" was not evaluated. Model results are summarized in paragraph 3.1.5. The quantity of large stone that would be required to construct each of the structures was then computed. The results of the model investigation found that extremely massive structures would be required to make a significant change in the flow regime of the Willapa channel. Estimated initial construction volumes for individual structures varied from 640,000 to 1,800,000 tons. Assuming an "in place" unit cost of $50/ton, the initial construction costs probably would range from $32 million and $90 million. The drawback of the high construction cost was compounded by high maintenance costs and the risk for unanticipated, and potentially adverse, consequences to the hydrodynamics and ecology of Willapa Bay.

Flow diversion structures were eliminated from further consideration because they do not appear to be either cost effective or environmentally acceptable, or verifiable as to the beneficial effect in reducing the flood and coastal storm damage threat to the Shoalwater Bay Indian Reservation. In addition, the analysis of channel migration (summarized in paragraph 2.3) found that the northward migration of the Willapa channel has stopped in the vicinity of the proposed project. Since the mid-1980s, the slope of the north bank of the main channel has been constant and has remained in a fixed position. This strongly indicates that the channel encountered hard strata that are resistant to erosion. Constructing a large and costly coastal structure in an attempt to initiate a change that may already be underway naturally does not appear to be in the best interests of the Shoalwater Bay Indian Tribe, the State of Washington, or the public in general.

4.3 Protective Structures

Although the northernmost Willapa channel has been constant and has remained in a fixed position since the mid 1980s seaward of the Shoalwater Reservation, combined extreme water levels and storm

waves will continue to erode the barrier dune system that extends southward on Graveyard Spit . Historically, this dune system has protected the Shoalwater Reservation and the Tokeland Peninsula shoreline from storm waves during periods of extreme water levels. Erosion and lowering of the barrier dune has exposed the Shoalwater Reservation and adjoining shoreline to increasing levels of flooding due to wave run-up and overtopping. The protective structures described below are designed to address the wave induced flooding that takes place during extreme water level storm events.

4.3.1 Sea Dike

The sea dike is a rock structure that is intended to replace the wave protection that was once afforded by the now deteriorated dune system. The structure has a top elevation of +20 feet MLLW, a top width of 14 feet, and a side slope of 1V on 2H (see Figures 4.6(a) and (b)). Two sea dike footprints are considered. The first alignment extends 12,500 ft along the eroded Graveyard Spit footprint. The second alignment extends 7,000 ft of Graveyard Spit immediately offshore of the Shoalwater Reservation boundary and then ties in toward the shoreline at the eastern boundary of the Reservation.

The 12,500 foot dike requires approximately 213,000 tons of underlayer and quarry stone, and 203,000 tons of armor stone, and is constructed along the crest of the deteriorated dune. Approximately 200,000 CY of sand is excavated to make way for the dike stone. Similarly the 7,000 foot dike requires approximately 120,000 tons of underlayer and quarry stone, and 114,000 tons of armor stone, and is constructed along the crest of the deteriorated dune. Approximately 112,000 CY of sand is excavated to make way for the dike stone. The excavated sand is re-graded over the dike, and planted with native dune grass. While the sea dike itself is designed to resist erosion by waves and currents, the sand covering the rock on the seaward side of the dike will erode over time, and will thus require periodic replacement.

The dike stone is brought to the construction site by truck. Access to the site requires construction of a 1-mile-long haul road from SR 105. The haul road will be removed at the completion of construction. The maintenance requirement for the sand covering the seaward face of the dike is assumed to be 100,000 cy at two-year-intervals. Replacement of 50 percent of the dike armor stone will be required at 25-year intervals.

The sea dike alternative assumes that the northward migration of the Willapa channel has halted seaward of the Shoalwater Reservation. Since the dike is not intended to address the channel migration, further channel encroachment could undermine and destroy the dike. The fact that the dike alignment is fixed at the time of construction, and can't easily accommodate even a minor change in the channel location, is a major disadvantage of this alternative. The sea dike is neither environmentally acceptable, nor supported by the Shoalwater Bay Indian Tribe.

4.3.2 Dune Restoration

As described in previous paragraphs, erosion and lowering of the barrier dune that extends southward on Graveyard Spit is exposing the Shoalwater Bay Indian Reservation and the Tokeland peninsula shoreline to increased flooding from storm waves during periods of extreme water levels. The dune restoration alternative is intended to rebuild and maintain the eroded dune system with sand dredged from the adjacent Willapa Bay entrance and channel. The restored dune is 12,500-feet-long, with a top elevation of +25 feet MLLW, a top width of 20 feet, and a side slope of 1V on 5H (see Figure 4.10). Like the sea dike, the dune is constructed along the crest of the existing eroded dune. The initial dune restoration requires approximately 600,000 CY of sand dredged from the entrance to Willapa Bay. To reduce wind erosion, portions of the dredged sand will be graded and planted with native dune grass.

The crest elevation is designed to prevent wave overtopping. This height is determined by factoring in all components contributing to extreme water level (e.g. astronomical tide, storm surge, wave setup, and wave run-up). The total water level is the sum of the still water level (tide, storm surge, setup) and dynamic water level (wave run-up). Figure 4.3 indicates an elevation of +14.6 ft MLLW corresponds to the 1% annual chance of still water level at the project. Wave run-up on a slope is computed using the Automated Coastal Engineering System (ACES v 1.07f) computer program and compared to recent methods given by Hughes (2004). Using the maximum wave height (i.e. 2 m or 6.5 ft) estimated along the barrier spit in Section 3.2.5, the wave run-up on the restored barrier dune slope is computed. A common parameter used is the run-up value exceeded by 2% of the run-ups (i.e. 2 waves out of 100 will overtop the dune). The ACES program computes this run-up to be 5.5 ft and the Hughes (2004) equation computes this run-up to be 7 ft. When run-up is included, an elevation of +21.6 ft MLLW corresponds to the 1% annual chance of total water level at the project. A barrier dune crest elevation of +25 ft MLLW will eliminate the threat of water levels from overtopping the barrier dune and the risk of flooding and erosion on the Shoalwater Reservation shoreline.

Over the last ten years, the erosion of the barrier dune has profoundly affected the channel that flows into North Cove. Figure 4.8 shows that, in 1994, the dune formed a continuous barrier separating North Cove from Willapa Bay and a single, well-defined channel entered the southern end of the cove. The tidal flow in this channel was strong enough to scour away sand that was being carried southward on the ocean side of the spit. In 1995, erosion of the dune resulted in the formation of a breach (see Figure 2.2.20). This additional entrance and exit for tidal flows, combined with the reduction in the cove volume due to infilling, resulted in a diminished flow through the channel. The flow through the North Cove channel was no longer strong enough to resist the southward encroachment of the spit, and the channel began migrating to the southeast. In 2003, a second breach developed in the spit decreasing the channel flow even further (see Figure 2.2.25). The 2004 aerial photograph (Figure 4.9) clearly shows that the migrating channel is now eroding the southern Tokeland Peninsula shoreline. Rehabilitation of the barrier dune will close the breaches, which will result in an increase in the flow through the channel.

Although the migration of the Willapa channel has halted, other littoral process will not be altered. Erosion by storm waves and currents will continue, and the restored barrier dune will require periodic nourishment on a recurring basis. The cost of mobilizing a large dredge to the project site is a major consideration in the volume of sand placed and resulting crest elevation of the restored dune. The lowest life-cycle cost is obtained by maximizing the periodic nourishment interval. For this reason, the initial dune dimensions maximize the volume of sand that is placed within the available plan area of the existing spit. A dune crest elevation of +25 feet MLLW can easily be achieved at this location, and approximates the elevation of the natural dune over the past several decades.

The reliability of the barrier dune against erosion is tested for various historic storm events using the SBEACH numerical model. This is discussed in Section 3.5. It was determined that the specified dune cross section will be reliable during the 1% annual (100 year) storm event, but will require periodic nourishment to provide this level of protection throughout the project life. Periodic nourishment requirements for the dune restoration were estimated by using topographic surveys of the dune to compute the sand loss that that occurred between 2000 and 2008. Based on observed erosion rates, the annual loss of sand from the dune, (above +6 feet MLLW), is estimated to be 50,000 cy per year.

For both initial construction and periodic nourishment, the sand will be pumped from a borrow site by a large pipeline dredge. A potential borrow site is located approximately 5,000 feet from the project, on the north side of the northern Willapa Bay channel. A similar construction process was successfully carried out by the Washington State Department of Transportation in 1998 for the SR-105 Emergency Stabilization Project. For that project, some 350,000 cy of dredged sand was pumped approximately 8,000 feet. This successful placement of sand by WSDOT immediately to the west of the project site eliminates any uncertainly as to the constructability of this alternative plan.

Under this alternative, the restored dune will provide the sole protection to the Shoalwater Reservation from storm waves. Therefore, maintaining the dune to its design dimensions will be critical, and the dune can not be allowed to deteriorate to a point that waves could overtop the structure. For this reason, the periodic nourishment requirement is assumed to be 250,000 cy at five-year-intervals (based on the observed annual erosion rate of 50,000 cy per year).

Like the sea dike, the dune restoration alternative assumes that the northward migration of the Willapa channel has halted seaward of the Shoalwater Reservation. The dune is not intended to address any further channel migration or even erosion (or accretion) of the lower beach, below +6 feet MLLW. The dune alignment on the spit may be readjusted slightly to the most effective location each time periodic nourishment is required.

4.3.3 Dune Restoration with Flood Berm Extension

The dune restoration with flood berm extension alternative combines restoration of the deteriorated barrier dune system with an extension of a shoreline flood berm that was constructed in 2001 and 2007 to protect a small portion of the Shoalwater Reservation. The dune restoration is identical in design to the dune restoration alternative described above in Paragraph 4.3.2. In addition, the existing flood berm is extended northward 4,000 feet and southward 2,770 feet (see Figure 4.7). When the 4,000-foot-long northward flood berm extension and 2,770-foot-long southward flood berm extension are combined with the existing flood berm, a continuous protective structure with a total length of 8,470 feet is formed. Figures 4.11 through 4.14 show the location of the flood berm in relation to existing features.

The purpose of the flood berm is to provide "backup" protection from wave overtopping during periods of high tide storms and thus allow flexibility in the periodic nourishment schedule for the dune restoration. The flood berm is intentionally porous; allowing water to filter through after the wave energy is dissipated. It is not intended – nor required – to be a levee that keeps elevated water levels from flooding interior lowlands. The flood berm will not be subjected to continuous or even frequent wave attack. Wave attack, when it occurs, will be over a 3-4 hour period, perhaps once or twice annually, and only if the barrier dune is sufficiently eroded prior to periodic nourishment. In the unlikely event that a true shore protection structure is required at some point in the future, the flood berm gradation will serve as the foundation for the two armor stone layer revetment described in Paragraph 4.3.4 below.

The flood berm extension utilizes a design that is similar to the existing flood berm. The flood berm extension is constructed of graded riprap with a top elevation of +17 feet MLLW, as verified through storm wave penetration simulations conducted for this study by CHL. The flood berm will have a top width of 16 feet, and a side slope of 1V on 1.5H. The flood berm design assumes that the barrier dune is in a deteriorated condition (and thus at such an eroded state that periodic nourishment is required) that was used in the "with dune" storm wave simulations by CHL. The riprap gradation was determined using the Corps' Automated Coastal Engineering System (ACES v 1.07f). Seattle District's extensive field experience with similar coastal structures along the Washington Coast was also applied to design of the flood berm. Assuming a +13.61 foot tide, a structure toe elevation of +8 feet MLLW (5.6 foot toe depth), and 2 foot (0.6 meter) incident wave height, the ACES "Rubble Mound Revetment Design" application computed that the rock should be graded with a minimum weight of 19.87 pounds, a maximum weight of 635.74 pounds, and 50% by weight greater than 158.94 pounds. The specified gradation will be "rounded" to a minimum weight of 10 pounds, a maximum weight of 500 pounds, and 50% by weight less than 200 pounds. The riprap "layer thickness" computed by ACES is 1.98 feet, but for reasons of constructability, and to minimize the potential for the piping of fines, the layer thickness was increased to 3 feet. The underlying filter (core material) gradation computed by ACES has a minimum weight of 0.05 pounds, a maximum weight of 1.67 pounds, with 50% by weight greater than 0.29 pounds. Based on past

experience by Seattle District, and to maximize quarry yield, this gradation was revised to a minimum weight of 0.1 pounds, a maximum weight of 10 pounds, with 50% by weight less than 1 pound. The ACES "Wave Run-up and Overtopping" application was used to compute the wave run-up to be 3.7 feet. Combined with a +13.61 foot tide, the maximum run-up elevation is calculated +17.31 feet MLLW. A design elevation of +17 feet MLLW was selected. Since the flood berm itself will be used for construction access, the berm top width is 16 feet. All construction materials are brought to the construction site by truck, and access to the site is along the structure itself.

The south flood berm extension requires approximately 25,000 tons of graded riprap, 15,000 tons of core material, and approximately 10,000 cy of excavation to make way for the riprap. The excavated material is re-graded over the flood berm and planted with native vegetation as an environmental and esthetic feature. The north flood berm extension requires approximately 35,000 tons of graded riprap, 14,000 tons of core material, and approximately 15,000 cy of excavation. All construction materials for the flood berm extension are brought to the construction site by truck, and access to the site is along the structure itself.

The restored barrier dune will provide primary protection from storm waves, but the presence of the flood berm allows considerable erosion of the barrier dune before periodic nourishment is required. The maintenance requirements for this alternative are assumed to be 500,000 cy at 10-year-intervals for dune maintenance, replacement of 25 percent of the flood berm riprap at 25-year intervals, and replacement of 5,000 cy of the top soil covering the seaward face of the flood berm at 25-year-intervals. However, the "backup" protection provided by the flood berm provides flexibility in the maintenance schedule for the dune restoration, allowing the maintenance interval to increase to at least 10 years verses every five years if the dune restoration-only alternative were implemented. This flexibility alleviates some of the concerns regarding availability and timing of funding for dune maintenance, and scheduling of relatively scarce dredging equipment, and the short four-month-long dredging "window" within which dredging equipment can safely operate in the severe wave climate at Willapa Bay.

4.3.4 Revetment

The revetment alternative consists of constructing an 8,470-foot-long rock structure to provide protection from shoreline erosion and coastal flooding due to storm wave overtopping during periods of extreme high tides. The revetment is designed for wave conditions that would result if the barrier dune erodes and lowers to the elevation of the surrounding inter-tidal area (approximately +8 feet MLLW) (see paragraph 4.1). The structure has a top elevation of +21feet MLLW, a top width of 8 feet, and a side slope of 1V on 1.5H (see Figure 4.15). The top elevation of the revetment is a function of the storm wave simulations performed by CHL. The barrier dune on Graveyard Spit has very nearly eroded to the point at which it does not modulate storm waves. In the absence of any other measure, the revetment will prevent further erosion of the shoreline, dissipate wave energy, and prevent storm waves from overtopping the shoreline and flooding tribal uplands.

Construction of the revetment requires placing approximately 55,000 tons of graded riprap and 64,000 tons of armor stone along the existing shoreline. The revetment is a porous structure designed to dissipate wave energy and to prevent waves from overtopping the structure and flooding tribal uplands. The graded riprap is the underlayer/filter material for the overlaying armor stone. The graded riprap and armor stone is brought to the construction site by truck and access to the site is along the structure itself. Approximately 24,000 cy of sand is excavated to make way for the structure. The excavated sand, along with approximately 40,000 cy of imported sand, is re-graded to create a shoreline dune over the revetment. The graded sand is then planted with native vegetation.

While the revetment itself is designed to resist erosion by storm waves, some of the sand covering the rock on the seaward side of the revetment probably will be eroded during extreme tide storm events. Maintenance requirements for the revetment are assumed to be replacement of 25,000 cy of sand covering the seaward face of the revetment every 10 years, and replacement of 25 percent of the revetment armor stone at 25-year intervals. As for all the protective structures, the revetment alternative assumes that the northward migration of the Willapa channel has halted seaward of the Shoalwater Reservation.

The revetment alternative abandons any attempt to preserve the existing barrier dune structure and does not address the filling of North Cove and eventual loss of the remaining Shoalwater Reservation inter-tidal habitat within North Cove. This alternative protects only the small upland portion of the Shoalwater Reservation. It was screened out because, unlike other available solutions, it fails to fully meet the criteria specified in the project authorization, and would leave approximately two-thirds of the Shoalwater Reservation (the North Cove embayment) unprotected from coastal erosion.

4.4 Incidental Benefits

This project is authorized to provide coastal erosion protection for the Shoalwater Bay Indian Reservation. All alternative plans have been formulated in an effort to fully respond to the project authorization. For coastal engineering reasons, all of the protective structures discussed above would provide some unintended "incidental" coastal erosion protection to privately owned shores in the immediate vicinity of the Shoalwater Reservation and/or to State Route 105. The objective of the "sea dike" and "dune restoration" alternatives is to protect the Shoalwater Reservation shoreline from further shoreline erosion and storm wave attack during periods of extreme high tides. Since strong southerly winds are associated with storm events in this area, both the sea dike and dune restoration alternatives must extend along the entire length of the existing eroded barrier dune to provide protection from locally generated waves. In addition, restoring the entire length of the barrier dune is the only practicable means to minimize, if not prevent, further infilling of the remaining inter-tidal area of North Cove within the boundary of the Shoalwater Reservation.

The flood berm and revetment are, by design, relatively porous structures, intended to prevent flooding caused by wave overtopping, but not to act as flood control levees. The alignment and extent of the structures are dictated by existing shoreline topography and wave exposure. For these reasons the southern portions of both the revetment and flood berm would be required to extend beyond the Shoalwater Reservation boundary in order to tie into high ground. The south extension of the flood berm and revetment would prevent further shoreline erosion and associated storm wave overtopping of the shoreline, thereby preventing back-flooding of tribal property and infrastructure. Likewise, the north flood berm and northerly extent of revetment would afford storm wave protection to a portion of State Route 105 which traverses the reservation along the shoreline. Note that the north flood berm lies entirely within the Shoalwater Reservation.

References

Federal Highway Administration and Washington Department of Transportation, 1997. Environmental Assessment, SR-105 Emergency Stabilization Project, North Cove, Washington.

Hughes, S.A. 2004. Estimation of wave run-up on smooth, impermeable slopes using the wave momentum flux parameter," *Coastal Engineering* 51, 1085-1104.

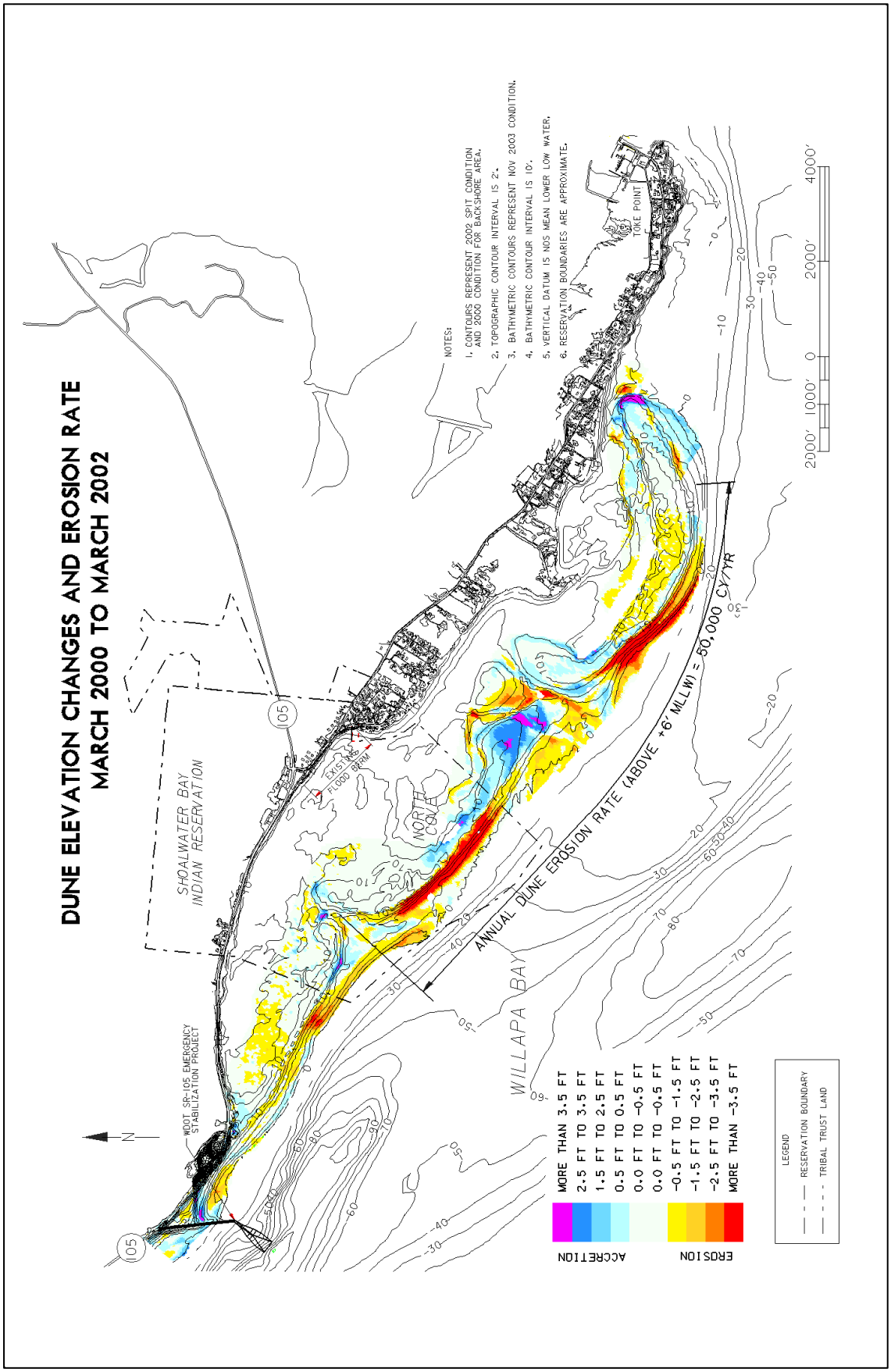

Figure 4.1 Dune elevation changes and erosion rate.

TOKE POINT, HIGHEST WATER ELEVATIONS 1973 - 2007	
TIDE ELEVATION (FT, MLLW)	**DATE**
14.41	NOV 14 1981
14.07	FEB 04 2006
13.87	DEC 11 1973
13.61	MAR 03 1999
13.41	DEC 03 2007
13.36	DEC 03 1982
13.23	DEC 01 2001
13.21	JAN 02 2003
13.16	JAN 27 1983
13.09	FEB 07 1978
12.97	JAN 18 1973
12.95	JAN 29 1999

Figure 4.2 Toke Point highest tides, 1973 - 2007.

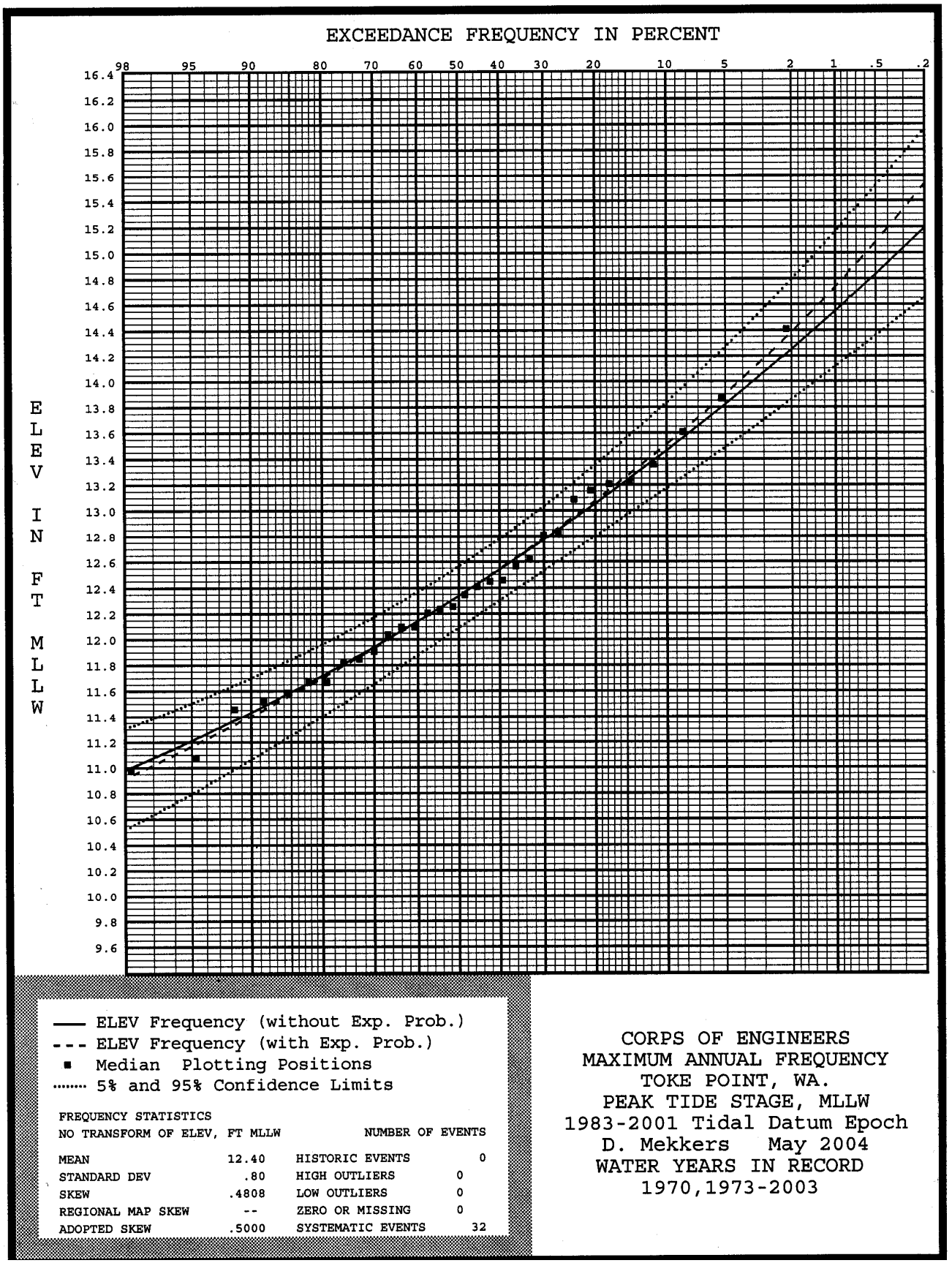

Figure 4.3 Maximum annual frequency curve for Toke Point, Washington.

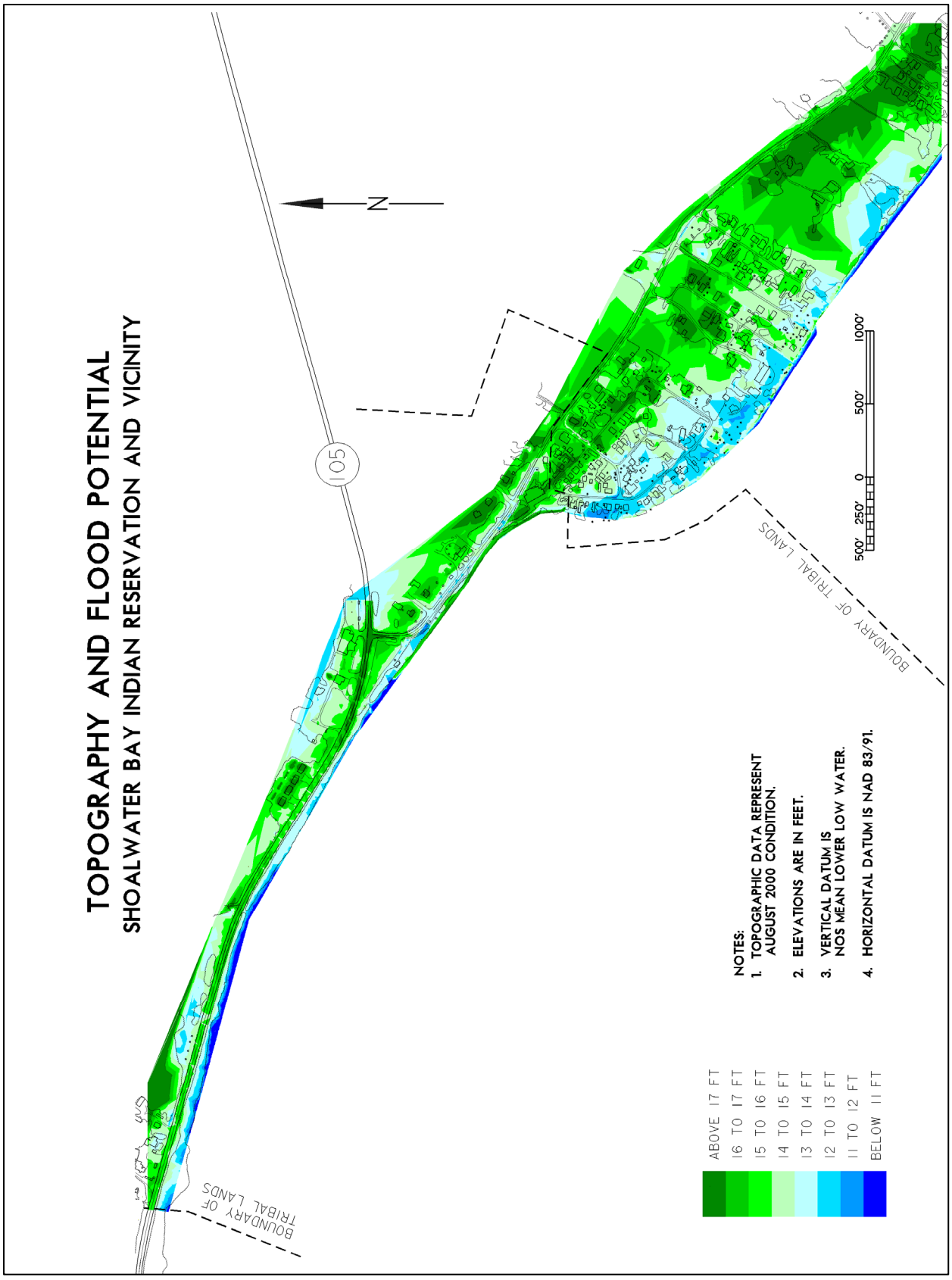

Figure 4.4 Topography and flood potential, Shoalwater Bay Indian Reservation and vicinity.

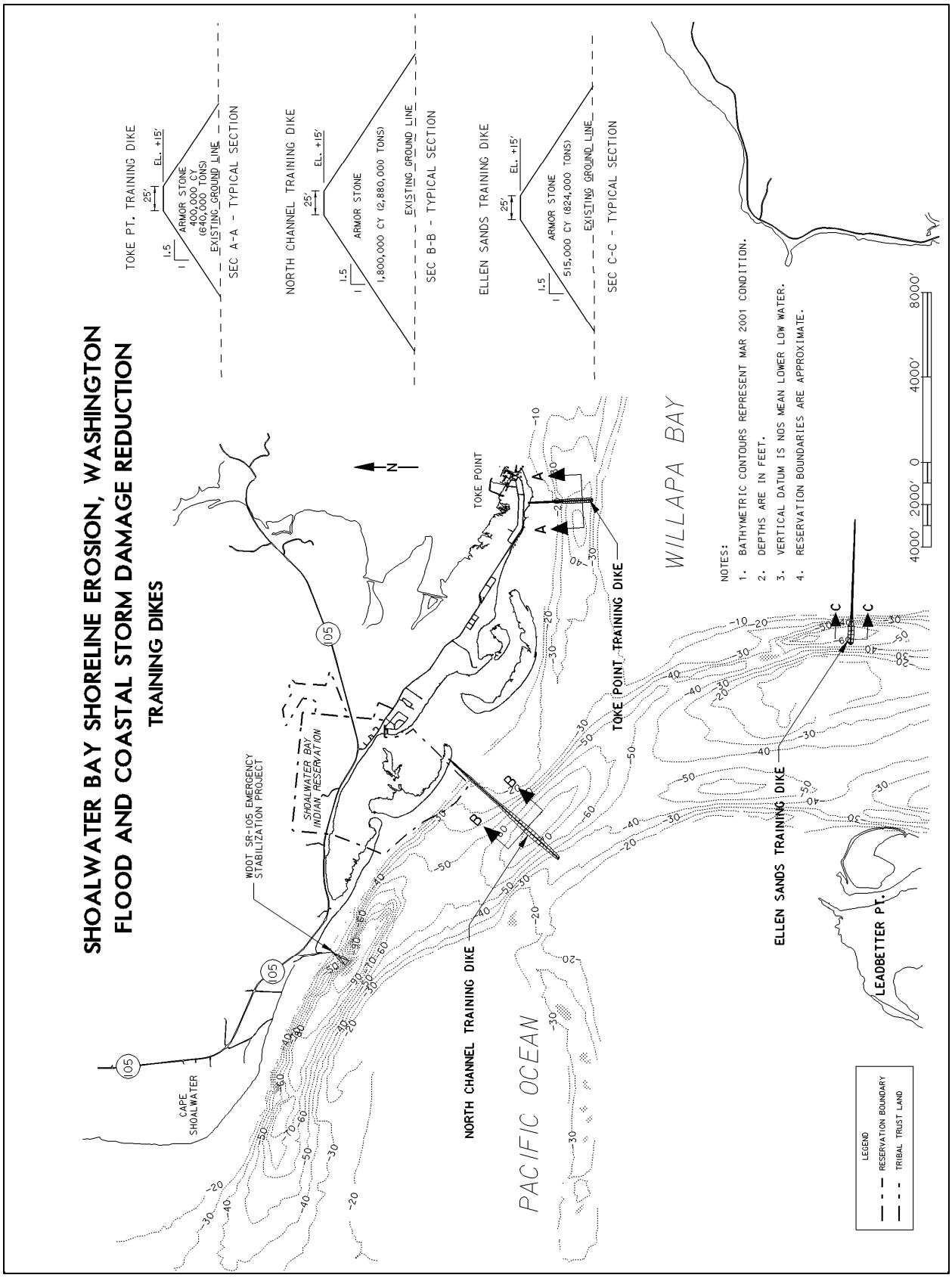

Figure 4.5 Training dikes, plan and section.

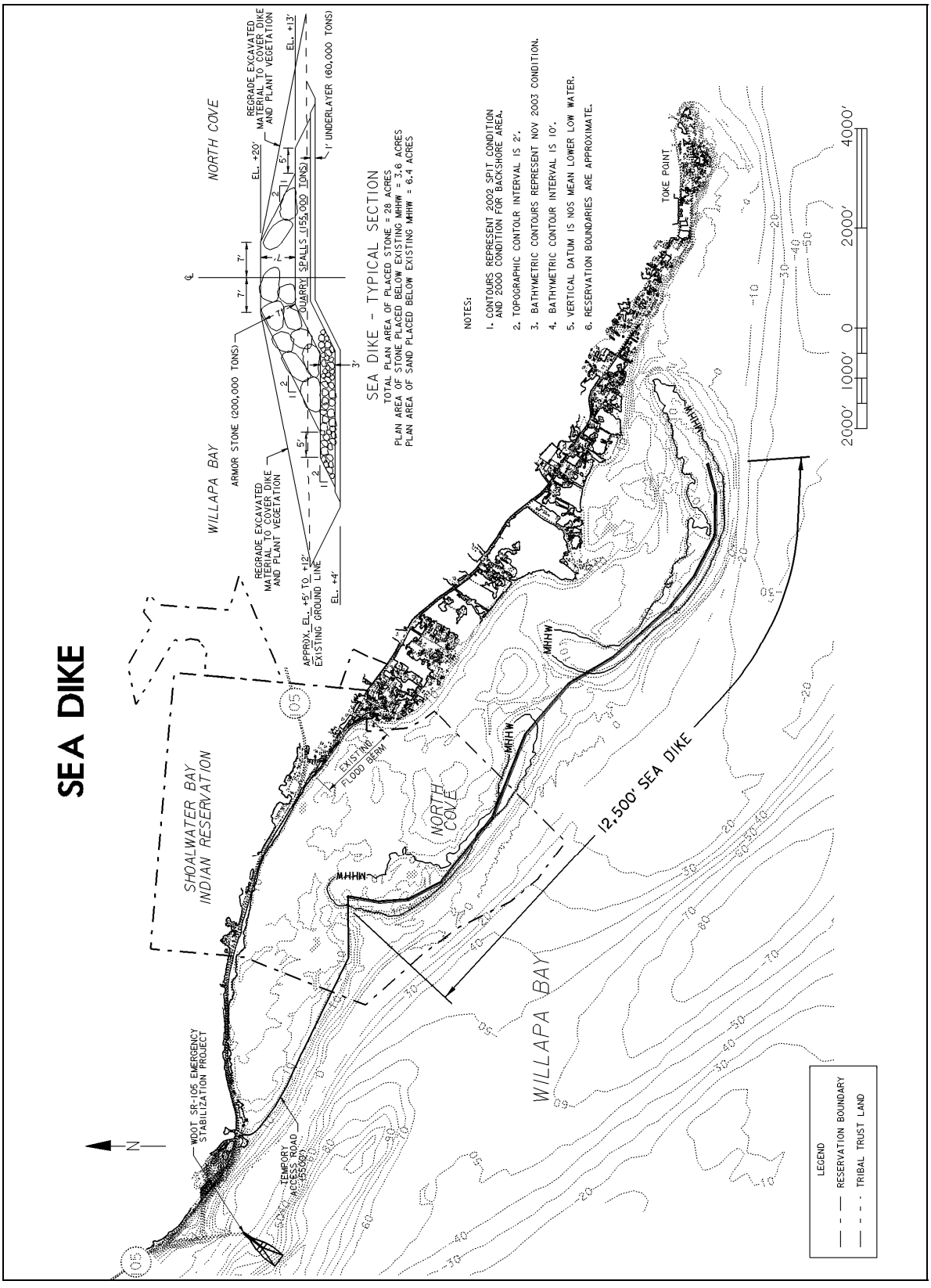

Figure 4.6 (a) Sea dike, plan and section.

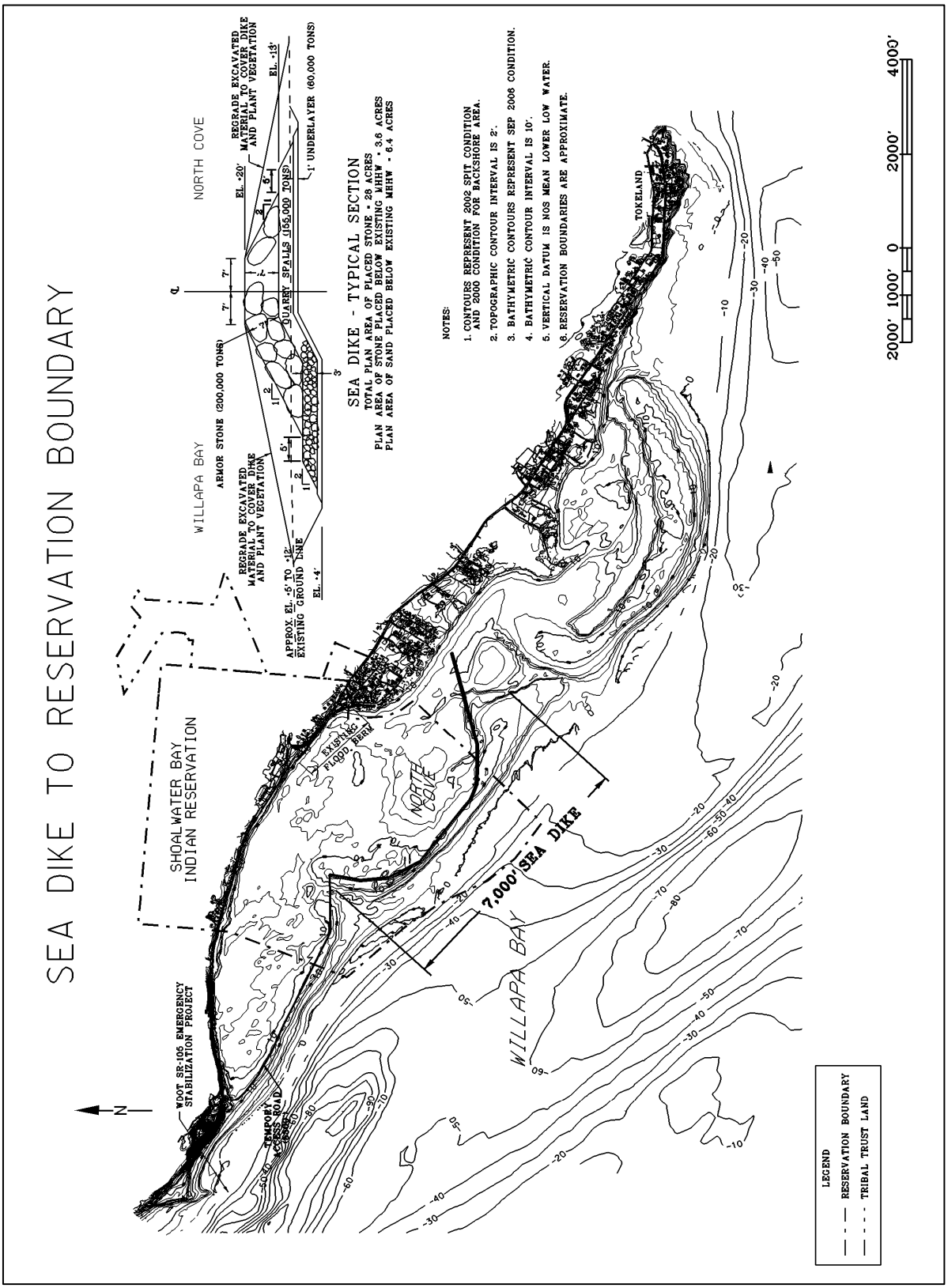

Figure 4.6 (b) Sea dike to reservation boundary, plan and section.

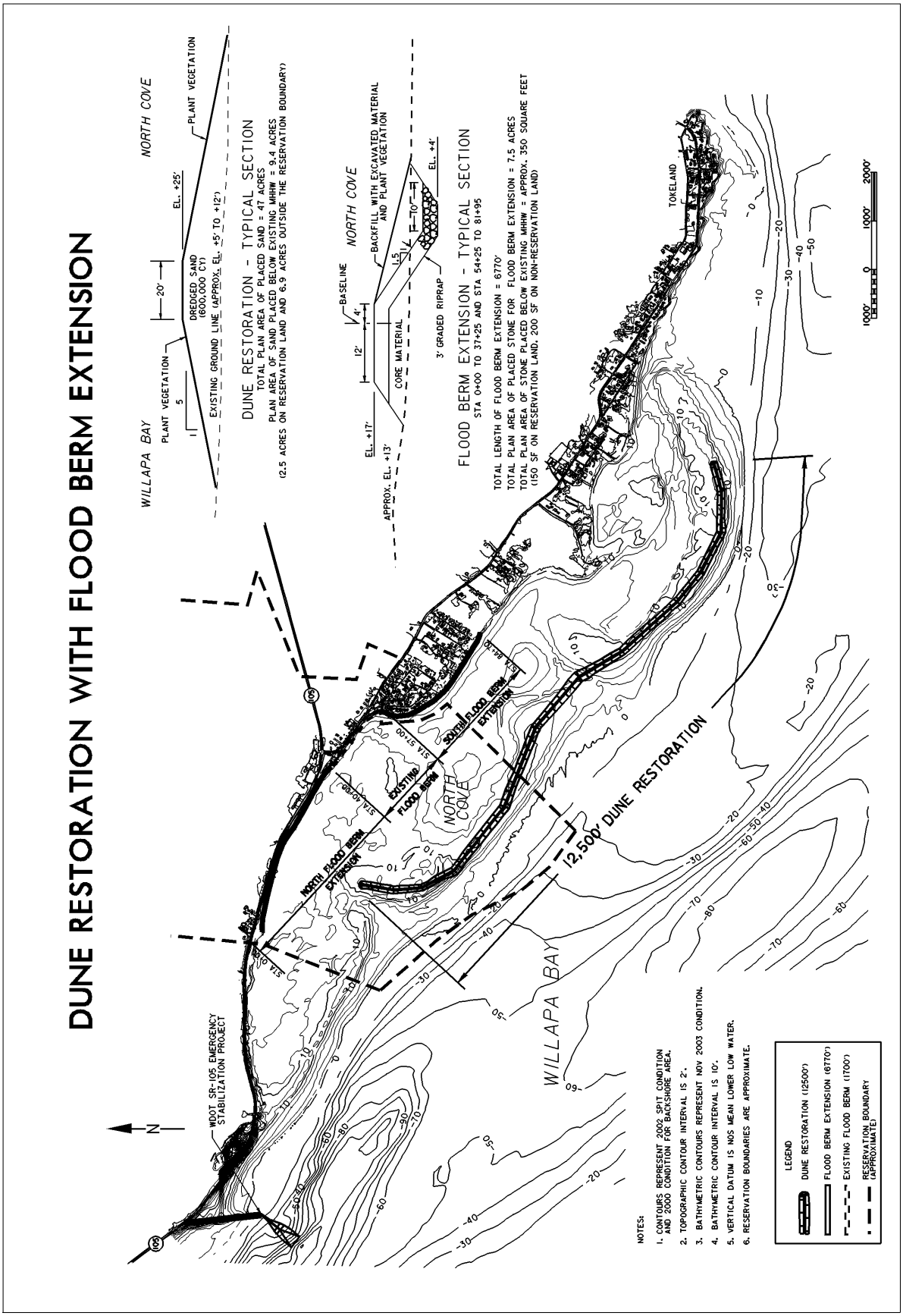

Figure 4.7 Barrier dune restoration with flood berm extension, plan and sections.

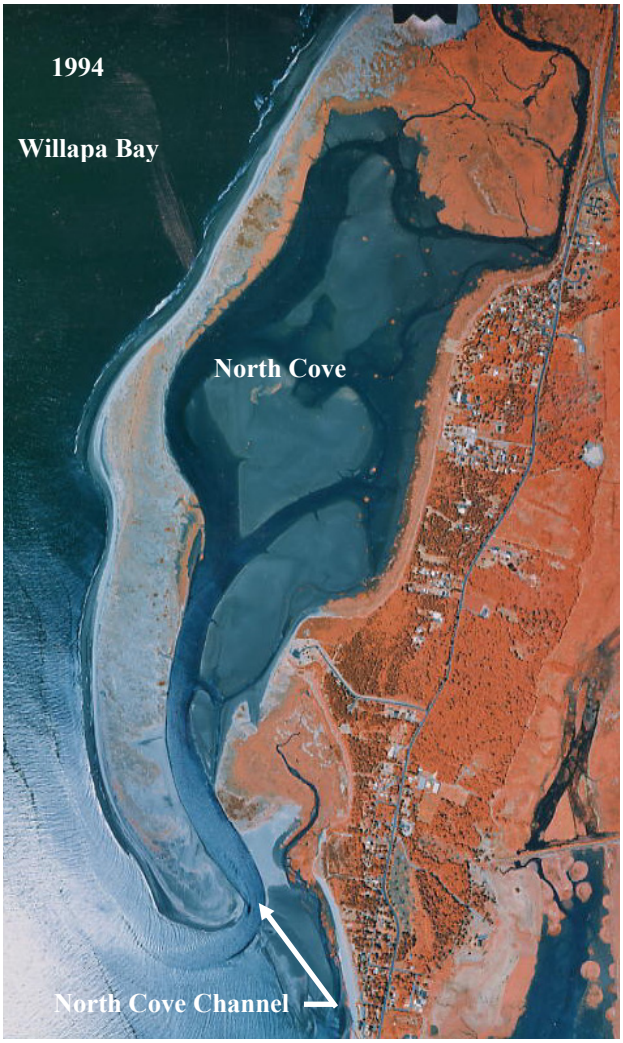

Figure 4.8 1994 Graveyard Spit configuration.

Figure 4.9 2004 Graveyard Spit configuration.

DUNE RESTORATION

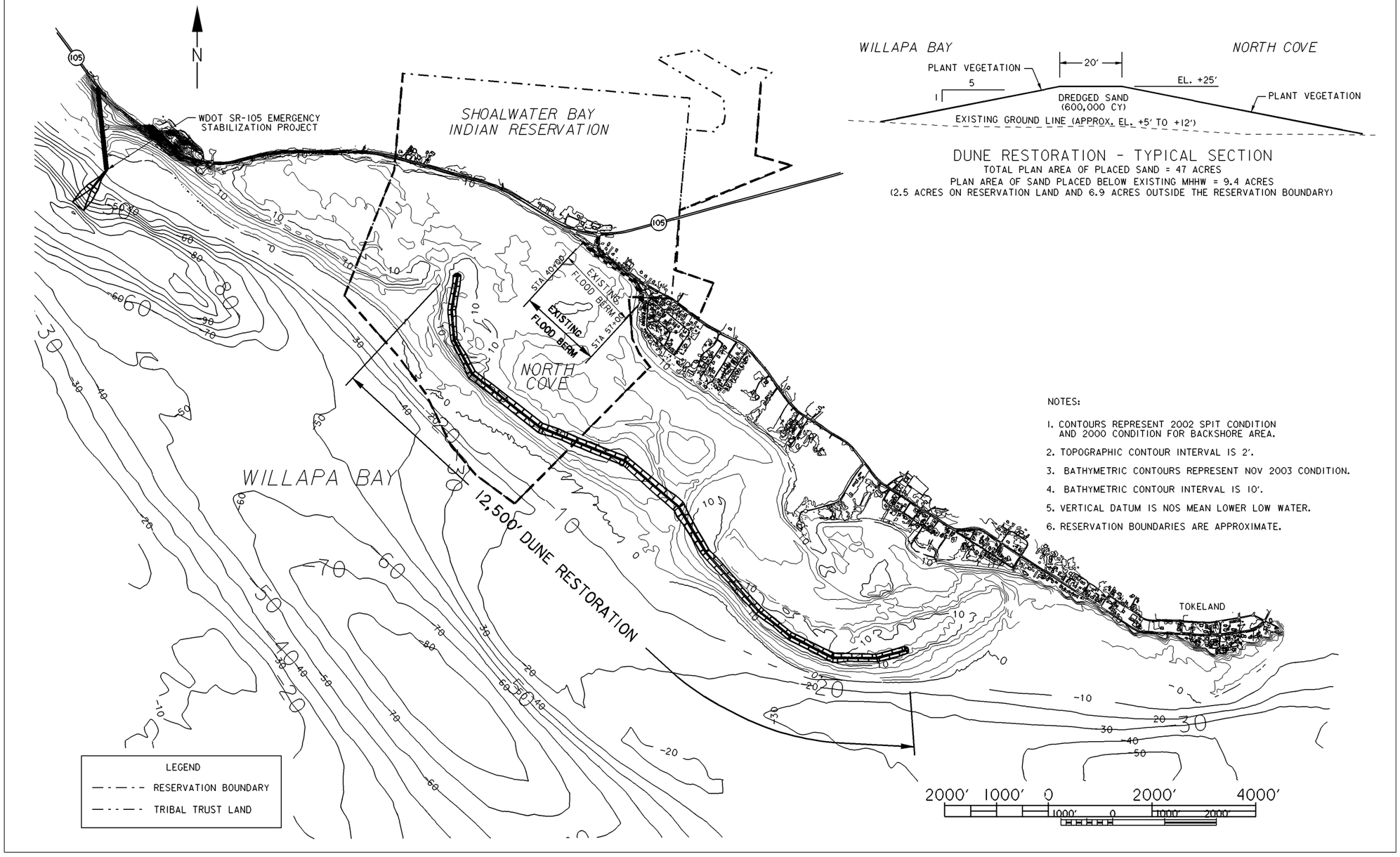

DUNE RESTORATION - TYPICAL SECTION

TOTAL PLAN AREA OF PLACED SAND = 47 ACRES
PLAN AREA OF SAND PLACED BELOW EXISTING MHHW = 9.4 ACRES
(2.5 ACRES ON RESERVATION LAND AND 6.9 ACRES OUTSIDE THE RESERVATION BOUNDARY)

NOTES:

1. CONTOURS REPRESENT 2002 SPIT CONDITION AND 2000 CONDITION FOR BACKSHORE AREA.
2. TOPOGRAPHIC CONTOUR INTERVAL IS 2'.
3. BATHYMETRIC CONTOURS REPRESENT NOV 2003 CONDITION.
4. BATHYMETRIC CONTOUR INTERVAL IS 10'.
5. VERTICAL DATUM IS NOS MEAN LOWER LOW WATER.
6. RESERVATION BOUNDARIES ARE APPROXIMATE.

Figure 4.10 Barrier dune restoration, plan and section.

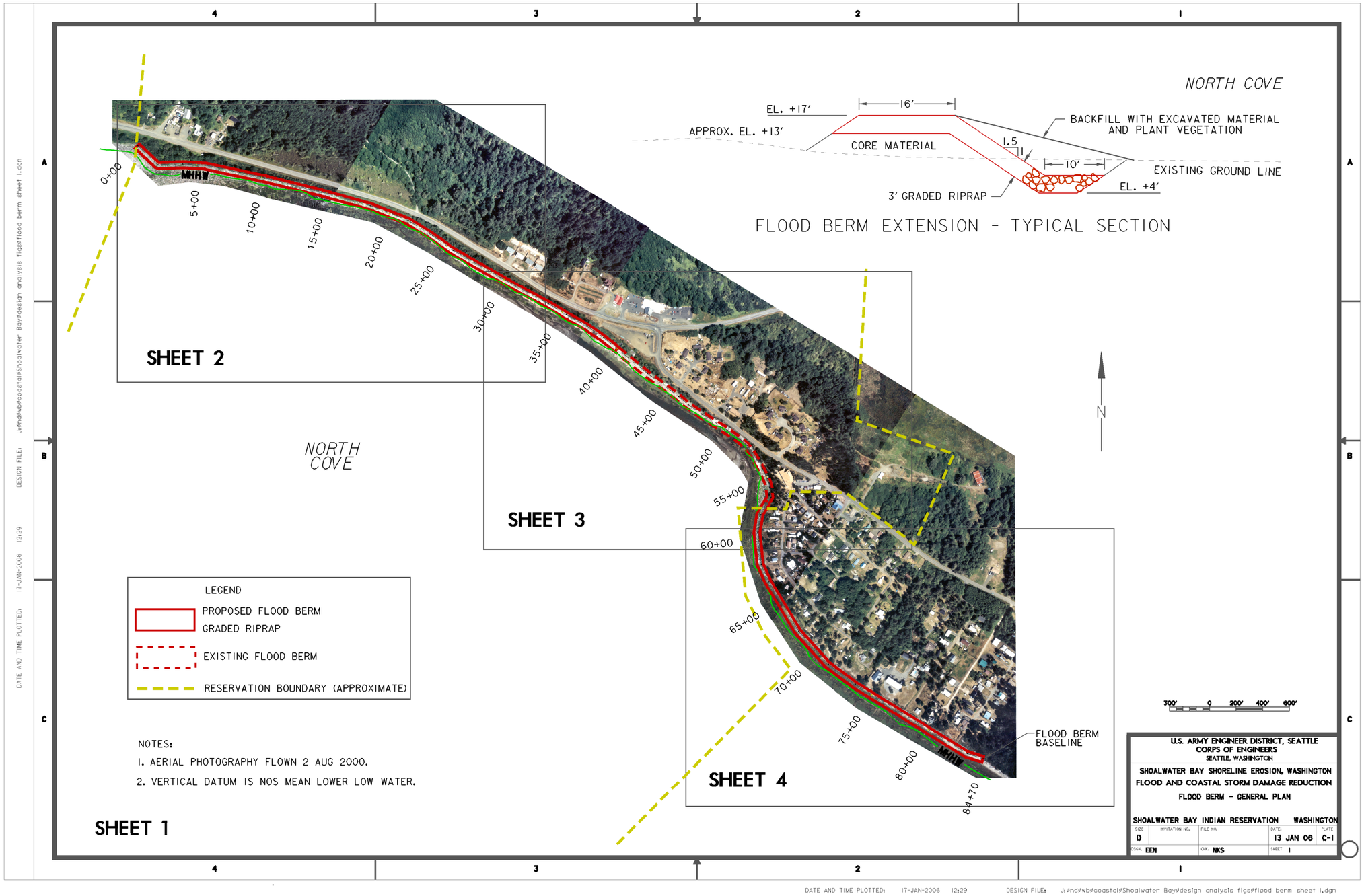

Figure 4.11 Flood berm extension, general plan and typical section.

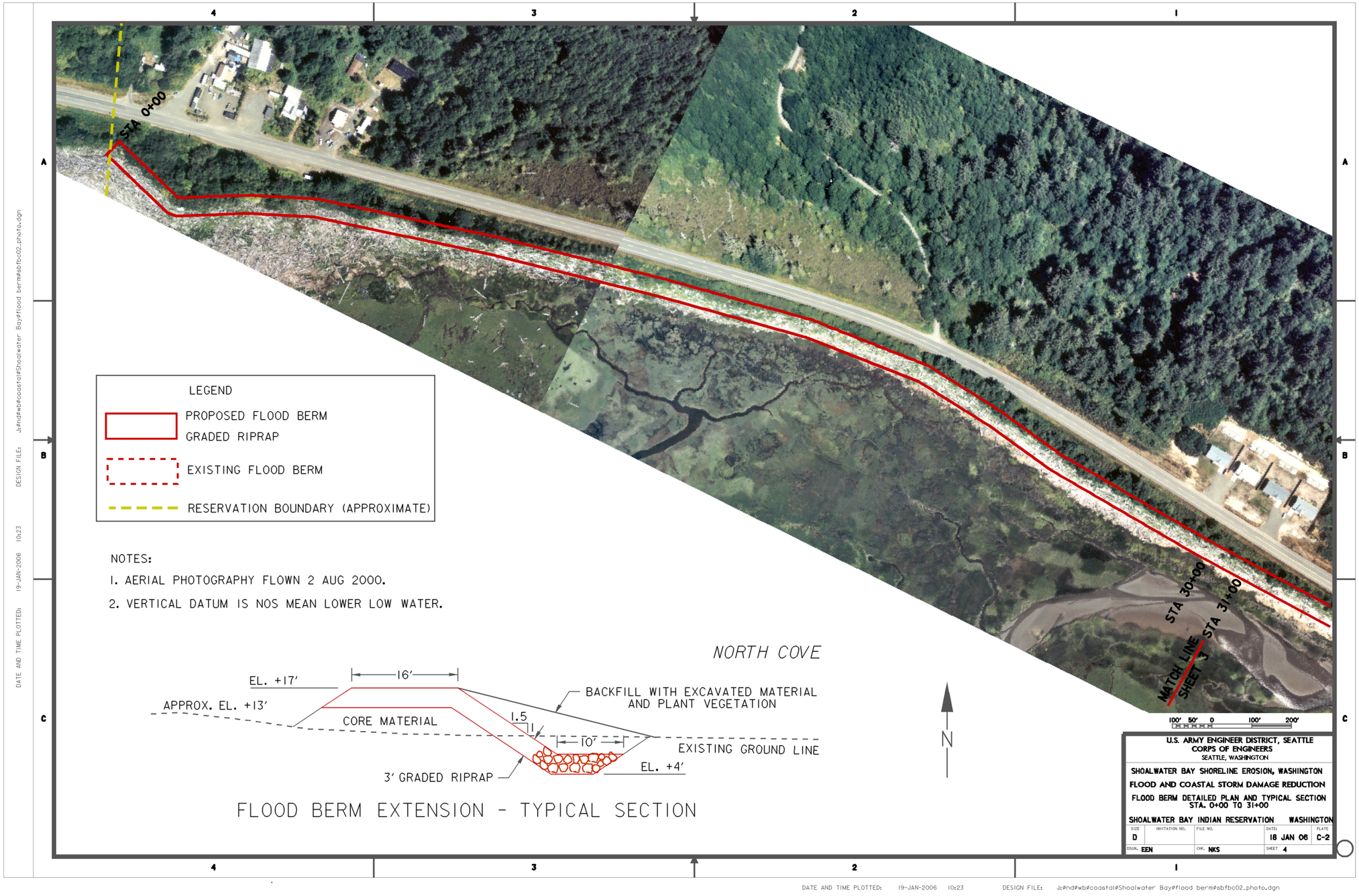

Figure 4.12 Flood berm detailed plan and typical section, station 0+00 to 31+00.

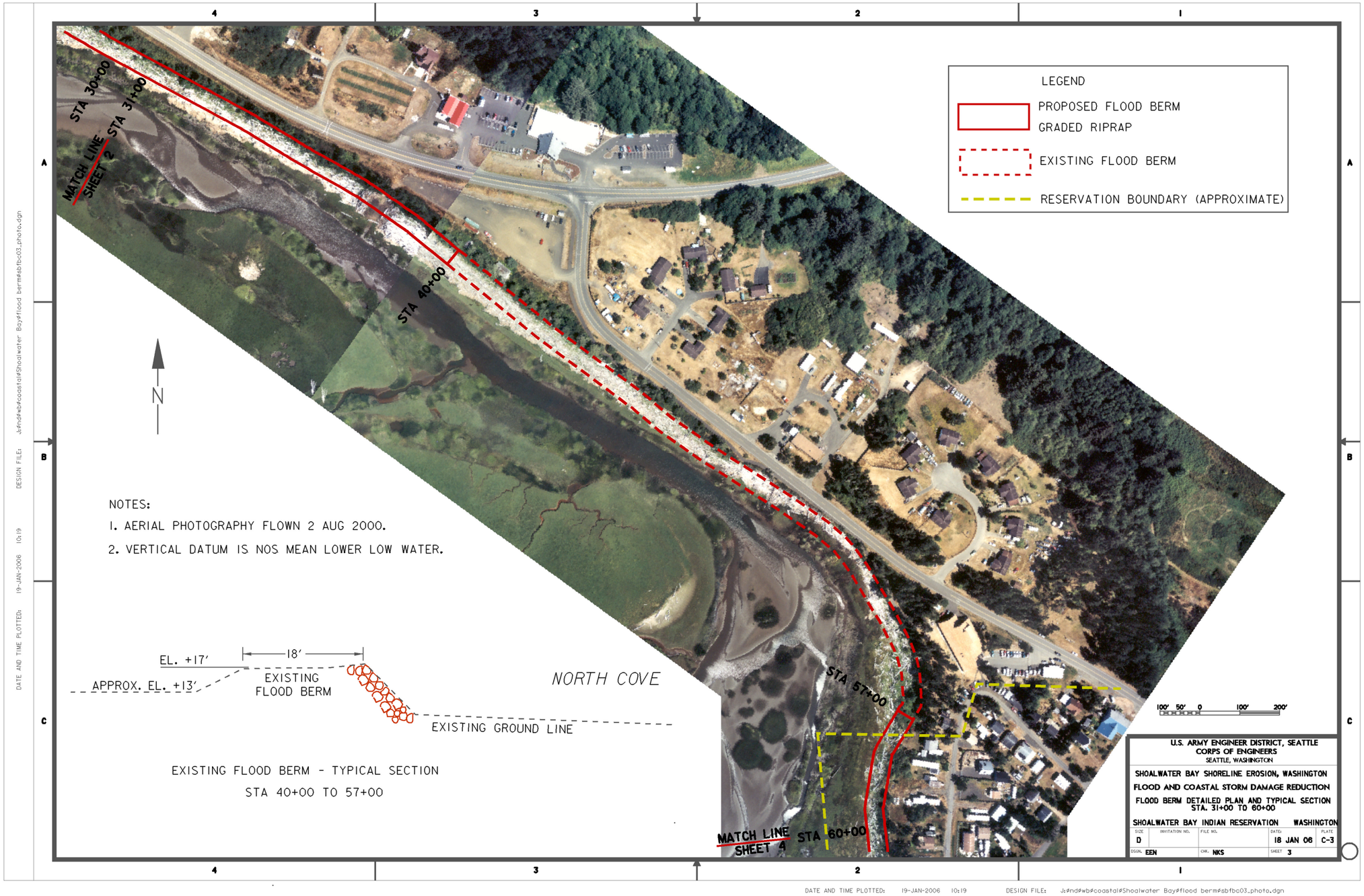

Figure 4.13 Flood berm detailed plan and typical section, station 31+00 to 60+00.

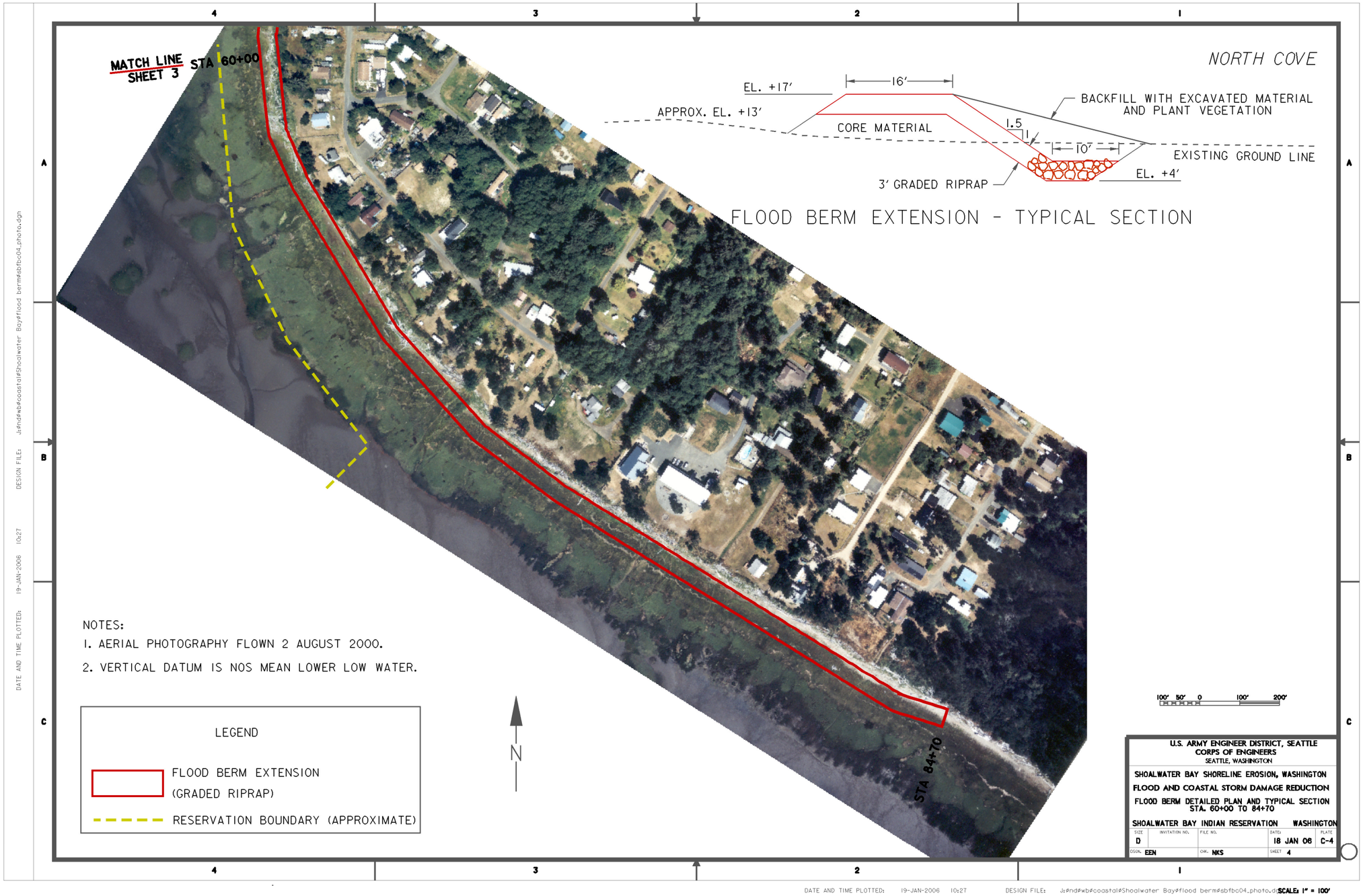

Figure 4.14 Flood berm detailed plan and typical section, station 60+00 to 84+70.

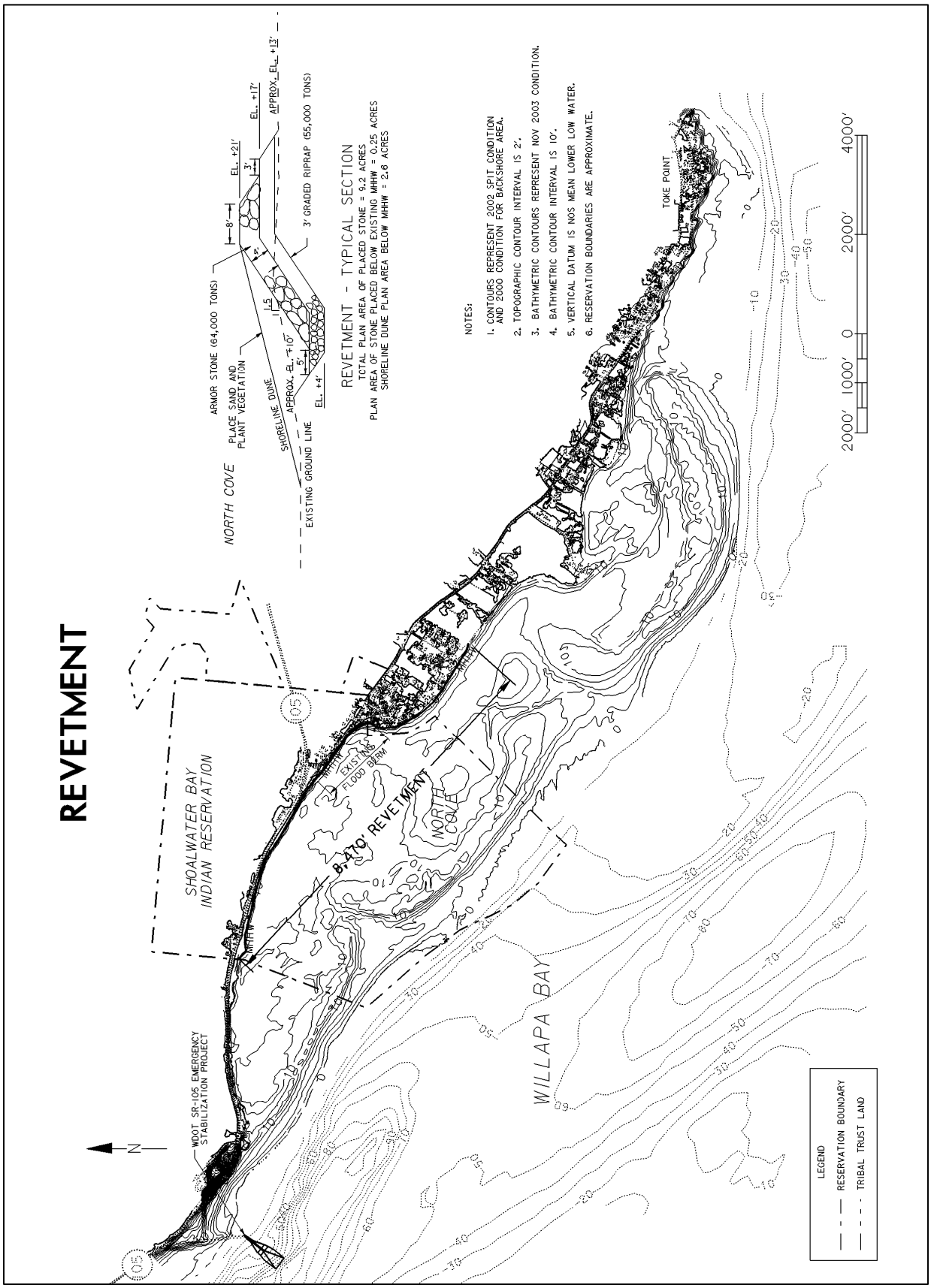

Figure 4.15 Revetment, plan and section.

5.0 Sand Borrow Sites and Beneficial Use of Dredged Material [16]

5.1 Sand Borrow Site Selection

The alternatives involving "dune restoration" will require access to a ready source of sand, for both construction and periodic nourishment. As described in Section 3.4.2, immense volumes of sand are moved by tidal currents in the vicinity of the Willapa bar and entrance. Figure 5.1 shows elevation changes that took place in the North Channel between 2000 and 2003. These changes confirm the conclusions of Section 2.3 that, in the area fronting the Shoalwater Reservation, the channel is now accreting and the channel thalwag is migrating southward. The area immediately seaward of the dune restoration site is now shoaling at a rate of greater than one million cy/yr, or almost 20 times the rate required to provide a supply of sand for the dune construction and periodic nourishment. As long as the natural accretion of sand at this location rapidly replaces the material being removed for periodic nourishment of the dune, this area appears to be an excellent (primary) borrow site for the dune restoration alternative. The primary borrow site is located on the north side of the North Channel (see Figure 5.2). However, the shoaling patterns are extremely variable. Monitoring of the borrow site will be required to ensure that this is the optimum borrow site location over time, and that the volume of material being removed does not significantly alter the tidal flow patterns or change the general trend of the channel thalwag movement away from the North Cove area.

Material will not be removed from the primary borrow site if bathymetric surveys indicate that the rate of natural accretion has decreased significantly. In the event that material cannot be obtained from the primary borrow site, an alternate (secondary) borrow site is located on the south side of the North Channel (see Figure 5.2). Sediment is now eroding from the vicinity of the secondary site at a rate of over 3.5 million cy/yr. Borrowing 50,000 cy/yr from this area is not expected to have any detectable effect on the ongoing sediment transport processes. Locating a sand borrow site on the south side of the North Channel will require a more complicated construction process involving pumping sand through a pipeline that extends approximately 8,000 feet, across (under) the channel, and along the shore to the dune restoration site. However, a similar procedure was accomplished very successfully in 1998 to construct a 350,000 cy beach fill for the State Route (SR) 105 Emergency Stabilization Project which is located to the west of Graveyard Spit. The SR-105 borrow site was located on the north side of the Willapa North Channel, and the sand was pumped approximately 8,000 feet. The SR-105 borrow site is located to the west of the proposed primary borrow site identified for the barrier dune restoration (see Figure 5.1). The SR-105 borrow site was originally located in water depths of 20 to 50 feet, and the volume of material that was dredged appears to be "background noise" compared to the natural bathymetric changes that have taken place.

[16] Written by Eric Nelson, U.S. Army Corps of Engineers, Seattle District

5.2 Beneficial Use of Dredged Material

In October – December 2000, the Corps of Engineers placed approximately 130,000 cy of maintenance dredged material at a beneficial use site located immediately offshore of the North Cove islands (see Figure 5.1). The material was placed in the hope that it would help to reduce the rate of erosion of the barrier dunes. Intensive monitoring was conducted within the disposal site. Figure 5.3 is an isopach that compares the elevation changes that were measured by surveys made prior to, and immediately after, placement of the dredged material. Figure 5.3 indicates that material was accumulating within the disposal site, but that material was not being transported landward onto the upper beach and Figure 5.1 indicates that little change has taken place within the site since the initial placement. The placement of maintenance dredged material appears to have no disadvantages, and continuing to place suitable maintenance dredged material in the vicinity of the primary borrow site would help to offset the material being borrowed for the dune maintenance.

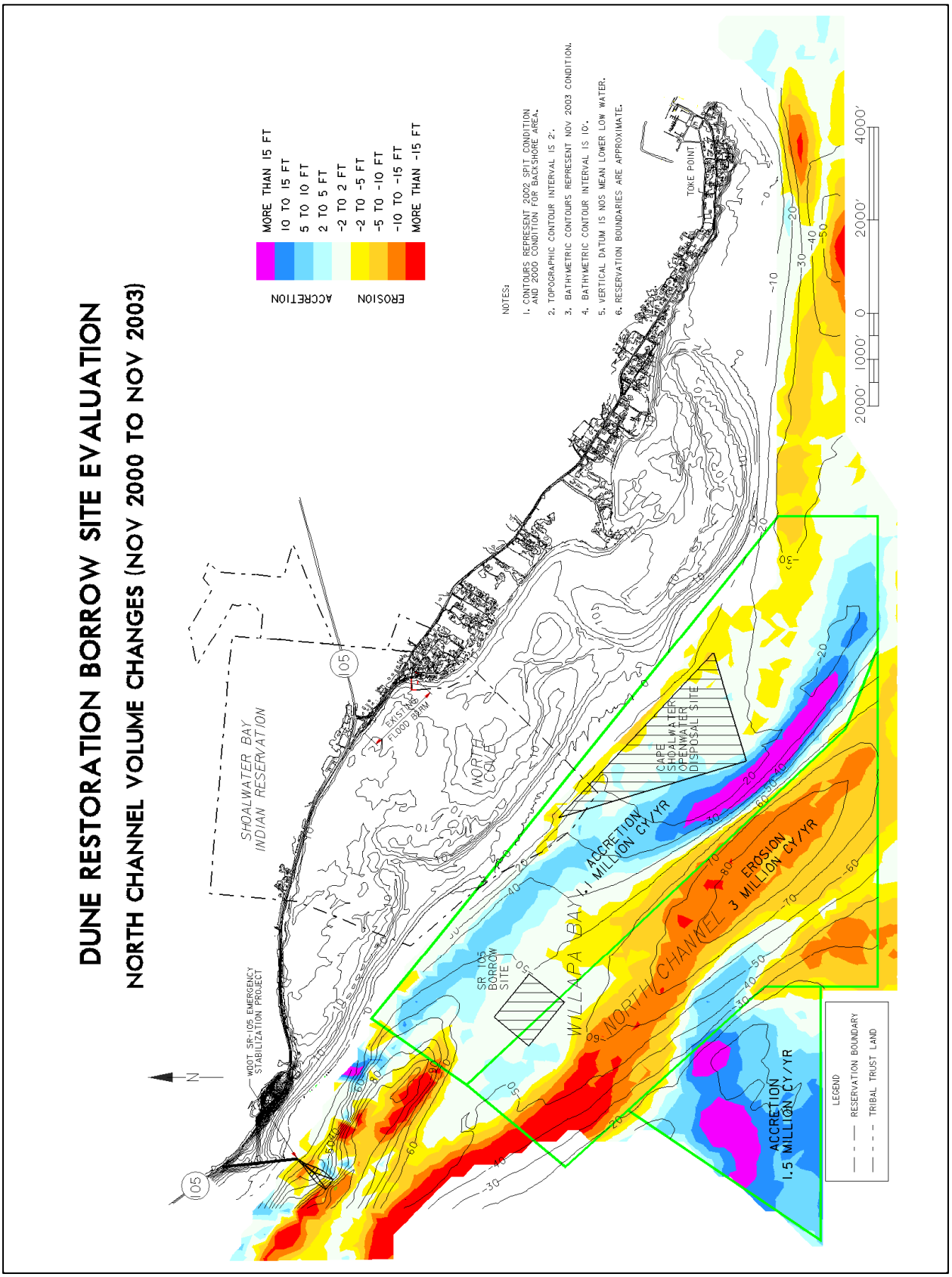

Figure 5.1 Dune restoration borrow site evaluation, North Channel volume changes.

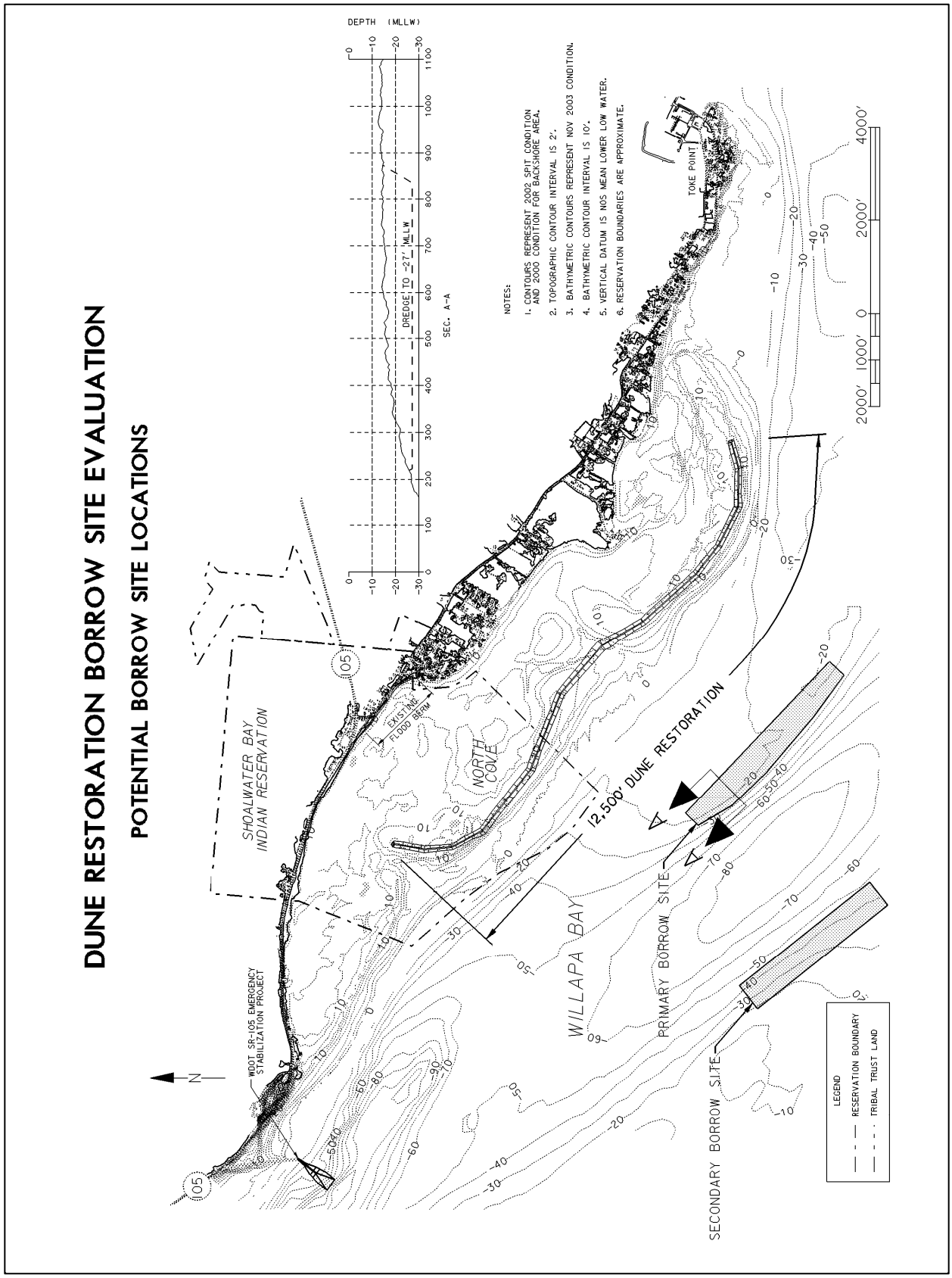

Figure 5.2 Dune restoration borrow site evaluation, potential borrow site locations.

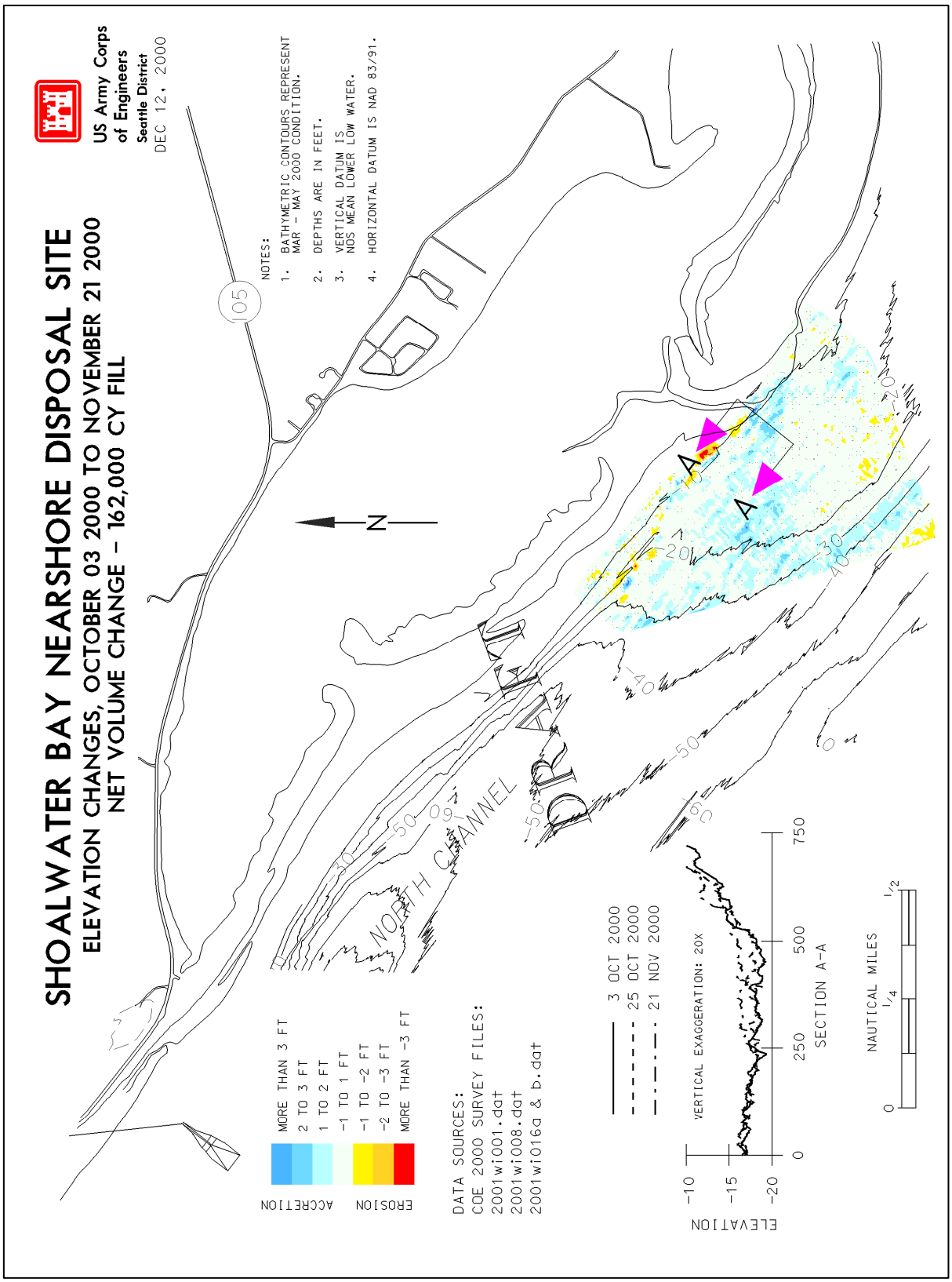

Figure 5.3 Shoalwater Bay near shore disposal site elevation changes. 3 October 2000 to 21 November 2000.

6.0 Incorporating Sea Level Change [17]

6.1 Sea Level Rise

In addition to other potential damaging consequences, sea level rise presents a threat to the reliability of coastal infrastructure. An increase in mean sea level in conjunction with storm surge and increased wave energy propagating further inland will inundate shorelines, bays, tidal wetlands, etc. exacerbating storm damage and coastal erosion. Incorporating the effects of sea level rise will be required in the long-term management of the barrier dune restoration. Previous guidance for incorporating sea level rise in Civil Works Projects has recommended the approach from the National Research Council (NRC, 1987). Recent interim guidance in the form of an Engineering Circular (USACE EC-1165-2-XXX, 2009) has been developed incorporating new information including projections by the Intergovernmental Panel on Climate Change (IPCC, 2007).

The interim guidance recommends that the local mean sea level be reevaluated every 5-10 years prior to nourishment for beach nourishment projects with reoccurring maintenance. The University of Washington Climate Impacts Group and Washington Department of Ecology (Mote et al. 2008) applies the findings of the IPCC to estimate local sea level rise for the Southwest Washington Coast. The study incorporates vertical land movement and local atmospheric dynamics to estimate the relative sea level rise projections for 2050 and 2100. The mean prediction for the by 2050 is a 5 inch sea level rise, with a worst-case scenario of 18 inches. By 2100, the mean prediction is 11 inches, with a worst-case scenario of 43 inches. Utilization of a soft engineering structure such as dune nourishment provides greater robustness against uncertainties associated with sea level rise. Prior to future periodic nourishment, the local sea level will be incorporated into the nourishment quantity and dune cross-section to maximize reliability while reducing risk associated with storm damage.

References

IPCC 2007. "Climate Change 2007: Impacts, Adaptation and Vulnerability. Contribution of Working Group II to the Fourth Assessment Report of the Intergovernmental Panel on Climate Change." [M.L. Parry, O.F. Canziani, J.P. Palutikof, P.J. van der Linden and C.E. Hanson, Eds.] Cambridge University Press, Cambridge, UK. Available at http://www.ipcc.ch/ipccreports/ar4-wg2.htm

Mote P., Peterson, A., Reeder, S., Shipman, H., and Binder, L.W. University of Washington Climate Impacts Group and Washington Department of Ecology. 2008. Sea Level Rise in the Coastal Waters of Washington State www.psat.wa.gov/climatechange

National Research Council. 1987. Responding to changes in sea level. Engineering Implications.

U.S. Army Corps of Engineers. 2009. Water Resource Policies and Authorities. Interim Guidance for incorporating sea level change. DRAFT.

[17] Written by David Michalsen, U.S. Army Corps of Engineers, Seattle District

End of Appendix 1
Engineering Analysis and Design